Fibre-reinforced Soil Based Construction Materials

Andrew John Corbin

Thesis submitted as partial consideration towards
the degree of Doctor of Philosophy

Mechanics Research Group
School of Engineering and Computing Sciences
Durham University, Durham
United Kingdom

August 2016

Fibre-reinforced Soil Based Construction Materials

Andrew John Corbin

Abstract

Soil based construction materials (SBCMs) are formed of a mixture of gravel, sand and clay which, when mixed with water, may be used for construction. They can be an environmentally-friendly alternative to more traditional construction materials such as concrete and fired brick. SBCMs commonly incorporate foreign material into the soil to enhance the material properties. Many guides on SBCM construction advocate the use of cement as a stabiliser to strengthen the material, which detracts from the environmental credentials that earthen construction materials possess. Alternatives methods to strengthen SBCMs are therefore needed.

In this thesis, waste wool fibres from a carpet manufacture are investigated as a potential alternative fibrous reinforcement in rammed earth (RE), and its effect on the behaviour of stabilised and unstabilised RE is assessed. Compressive tests, shear tests and splitting tests are performed to study the effect of fibrous (wool) and chemical (cement) stabilisation on RE, and recommendations on further use of these materials are made. Tests are also performed to investigate the shrinkage of different clays (bentonite and kaolinite) used in RE when mixed with sand or wool, in order to determine the effects of these materials on shrinkage behaviour. Finally, advice is provided regarding the use of fibrous reinforcement in SBCMs, which is applicable to both the SBCM industry and research, and new and pre-existing research areas are identified to prompt further study.

Declaration

The work in this thesis is based on research carried out in the Mechanics Research Group, School of Engineering and Computing Sciences, Durham University. No part of this report has been submitted elsewhere for any other degree or qualification and it is all my own work unless referenced to the contrary in the text.

Parts of this work have been used or reproduced in the following:

Published Conference Papers

A.J. Corbin and C.E. Augarde. (2015). Investigation into the shear behaviour of rammed earth using shear box tests. *Proceedings of the 1st International Conference on Bio-based Building Materials (ICBBM2015)*, Amiziane & Sonebi (eds), Clermont-Ferrand, RILEM Publications S.A.R.L.:Bagneaux, France. 93-98

A.J. Corbin and C.E. Augarde. (2014). Fracture energy of stabilised rammed earth. *Procedia Materials Science*, 3, 1675-1680.

Author Contributions

D. Readle, S. Coghlan, J.C. Smith, A.J. Corbin and C.E. Augarde.
Fibre reinforcement mechanisms in earthen construction materials.
In *ICE Proceedings - Construction Materials*, available ahead of print, 14 Oct 2015

Acknowledgements

I would like to take this opportunity to thank Professor Charles Augarde for his generous and unwavering support and guidance throughout my PhD and previously during my final year undergraduate research project. Charles, without your support, encouragement and belief in me, I would not have had the opportunity to do any postgraduate research, and for that I am deeply grateful.

On a more formal note, this research would not have been possible without the generous funding from the UK Engineering and Physical Sciences Research Council (EPSRC).

I would like to thank all those in the School of Engineering and Computing Sciences who have helped me through my PhD, be it providing advice on laboratory procedure, guiding me toward documents and people who were able to help when I got stuck, or through casual conversations during coffee breaks and lunch. To Joe, Chris, Adam, Jack, JD and all those who have lent me support, advice or simply a listening ear, I would not have started this without you. I would like to thank Steve Richardson and Kevan Longley in particular for their practical support, guidance and encouragement in the laboratory where I spent many long hours.

I would also like to thank Dr. Daniela Ciancio at the University of Western Australia who gave me the opportunity to study abroad for 3 months in 2014. Thank you also to Dr. Chris Beckett and everyone in Perth who helped me to settle in Australia for the duration of my study.

Thank you to my family and friends, who have given me so much over the years and, without whom, I would not be who, or where, I am today. Thank you for believing in me, especially when I didn't believe in myself. Thank you also for listening to my extensive monologues extolling the benefits of earthen construction - I promise that I will engage myself in other projects so that our conversations may become a little less soil-orientated.

Finally, and most importantly, I would like to publicly thank my amazing wife Abbey, who has shown me unwavering love and support throughout my PhD. Thank you for being there for me, and I promise that I will endeavour to be as supportive of you in the future as you have have been of me over the last few years. Thank you for distracting me when I needed it and encouraging me to work when I need to. Thank you also for your many hours of proofreading. I can say for certain that this would not have been possible without you.

Andrew Corbin

August 2016

Contents

List of Figures

List of Tables

Acronyms

DST	direct shear test
LEFM	linear elastic fracture mechanics
OWC	optimum water content
SBCM	soil-based construction material
RE	rammed earth
UCS	unconfined compressive strength
WST	wedge splitting test

Chapter 1

Introduction

Soil has been used as a construction material for thousands of years (Jaquin et al., 2008a). In the last few decades, earthen construction has seen a revival, triggered in part by a desire for a more sustainable existence, leading to a surge in interest in earthen construction research.

There is current uncertainty within research circles as to the most appropriate approach for performing research into the analysis of earthen construction, for example whether to consider it as a geotechnical material, therefore applying unsaturated soil mechanics, or whether to take a macroscopic approach, similar to the approach taken when analysing concrete, and therefore applying a different analysis. It is likely, however, that both approaches are valid for different situations in earthen construction. For example, a macrostructural analysis is likely to be more appropriate when cement is added to soil mix, as it behaves in a similar matter to that of weak concrete, while an unstabilised soil might be more appropriately modelled as a compacted unsaturated soil.

This thesis considers the structural behaviour of rammed earth (RE), by presenting studies into the change in behaviour when compacted with cement and/or wool stabilisation. It analyses the material behaviour from a macroscopic perspective, but with consideration of the microstructure in an attempt to combine the two different approaches.

1.1 Thesis aim and primary research areas

The primary aim of this thesis is to investigate the potential use of waste carpet fibre, a waste stream from the carpet manufacturing industry, as the fibrous reinforcement in earthen construction. This thesis also aims to investigate how this material behaves when mixed into soils stabilised with cement. In order to perform a complete study into this area, this aim may be divided into three primary research areas and associated objectives as follows:

- The effect of cement stabilisation on the properties of rammed earth;
  - To investigate the effect of cement stabilisation on the compressive strength of RE, and to confirm that stabilisation of the soil used in this thesis behaves in a similar manner to that presented in other research.
  - To establish the effect of cement stabilisation on the shear strength of RE, and also to investigate the viability of using a less well-used test for this property within soil-based construction material (SBCM) research.
  - To determine the effect of cement stabilisation on the fracture energy of RE, testing the viability of using a test not used to date within earthen construction.
- The effect of wool reinforcement on the properties and behaviour of rammed earth;
  - To establish the effect of waste carpet fibre reinforcement on the compressive strength of RE, and to determine if the behaviour of the samples is similar to samples with fibrous reinforcement in other research.
  - To determine the effect of waste carpet fibre reinforcement on the shear strength of RE, and to further determine if the samples behave similarly to other research with other fibrous reinforcement.
  - To determine the effect of waste carpet fibre reinforcement on the fracture energy of RE.
  - To investigate if and how the addition of wool affects shrinkage of RE.
- The effect of cement stabilisation and wool reinforcement on the properties of rammed earth.
  - To establish the effect of cement stabilisation and waste carpet fibre on the compressive strength of RE.
  - To investigate the effect of cement stabilisation and waste carpet fibre reinforcement on the shear strength of RE.
  - To determine the effect of cement stabilisation and waste carpet fibre on the fracture energy of RE.

1.2 Thesis overview

The thesis is structured as follows. An introduction to many of the different types of earthen construction is presented in Chapter 2, alongside a summarised history of relevant discoveries in fracture mechanics and a section highlighting current gaps in knowledge. Chapter 3 presents the results and

subsequent analysis of four investigations into the mechanical failure mechanisms of RE, focussing on the effects of the addition of wool and cement. One test investigates unconfined compressive strength (UCS), while the other three study shearing failure using variety of tests and loading conditions. Chapter 3 also presents a examination of RE using a scanning electron microscope in order to identify microstructural features of the samples.

Chapter 4 investigates the splitting failure of RE using a test not previously used for earthen materials, the wedge splitting test. A novel method of calculating the fracture energy is used, due to difficulties which arose when using the original method designed for use within concrete assessment. The fracture energy is calculated and comparisons are drawn between the fracture energy of unstabilised RE and of RE stabilised with wool and cement.

In Chapter 5, a set of experiments investigating shrinkage of clay used for RE is presented, analysing the effect of the addition of sand particles and wool to the clay/water mix. This is performed to investigate possible methods of making 'unsuitable' soils (such as those containing expansive clay) more suitable for construction.

Chapter 6 presents a summary of the research topics, setting out how the aims and primary research areas of the thesis have been achieved.

Finally, Chapter 7 presents a summary of the conclusions made throughout this thesis, alongside a discussion into the implications for SBCM construction, and suggestions for further research.

Chapter 2

Background to this research

Over the past couple of decades, there has been a notable increase in the research, development and implementation of new sustainable construction methods, in part due to the increasing awareness of climate change and the impact of human activities on our surroundings. Alongside new technologies, some older construction materials are being revisited in order to assess their suitability for use in modern construction. One such construction material is soil, or more specifically *subsoil*, which is defined as soil without any organic material present. For simplicity throughout this thesis, any references to soil actually refer to subsoil.

Soil has been used for construction around the world for thousands of years; the oldest surviving buildings are over 8,000 years old (Jaquin et al., 2008a). While in antiquity it was generally used due to low material cost and availability of cheap labour, earthen construction has decreased in popularity over the centuries for a number of reasons, including the rising cost of labour and the availability of more advanced construction methods and materials. However, with the revival of more sustainable approaches to construction, soil (also known as 'earth' in some literature) is receiving more interest as an environmentally-friendly alternative to some modern construction methods.

2.1 An introduction to soil-based construction

Many modern earthen construction methods are still largely the same methods that have been used for millennia around the world, although adaptations have been made to some methods now that more modern equipment is available. While some of the main soil-based construction methods are very different, they all use soil as the primary ingredient. Soil-based construction takes many forms, which can be broadly split into three categories according to construction technique: compacted earth, moulded earth and formed earth.

- **Compacted earth** construction techniques use high static or vibration forces to compact the soil and reduce the volume and void space, hence increasing density and strength. Examples of compacted earth techniques include compressed earth blocks and rammed earth (also known as pisé). Compressed earth blocks are made by compressing soil in a mould, usually with a hydraulic or manual press applying a static load. Rammed earth is constructed by dynamically compacting soil between two faces of a metal or wooden formwork, usually using either a manual or pneumatic tamper.

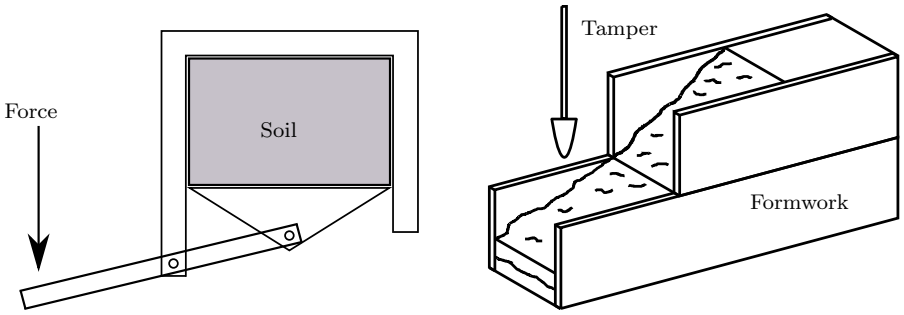

(a) Compressed earth block. (b) Rammed earth.

Figure 2.1: Schematic diagrams of compacted earth construction techniques.

- **Moulded earth** construction techniques involves the moulding of earth bricks which are usually dried before use in construction. Examples of moulded earth techniques include extruded earth blocks and adobe. Extruded earth blocks are typically made using an hydraulic extruder, from which the desired block length can be cut. Adobe is one of the earliest earthen construction techniques, and is made by shaping soil, typically with a high clay and water content and often with straw mixed through it, into bricks either manually or using a mould (Figure 2.2b) and left to dry in the sun.

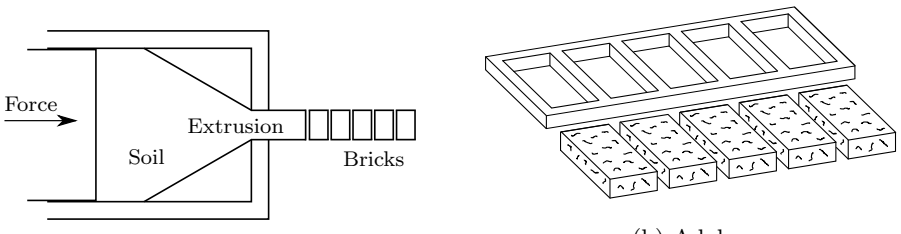

(a) Extruded earth block. (b) Adobe.

Figure 2.2: Schematic diagrams of moulded earth construction techniques.

- **Formed earth** construction techniques typically involve manually forming the earth structure by moulding it into shape in-situ. Examples of formed earth techniques include cob and daubed earth. Cob is made by stacking balls of earth mixed with straw and then compacted by people hitting and

walking on it, in order to form a solid wall. Daubed earth is constructed by applying a clay-rich soil to the external surfaces of a latticed framework made of wood and vegetable matter. This latter method is commonly known as 'wattle and daub.'

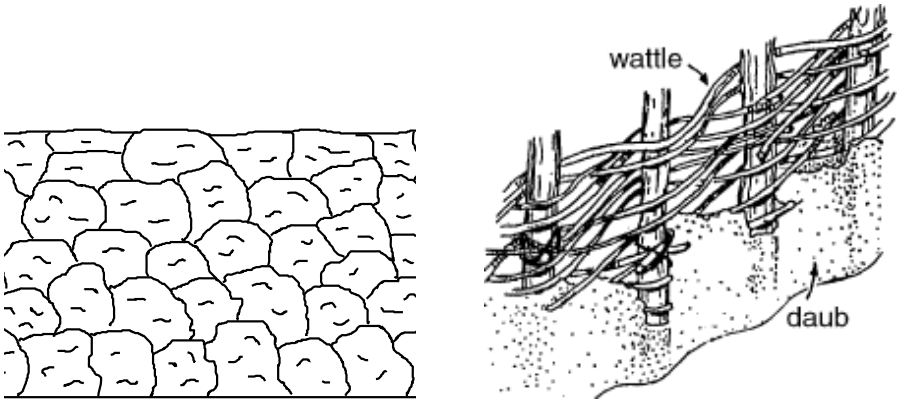

(a) Cob. (b) Daubed earth, from Harris (1975).

Figure 2.3: Schematic diagrams of formed earth construction techniques.

The majority of soil-based construction methods described above may be referred to both as construction *materials* and as construction *methods*. It is the *material* that is of primary interest in this thesis, which is referred to in some literature as a soil-based construction material (SBCM), and it is this acronym that will be used in this thesis to refer to all materials that use soil as the primary ingredient, such as those detailed above.

The majority of earthen structures are constructed such that the walls are load-bearing, but daubed earth relies on a supporting framework. Compacted earth construction uses a temporary formwork to create the structure, which is then removed soon after construction, while a moulded earth construction is built up in stages using the constructed blocks, similar in procedure to a contemporary brick-built structure. Experiments presented in this thesis were primarily performed to investigate rammed earth (RE), a compacted earth construction technique, although as compacted earth and moulded earth construction share many mechanical and load-bearing properties, this research may also be applicable, at least in part, to other SBCMs such as compressed earth blocks or adobe.

SBCMs have a number of advantages over more traditional brick and concrete constructions. For example, SBCMs typically use the soil from the construction site, unless the particular properties of the local material should be found to be unsuitable for construction. This drives down material cost and lowers CO_2 emissions from material transport. Buildings made of soil are also known to have good thermal properties as soil has a very high buffering capacity, which results in a more stable environment within an earthen structure (Walker et al., 2005). This makes it a particularly good building material in hot countries as it stores heat during the hottest part of the day and releases heat in the evenings.

However, SBCMs also have a number of drawbacks, particularly when compared to fired brick and concrete. SBCMs are labour intensive, which can cause construction to be impractical in areas where labour is expensive. Many also require complex construction methods and specific construction moulds or formworks, such as RE (Houben and Guillaud, 1994). Moreover, they are generally perceived to be not as durable and of lesser quality in comparison to bricks and concrete, particularly when exposed to rainwater. As a result, in the UK, SBCMs are currently generally used only for small structures by private individuals and environmentally conscious companies.

SBCMs can be modified in order to improve material properties such as compressive strength or durability. This is typically achieved through the addition of stabilisers, and such soil mixes are referred to as *stabilised* soils. Soil mixes without stabilisation are known as *unstabilised* (Hall et al., 2012). An unstabilised SBCM is created from a pure soil mix without any additives, either taken from the soil on a construction site, or manufactured from different components to form an artificial soil with similar properties to a 'natural' soil. A stabilised SBCM is created from a soil mix similar to that used in unstabilised SBCMs but with one or more additives designed to alter the behaviour or properties of the material. Stabilised SBCMs can further be subdivided into chemically stabilised (generally referred to simply as 'stabilised') and mechanically stabilised (generally referred to as 'reinforced'). Chemically stabilised soils typically contain cement or lime, although other additives such as asphalt are occasionally used (Houben and Guillaud, 1994). The chemical stabilisation acts as a binder to enhance the strength of the material or to improve other properties such as water imperviousness, durability or ductility. Mechanically stabilised (reinforced) soils usually contain discrete physical objects which bind the material together, such as natural or artificial fibres (Hall et al., 2012). Two commonly used materials are straw (e.g. Lenci et al., 2012) and plastic (e.g. Binici et al., 2007), and these and other materials used are discussed in greater detail in Section 2.3.2.

2.1.1 Existing research

The renewal of interest in sustainable construction techniques over the past decade or so has triggered global interest in SBCMs (also referred to in literature as 'compacted unsaturated soil' or 'earthen construction') and research has been performed in countries around the world including Canada (e.g. Rampino et al., 2000), Australia (e.g. Ciancio and Gibbings, 2012), Spain (e.g. Sánchez et al., 2012), Saudi Arabia (e.g. Al Shayea, 2001) and France (e.g. Nowamooz and Chazallon, 2011). Some construction standards and advisory documents have been published in some countries including the USA, Australia, India, New Zealand, Brazil, Kyrgystan, Nigeria and Zimbabwe (Schroeder, 2012). These guides were published to advise on structural design and construction using RE and other earthen construction techniques, however many of these guides are now out of date either due to the research that has been

performed since the guides were published, over 20 years ago in some countries, or due to increased awareness of the fallibility of some recommended tests. For example, Smith and Augarde (2013) reports on an investigation into the viability of the drop test, a traditional, widely-used and generally recommended method of obtaining the optimum water content of a soil. The results of the test varied hugely depending on several factors, primarily on the experience of the test operator, and also noted that different guides call for different procedures, thereby calling the validity and universality of the test into question.

While a limited amount of research has been performed tracking historical construction (Jaquin et al., 2008a), undertaking archaeological studies of historic earthen construction (Sánchez et al., 2012) and providing recommendations for building conservation (Jaquin and Augarde, 2012), more research has been performed into unstabilised SBCMs, in order to improve understanding of how the material works and to develop ways to enhance some material properties without sacrificing others.

Research has highlighted that while some basic mechanisms of building with SBCMs are thought to have been established, it is still not a completely understood material and more investigations need to be performed in order to further our understanding of the material. Research is continuing into how to improve strength and other mechanical characteristics of the material, as well as into the development of new computational and analytical tools to help us understand both the macrostructural (i.e. relating to the material as a whole, treating it as a part of a structure) and the microstructural processes (i.e. relating to the microscopic properties of the material, that is the relationships and interactions between the different soil particles) behind its structural behaviour. Only by further experimentation and analysis will the materials, methods and structural processes have a chance of being fully understood.

Hall and Djerbib (2004b) performed a scientifically thorough and detailed investigation into the compressive strength of rammed earth, by testing a series of rammed earth cubes to investigate how particle size distribution affects the compressive strength and density of the sample. It was found that using blended graded quarry materials is not only a suitable substitute for 'natural' soil when constructing rammed earth samples, but it also had a number of advantages over using 'natural' soil for experimental work. Using purchased quarry-grade materials and manufacturing the soil in the lab enables greater control of variables such as water content and particle size distribution. A manufactured soil also has less variability between different mixes, and thus creating an 'artificial' soil mix has become normal procedure in scientific investigations into RE where it is important to minimise natural soil variation. A manufactured soil also enables other researchers to create a near-identical soil for the purposes of building upon established research without the requirement of access to the particular area from which the 'natural' soil was taken. Additionally, Hall and Djerbib (2004b) proposed a production method for creating very similar and uniform rammed earth cubes that could be used for determining compressive strength, a crucial measure of the suitability of soil mix for earthen construction. As in concrete research

and manufacture, unconfined compressive strength (UCS) is used in earthen construction as a universal test for an initial indicator of soil and/or stabiliser suitability, determined either through the unconfined compressive testing of cube samples (Schroeder, 2011), prismatic samples (Maniatidis and Walker, 2008) or cylindrical samples (Ciancio and Gibbings, 2012).

2.2 Unstabilised SBCMs

A soil mix is typically composed of a combination of different sized materials - termed gravel, sand, silt and clay according to size - with spaces between them known as *pores*. When the pores are full of air, the soil is termed *dry*, while if the pores are full of water the soil is termed *saturated*. It is when the pores contain a mixture of air and water that the soil is termed *unsaturated*, and it is unsaturated soils that are required for the majority of earthen construction methods.

2.2.1 Existing research

Unsaturated soils are used for earthen construction because saturated or dry soils are unable to form solid structures, and because unsaturated soils are compressible into a denser, stronger form. One of the most critical areas of research in unstabilised SBCMs is understanding the underlying behaviours of the material and to discover what the greatest factors that affect the material strength are, such as construction method (e.g. compactive effort), construction materials (e.g. particle size distribution) or material properties (e.g. optimum water content). The experiments reported in Hall and Djerbib (2004b) found that the compressive strength of the material after compaction is not related to the dry density of the soil at a given compactive effort, which suggested that more complex material properties are present in RE than perhaps were initially predicted. The compressive strength was also found to vary with the particle size distribution, finding that the percentage of clay in the soil has the greatest effect on the compressive strength of rammed earth, with a 30% clay content producing cubes with consistently high compressive strength values compared to soils with 10% or 20% clay. However, it is likely that it is the size of the pores between the particles, rather than the size of the particles themselves, that causes the increase in strength, due to suction within the soil being the cause of the material's strength as discussed in Section 2.2.2.

Substantial research into unstabilised SBCMs has focussed on the effects of water before, during and after construction as it is of crucial importance to the development of material strength. Such investigations include determining the optimum water content of the soil, defining the processes of suction (Rampino et al., 2000; Beckett et al., 2015b), analysing the effect of moisture ingress (Hall and Djerbib, 2004a) and studying rate of erosion (da Silva et al., 2012). Research has not been limited to the role of

water, however, as research has been undertaken to understand the detailed structure of SBCMs using x-ray computed tomography (XRCT) (Beckett et al., 2013; Smith et al., 2014), as well as research into shrinkage (Ciancio et al., 2013), thermal properties (Ciancio, 2011; Taylor et al., 2012), tensile strength (Lenci et al., 2009; Bui et al., 2014b; Beckett et al., 2015b) and into the application of different loading conditions such as dynamic loads (Bui et al., 2011). Furthermore, computational modelling of RE has been attempted using finite element analysis (Nowamooz and Chazallon, 2011) and the strut-and-tie model (Ciancio and Robinson, 2010), although the variability between different earthen materials creates various challenges that need to be addressed before modelling of SBCMs can be relied upon to produce consistently accurate results.

2.2.2 The role of water in SBCMs

Water is crucial within the construction of SBCMs for two reasons. Firstly, it contributes to the level of compaction during construction: For example, compacting a sample at optimum water content will result in a higher density than the same soil compacted at higher or lower than optimum (Hall and Djerbib, 2004b), assuming that all other factors (such as compactive effort and method) remain constant. Secondly, water mobilises the internal friction between the soil particles after construction through suction between soil particles (Gerard et al., 2015).

Suction is known to be the main cause of cohesion between particles in an unsaturated soil, and has likewise been found to be the main cause of cohesive strength in unstabilised SBCMs (Jaquin et al., 2008b). Suction in unsaturated soils consists of two different components: *matric* and *osmotic* suction (Krahn and Fredlund, 1972). While matric suction results from the air/water relationship in the unsaturated soil pores, osmotic suction is the 'chemical potential energy difference between the soil water and the pure water' (Jaquin, 2008), which results from the change in the chemistry of the water when mixed into the soil. Matric suction is composed of two different parts: capillary and adsorptive suctions (Tuller et al., 1999), which, together with osmotic suction, combine to make the *total suction* Ψ (Gens, 2010).

$$\Psi = (C + A) + \pi \tag{2.1}$$

where C is the capillary suction, A is the adsorptive suction and π is osmotic suction. The matric suction is also calculated as the difference between the water pressure (u_w) and the air pressure (u_a) within the soil pores.

The layer of adsorbed water surrounding the soil particles is reported to contain very high levels of suction as a result of the chemical bonding between the water and the particles (Jaquin, 2008). Capillary suction, however, is derived from water surface tension of the menisci between soil particles (Lourenco

et al., 2008) and is much weaker when the soil has a high water content. As the soil dries, shrinkage of the menisci increases the negative pore water pressure in the menisci between the soil particles (Augarde, 2012; Jaquin et al., 2009), increasing the water surface tension and hence the capillary suction and, subsequently, the total suction Ψ in the soil. It is currently unknown to what extent the different suctions contribute to the strength of unstabilised SBCMs. While matric suction is assumed to be the main cause of strength within unstabilised RE, osmotic suction has not been studied within a SBCM context to the author's knowledge. Additionally, it is not known exactly how the capillary and adsorptive suctions contribute to the matric suction component of Ψ at different water contents. It was reported in Jaquin (2008) that the matric suction measured in very dry RE samples using a tensiometer are too high for capillary suction alone (above 1500kPa), suggesting that adsorptive suction provides a considerable portion of the matric suction, although this has yet to be confirmed. Hereafter, unless specified otherwise, the term *suction* refers to the *total suction* Ψ.

Figure 2.4 shows heavily simplified arrangements of an unsaturated soil. It is noted that, in practice, the soil particles would not be spherical. Additionally, there is inherent fallibility in portraying complex three-dimensional soil-pore arrangements in a two-dimensional framework, however the approximation made for both of these issues is sufficiently accurate to enable comment. Figure 2.4a shows a soil sample near saturation, with a high proportion of water to air present in the sample. The sample is not fully saturated, as evident from the presence of a solitary air pocket in the centre of the sketch. Moreover, as the air : water ratio is low, the pore water pressure is only slightly negative, resulting in a low amount of matric suction. Drying the sample shrinks the amount of water present such that the soil might look similar to that shown in Figure 2.4b. The removal of water from the menisci creates a high air : water ratio and a highly negative pore water pressure between particles. This creates a strong suction pulling the particles together, increasing the bond strength and hence the overall strength of the material.

It has been established that the strength of unstabilised SBCMs, such as rammed earth, primarily results from suction bonding between particles due to a highly negative pore water pressure, which is the result of a decrease in percentage water content in the sample. It therefore follows that an increase in percentage water content after construction would reduce the negativity of the pore water pressure, therefore reducing suction and hence, strength. This effect can be seen in Bahar et al. (2004), after samples were soaked in water for 48 hours. Heath et al. (2009) shows that this large drop in strength is not seen after large increases in relative humidity (such as that exhibited within a shower room), but only after submersion, and reported that a high relative humidity did not produce significant reductions in compressive strength. Bui et al. (2009) presents results from a 20-year experiment which left rammed earth walls exposed to the natural environment (e.g. wind, rain, sun), albeit with a covering on the top surface to prevent vertical water ingress. The walls were analysed using stereo-photogrammetry, whereby

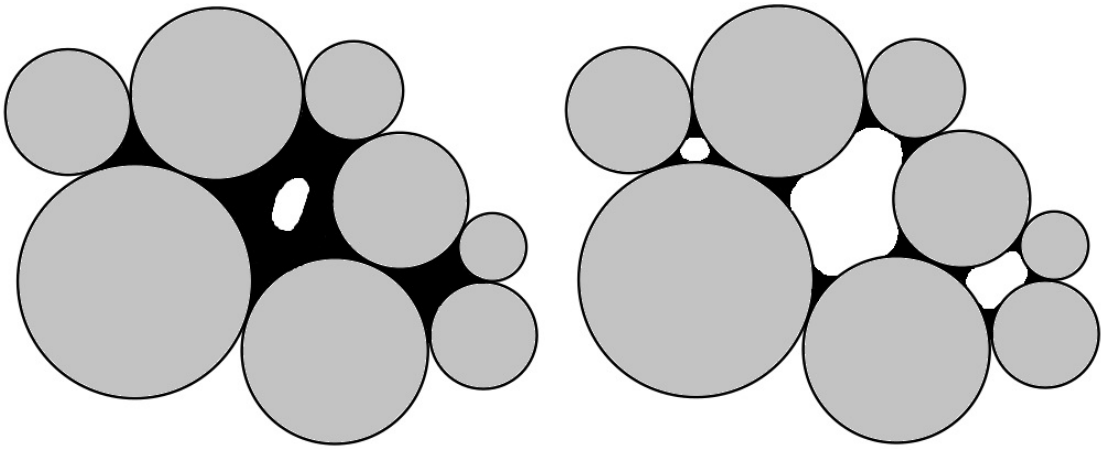

(a) Sketch of idealised soil with high water content and low pore water pressure.

(b) Sketch of idealised soil with low water content and high pore water pressure.

Figure 2.4: Idealised sketch of soil particles, water and air arrangement in an unsaturated soil at high and at low water contents. For simplicity and demonstration of the ideas presented, menisci that would border the outside of the sketch are not shown, and clay particles are shown as spheres opposed to plates, inspired by the images in Lourenço et al. (2012).

two photos are taken from different locations and later combined to create a 3D image. Results showed that erosion from regular weather was small and a design life of 62.5 years before the walls tested would show a 5% thickness reduction due to erosion was extrapolated. It may therefore be concluded that humidity does not greatly contribute to the weakening of SBCMs, however submersions within water, such as during a flood, will cause catastrophic failure of unstabilised SBCMs. Whilst suction must be mentioned when discussing the strength development of unstabilised RE, it must be acknowledged that suction in the material is very difficult to measure accurately. Tensiometers, such as those developed by Lourenço et al. (2006), are very good at measuring in-situ suctions up to around 2MPa. However, as suction within RE is known to be in the 100s of MPa (Jaquin et al., 2008b), the filter paper test is more appropriate for suctions around these values (Bui et al., 2014a). However, this test cannot be performed on in-situ material as it requires specially-made samples. This means that the suction within a particular sample of RE, for example, is very difficult to accurately determine.

As water is therefore crucial to the strength of SBCMs, methods must be developed to improve the properties of the soil such that suction bonds may be adequately formed and maintained. Compacting a soil sample at its optimum water content, which is the water content at which the dry density of the sample is at its maximum, is considered to the most reliable method of maximising the material shear strength (Jaquin and Augarde, 2012) although it is known that there is a complex relationship between optimum water content and suction (Heath et al., 2004). A material compacted to a higher density will have smaller voids between particles which will then enable more, stronger menisci to form, increasing the material strength. Determining the optimum water content of the material is therefore crucial as a

samples compacted at a water content different to optimum will not compact to the same volume and hence will not be as dense and therefore not as strong as samples compacted at optimum water content, assuming that the compactive effort remains constant.

2.2.3 The role of clay in SBCMs

As the primary construction material of most SBCMs is soil, it is from soil mechanics that many procedures, analyses and symbols are used. In traditional soil mechanics, 'clay' can refer to one of two types of particle. Firstly, it can refer to particles less than 2μm in diameter (i.e. a limestone, ground into a very fine powder may, on occasion be called 'clay' within traditional soil mechanics), or secondly and more specifically, it can refer to an aluminosilicate mineral (composed of aluminium, silicon and oxygen) which has a high plasticity when mixed with water and a net negative electrical charge. It is the latter type of particle to which all future references to 'clay' in this thesis relate.

The majority of clays are made up of different combinations of *sheets* of silica and gibbsite. The silica sheet consists of a tetrahedral arrangement of oxygen atoms bonded with a silicon atom, and combined such that 3 of the four oxygen atoms are shared between the surrounding tetrahedra as diagramatically represented in Figure 2.5a. Gibbsite sheets consist of octahedral arrangements of oxygen or hydroxyl atoms around cations of Al^{3+} (gibbsite). A diagrammatic representation of gibbsite is shown in Figure 2.5b.

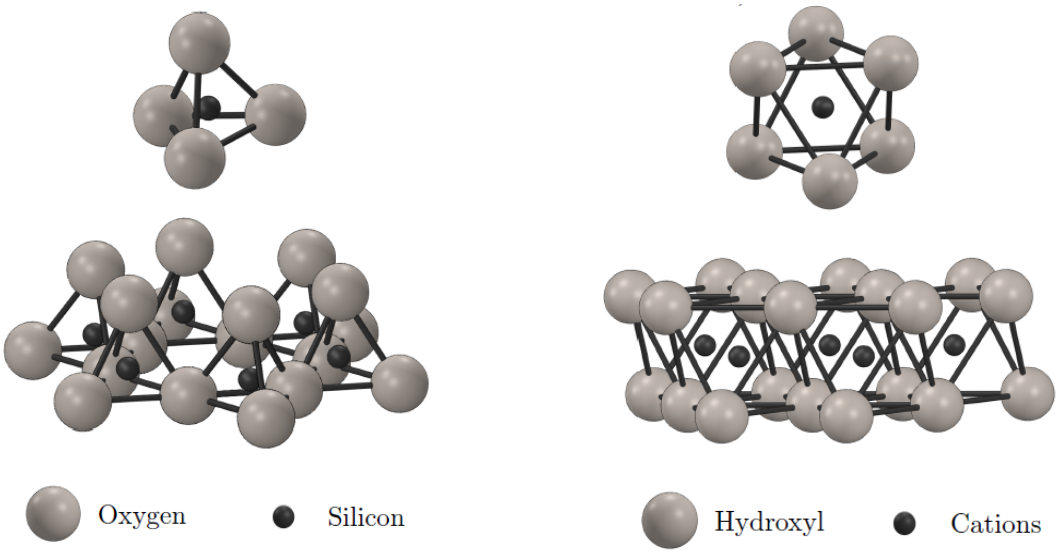

(a) Silica. (b) Gibbsite.

Figure 2.5: Diagrammatic representations of silica and gibbsite, in *particle* (top) and *sheet* (bottom) form, adapted with permission from Smith (2015).

A *layer* of clay is made up of clay sheets bonded using different methods depending on the type of clay (Bailey, 1971). The most common clay mineral groups are kaolinite, illite and montmorillonite.

Kaolinite

Kaolinite has the simplest structure of the clays, consisting of a sheet of silica attached to a sheet of gibbsite (Figure 2.6a). It is the least reactive clay, that is, it is the clay which has the smallest amount of swelling upon contact with water, as it has few exchangeable cations in its structure, and has strong inter-layer bonds. Kaolin particles are between 0.1 - 4 μm by 0.05 - 2 μm in size, and are the largest of the clays (Powrie, 2013).

Illite

Illite has a three-sheet structure, composed of a sheet of gibbsite between 2 sheets of silica (Figure 2.6b). The layers are separated by potassium ions resulting from its formation process. Illite particles range from 0.1 μm to a few micrometres in length, although they may be as small as 3 nm thick (Powrie, 2013).

Montmorillonite

Montmorillonite (also called Smectite) is a three-sheet structure, composed of a sheet of gibbsite with a sheet of silica on either side, in the same configuration as Illite (Figure 2.6c). In montmorillonite, however, the layers are separated by cations such as Sodium or Calcium, which result in weak inter-layer bonds (Powrie, 2013). These weak bonds allow the soil to expand when in contact with water, leading to soils containing montmorillonite being referred to as *expansive soils*. Montmorillonites are among the smallest of the clay particles, in part due to the weak inter-layer forces, and are generally 1 - 2 μm in length. For a more detailed explanation of the mineralogy of these and other clays, the reader is referred to Grim (1962), Craig (2004) and Powrie (2013).

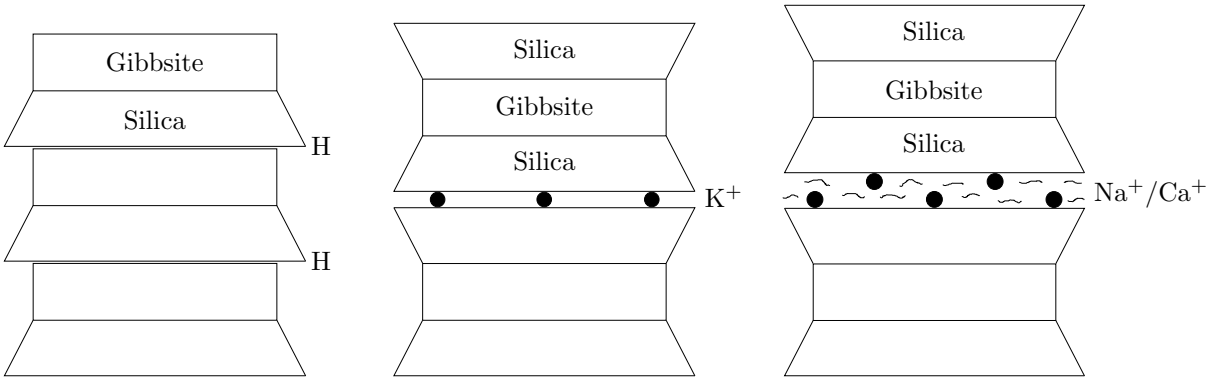

(a) Kaolinite. (b) Illite. (c) Montmorillonite.

Figure 2.6: Sketches of the three most common types of clay.

Clay is known to play a major role within the strength and integrity of SBCM as it contributes to and enhances the inter-particle bonding in two distinct ways. Firstly, some clay particles (e.g. Illite and Montmorrillonite) are able to hold an electrostatic charge due to the free ions within the particles creating an attractive force between particles (Grim, 1962). This charge enables the clay particles to adhere to each other, providing a small source of soil strength. Secondly, and arguably more importantly, the clay coats the individual particles of silt, sand and gravel (Jaquin and Augarde, 2012), and, upon contact with water, are known to fill the menisci bridges between particles, creating a so-called *clay bridge* (Gelard et al., 2007). These clay bridges enhance the strength of the soil as they allow a smaller change in water content to create a larger change in pore water pressure, and hence, suction.

It is generally recommended that SBCMs use kaolinite clay-bearing soils over illite and montomorrillonite as the expansive nature of illite and montmorrillonite increase the likelihood of undesirable shrinkage cracks appearing in the material, which would indicate weaknesses in the structure, particularly if subsequently exposed to water.

2.3 Stabilised SBCMs

Stabilisers are commonly added to RE and other SBCMs to affect the material behaviour (Hall et al., 2012), as has been done for thousands of years. As previously mentioned in Section 2.1, stabilisers generally fall into two different categories: chemical (*stabilised*) or physical (*reinforced*). Chemical stabilisers use chemical reactions to strengthen the soil matrix between individual soil particles, while physical stabilisers create links across larger areas of soil, binding large clumps together.

2.3.1 Chemical stabilisation

Chemical stabilisers use chemical reactions to bond particles together. Such reactions are generally irreversible and, if the stabiliser is mixed effectively into the soil, produce very strong particle bonds with the material. Chemical stabilisation generally creates samples with a higher UCS, better resistance to water ingress and improved durability. However, as SBCMs are generally very environmentally friendly construction methods, it is therefore often perceived to be undesirable to add chemical stabilisers to the soil mix as the material then loses its environmental credentials. However, it is recognised that chemically stabilising an SBCM can reduce construction and maintenance costs while improving the material's mechanical and potentially environmental performance, as it can also end up using less material than a regular unstabilised structure, therefore reducing its environmental footprint. However, the author has only been able to find anecdotal evidence to support this.

While lime was the chemical stabiliser of choice in antiquity until the development of Portland cement

in the early 19th century (Houben and Guillaud, 1994), cement is currently the recommended chemical stabiliser in the majority of construction books and guides for SBCMs (Brink and Rush, 1966; Walker et al., 2005; Easton, 2007) and is by far the most commonly used chemical stabiliser in earthen construction, with the use of *quicklime* and *lime* a distant second (Danso et al., 2015). Other materials such as asphalt (Burroughs, 2006), gypsum (Binici et al., 2007), alabaster (Serrano et al., 2012) and fly ash (Cristelo et al., 2012) have been used in some investigations, although they have yet to gain much momentum despite some advantages that some of these materials have over cement. Fly ash, in particular, is a good alternative to cement as it is a waste product from the burning of coal, and as such is much less resource-intensive to obtain than cement, therefore making it more environmentally friendly. However, pulverised fly ash, or PFA, needs activation through chemical activation (using sodium silicate) or mechanical activation (by heating to a known temperature) (Hela and Orsáková, 2013). It is already commonly used in concrete production as a substitute for portland cement, and as such could work well as a substitute in SBCMs.

Lime is produced by heating limestone or chalk to form *quicklime* (CaO), which becomes *slaked lime* ($Ca(OH)_2$) when combined with water. Once re-exposed to air, the *slaked lime* reacts with carbon dioxide (CO_2) in a process known as *carbonation* in order to form calcium carbonate ($CaCO_3$), more commonly known as limestone. Portland cement is traditionally a mixture of calcium monoxide (CaO) and silicon dioxide (SiO_2) in a ratio of at least two parts CaO to one part SiO_2, but it also often contains other materials such as gypsum or Aluminium Oxide (AL_2O_3) which affect its properties, such as rate of pozzolanic reaction or workability.

Stabilisation and clay

It was previously mentioned (Section 2.2.3) that SBCMs use kaolinite clay-bearing soils over illite or montomorrillonite clay soils due to the expansive nature of illite and montmorrillonite. This recommendation is also generally extended to chemically stabilised SBCMs, although for an alternative reason. Different clays are known to react to chemical stabilisers in different ways, depending on the stabiliser used. Sherwood (1993) reports on the behaviour of clays when mixed with cement or lime and, while the research was focused toward application within road pavement construction, the basic theory is very similar and may therefore be applied to SBCMs. It was reported that cement is generally better for stabilising soils than lime as it produces a stronger resultant product, however it is conceded that lime is useful when cement is not appropriate, such as for very wet soils, or soils that contain high amounts of montmorrillonite. Lees et al. (1982) recommends that such soils are stabilised with lime rather than cement as the soils react more favourably due to the chemistry of the montmorrillonite clay.

Both cement and lime, when brought into contact with water, use a pozzolanic reaction to create

a cementitous matrix structure. This is widely known to happen over a long period of time (around 28 days or longer) which gradually strengthens the material. Lime-stabilised soils, however, also have the potential for a more instantaneous reaction, as the aluminosilicates within the clay portion of the soil partially dissolve in the high pH of the lime, which in turn hastens cation exchange which turns sodium (Na) and hydrogen (H) particles into calcium (Ca). This also reduces the plasticity of the soil by flocculation of the clay particles (Sherwood, 1993). Therefore, soils with a high cation exchange capacity, such as soils which contain montmorrillonite clay, should be stabilised with lime as it will produce a more beneficial response, both in the short- and long-term. It is also recommended in Sherwood (1993) that, as the plasticity of the soil is heavily affected by the lime stabiliser, the plasticity index may be used to determine whether a lime or cement stabilisation may be more appropriate. Sherwood (1993) suggests that a soil with a plasticity index (PI) of below 10% is stabilised with cement and a soil with a PI of above 25% is stabilised with lime.

It has been established why different clays react to different stabilisers, however it is unknown whether the particle size distribution also has a secondary effect on the effectiveness of soil stabilisation. To state this more clearly, it is unknown how two different soils, with the same particle size distribution, but one containing clay as the 'clay' fraction and one containing powdered rock as the 'clay' fraction, would react to different stabilisation materials and amounts; whether the soil with clay would produce a different behavioural response than the soil with powdered rock. It is suggested that cement stabilisation would have similar effects on both materials, however the lime might have different effects depending on the clay type as per the cation exchanges discussed above. It is also suggested that the powdered rock soil would behave very similarly to a kaolinite-clay soil as kaolinite is known to be non-reactive when mixed with lime or cement, as powdered rock is expected to be.

Stabilisation suitability

It is essential when using stabilisers that checks are made to ensure that the stabilisation is effective, specifically with regards to the amount of stabiliser used and the raw soil's properties. Unconfined compressive strength (UCS) is commonly used in concrete and unstabilised RE literature for this purpose, and it has subsequently been adopted for use in stabilised earthen construction investigations in order to determine the suitability of the chemically-stabilised soil mix for earthen construction. Burroughs (2008) proposes a universal acceptance system for the suitability of a soil for stabilisation, resulting from tests of 197 different samples with varying particle size distributions and cement/lime quantities. Burroughs (2008) presents a decision tree dependant on the measurement of linear shrinkage and plasticity index, from which a soil's suitability to stabilisation can be determined. The soil mix is classed as 'suitable' if the resulting cube strength of the stabilised sample is 2MPa or greater (tested under *dry* conditions,

typically when the samples have been air-dried for 14 or 28 days). While the methods were scientifically thorough, it has since been suspected that there are more factors that make a soil suitable or unsuitable to use than shrinkage and plasticity index, and alternative chemical or mechanical stabilisation materials may enable a soil to be suitable for stabilisation, or may result in a soil being unsuitable, contrary to the proposed classification method.

Ciancio et al. (2013) reports on a review of a greater variety of tests to determine properties including plasticity index, liquid limit, linear shrinkage and erosion index, all of which are recommended in different design guides to use for determining a soil's suitability for construction. It was concluded that many of the existing guidelines were contradictory, for example a test from one set of guidelines suggested that the soil is favourable for construction, whereas a different test from a different set of guidelines found the same soil unfavourable. Due to the conflicting tests, it was proposed that unconfined compressive strength (UCS) remains the primary test of a soil's suitability for construction as different soils with different optimum water contents, particle distributions, plasticity index and shrinkage properties may produce the same UCS and may subsequently be used successfully in earthen construction. Additionally, Ciancio et al. (2013) confirms that some raw soil properties, such as a high clay content, might make a soil unfavourable to stabilisation. Some more recent investigations into stabilised soils using soil mixes without clay have subsequently been performed for this reason (Beckett and Ciancio, 2014a; Beckett et al., 2015a).

Despite the potential effects of clay on the effectiveness of different stabilisation materials mentioned above, the majority of investigations into properties and behaviour of stabilised SBCMs are performed on cement-stabilised, clay-bearing soils. Such investigations typically use concrete-industry standard tests for evaluation and comparison. Investigations have been performed into compressive strength (Jayasinghe and Kamaladasa, 2007), axial loading of columns (Tripura and Singh, 2015), lateral loading of walls (Ciancio and Augarde, 2013), the effect of climate (Hall, 2007) and heat transfer (Beckett and Ciancio, 2014b), among other topics. As in unstabilised RE research, the effect of water before, during and after construction has been studied, including shrink-swelling cycles in lime stabilised RE (Du et al., 1999) and the erosion and water absorbtion of cement-stabilised RE (Kariyawasam and Jayasinghe, 2016).

One such paper, Ciancio and Augarde (2013), presents research into lateral loading on a cement stabilised rammed earth wall, and created and compared an elastic and an 'ultimate strength' computational model. The elastic model provided a 'better prediction of the experimental results than the ultimate strength analysis,' although the elastic method still calculated a difference of up to 20% between the analytical model and the experimental results. It was concluded that the analytical methods 'correctly estimate the capacity of the wall to resist lateral wind pressure' but only when subjected to strict laboratory conditions. Further investigation into fracture of rammed earth was recommended as

the results of the ultimate state analysis 'significantly' underestimated the capacity of the wall, indicating that the energy required to fracture the samples may have had a greater effect on the results than had initially been predicted (Ciancio and Augarde, 2013). It was subsequently recommended that an investigation into the fracture energy of RE would be beneficial to understanding the ultimate capacity of the material.

2.3.2 Mechanical stabilisation

Mechanical stabilisers use the addition of foreign materials to help bond particles together by contributing to and enhancing, rather than replacing, the strength of the natural suction bonding. Mechanical stabilisers, along with the soil material, may also in some cases be recovered and re-used if the structure is dismantled.

While steel rebar is ubiquitously used in concrete construction, it is only occasionally used with earthen construction as it provides very localised reinforcement which relies on effective bonding with the material immediately surrounding it in order to enhance the tensile strength of the material, something which is generally not an issue in concrete construction. Rammed earth relies on either suction or small amounts of cement (less than 10% by mass) for strength, however, and as such does not form as strong bonds with the steel rebar as concrete does. This behaviour has been observed in an unpublished undergraduate final year project (Corbin, 2012) during a series of three-point bending tests on a RE lintel reinforced with steel rebar. A simply supported, steel rebar-reinforced lintel was subjected to an increasing vertical displacement applied at the mid-span, and material was observed to fall from the underside of the sample, exposing the rebar long before the ultimate strength of the sample was reached. Lilley and Robinson (1995) and Ciancio and Robinson (2010) describe two of very few other investigations which added steel rebar to unstabilised and stabilised SBCMs. Lilley and Robinson (1995) details a test investigating the use of steel rebar in rammed earth lintels. No increase in ultimate load from the inclusion of steel reinforcement was found, although it was noted that the reinforcement did appear to limit damage in these cases to the area directly above the opening below the lintel, as opposed to a more widespread failure surrounding the lintel. Steel rebar is therefore typically advised against in earthen construction as it does not distribute forces evenly through the surrounding material as in concrete, acting instead only as a support for the material above it, and providing little strength improvement to the material below it. It is also advised against because it is very susceptible to corrosion in permeable materials such as RE, and as such would not be suitable for use in earthen construction.

It is therefore more common that fibrous reinforcement, distributed evenly throughout the construction material, is used to physically stabilise SBCMs, and such reinforcement can be divided into either 'natural' or 'synthetic' fibres. Examples of 'natural' fibres used and investigated in SBCMs include wool (Aymerich

et al., 2012; Readle et al., 2015), hemp (Aymerich et al., 2016; Dugdale, 1960), seaweed (Achenza and Fenu, 2006) and straw (Clementi et al., 2008; Quagliarini and Lenci, 2010; Schroeder, 2011; Serrano et al., 2012), while 'synthetic' fibres include plastic (Binici et al., 2005), nylon (Kumar and Tabor, 2003), fibreglass (Consoli et al., 1998) and steel fibre (Boominathan et al., 1991).

As SBCMs are often used for their environmental benefits, it is generally considered important that any fibrous reinforcement is obtained from a renewable source. Indeed, in some SBCMs, such as Adobe and Cob, it is traditional that straw, a highly renewable resource, is mixed into the soil to help to bind the material together, which is why it has received an uneven amount of attention in research compared to other viable fibrous reinforcements. However, there are other potential sources of suitable fibres, for example from manufacturing waste streams, which may be of even greater benefit both to the structural properties of the building but also to the environment, as otherwise the waste might proceed to landfill. Examples of such reinforcement include rubber (Serrano et al., 2012; Turgut and Yesilata, 2008), and polystyrene fibres (Binici et al., 2005).

2.4 An introduction to fracture energy

It has previously been discussed that SBCMs are often stabilised to increase the strength of the material, and that strength is assessed from a mechanical perspective. An alternative approach to studying the strength of materials is that of fracture mechanics, which is the study of the development and propagation of cracks in any material from an energy-based approach.

2.4.1 Development of classical fracture theory

Inglis (1913) proposed the first basic principles of classical fracture mechanics, and outlined an elastic solution for stresses at the tip of an ellipsoidal cavity in an infinite solid, based on experiments studying cracks in glass. It was found that as the short axis of the crack tends to zero (i.e. the 'crack' gets narrower), the stress at the vertex tends towards infinity. This infinite value is also known as the 'stress singularity' and is not possible outside a theoretical framework, therefore an alternative was needed. Griffith (1921) concluded that stress should not be used as a failure criterion as the stress at the crack tip in an *elastic* continuum is infinite irrespective of the size of the load. Instead, an *energy* failure criterion was proposed, which formed the foundation of classical linear elastic fracture mechanics (LEFM), which states that a crack will propagate if the energy required to extend a crack by a unit surface area equals or is exceeded by the energy available do so. This required energy was assumed to be equal to twice the specific surface energy of the elastic solid ($2\gamma_s$). The specific surface energy γ_s is the energy required to break the bonds in the material microstructure, creating a new unit area of surface.

The proposed approach in Griffith (1921), however, was based on a very simplified model of a crack, and hence did not take any account of any material properties such as roughness, tortuosity, microcracking, frictional slip or substantial plasticity. $2\gamma_s$ was soon replaced by the general crack growth resistance $\mathcal{R}$, which is constant in simple analyses and unique to each material.

Subsequent research did not continue until the 1940s, triggered in part by the unexpected failure of several metal structures, including the hulls of the U.S. Navy's 'Liberty' ships during WWII. Research around this time produced a general form of the work presented in Griffith (1921) and linked $\mathcal{G}$, the energy release rate, equal to the energy available to increase the length of a crack by a unit area, to the elastic stress and strain fields. Experimental work, however, was focussed on the determination of $\mathcal{R}$, as it was, and still is, one of the basic challenges in fracture mechanics (Bazant and Planas, 1998).

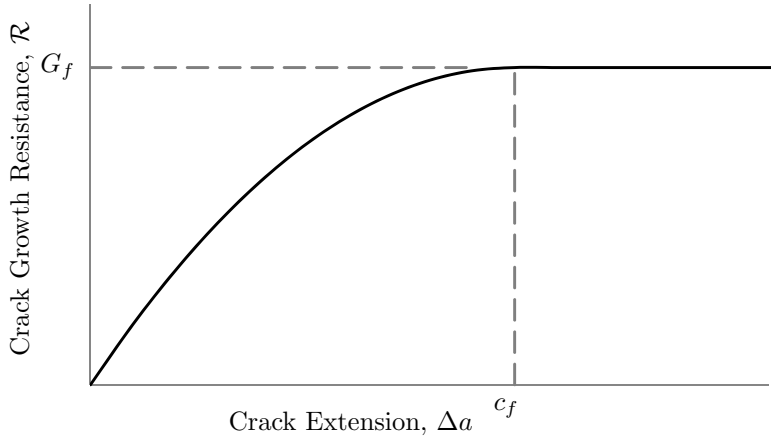

Figure 2.7: Typical $\mathcal{R}$-curve.

The primary way that $\mathcal{R}$ values are displayed is a via a $\mathcal{R} - \Delta a$ curve, more commonly known simply as the $\mathcal{R}$-curve, where Δa is the crack extension, as proposed in Irwin (1960). An example of such a curve is given in Figure 2.7. The figure shows that as the crack extends, the crack resistance increases up until a threshold G_f is reached. Further developed in Krafft et al. (1961), the $\mathcal{R} - \Delta a$ curve may also be expressed in a formulaic arrangement (Equation 2.2), where c_f is the value of the crack extension at which the $\mathcal{R}$-curve plateaus and the fracture energy of the material is the value of the resistance at the plateau. $R(\Delta a/c_f)$ is a dimensionless function.

$$\mathcal{R} = G_f R\left(\frac{\Delta a}{c_f}\right) \tag{2.2}$$

By definition, the energy required to produce a crack extension of length Δa is $\mathcal{R}\Delta a$. Therefore, fracture work $\mathcal{W}_F$ per unit thickness b may be calculated as

$$\frac{\mathcal{W}_F}{b} = \int_0^{\Delta a} R(\Delta a)\ \ d\Delta a \tag{2.3}$$

which equals the area under the curve in Figure 2.7.

However, determination of Δa is very difficult to obtain experimentally, due to the impracticality of taking measurements of the length of an extending crack. Such curves are now normally obtained through methods using LEFM computational modelling. Another major drawback of the $\mathcal{R}$-curve is that it is heavily dependent on and affected by the specimen size, shape and structure (Bazant and Planas, 1998).

The second major breakthrough in LEFM, presented in Irwin (1957), proposes the stress intensity factor $\mathcal{K}$ as a measure of the stresses close to the crack tip, and relates the stresses to the energy release rate $\mathcal{G}$. $\mathcal{K}$ has a large advantage over $\mathcal{G}$ as the stress intensity factors are additive, while $\mathcal{G}$ is not. However, $\mathcal{K}$ is also limited to linear elasticity, as opposed to the more general $\mathcal{G}$. The final major breakthroughs in the foundation of LEFM were presented in Rice (1967) and Rice (1968), which defined the J-integral, which links the energy release rate $\mathcal{G}$ to the stress and strain fields in any elastic material, linear or nonlinear, subsequently forming the basis of elastoplastic fracture analysis.

LEFM has continued to be used, developed and adapted as it is a very useful tool for analysing fracture in very brittle samples which have no plastic region, however it should not be used for materials which undergo substantial plastic deformation. In these cases, elastic plastic fracture mechanics (EPFM) should be used instead. LEFM is also known to overestimate the load-bearing capacity of typical structures, which lead to new models being proposed using non-linear fracture mechanics (NLFM) approaches (Rossi et al., 1991). Many different models were created using NLFM to analyse fracture in a non-brittle materials, two of which were the equivalent elastic crack model, also called the equivalent crack model, and the cohesive crack model. A brief outline and description of these two models are presented below. For a more in-depth discussion of these two models, and of many other models which use LEFM or NLFM, the reader is referred to Bazant and Planas (1998).

Equivalent crack model

The equivalent crack model (ECM) approximates the nonlinear zone in the material by decreasing the stiffness of that area such that it becomes equivalent to a crack extension. It is a similar approach to LEFM, however $\mathcal{R}$ varies according to the geometry of the sample, i.e. $\mathcal{R}$ reduces as the crack extends. It is crucial, therefore, that $\mathcal{R}$ is correctly determined in advance.

Jenq and Shah (1985) proposes one of the most complete ECMs, the *two parameter fracture model*, which enables the inclusion of nonlinear crack growth prior to peak load in the analysis, and which in turn led to test recommendations for the fracture characteristics of concrete. One consequence of this work was that it encountered the problem of size effect in concrete, which is the effect of the size of the sample with respect to the size of the largest particles of the material makeup. In practical terms, the scaled-up response of a small sample would be different to the response of a sample of the larger size, if the same

material was used in both samples. The variation would be due to the differing ratio of largest piece of constituent material (i.e. gravel in concrete) to sample size. A simple approximation for concrete was developed in Bazant (1984) and subsequently used as the basis for further determination for nonlinear fracture properties. The term 'size effect' also includes considerations such as boundary effects and is described in full detail in Bazant and Planas (1998).

Cohesive crack model

The cohesive crack model (CCM) was developed to simulate nonlinear material behaviour near the crack tip. First proposed in Barenblatt (1959) and extended a few years later (Barenblatt, 1962), the model aimed to relate crack growth resistance to the atomic binding energy, while also releasing the stress singularity which featured in Inglis (1913). In the model, the crack is assumed to extend and open, whilst transferring stress from one crack face to the other, simulating inter-atomic forces by introducing cohesive stresses onto the newly formed crack surfaces such that the stress singularity would disappear. It was postulated that the shape of the crack was independent of the specimen size and shape, and that the proposed cohesive forces were only applicable to a small area immediately adjacent to the crack tip. The pre-existing parameter of energy release rate, $\mathcal{G}$, also known as external work, was balanced with the proposed cohesive forces, equal by definition to $2\gamma_s$, thereby linking to the initial solution reported in Inglis (1913).

Dugdale (1960) further developed the CCM by taking a different approach and modelling macroscopic plasticity as opposed to microscopic atomic interactions, while still removing the stress singularity. Although it was heavily simplified and did not actually model fracture itself but instead extended the plastic zone infinitely, this approach set the ground for several new models, one of the most significant within analysis of quasi-brittle materials such as RE and concrete being the fictitious crack model.

Fictitious crack model

The fictitious crack model for concrete was the first major model to allow fracture mechanics analysis to be performed without the requirement for a pre-existing crack, although it is identical to the cohesive crack model if a pre-existing crack is modelled. It is able to link the classical strength-based crack initiation to a more appropriate energy-based crack extension and describes the complete process from crack initiation to sample failure. Proposed in Hillerborg et al. (1976), it considers the tensile strength f_t, specific fracture energy G_F and the tensile softening diagram of the material. The tensile softening diagram of a material is a graphical representation of the decrease in stress under increasing deformation, typically plotted on a normal stress (σ) - strain (ϵ) plot, although normal stress (σ) - displacement (δ) plots may also be used. Two different softening curves were proposed by Hillerborg et al. and are shown

in Figures 2.8a and 2.8b. Figure 2.8c shows the general curve now developed which can be applied to any material. Each plot in Figure 2.8 is a stress (σ) - displacement (δ) curve, where f_t is the flexural tensile strength, which is the stress at failure under bending loading conditions.

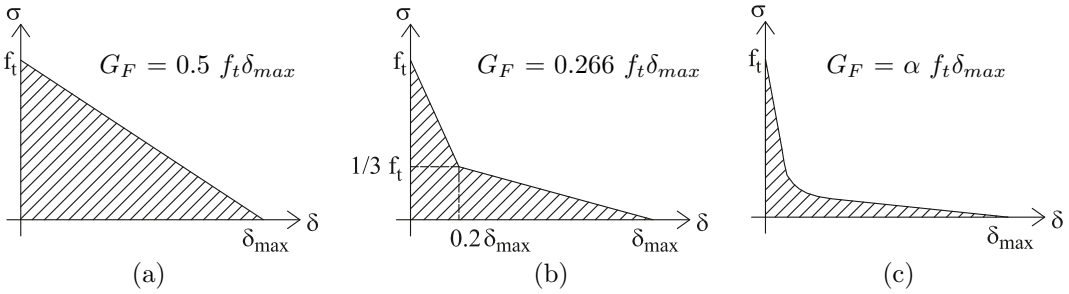

Figure 2.8: Tensile softening curves for cohesive crack models as presented in Ciancio and Augarde (2013).

α (Figure 2.8c) is a material variable, equal to approximately 0.15 within concrete and assumed to be similar for RE (Ciancio and Augarde, 2013). Using any of the softening curves, the cohesive fracture energy G_F can be determined by calculated the area under the softening curve. Determination of G_F using this method, however, is reliant on the calculation of the softening curve parameters from an accurate computational model, so a more direct way of measuring G_F was required. Hillerborg (1985) proposed an alternative to an analytical method by using an experimental method to directly determine G_F, which is now known as the three point bending test. This test involves resting a cuboidal sample on two supports and applying a vertical displacement at mid-span, taking measurements to calculate responses and calculate the fracture energy by calculating the work applied to the sample. Once calculated, G_F may be divided by the crack length in order to obtain G_f, the specific fracture energy, which is equivalent to to $\mathcal{W}_F/b$ from Equation 2.3. This test is discussed in greater detail in Chapter 4, alongside discussions of the advantages and disadvantages of this approach.

The study of fracture mechanics is a massive area of research, and as such there are many different notations for very similar or identical parameters which are no longer in use (for example G_c, used in Petersson (1980), is equivalent to G_f but is no longer in common usage). There are also different symbols for fracture energy that relate to its calculation under a specific set of circumstances that were not relevant for investigation at this time. One such example is that of G_R, which is the fracture energy calculated when it is dependent on historical motion of the crack (Bazant and Planas, 1998).

2.4.2 Current fracture theory

Current fracture mechanics theory (Bazant and Planas, 1998) is primarily based on two assumptions:

- Failure occurs in a material when the input energy exceeds the material capacity.

- After fracture, any excess energy is transferred to another part of the material through the internal material structure.

Widely accepted current theory about cracking in any material states that when a cracked plate undergoes local displacement, the area around the crack tip undergoes elastic deformation. Once the stress in this area reaches the yield stress of the material, plastic deformation begins. When the plastic limit of the material is reached in an area, generally adjacent to the existing crack, the material fails in that location and the crack is extended. Excess energy is then transferred to a new area which experiences elastic deformation, and so the pattern repeats, extending the crack until force equilibrium is reached. This process directly implies that the greater the yield strength and ultimate capacity of the material, the greater the maximum stress that can be sustained by the material and the greater the crack resistance. It follows that a brittle material, which has a very small or negligible plastic region, will undergo little physical deformation and so will fail swiftly and dramatically. A material with a large elastic and plastic regions, however, will physically deform and provide visible warning of imminent failure. Different existing models and analyses consider different shapes and sizes of the plastic zone at the crack tip in order to calculate material capacity, ranging from spherical models to the Tresca or Von Mises criterion zones (Broek, 1974).

2.4.3 Fracture of SBCMs

Fracture of soils has been studied for number of years, while fracture of SBCMs is a very recent research area. As fracture in both materials is similar, it is difficult to distinguish in literature where the research in SBCMs began. Among the first to bridge the gap between regular soil mechanics and SBCMs is the work reported in Lenci et al. (2012) and Aymerich et al. (2012). The majority of investigations performed to date use the three point bending test as proposed in Hillerborg (1985), but subsequent analyses substantially differ. Aymerich et al. (2012), for example, presents results in joules of absorbed energy specific to the samples tested, while Lenci et al. (2012), for example, followed traditional fracture mechanics theory to determine the $\mathcal{R}$-curve of the samples using the *two parameter model* as proposed in Jenq and Shah (1985). In order to perform this analysis, however, it was assumed that the material was very brittle, thereby allowing LEFM analysis to be performed. While this is a reasonable assumption in unstabilised earthen construction and soils (e.g. Wang et al., 2007), there is strong evidence that this is not the case in fibre-reinforced earthen construction and soils, as shown in Aymerich et al. (2012, 2016). Conversely, Parisi et al. (2014) reports on clear evidence of brittle behaviour in a compacted 'silty soil', suggesting that the brittle behaviour of earthen construction varies according to the properties of the soil and the type of fibrous reinforcement. Finite element modelling of RE is still in its infancy, and while investigations with varying degrees of success have been performed (Ciancio and Robinson, 2010;

Nowamooz and Chazallon, 2011), Heath (2008) proposes an alternative strain-based NLFM approach which is reported to have advantages over more regularly used finite element analysis approaches, such as reduced computational time and improves convergence during the iterative process implementing the model into the strain-based finite element code.

The majority of the research published, however, has not considered the self-weight of the sample during experimentation. Indeed, it was assumed in Lenci et al. (2012) that self-weight is negligible, which is specifically advised against in fracture mechanics literature (Bazant and Planas, 1998). Wang et al. (2007), however, attempted to overcome self-weight considerations by performing the Three Point Bending Test horizontally such that the self-weight is parallel to the crack and the applied load is applied horizontally to the sample, hence removing its effect on the fracture energy. However, no suggestions were made about how this arrangement affected the test results, such as friction effects artificially increasing the fracture energy of the sample.

Additionally, no authors are known to have considered size effect, a consideration well established in concrete fracture literature for which several different approaches have been considered and proposed (e.g. Achenza and Fenu, 2006). Thus a new approach is needed from quasi-brittle fracture mechanics in order to progress the understanding of fracture in rammed earth and other SBCMs, which removes the consideration of size effect and self-weight on the sample. One potential solution is discussed further in Chapter 4.

2.5 Research Gaps

Throughout the previous sections, the current understanding of different aspects of earthen construction research has been outlined. It has also been acknowledged that current understanding of SBCMs is not complete, and further research is needed in order to comprehend different aspects of earthen construction that are not yet fully understood. A few key areas have been identified for research for this thesis, and it is recognised that there are still many other areas that need research. These research areas, plus other identified in this thesis, are outlined in Section 7.4.

While fibrous reinforcement has been found to generally improve material properties of soil (Hejazi et al., 2012) and of concrete (Zheng and Feldman, 1995), new sources of fibrous reinforcement should be identified either to use waste material from another manufacturing process, or else to use renewable material, in order to help maintain the material's environmental credentials. Waste carpet fibre from industrial processes has been found to improve the properties of 'substandard' soil (Miraftab and Lickfold, 2008) and has been used to improve the UCS of a clay soil (Mirzababaei et al., 2012). Its effect on sandy soils, and its effect on shear has been less well investigated, however. Waste carpet fibre has also been

used within concrete with positive effects on the energy absorbtion and ductility properties of the material (Wang et al., 1994).

The triaxial test is most commonly used to determine shearing properties of SBCMs (e.g. Cheah et al. (2012)) and the direct shear test has generally been overlooked for research in this area. The direct shear test is a very simple, easy test to perform, and the apparatus is ubiquitous in soil mechanics laboratories around the world, therefore expanding opportunities for this test to be performed. Other advantages and disadvantages of the direct shear test over the triaxial test are outlined in Sections 3.4.1 and 3.5. The tests have been compared in soil mechanics literature (Maccarini, 1993), which found that the tests displayed slightly different behaviour under repeated loading and unloading cycles.

Very little research has been found that investigates fracture of SBCMs, with Ciancio and Augarde (2013) identifying that the neglection of consideration of fracture energy in the experiments described led to an underestimation of the lateral capacity of wall section. Lenci et al. (2012) and Aymerich et al. (2012) performed different investigations into fracture of SBCMs, and finite element modelling has been attempted (Ciancio and Robinson, 2010; Nowamooz and Chazallon, 2011), but all the research retrieved has used the three point bending test, which has a number of drawbacks, and these drawbacks are still present in earthen construction material investigations. These drawbacks, and an alternative test that eliminates the majority of them, are discussed in detail in Section 4.1.2.

Chapter 3

Mechanical behaviour

3.1 Introduction

Understanding the mechanical behaviour of different soil-based construction materials (SBCMs) is crucial to being able to use them in a variety of different situations. The most commonly researched material property is compressive strength, and is also the most commonly used property to define soil suitability (Section 2.1.1), and it is recognised that understanding strength development in unstabilised (Schroeder, 2011) and stabilised (Maskell et al., 2013) SBCMs is crucial to understanding the material such that it may be used more widely. Other mechanical characteristics have been studied such as tensile strength (Jaquin et al., 2008b) and dynamic loading (Bui et al., 2011), microstructural analysis has been performed (Smith et al., 2014; Cristelo et al., 2012) and attempts have been made to model the material using finite element analysis (Nowamooz and Chazallon, 2011) and other models (Caporale et al., 2014; Piattoni et al., 2011).

This chapter presents four different tests investigating the influence of cement content, wool content and water content on the mechanical behaviour of rammed earth. A commonly-used test to investigate the unconfined compressive strength is described, before three tests not normally applied to SBCMs are detailed. Two of the tests are standard tests in geotechnical engineering performed to investigate shear behaviour of a soil - the direct shear test and the triaxial test. The third non-standard test is an unconfined cylinder compression test, performed on a slender column. A Scanning Electron Microscope (SEM) was also used to investigate the structure of the sample at a small scale in order to further investigate the role of the small fibres on the soil, which were first identified as having a distinctive role in sample strength while performing the direct shear test. Results are presented for the material which is not commonly subjected to many of these tests and comments are made upon the applicability of these standard geotechnical tests to SBCMs. Details are also presented of the soil selection and manufacturing

procedure, and sample identification nomenclature, which were used for all samples unless otherwise stated.

3.2 Material information and preparation

Investigations into rammed earth have previously found that it is a highly variable material with large variation between supposedly identical samples. It is commonly advised, therefore, when performing investigations into its behaviour, that steps are taken to minimise the effect of natural variation in the material by minimising experimental error. One way this was achieved in the experiments described below was through the design and creation of an 'artificial' soil, as opposed to using a 'natural' soil obtained from site, as first proposed in Hall and Djerbib (2004b). Another way this was achieved was through creating multiple samples for each data point such that data point outliers might be identified and that points might be combined to produce an average value, therefore minimising the effect of experimental error. Details of experimental control are provided in the 'Sample Production and Testing' section of each test where appropriate.

3.2.1 Soil

'Soil' typically refers to natural earth, which often includes some topsoil and organic matter. As organic material is generally excluded from SBCMs, it is in fact subsoil that is used for construction. For ease of nomenclature, however, 'subsoil' is typically simply referred to as 'soil' in SBCM literature, and this has been adopted for use in this thesis. Natural soils are typically characterised using a particle size distribution curve, which divides the soil into 'gravel', 'sand', 'silt' and 'clay' constituents according to particle size (British Standard BS1377-2). Therefore an artificial soil was created using materials which were combined to make a similar, suitable alternative. Gravel and sharp sand were obtained from a builders' merchant, after which they were dried and subsequently sieved so that they might be used in the soil mix. The gravel was sieved to between 2mm and 10mm, while the sand was sieved to less than 2mm. Speswhite, a kaolin clay, was used for the clay fraction for the majority of samples and was sourced pre-dried, powdered and bagged from Imerys Minerals Limited. Chemical analysis provided on the manufacturer's product data sheet states that the kaolin clay is on average 47% Silicon Dioxide (SiO_2) and 38% Aluminium Oxide (Al_2O_3) by mass. The mean particle size is approximately 0.7μm. A few tests used a sodium bentonite clay to compare the behaviour of samples with different clay, as described in the relevant sections. The bentonite clay was also sourced pre-dried, powdered and bagged, from RS Minerals Ltd.

The standard method of soil characterisation is through a particle size distribution curve, although

numerical methods are sometimes used to refer to individual soil mixes in text without heavy reliance on a plotted curve. In Hall and Djerbib (2004b), a three-digit identification code (e.g. 523) was proposed, whereby the single digits represent the ratio of sand : gravel : silty-clay (e.g. 5:2:3 for the previous example), and also total 10 for simplicity. Note that the 'silty-clay' figure is a combination of the silt and clay fractions. Smith and Augarde (2013) proposes an alternative notation which, although slightly less concise in presentation, contains greater detail about the soil mix. The alternative notation, which is used for the experiments detailed below, includes a reported margin of error calculated by means of a *maximum weighted percentage error* (MWPE) in Equation 3.1.

$$MWPE = max(|Cl - a|, |Si - b|, |Sa - c|, |Gr - d|) \tag{3.1}$$

where *Cl*, *Si*, *Sa*, and *Gr* are the *designed* soil fractions and *a*, *b*, *c*, and *d* are the *measured* soil fractions of clay, silt, sand and gravel respectively.

The soil identification code takes the form 'Clay : Silt : Sand : Gravel [MWPE]' (e.g. 11:26:49:14[1.8]) whereby each value may be reported to several decimal places if needed, but also has the benefit of including an optional error margin. It was recognised that many authors do not differentiate between the silt and clay portions of their soil, so a shortened version was also proposed, of the form 'Silty-Clay* : Sand : Gravel [error]' (e.g. 37*:49:14[1.8]) whereby the asterisk indicates that the silt and clay fractions have been combined.

SBCMs typically contain a mix of clay, silt sand and gravel, however, it was not always possible for the samples made for these investigations to do the same. Gravel was not used in the majority of samples tested in these investigations due to restrictions set by the testing equipment instructions and sample size, also called the size effect, whereby testing of small-scale samples must be done with care in order for sample properties to scale appropriately, as gravel would have a larger effect on sample homogeneity in smaller samples than it would in real-world situations. The soil used for the majority of the investigations presented used the soil mix 30*70:00[2.2], although some investigations used the soil 30*:60:10[2.2]. The only samples which were constructed with the soil 30*:60:10[2.2] were the tests constructed for the unconfined compressive strength (UCS) tests in Section 3.3 and the wedge splitting tests in Chapter 4. Tests were originally to be performed on the same soil, 30*:60:10[2.2], however tests performed after the initial investigations, such as the direct shear test, were unable to use gravel due to maximum particle size requirements of the testing apparatus. Gravel was not introduced to the subsequent tests in order to minimise the variation in the soil and hence produce results from which more reliable comparisons and conclusions can be made. The removal of gravel from a SBCM is known to reduce the Young's modulus of the material by up to 400%, affect the void structure of the material and increase the compressive strength Smith (2015), it was deemed acceptable to remove gravel as the tested

material may be considered to be representative of the inter-aggregate part of the soil (Beckett et al., 2013).

The sand and clay were added to a Hobart planetary mixer and mixed until the two materials were evenly combined by eye. Water was then added slowly to the mix and left for 24 hours in sealed containers to allow the water to equilibrate through the soil. Samples were stored at $20^{\circ} \pm 2^{\circ}$ and at $60\% \pm 5\%$ relative humidity. When fully combined, the soil was split into different batches, with each batch containing enough soil to make the number of samples required plus a small amount remaining as a contingency. A 1kg soil sample was retained from each soil mix prior to separation into soil batches in order to confirm the desired specification of the soil, calculate the MWPE, and obtain a particle size distribution curve. A wet sieve test was performed first to remove all particles smaller than 63μm by rinsing the soil through a sieve. Soil that passed through the 63μm sieve during the wet sieve analysis was dried in an oven at 105° and further characterised using a sedimentation test by the pipette method (British Standard BS1377-2). Soil retained on the 63μm sieve was also dried in an oven at 105°, after which a dry sieve test was performed. The obtained particle size distribution curve for soil 30*:70:00[2.2] is shown in Figure 3.1.

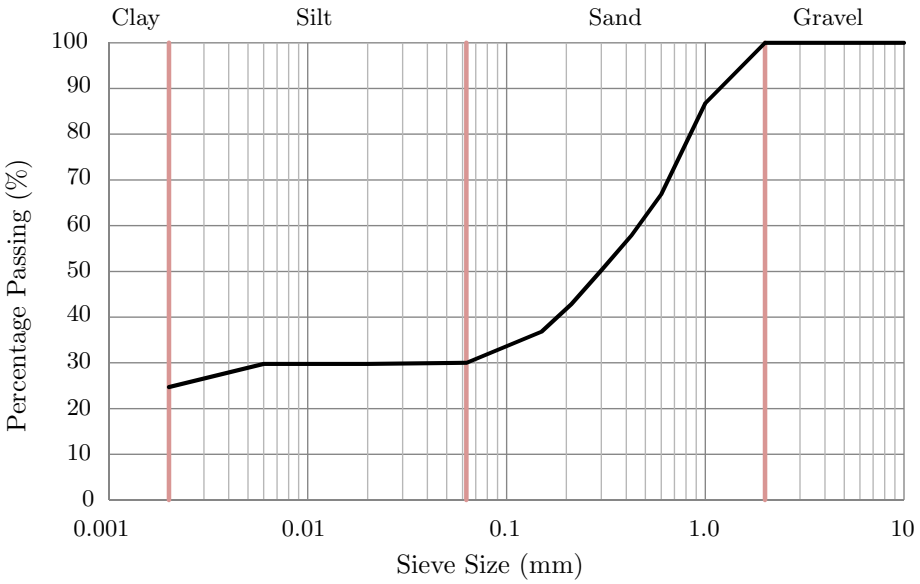

Figure 3.1: Particle size distribution curve for soil ID 30*:70:00[2.2].

The soil 30*:70:00 was found to have an optimum water content of 11%, obtained by performing a series of vibrating hammer compaction tests (British Standard BS1377-4, 1990), plotting the results (Figure 3.2) and determining the water content at the maximum dry density according to the method detailed in the British Standard BS1377-4. The highest value of dry density on the best-fit curve corresponds to the optimum water content of the sample. All samples were compacted at their optimum water content. The vibrating hammer test was used as it is the most similar to compaction method for rammed earth (RE),

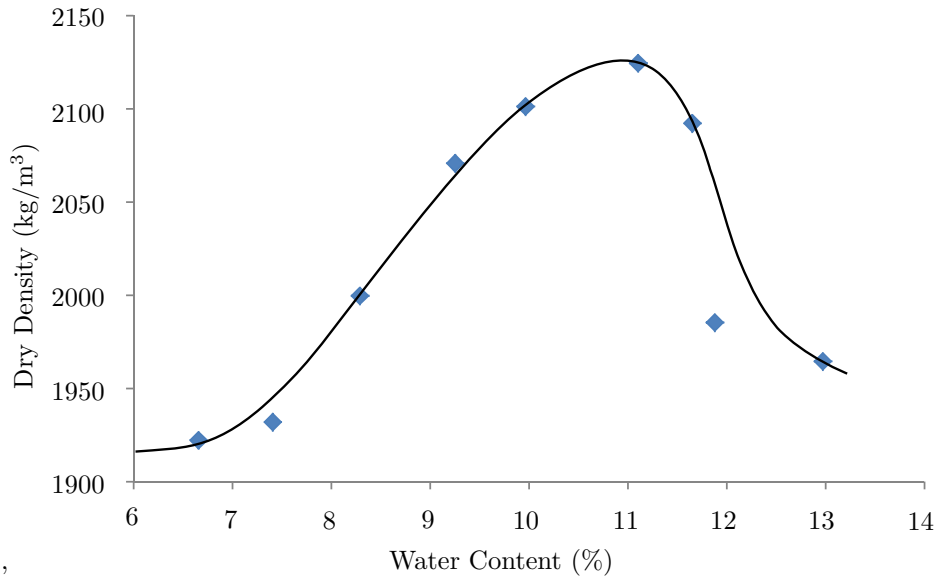

,

Figure 3.2: Water content vs. maximum dry density of soil 30*:70:00[2.2], obtained from a vibrating hammer test.

which was an important consideration as compactive effort is known to affect optimum water content of soils - a higher compactive effort will result in a lower optimum water content (Beckett, 2011).

3.2.2 Stabilisers

In the majority of investigations performed, both a chemical and a physical stabiliser were used in order to investigate the effects of their individual and combined inclusion into the material.

Chemical stabiliser

The most commonly used chemical stabilisers in SBCM construction are cement and lime. Cement was used as a chemical stabiliser in these experiments because it is the most widely-used stabiliser in earthen construction and it is also readily available all around the world. The cement used in these experiments was a CEMII Portland-Limestone cement, supplied by *Tarmac Trading Ltd.*

Physical stabiliser

Waste carpet fibres were used as a source of wool for a physical stabiliser, obtained from the waste stream of a carpet manufacturer and provided in woven mats consisting of hundreds of wool strands. To prepare them for sample construction, the mats were firstly cut into strips of around 40mm width. The wool strands were then separated from the strips, each strand being made up of many smaller fibres. The strands were 0.7mm in diameter when compressed and approximately 3mm diameter when relaxed, measured using a micrometer. Tensile tests were performed on 15 wool strands using a Lloyds tensile

testing machine. The average tensile strength of a wool strand was found to be $69.2 N/mm^2$. The fibres were 2μm in diameter. To clarify the nomenclature for referring to the different scales and part of the carpet waste material, *wool* refers to the material, *wool* was provided in *mats* made of hundreds of *strands*. Each *strand* is made up of many *fibres*. This nomenclature is used throughout this thesis. Figure 3.3 shows a photograph of a wool strand, with the fibres clearly visible.

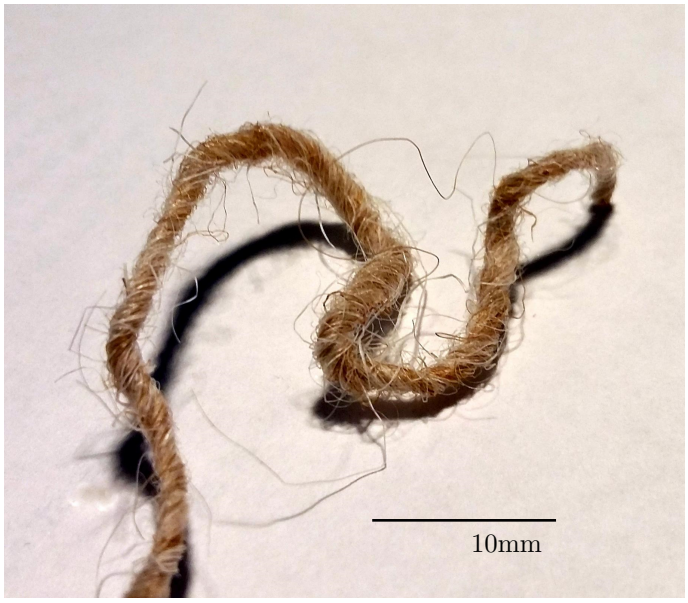

Figure 3.3: Photograph of a wool strand with fibres.

Soil batches containing cement or wool fibres were mixed with a slight variation from the method described in Section 3.2.1. After the equilibration period, soil batches which were to contain cement were re-placed into the Hobart planetary mixer with the cement and the appropriate additional mass of water to maintain the optimum water content of the pure soil. The cement was added after equilibration of the soil as cement starts hydration as soon as it comes into contact with water, which would result in any cement present during the equilibration process start to form solid lumps of cemented clay, rendering the soil unworkable. Total water added to the sample was equal to the optimum water content of the soil, and no additional water was added to the sample to allow for cement hydration or to take account of the change in particle size distribution and hence pore size distribution. This was done to minimise the variability in the sample, although it is recognised that this may, on occasion, lead to a weakening of the sample. This is discussed in more detail when this effect is observed in Section 3.4.3. Wool tended to clump when attempts were made to mix it into the soil using the planetary mixer, so the wool was mixed into individual samples by hand to achieve even wool distribution.

Another consideration in the soil mixing process was the role of equilibration. The benefits of equilibration have not, to the author's knowledge, been studied in SBCM literature. It is generally thought

that equilibration allows the water in the sample to equalise throughout the soil, to ease compaction and help to create a denser, and hence stronger, material. This has yet to be investigated scientifically, however, and if it does not have an effect on either the compaction quality or strength of the material, then then large amounts of time during construction could be saved, and would also negate the risk of water loss during equilibration, as it was observed that the inside of the storage container was damp from condensation, implying that some water had left the soil. If, however, equilibration is found to improve the compaction or strength, the mix might still produce more favourable properties if the dry parts of the construction material (soil and cement/lime) is added and mixed together before water is added immediately prior to construction, instead of the procedure used for these experiments. This alternative method would ensure a more even distribution of cement throughout the soil mix, as opposed to the cement coating small balls of wet soil, which was observed during soil mix construction, and is discussed further in Section 3.4.3.

3.2.3 Sample identification system

Samples across the majority of experiments were given identification codes of the same format such that it might be easier to refer to and compare the properties and results of different samples.

Each batch of soil was given an ID of the form WnCm where n and m indicate the percentages of Wool and Cement respectively. As the wool in some tests was used in increments of 0.5%, in order to simplify the notation the n indicating the wool percentage records double the value of wool percentage, i.e. W2 corresponds to 1% wool by mass and likewise W3 to 1.5%. As the cement content was only increased in integer increments, the Cement value m can be read directly, i.e. C4 corresponds to 4% cement by mass.

As each soil batch held a unique identification code, so did each individual sample tested using that batch. The code took the form T-WnCm-X, where T is the code for the test (Test ID) used on that sample, WnCm is the identifier for the soil batch (Batch ID), and the hyphenated suffix X indicates the sample number in the test batch (Sample ID). To give an example, sample T-W1C6-3 is a sample tested for the triaxial investigation, constructed using a soil containing 0.5% wool and 6% cement by mass and is the 3rd sample in the batch (typically consisting of 6 samples). Test IDs are provided in the 'Sample Production and Testing' section of each test, along with details of any minor deviations and other soil mixes which were not used in other investigations.

Tests which did not use this sample identification system are limited to the Unconfined Compression Tests in Section 3.6 and Shrinkage Tests in Chapter 5. Reasons for this and local sample identification systems are provided in their respective 'Sample Production and Testing' sections.

3.3 Unconfined compressive strength

Unconfined compressive strength (UCS) is a fundamental material property that is routinely used to categorise, compare and check the quality of different construction materials. The UCS of a material can be determined through testing of different shaped samples including prismatic and cylindrical samples, although the predominantly used sample shape in construction is the cube. This is particularly the case in concrete construction, where cube samples are used so frequently that the test is often referred to simply as the 'Cube Test' and results are often quoted as the 'Cube Strength.'

3.3.1 Background to the cube strength test

There are three different ways to determine the UCS of RE, using three different sample shapes: prismatic (e.g. Maniatidis and Walker (2008)), cylindrical (e.g. (Ciancio and Gibbings, 2012)) and cube (e.g. Hall and Djerbib (2004b)). The cube shape is commonly used because it is a very simple, easily repeatable, reliable test in concrete construction, and evidence so far has suggested that it is similarly reliable in earthen construction (Hall and Djerbib, 2004b). Although cylindrical samples may be more commonly used around the world, no work has been found that directly compares the three methods of determining compressive strength in earthen construction. It was the aim of this investigation to use a well-established, easy test, familiar with industry and in research, to investigate the effect of wool and cement on the material. From a scientific perspective, there should be no significant difference in strength obtained using the different tests, and the outcomes of the investigation presented below should be identical to a similar investigation performed using a different shape specimen.

The UCS of a material is obtained by applying an evenly-distributed, increasing displacement to the top surface of a cube of solid material, until the peak load is reached and the sample fails. The maximum load, typically applied through displacement controlled testing apparatus, is then converted into a maximum vertical stress according to the surface area of the test cube in contact with the applied load.

3.3.2 Sample production and testing

The soil was manufactured as described in Section 3.2.1, to the specification 30*:60:10 in batches of 42kg which provided enough soil for 6 cube test samples and 6 wedge splitting test samples per soil batch. Details of the wedge splitting test samples and subsequent investigation are presented in Chapter 4. Cube test samples were constructed in batches of 6, each batch containing a different amount of cement (0, 2, 4, 6, 8 or 10% by mass) and wool (0, 1 or 2% by mass). Sample IDs were assigned according to the method described in Section 3.2.3, with the test ID 'U'.

Samples were compacted in 3 layers in a metal cube mould with internal dimensions 102.5 x 102.5 x 102.5 mm. Each layer was compacted with a vibrating rammer for 30s per layer, which was judged to be sufficient for full compaction, after which the top was levelled to the top of the mould to ensure that the samples were constructed to the same volume. Samples were removed from the mould immediately after compaction and left to dry in an indoor, open environment for 14 days. On the day before testing, each sample was coated in a thin layer of white paint on four sides, in order to observe cracking behaviour during testing more clearly. On the following day, 14 days after construction, the samples were tested in a displacement-controlled compressive strength test rig. Figure 3.4 shows the test arrangement. It is noted that the load is not central to the cube in the image, and the reader is assured that this image was taken for illustrative purposes only - the load was ensured to be applied centrally to each of samples during testing. A load spreader was placed on top of the sample to ensure an even stress distribution across the top surface of the cube and an increasing vertical displacement was applied to the base of the sample. The load was measured using a proving ring and the peak load was recorded. A non industry-standard machine was used for this experiment as a higher load resolution was required at lower load levels than the more commonly-used equipment can provide.

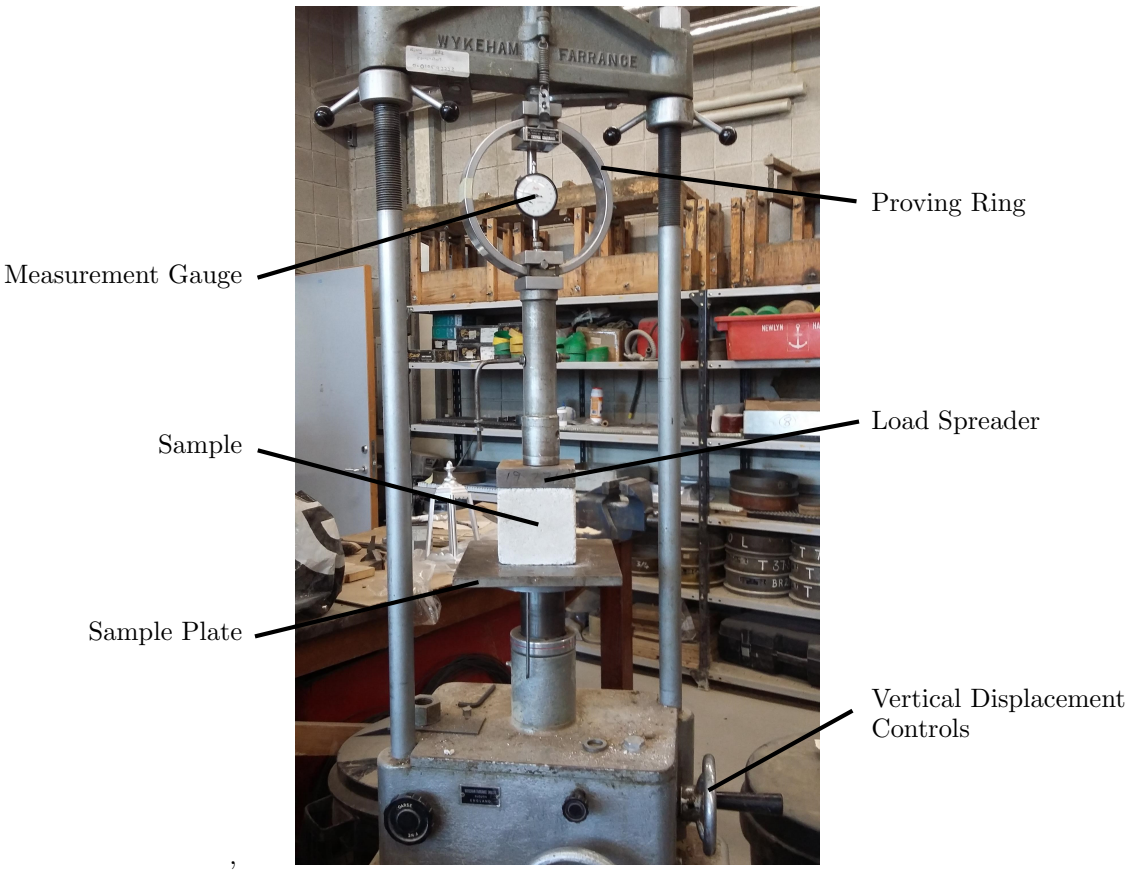

Figure 3.4: Unconfined compressive strength test rig. Photo for illustrative purposes only.

3.3.3 Results and discussion

It was observed during testing that all samples broke in an hourglass shape, similar to the pattern commonly observed during concrete cube testing (Hughes and Bahramian, 1965). This indicates that forces are being distributed evenly throughout each sample, in a similar distribution pattern to that which is observed in the failure of concrete cubes. This suggests that the presence of wool does not affect compressive stress concentration patterns or stress paths in the sample.

Maximum loads recorded on the loading ring were converted into maximum vertical stress to obtain the UCS by dividing the maximum load (N) by the area of the sample in contact with the loading plate (mm^2). In this case, as the object under stress is a cube of sides 102.5mm, the maximum force load was divided by 102.5 x 102.5 mm^2. Figure 3.5 shows a plot of UCS against percentage cement content of the sample, grouped by percentage mass of wool content of the sample.

Appendix A contains the raw data for Figure 3.5. Details of sample dry density and water content taken from the sample after testing have, unfortunately, been lost since the tests were conducted, although all samples were mixed with the same mass of soil and compacted at the same water content.

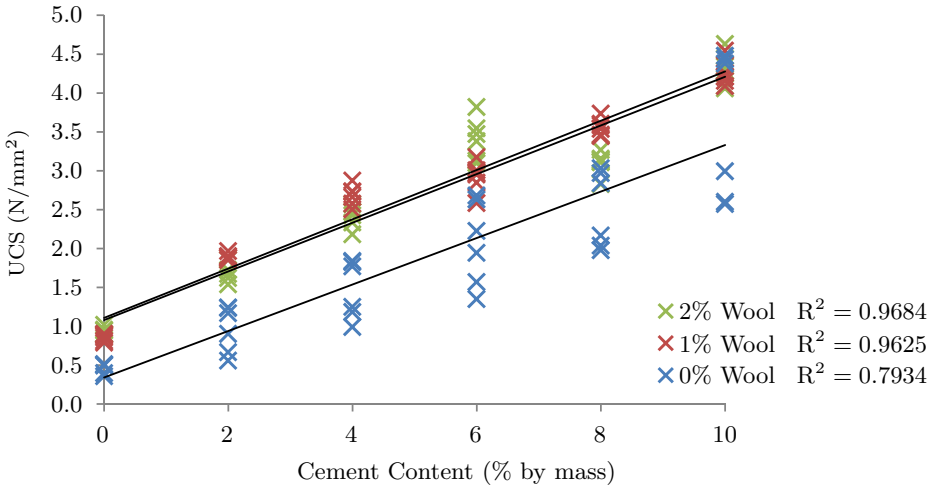

Figure 3.5: Plot of UCS against percentage cement content, grouped by percentage wool content.

Figure 3.5 clearly shows that adding either wool or cement increases UCS independently of the other stabiliser. This is in clear contrast with many experiments on fibre-reinforced concrete, such as Zheng and Feldman (1995) or Reis (2009), which both found that adding fibres decreased the UCS of the samples. However, Wang et al. (1994) also found that compressive strength was generally higher with 1% fibre than with either 0% or 2%. The fibres used in those experiments were also carpet fibres, and the suggested reason for the drop in strength at 2% fibre content was that the fibres "might have caused a strength reduction, or they might have delayed the development of compressive strength with age". However, the latter reason does not account for why the strength increased with 1% wool, and therefore it is more likely that the greater amount of wool weakens the sample.

Figure 3.5 also suggests that the amount of wool added to the sample has a lesser effect on the sample than whether wool is included or not, as the figure clearly shows that UCS values of the samples with 1% and 2% wool follow similar average increases in strength with increase in cement content. Moreover, the addition of wool to the soil mix increases UCS by a constant of approximately 0.8N/mm^2. Clearly, neither adding one piece of wool to the sample nor making a sample contain 90% wool by mass would improve the sample mix UCS, therefore there must be an upper and a lower limit to this relationship. Little is known about the relationship between wool content and increase in UCS from these experiments, although three proposals for this relationship are presented in Figure 3.6.

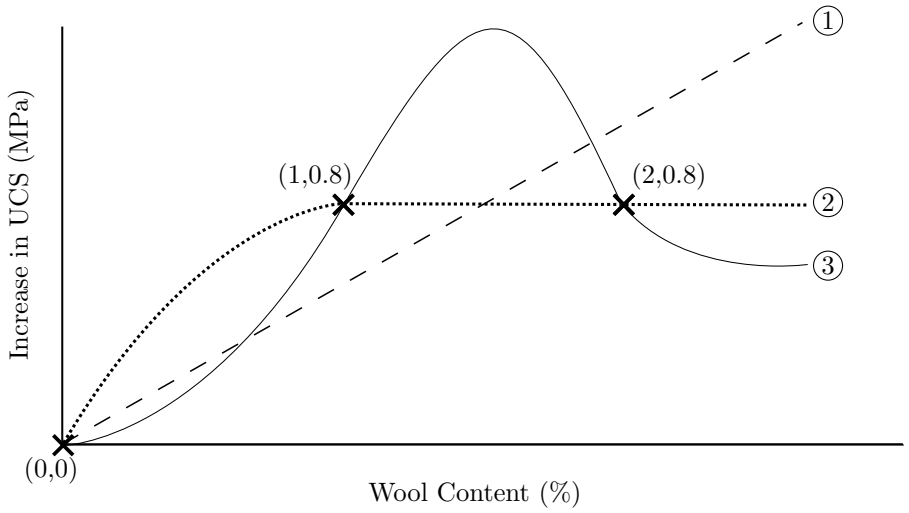

Figure 3.6: Potential relationships between wool content and increase in UCS.

Figure 3.6 plots the three known points relating UCS and wool content and suggests three different relationships between them. Relationship ① is linear and, as a result, only passes through one of the known data points, at (0,0). This interpretation implies that there is a high level of error in the non-zero measurements taken, and that the equal improvement to UCS is largely coincidental. While it is recognised and accepted that there is a large amount of individual result variation as seen in Figure 3.5, the process of taking six samples and taking an average should remove the effect of random experimental error. Equally, if systematic error was present in testing, then more evidence should be seen in Figure 3.5, for example adding wool making no difference to the increase in UCS at all. Therefore it is unlikely that a linear relationship between wool content and increase in UCS is accurate.

Proposed relationship ② starts with a rapid increase in UCS as wool content increases, before levelling off to remain at 0.8 N/m^2. This relationship has a distinct advantage over the linear relationship ① as the line passes through all known data points. However, this also implies that the wool content only affects the UCS up to a point, after which the wool has no effect, either positive or negative, on the UCS of the sample. This relationship is also impractical as proved if an extreme case is considered. It was

observed during testing that the samples with 2% wool were struggling to keep the structure after removal from the mould. Indeed, it is described in Chapter 4 how some samples were unable to be constructed due to a high wool content. Allowing a very generous case that the sample will maintain integrity at up to 5% wool, it is suggested that by 10% wool the sample will actually be weaker than it was without wool. Thus at some point the 'increase in UCS' must turn negative (thereby implying that adding wool will make the sample *weaker*), clearly refuting the suggested path of relationship ②.

It is recognised that relationship ② might be adapted such that, instead of increase in UCS remaining constant after the third data point, it might instead decrease to the x-axis and beyond, finishing near a negative value equal to the UCS of the sample without wool, thereby stating that the sample has near zero compressive strength as a result of the wool weakening the sample. However, it seems unlikely that the wool between 1% and 2% content would affect the compressive strength in no way at all. It is much more likely, then, that the relationship between wool content and increase in UCS is similar to the shape of relationship ③, which starts with a slow increase of UCS as wool content increases and follows with an increasing rate of improvement until it reaches the maximum increase in UCS somewhere between 1% and 2% wool content. After this point, the benefit of the wool (i.e. increase in UCS) decreases before turning negative and asymptotes towards a negative value equal to the initial UCS of the sample mix before wool had been added, such that the net compressive strength of the sample is zero. This relationship could be confirmed or refuted with a series of simple experiments including a wide range of different wool contents, and would potentially lead to discovering an *optimum fibre content* for the soil mix, which would be dependent on the type of fibre (wool in this case).

It is also noted that adding wool and cement will affect the soil in other ways, other than the values of UCS, some of which are explored in detail in experiments presented later in this thesis. Also noted previously in Figure 3.5 are R^2 values, which are a statistical measure of how close the line of best fit is to the data set provided, calculated through the least-squares method. The R^2 values clearly indicate that the variability of the UCS of cubes not containing wool is much greater than the variability of those with 1% or 2% wool. Samples containing 10% cement, in particular, had wide ranging values of UCS (between 2.57 and 4.48 N/mm^2). This implies that the addition of wool helps to distribute stresses evenly though the sample, potentially transferring loads from weaker to stronger areas, removing some variability in the sample.

Figure 3.5 also suggests that the same UCS can be achieved from two different soil mixes - one with cement and no wool, and one with some added wool and a lesser amount of cement. Thus an alternative to cement stabilisation can be proposed for application in earthen construction: to design a mix to a given UCS, it is possible to add a percentage of wool (or other natural waste fibre material) to the soil mix and hence reduce the amount of cement needed to attain the desired compressive strength. Use of

wool in stabilisation, therefore, does not only use a waste material from another manufacturing process, but also reduces the amount of cement required, hence reducing the carbon footprint of the construction. However, this may not be the case for all soils used in all earthen construction methods, and the addition of wool may negatively impact the material properties in ways that will be explored in Section 3.4. Clay, in particular, plays a crucial role in the strength of rammed earth (Jaquin et al., 2009) and it is not fully known how cement and wool affect the role of clay in earthen construction. It was reported in Burroughs (2008) that effectiveness of stabilisation is dependant on low shrinkage and low plasticity index, both of which are dependant on the properties of the clay. It therefore follows that variation in the clay properties would also affect the viability of wool replacement of cement, resulting in the earlier proposal being subject to the soil properties.

3.4 Direct shear strength

As the primary material in the majority of SBCMs is compacted subsoil without organic matter (Section 3.2.1), soil mechanics is often applied to SBCMs in an attempt to understand the underlying material structure and behaviour. In the same way that tests from concrete research have been adapted for use in earthen construction (such as the UCS test in Section 3.3), tests from soil mechanics can also be adapted for use in a similar fashion.

While investigations into the development and improvement of compressive strength are very common in SBCMs, shear strength has received relatively little attention despite it being a very important material property. For example, consider the UCS test as described in Section 3.3. The test is used to calculate the compressive strength of RE, however the mode of failure is clearly shear, as can be seen in the classic diagonal 'hourglass' shape of the post-failure sample. It is shear strength, therefore, that is the fundamental strength of RE, and thus it requires further investigation such that the source of strength can be fully determined, be it from suction, friction or other soil properties yet to be identified.

Shear strength of rammed earth is a relatively new area of investigation and, as such, little work has been done to quantify the most appropriate test for determining the shear strength of earthen construction materials. One investigation, reported in Cheah (2014), outlines a program of triaxial and triplet tests on RE samples, and reports that the 'triaxial test better represents the diagonal shear failure which is the predominant shear failure mode for rammed earth walls in practice' and that performing a triplet test is 'more difficult and expensive' and the samples are 'not as convenient or safe to transport and test' than triaxial specimens. Two tests commonly used in traditional soil mechanics for determining the shearing behaviour of soils are the direct shear test and the triaxial test, although only the triaxial test has been previously used in SBCM investigations.

To the author's knowledge, the direct shear test has not been used before on SBCMs, although it is suspected that tests on unsaturated soils will often produce similar results, particularly those testing fibre-stabilised soils. For example, Bouhicha et al. (2005) details a set of experiments on barley-straw reinforced composite soil, and found that, among other things, fibrous reinforcement increased the flexural and shear strengths of the material and altered the failure to be more ductile than without reinforcement. The importance of an optimum reinforcement ratio was also discussed, above which the compressive strength was seen to plummet. It is recognised that this may be similar to the *optimum fibre content* discussed in Section 3.3.3.

This section presents a detailed investigation into the direct shear test, while Section 3.5 presents a triaxial investigation of rammed earth samples and reports on a comparison of the results.

3.4.1 Background to the direct shear test

The direct shear test, also known as the shearbox test, is used to determine the relationship between normal and shear stress of a soil. It is described in full detail in the British Standard BS1377-7, and consists of a horizontally split metal box of internal dimensions 60mm x 60mm in plan view, in which a soil sample, 20mm in thickness, is placed (Figure 3.7). Porous stones, placed above and below the sample, help to dissipate any increase in pore water pressure if non-dry samples are tested. A load spreader is then placed on top of the sample, and a normal load, N, is applied to the top face of the sample via a hanger. It is suggested that the test is adapted according to the properties of the soils being tested. The two main areas for adjustment are the shear rate, or rate of testing, and the range of applied normal loads. Bolton (1991) recommends varying the shear rate for sand (1mm/min), silt (0.01mm/min) and clay (0.001mm/min) to allow any buildup of pore water pressure to dissipate, and, if the sample is a sand, it is recommended that it is lightly compacted to a known specific volume. In the testing programme described here, normal stresses were applied according to the expected stresses in a wall as described in Section 3.4.2.

In this test, horizontal (x) and vertical (y) displacements are measured at the locations marked in Figure 3.7. The vertical displacement must be measured as close to the normal load as possible in order to improve accuracy, as the load spreader is known to occasionally rotate during testing resulting from uneven compaction or dilation of the sample. The proving ring (Figure 3.7) measures the horizontal shear force, F. The motor drive is engaged and horizontal force and both displacements (x and y) are recorded. It can be assumed that the pore water pressure is zero as the test is performed drained (i.e. it allows any pore water pressures to dissipate), provided that the test is performed at a slow enough rate (Bolton, 1991). The normal stress, σ_n, and the shear stress, τ_s, are obtained by dividing the forces N and F respectively by the initial cross-sectional area of the sample, A. Direct shear test data are conventionally

presented as plots of shear stress τ_s against horizontal displacement x and vertical deformation y against horizontal displacement x (British Standard BS1377-7).

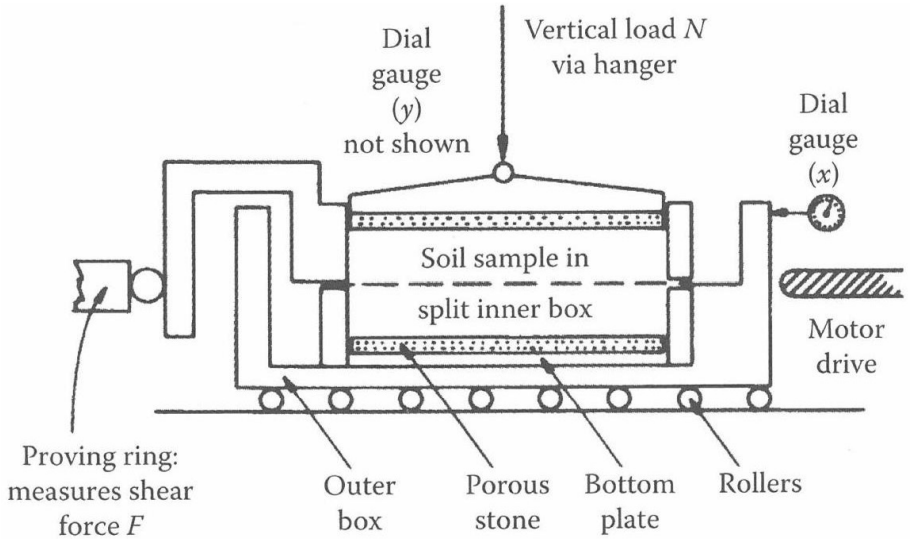

Figure 3.7: Schematic of the direct shear test, from Powrie (2013).

The direct shear test is easy to use, tests are cheap to replicate and the equipment needed is minimal and ubiquitous within soil engineering laboratories around the world. However, it is not without its faults as the sample is forced to shear across a prescribed plane and the test creates high stress concentrations within the sample. These disadvantages are minor, however, and will have minimal effect on the results of the tests performed.

3.4.2 Sample production and testing

Direct shear test samples (60 x 60 x 20mm) were constructed in a single layer in a specially constructed formwork to fit the direct shear test rig. A large number of samples were constructed in order to improve reliability of the results and to obtain a realistic understanding of the material as per described in Section 3.2.1. The soil was mixed in batches, each containing enough soil for 6 identical samples. Wool (0, 0.5, 1.0 or 1.5% by mass) and cement (0, 2, 4, 6, 8 or 10% by mass) were added to each batch to produce 24 unique batches of soil. Four additional sample batches with no wool or cement were created, each with a different water content at compaction (8%, 10%, 12% and 14%), in order to investigate the effect of initial water content, and hence density of the sample, on shear strength. Each sample was given an identification code as described in Section 3.2.3, with the Test ID 'D'. The soil batches created with varying water contents were given the sample IDs L1 to L4 in ascending water content (i.e. L1 contained 8% water, while L4 contained 14% water). The total number of samples created was 168.

The samples were air dried for a minimum of 7 days, by which point their masses had stabilised. Measured 'water contents' at test varied between 0.5% and 1.5%, although these calculated values did not take account of the cement addition. If the mass of cement and proportion of water used within the cementation reactions was added to the mass of the sample, all calculated water contents at test dropped to less than 0.8%. Samples were not physically dried in the oven after each test to obtain measured water contents, and so water contents at test were calculated from initial masses, cement content and water content added, alongside the calculation proportion of water used within cementitious reactions as calculated in Jones (2015). It is noted that a small amount of water within unstabilised samples would affect the behaviour of the sample, however it is expected that water within stabilised samples would not affect the behaviour due to the different source of particle bonding (i.e. cementation opposed to suction).

Each sample was placed in a shear box rig and the test was performed as described in Section 3.4.1. In every batch of 6 samples, 2 were tested at 25kPa, 2 at 50kPa and 2 at 75kPa normal stress (σ_n), which was achieved by adding different masses to the hanger applying the vertical load V. These values were selected after calculations were made to find the expected stress at the base of a 2.4m tall RE wall with a density of 2000kg/m^3 as in Equation 3.2.

$$\sigma_n = \gamma \times H \times A \tag{3.2}$$

where σ_n is the applied normal stress, γ is the material density, H is the height of the wall and A is the area of the plan view of the direct shear test (DST) sample. σ_n was found to equal 47 kPa. Thus 25 kPa, 50kPa and 75 kPa were selected to provide stresses below, equal to, and above the expected design stress.

One linearly variable differential transducer (LVDT) was used to measure horizontal displacement of the shear box, while a second LVDT was used to measure vertical displacement of the sample. The motor drive applied a displacement at a rate of 1mm/min, which was selected as recommended by Bolton (1991) (Section 3.4.1). As the samples in this investigations are largely sand, this was judged to be slow enough for any pore water pressure to dissipate, especially considering that the samples were tested at a very low (less than 1.5% by mass) water content. The average duration of the direct shear tests performed was approximately 10 minutes. Output values of horizontal displacement were converted into the horizontal load and then divided by the cross-sectional area of the sample in plan view to calculate the shear stress. Shear stress (τ_S) and vertical displacement (V) were then plotted against horizontal displacement (H) for each sample as per the example in Figure 3.8.

Maximum shear stress (τ_S) of each sample was then plotted against the normal stress (σ_n) following standard procedures of the direct shear test as described in British Standard BS1377-7 to form a plot similar to that in Figure 3.9.

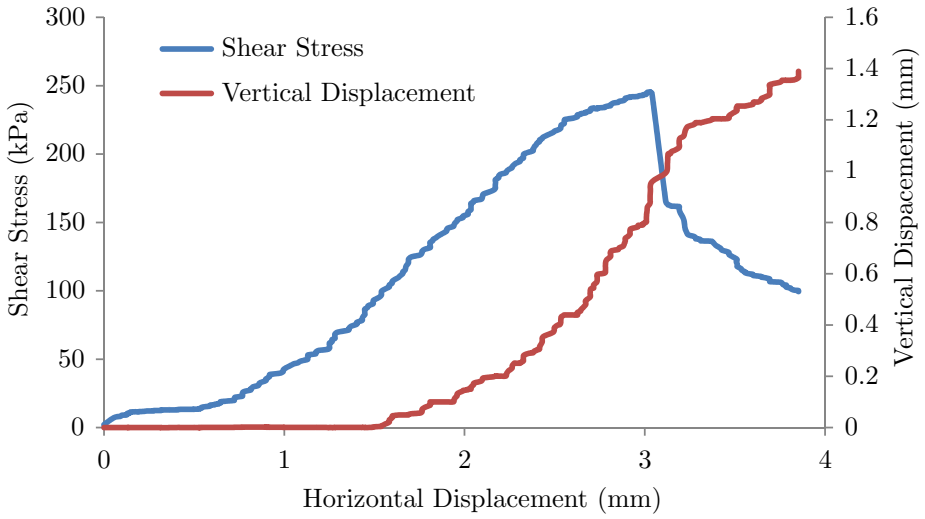

Figure 3.8: The direct shear test response curve of sample D-W1C6-6, plotting shear stress (τ_S) and vertical displacement (V) against horizontal displacement under normal stress (σ_n) equal to 75kPa.

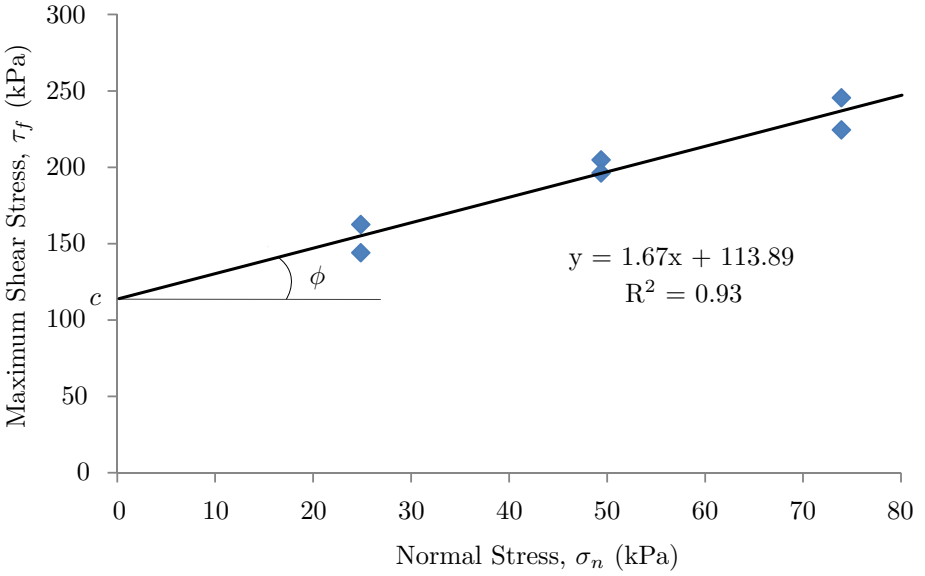

Figure 3.9: Determination of c and ϕ for soil batch D-W1C6.

The line of best fit in the figure follows an equation of the form

$$\tau_f = c + \sigma tan\phi \tag{3.3}$$

where τ_f and σ are the shear stress and normal stress respectively.

The Mohr-Coulomb criterion (Equation 3.3) was then applied (Bui et al., 2014b) to calculate apparent cohesion (c), hereafter referred to simply as 'cohesion', and angle of shear resistance (ϕ) as shown in Figure 3.9 through reading the y-intercept and calculating the gradient of the line of best fit respectively. The angle of shear[ing] resistance is an alternative form of the coefficient of friction, and is equal to the angle at which an internal resistance force lies at, compared with the normal, when a vertical and horizontal

force are applied to the material in such a combination that the material is about to move laterally. Cohesion is defined as 'the shear strength of a soil when subjected to zero normal stress or confining pressure' (Head, 1982). In the example shown in Figure 3.9, c is 114kPa and ϕ is 59°.

In traditional soil mechanics, it is common to adopt the Mohr-Coulomb strength criterion to use values of effective stress as proposed by Terzaghi (1936), whereby the overall stress state σ is related to the effective stress σ' and the pore water pressure u according to Equation 3.4.

$$\sigma = \sigma' + u \tag{3.4}$$

The effective stress σ' is then used with the Mohr-Coulomb criterion to determine effective cohesion c' and effective angle of shear resistance ϕ', according to the same methods for determining c and ϕ in Equation 3.3. The effective stress in a soil is the stress that affects the rigidity of the soil, that is how well the soil remains as a solid block when subjected to a load. However, the effective stress as proposed in Terzaghi can only be used if a number of assumptions about the soil are valid. One such assumption is that the soil is fully saturated. As this is not the case in the samples in this investigation, as in fact the samples are highly *un*saturated, Terzaghi's effective stress cannot be used. Effective stress of unsaturated soils was not used due to the unknown parameters of the soil matrix. Additionally, no values of pore water pressure have been determined, therefore all results were calculated as values of total stress σ, and subsequently used to calculate values of c and ϕ.

It is noted that the due to the graphical determination of ϕ and c (Figure 3.9 and Equation 3.3), that a line of best fit is drawn between a number of different points, changing one variable will naturally change the other (i.e. altering the angle of the line, ϕ, will result in a change in cohesion, c) and thus these variables are inherently dependant on one another. It is also essential that an appropriate line of best fit is selected as the reliability of ϕ and c are unequivocally linked to the justification of the selected line. On occasions where there is uncertainty as to the location of the line of best fit, a minor alteration to the angle of shear resistance ϕ will result in a large change in cohesion. Low correlation between data points will cause a small uncertainty in determination of ϕ, and will result in a large uncertainty in c. Thus ϕ must be considered to be the more important variable.

This effect can be demonstrated by considering the determination the line of best fit for soil batch D-W1C6 shown in Figure 3.9, which was calculated using the method of least squares. Figure 3.10 shows that, through the selection of use of different data points, values of ϕ and c can vary considerably. Figure 3.10 shows the same data points as in Figure 3.9, with some points (highlighted in red) not included in the linear regression calculation. In each figure, two different points have been removed to alter the line of best fit to the extreme values of ϕ and c.

While data points cannot obviously be ignored for convenience, this does illustrate that minor changes

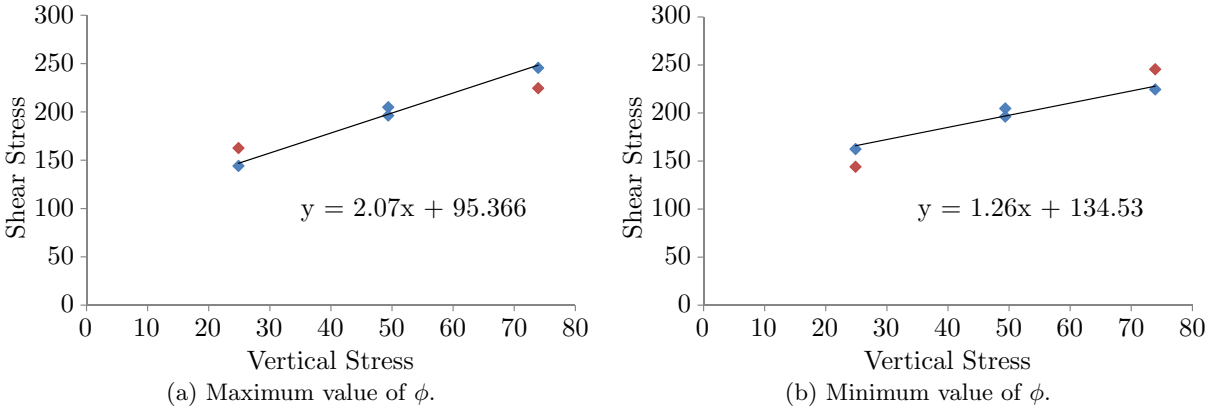

(a) Maximum value of ϕ. (b) Minimum value of ϕ.

Figure 3.10: Graphs determining values for ϕ and c resulting from data point exclusion from soil batch D-W1C6.

in recorded values can massively affect the calculated values of of ϕ and c. If the points in red had not been recorded, or had the value of them been closer to the other data point in its 'pair', there is great potential for variation. The range of potential values of ϕ extends from 52° to 64° and potential values of c range from 95 kPa to 135 kPa. Any uncertainty in line location, and hence in value of ϕ and c, is greatly increased in plots where the data points show little correlation.

When the samples were being constructed, a higher compactive effort was required for the samples tested in this investigation than is usually applied to soil mechanics samples undergoing tests, and therefore a different construction method was required, and samples were hence compacted in a separate mould before being transferred to the shear box. While the procedure was not perfect, and may have resulted in occasional stress concentrations, the experiment was deemed to be valid as the comparative nature of the work was unaffected. This imperfect procedure necessitated a design of the separate mould such that the samples would fit as neatly as possible in the apparatus. Unfortunately, as a perfect fit is rarely possible, it was noted during sample insertion that some samples were tighter fitting in the mould than others, and this was often found to be due to wool sticking out of the side of the sample. During testing, some samples were noted to fail in an 'incorrect' manner, resulting in their results being unusable. It is thought that some of these failures could have been to the imperfect sample size, although it could have also been due to sample imperfections such as uneven soil mixing, specifically regarding mixing of the cement and wool, or uneven compaction of the sample. In the cases where the sample failed 'incorrectly', either due to sample failure before testing or due to an irregular crack path, fewer than the designed 6 repeat samples were therefore used to calculate ϕ and c. Reasons for sample exclusion were as follows:

- *Incorrect Failure* (IF). Samples that failed incorrectly, such as diagonally up through the sample or shearing off at a corner, rather than horizontally through the sample as designed.
- *Pre-test Failure* (PF). Samples that failed prior to testing, in general due to excess wool causing

the sample to feature a crack path through the sample prior to testing.

- *Triax Freeze* (TF). The data logging program used, *Triax* (Toll, 1999), froze partway through this test, resulting in no readings being taken over part of the test peak shear stress.

Figure 3.11 shows example photographs of some samples which were judged to have failed incorrectly and were therefore excluded from further analysis. Samples were judged to have failed 'correctly' if the sample had split evenly between and parallel to the top and bottom surfaces of the sample, and the two halves had remained intact.

(a) Example of Incorrect Failure (IF) in sample D-W0C10-1. Note the diagonal failure across the front right corner of the image and the lack of other failure in the rest of the sample.

(b) Example of Pre-test Failure (PF) in sample D-W2C6-4. Note the uneven wool showing near the front of the image and the cross-shaped fracture on the top surface of the sample.

Figure 3.11: Examples of incorrect sample failure during direct shear test.

Table 3.1 shows the number of successful samples tested in each batch, details of sample exclusion, and calculated values of ϕ and c. Extra to the occasions where too few sample results were due to incorrect sample failure, 2 additional samples were made in the first batch ID D-W0C0, in the case of multiple sample failure at the start of experimentation. Values of normal stress and maximum shear stress of each sample are presented in Appendix B, while the plots used to calculate values of ϕ and c are presented in Appendix C. Table 3.1 also shows the R^2 value, that is a measure of how well the line of best fit aligns to the data points. While some R^2 values are fairly high (e.g. D-W0C0 - 0.91 and D-W2C6 - 0.90), it is noted that some R^2 values are very low (e.g. D-W2C0 - 0.02 and D-W3C6 - 0.08), resulting from a clear lack of correlation between data points. This apparent lack of correlation is likely due to the wool present in the sample affecting the results by making the samples heterogeneous, although it is recognised that this is difficult to prove, and this is discussed in further detail in Section 3.4.6.

Although the variation in the angle of shear resistance reported is high (ranging from 7° to 76°), it must be noted that over 80% of the samples lie within 26° of each other, and the majority of the exceptions to this have a low R^2 value. Additionally, the variation in ϕ of RE has not received any attention - while studies have been found that investigate the shearing properties of RE using the triaxial test, as

Table 3.1: Direct shear test samples.

Batch ID	No. of Samples	R^2	ϕ (°)	c (kPa)	Reason for Sample Failure
D-W0C0	8	0.91	67	58	
D-W0C2	5	0.32	52	144	IF
D-W0C4	6	0.80	53	133	
D-W0C6	6	0.89	76	48	
D-W0C8	6	0.83	65	145	
D-W0C10	5	0.20	55	177	IF
D-W1C0	6	0.36	48	95	
D-W1C2	6	0.41	41	131	
D-W1C4	5	0.40	66	128	IF
D-W1C6	6	0.93	59	114	
D-W1C8	6	0.77	48	102	
D-W1C10	5	0.15	50	169	TF
D-W2C0	4	0.02	8	103	IF, IF
D-W2C2	6	0.75	54	54	
D-W2C4	6	0.40	60	32	
D-W2C6	4	0.90	65	48	PF, PF
D-W2C8	5	0.36	54	83	PF
D-W2C10	6	0.12	47	68	
D-W3C0	6	0.36	32	40	
D-W3C2	4	0.84	62	0	PF, PF
D-W3C4	6	0.61	62	4	
D-W3C6	5	0.08	51	29	PF
D-W3C8	6	0.18	7	74	
D-W3C10	6	0.78	58	0	
D-L1	6	0.53	26	71	
D-L2	6	0.85	57	66	
D-L3	6	0.71	63	53	
D-L4	6	0.75	42	80	

described later in this section, none have been found to quantify any variation in the results. While the values of cohesion and angle of shear resistance found performing this test may seem unrealistic, there author can find no other highly compacted soil samples experiments performed using the direct shear test to compare the work to. In addition, this test is being used for comparative purposes to identify any changes in the material behaviour, therefore conclusions made regarding the relative difference between samples is likely to still apply under other test conditions.

3.4.3 Experimental observations

During experimental design, it was originally planned to test additional samples containing up to 2.0% wool, as per the samples used in UCS testing. This, however, proved impractical as the volume of wool required was too much for the small samples to contain and hence all the samples collapsed when removed from the mould. It is noted that the UCS cubes did not fail in a similar manner, and this is likely due to

the difference in the sizes of the different samples, specifically with regards to the dimensions of the wool relative to the smallest dimension of the sample. During direct shear test sample construction, it was observed that any wool strands on the surface of a sample visibly expanded immediately after the sample was removed from the construction formwork (which caused the problems with inserting the sample into the test rig as mentioned in Section 3.4.2). It therefore follows that samples containing over 2% wool appear not to have enough soil to bind the sample together. As the samples constructed at under 2.0% wool did not expand and collapse after removal from the formwork, it can be assumed that the wool in the sample remained under compression, held by the surrounding soil. This has strong implications for sample behaviour, and possible effects of the internal forces stored in the wool are discussed in Section 3.4.6.

It was also noted that the two halves of a sample which contained wool often remained connected after testing had been performed and failure had occurred. This was occasionally due to full wool strands crossing the gap, but it was usually instead due to the fibres bridging the soil failure line. Wool strands at least partly lying in the crack zone remained attached to at least one, and often both, sides of the sample, and sometimes scissors were needed to separate the two sample halves in order to see the fracture plane. Figure 3.12 shows the two sides of the fracture plane in sample D-W1C4-1.

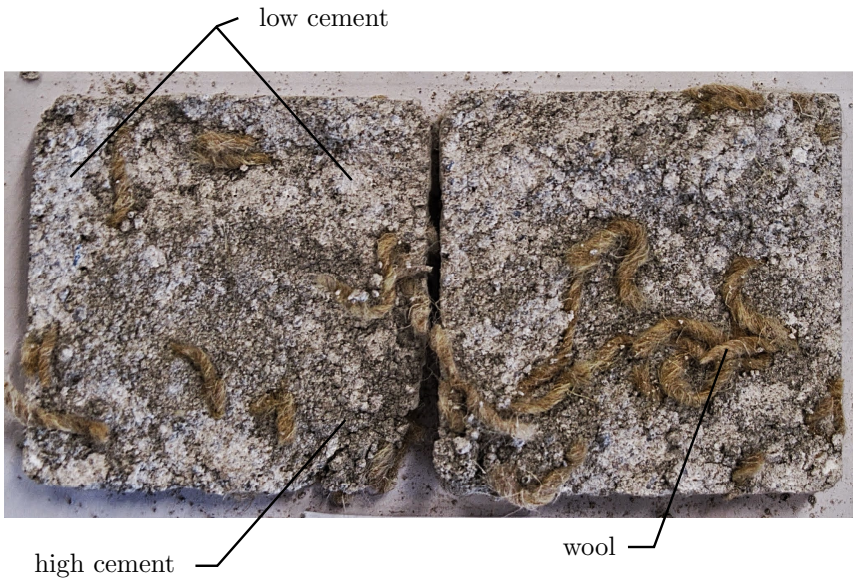

Figure 3.12: Photograph showing the top (L) and bottom (R) halves of the fracture plane of sample D-W1C4-1.

The soil appears pale in the image as the clay fraction of the soil was purchased clean, and is hence white. Darker, grey sections indicate areas of increased cement percentage, which is likely a result of uneven cement mixing through the sample due to the limitations of the soil mixing process. As cement was added after the soil had been mixed and left to equilibrate (from the method and reasons presented

in Section 3.2.1), the cement coated any existing clumps of soil as opposed to mixing evenly throughout the soil. These cement-coated soil clumps are labelled in the Figure 3.12 and can be indentified by distinctive areas of pale soil surrounded by a dark grey line of cement. Wool can also clearly be seen in the Figure, which shows that wool was present in the crack zone. Samples with no wool, and hence no wool in the crack zone, were observed to shear along macroscopically linear crack planes, while samples with increasing amounts of wool (and hence increasing amounts of wool in or adjacent to the crack zone) had increasingly uneven fracture planes. This is discussed further in Section 3.4.6.

3.4.4 Discussion on the direct shear test response curve

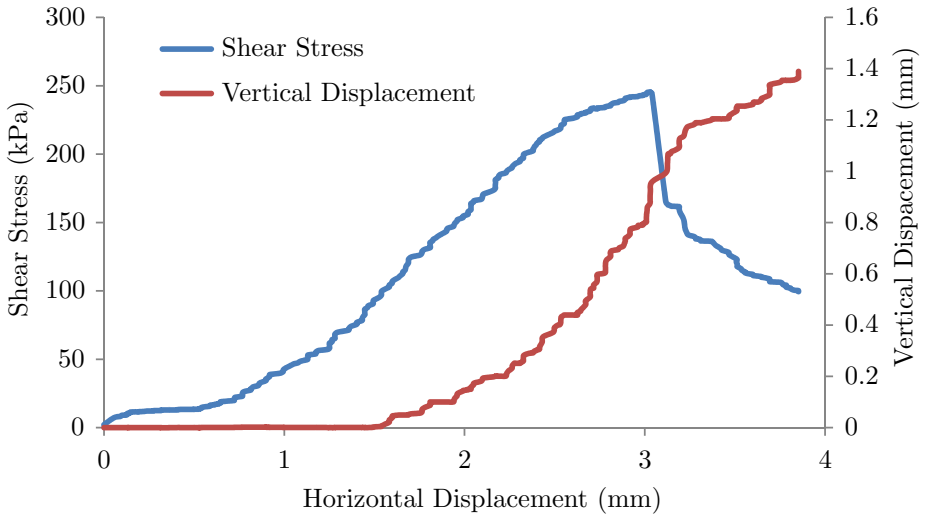

Figure 3.13: The direct shear test response curve of sample D-W1C6-6, plotting shear stress (τ_S) and vertical displacement (V_S) against horizontal displacement.

Figure 3.13 shows an example response curve, from sample D-W1C6-6, which plots shear force and vertical displacement of the sample against horizontal displacement of the test rig. Direct shear tests performed on geotechnical samples often display initial sample compression, shown by a drop in vertical displacement at the start of the test curve, followed by sample dilation after sample failure. It is suggested that this behaviour (that is, the observed volumetric compression) is only typical in samples that are not fully compacted, as samples which are heavily compacted to a maximum density would not be expected to compact further under the small vertical stress applied during the test. Considering that the samples were compacted under a higher vertical pressure than was applied during the direct shear test, the samples would not be expected to compact further during the loading phase of the test, and will therefore be expected to expand under shear loading as the particles move past each other. Initial compaction (from a negative dilatancy angle) is not seen in Figure 3.13 as the soil sample is fully compacted prior to testing and will therefore exhibit no further contraction. Figure 3.13 exhibits positive vertical displacement after around 1.5mm horizontal displacement, which confirms the expected behaviour.

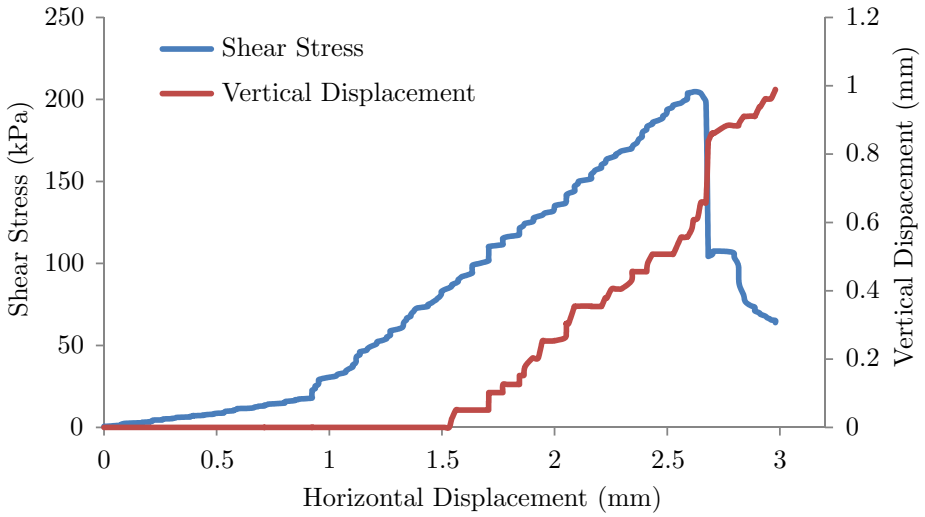

Figure 3.14: The direct shear test response curve of sample D-W1C6-3, plotting shear stress (τ_S) and vertical displacement (V_S) against horizontal displacement.

While this behaviour was observed in the majority of samples, no pattern could be identified as to when dilation begins, nor its maximum value, nor indeed whether it occurs at all. Additionally, the majority of samples displayed large amounts of dilation, such as that shown in Figure 3.13, as shear stress in the sample reached its maximum, which then extended after failure had occurred. Indeed, many response curves featured a sudden increase in vertical displacement as shear stress dropped as a result of sample failure, such as that shown in Figure 3.14. The drop in shear stress signals sample failure, while the corresponding dilation results from the sample expansion during failure. This expansion is due to soil particles moving over each other, and increasing sample height as a result.

It was also observed that many direct shear test samples, particularly those that contained wool, retained a considerable residual strength after peak shear strength had been reached and the sample had failed (see the post-peak curve in Figure 3.13). This behaviour had been previously reported in Consoli et al. (1998), where it was attributed to the addition of, in that case, fibreglass fibres. It therefore follows that this behaviour seen in the experiments described above may result from the presence of wool strands in the sample.

It is proposed that this residual strength is due to the fibre part of the wool, identified in Section 3.4.3, with the wool strands essentially acting as a 'carrier' for the fibres that provide the enhanced strength. Fibres which were embedded into the sample continued to hold the sample together after the macrocrack had formed, resulting in the residual strength seen in Figure 3.13. This proposal is further explored using SEM analysis in Section 3.7.

3.4.5 Experimental analysis of the effect of cement content on sample behaviour

Figure 3.15 shows the values of ϕ and c from Table 3.1, plotted against each other and arranged by cement content, as calculated through the method detailed in Section 3.4.2. The figure shows a wide variation in c (0kPa - 180kPa) and in ϕ (8˚- 76˚). While these values might appear high compared to typical geotechnical material investigations, it must be noted that RE by definition is highly unsaturated, heavily compacted, and in this case has fibrous and cementitious reinforcement. All of these factors would be expected to alter the properties of the soil, particularly ϕ and c as both are dependent on how well particles remain attached to one another when subjected to stress. Similar high values of ϕ and c have been found in other studies. For example, in Consoli et al. (1998) it was found that adding 1% cement by mass to a sandy soil increased c by 46.8kPa from 9.9kPa to 56.7kPa and increased ϕ to a lesser degree by 6˚ from 35˚ to 41˚. While the results obtained by that investigation inhabit a smaller range than reported in the investigation above, it is clear that high ϕ values are possible in cemented soils. Moreover, it is stated in Consoli et al. (1998) that cohesion is linked to cement content.

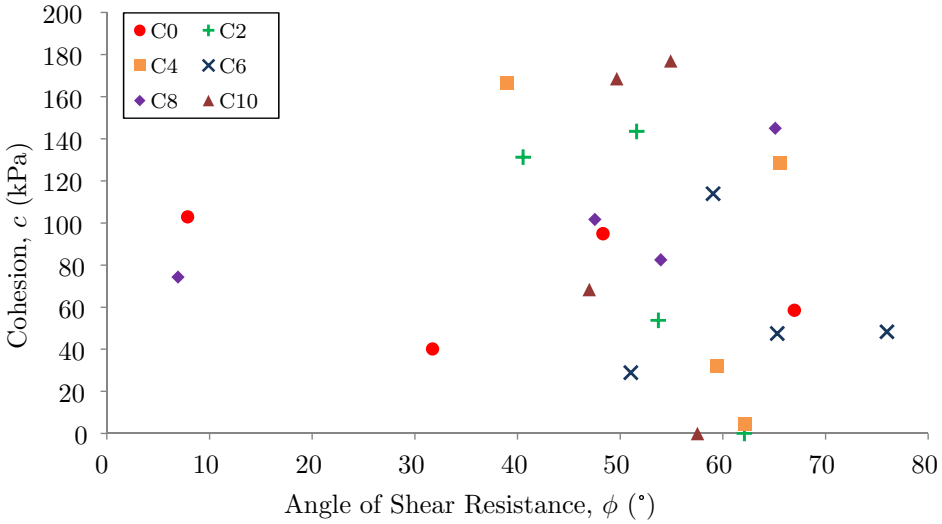

Figure 3.15: ϕ vs c of samples arranged by cement content.

The results of this investigation, in contrast, show no evidence of a similar increase (Figure 3.15) as there is no correlation between the samples with the same amount of cement, neither is there a correlation between samples with lower cement contents compared with higher cement content. While it might be suspected that this is due to the addition of the wool in the samples (as opposed the fiberglass used in Consoli et al. (1998)), it is noted that the samples without wool do not show a regular increase in ϕ with an increase in cement content (Figure 3.16), neither is any evidence seen of any link between cement content and cohesion. To find the source of the difference between results, differences between the soils, the stabilisation and the construction and testing method must be considered. Firstly, the soil used in

Consoli et al. (1998) could be categorised using the method detailed in Section 3.2.1 approximately as 8:31:61:0, or as 39*:61:00. This initially appears similar to the soil used in these experiments (30:60:00), although the main difference is in the composition of the 'silty-clay' fraction of the mix. While the 'silty-clay' fraction of the soil mix used in the experiments detailed above is mostly clay with a negligible amount of silt, the portion in Consoli et al. (1998) is largely silt. This difference in the makeup of the smallest particles, which are known to have a large effect on suction and hence strength (Jaquin and Augarde, 2012), could be the cause of this difference.

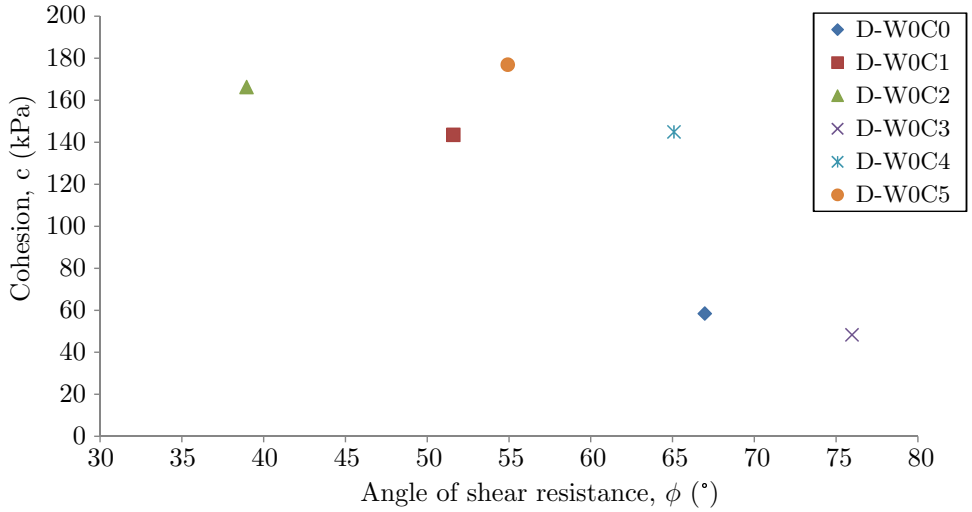

Figure 3.16: ϕ vs c of samples containing no wool, arranged by cement content.

The second potential source of difference between results is the range of cement and fibre contents tested. In Consoli et al. (1998), cement was added up to 1% by mass and fibres were added up to 3% by mass. While the mass of wool added was similar to the tests presented above, the mass of cement was up to a tenth of that added to the samples detailed above, the effect of which is discussed below.

Figure 3.15 shows two distinct outliers with unusually low values of ϕ. The plots used for calculation of ϕ for sample batches D-W2C0 and D-W3C4 are shown in Figures 3.17a and 3.17b respectively. While Figure 3.17b shows that some data points have been excluded from the plot due to incorrect sample failure as identified in Table 3.1, it is clear that the line of best fit of the remaining samples (shown in black) may not correctly display the accurate values of ϕ and c for the soil. This is the same for sample batch D-W2C0 in Figure 3.17a, except that all data points were valid in that instance. Instead, it is more likely that the actual lines of best fit for each of the data sets lie approximately on the red lines superimposed on the image. The red 'line of best fit' for batch D-W2C0 (Figure 3.17a) discounts both shear stress values calculated at highest normal stress, while the red 'line of best fit' for batch D-W3C4 discounts only the lower of the two shear stress values at highest normal stress. The red alternative lines of best fit result in values of ϕ and c which lie much closer towards the main body of data points in Figure 3.15; at $\phi = 23^{\circ}$, $c = 65$ kPa (D-W2C0) and at $\phi = 33^{\circ}$, $c = 86$ kPa (D-W3C4).

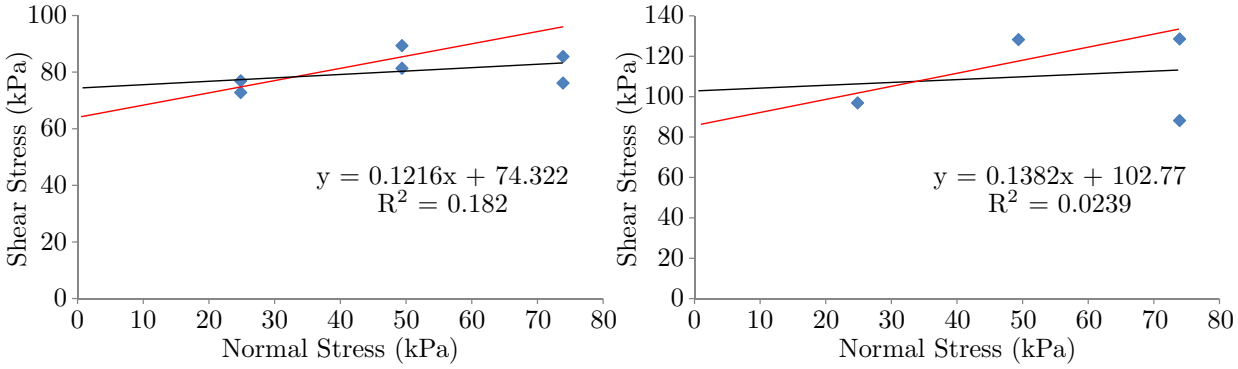

(a) Sample Batch D-W2C0.

(b) Sample Batch D-W3C4.

Figure 3.17: Plots of sample batches D-W2C0 and D-W3C4 used to determine ϕ and c.

However, while this analysis does result in some more realistic values of c and ϕ, the method raises some issues, particularly regarding the apparent discarding of a substantial number of supposedly valid results, depending on the soil batch (either a third or a quarter in the examples given above). It is therefore recommended that a greater number of duplicates are performed in future investigations such that erroneous data points might be more easily distinguished. It is recognised that the necessary data exclusion suggests that the DST might not be the most appropriate method of determining shear properties of RE, however two important things must be noted. Firstly, it is the apparatus and the test arrangement that caused some of the erroneous data. Secondly, and perhaps more importantly, it has been and will be shown that the test does produce recognisable trends and patterns in result analysis, which means that fair conclusions can therefore be drawn from the data.

Figure 3.18 shows plots of peak shear stress against cement content of samples containing no wool. Results are separated into different plots according to difference in applied normal stress: 25kPa, 50kPa and 75kPa respectively. All the figures show a clear increase in peak shear stress as cement content increases, although it is noted that there is considerable variation in the results, both with individual samples and between different applied normal loads. It is well established that adding cement to a RE mix increases unconfined compressive strength (for example in Jayasinghe and Kamaladasa (2007)) and these results show that increased cement content also increases peak shear stress of the sample.

In stabilised RE, cementitous bonds are the major source of inter-particle bonding, and hence strength, whereas at lower or zero values of cement content (i.e. unstabilised RE), matric suction becomes a significant source of strength (Jaquin et al., 2009). Cementitious bonds are, by nature, strong yet very brittle, which increases shear (and compressive) strength. The brittleness of the bonding implies that peak stress might be reached at a lower horizontal displacement than samples held through suction, however no pattern could be observed (Figure 3.15).

The construction method must also be considered when analysing the effect of cement addition to

RE, specifically with regards to how the cement was mixed into the sample. Not only was the cement added after equilibration, thereby allowing the cement to coat soil clumps as identified in Section 3.4.3, as opposed to mixing evenly through the soil, but no additional water was added to take account of the requirement amount for cement hydration. Some additional water was added with the cement so as to keep the water content constant at 11%, but by prioritising maximising compaction and keeping the sample at optimum water content, it is possible that the amount of water in the samples was not enough to allow the cement to undergo complete hydration, thereby leaving some unreacted cement in the soil matrix. It has previously been found (Jones, 2015), that there is a limit at which cement ceases to be effective due to lack of water present in the sample for hydration to occur, however when the chemical calculation of hydration is considered, there needs to be 4.2 times as much cement as water by mass (Jones, 2015). Considering the worst case in the samples above, there was 10% cement and 10% water clearly enough water for full hydration to occur. However, considering the makeup of the cemented structure that of balls of soil surrounded in cement it is possible, if unlikely, that some pockets of cement remained unreacted within the material in areas of minimal water. However, this scenario is judged to be fairly unlikely and so the cement may be assumed to be fully hydrated. Thus it may be concluded that compacting samples at optimum water content, whether containing cement or not, is the most appropriate method for sample comparison.

3.4.6 Experimental analysis of the effect of wool content on sample behaviour

It was observed that samples containing wool failed along uneven fracture planes, compared to those samples without wool present (see Section 3.4.3). The following hypotheses are proposed to explain this effect, assuming that failure initiates via fracture propagation as described in Section 2.4:

a) Wool in the sample adds areas of weakness. As shear stress increases in the sample, the crack is diverted to weaker areas which have less shear strength. Once the crack has found its way to a piece of wool, the wool then allows the crack to travel more freely through the sample. The overall effect is to decrease the overall crack energy needed for the sample to fail.

b) Wool present in the sample forces the growing crack path to change direction, making the crack path longer and the crack plane larger, which increases the maximum shear force.

Figure 3.19 shows plots of peak shear stress against wool content, for samples containing no cement. Results are separated into different plots according to applied normal stress - 25kPa, 50kPa or 75kPa respectively. Each plot shows a clear decrease in peak shear stress as percentage wool increases, each with a similar rate of decrease. It is likely that this behaviour is due to wool reducing bonding between particles. This thought is reinforced by observations made in Section 3.4.3 that samples containing larger

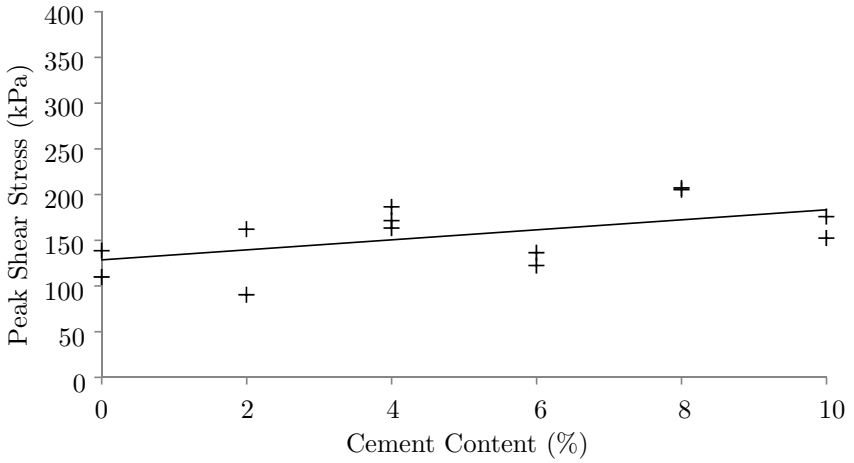

(a) The relationship between peak shear stress and cement content in cement-stabilised samples without wool reinforcement, tested at 25kPa applied normal stress.

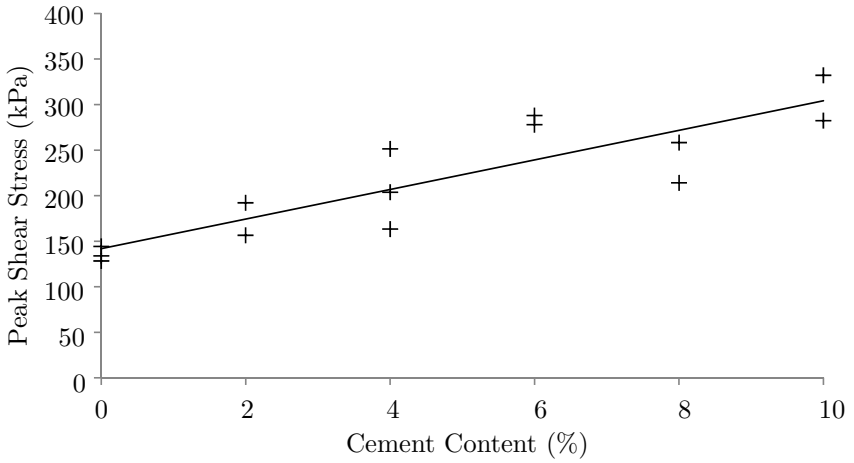

(b) The relationship between peak shear stress and cement content in cement-stabilised samples without wool reinforcement, tested at 50kPa applied normal stress.

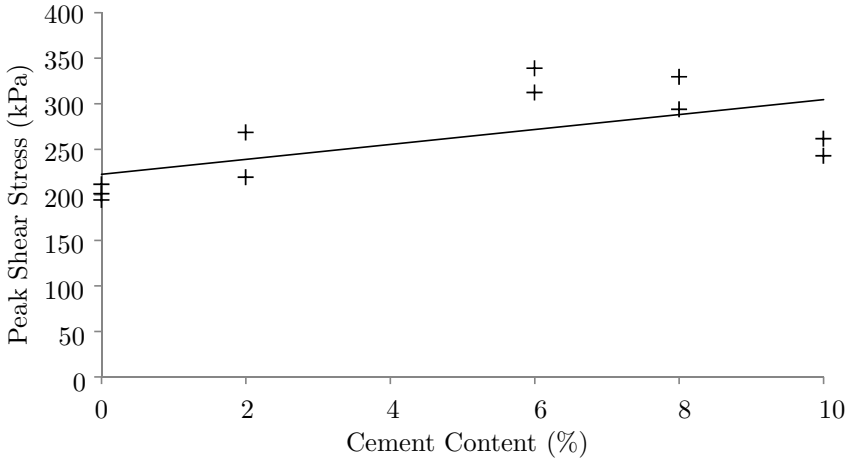

(c) The relationship between peak shear stress and cement content in cement-stabilised samples without wool reinforcement, tested at 75kPa applied normal stress.

Figure 3.18: The relationship between peak shear stress and cement content in cement-stabilised samples without wool reinforcement, tested at different applied normal stresses.

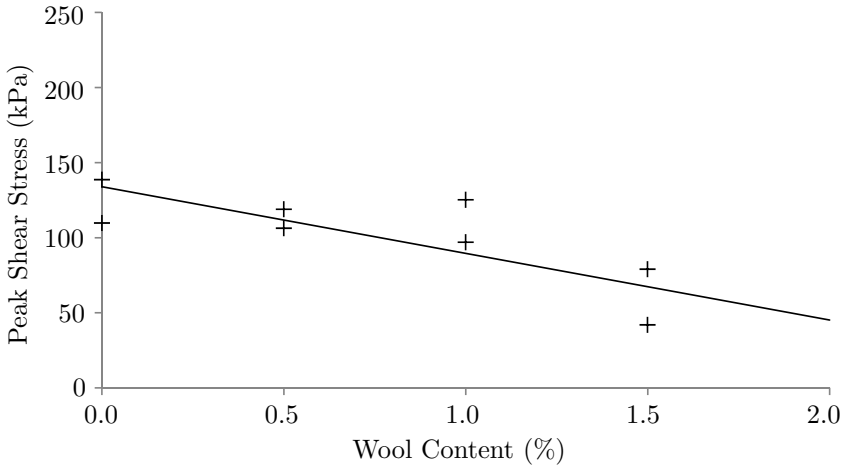

(a) The relationship between peak shear stress and wool content in wool-reinforced samples without cement stabilisation, tested at 25kPa applied normal stress.

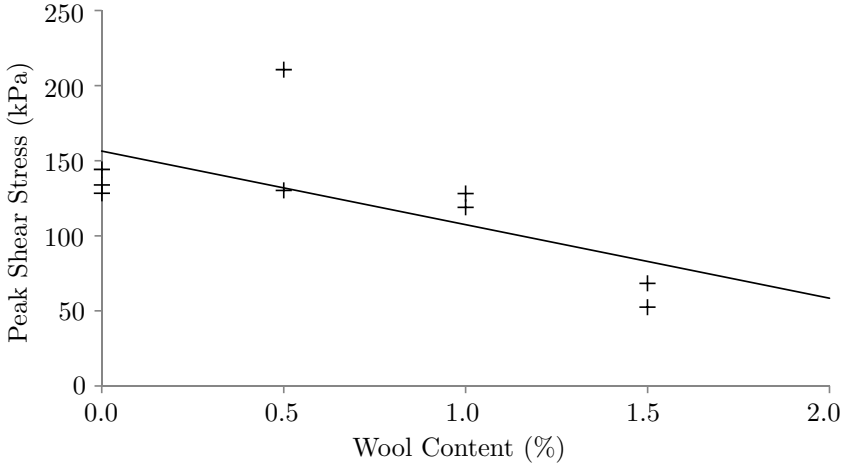

(b) The relationship between peak shear stress and wool content in wool-reinforced samples without cement stabilisation, tested at 50kPa applied normal stress.

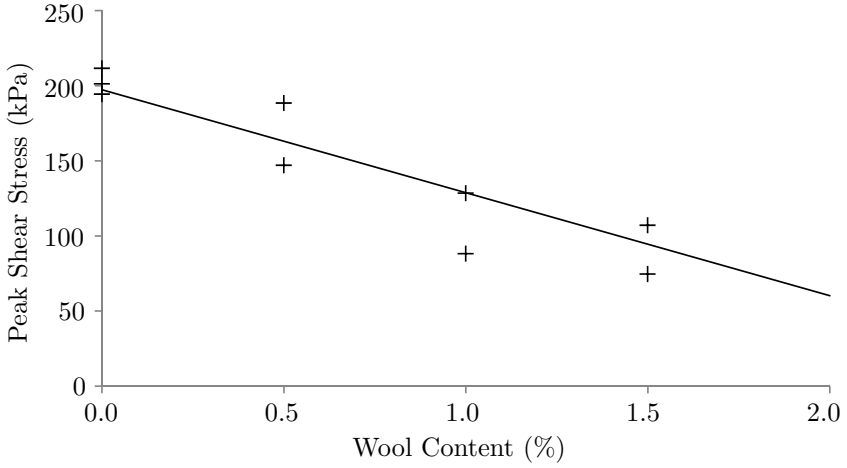

(c) The relationship between peak shear stress and wool content in wool-reinforced samples without cement stabilisation, tested at 75kPa applied normal stress.

Figure 3.19: The relationship between peak shear stress and cement content in wool-reinforced samples without cement stabilisation, tested at different applied normal stresses.

percentages of wool were more likely to collapse after sample construction. Table 3.2 shows a clear decrease in dry density as wool is increased, further supporting this theory.

Table 3.2: Effect of wool on sample density.

Wool Content (%)	**Average Dry Density (kg/m^3)**
0	2131
0.5	2084
1.0	2015
1.5	1938

During sample construction it was decided that the same amount of water would be added to each sample, independent of whether cement or wool was included in the sample batch mix. This was done in order to facilitate direct comparison between samples with and without cement and/or wool. This meant that some samples, particularly those with high amounts of cement, were not compacted at optimum water content as the addition of cement would likely affect the optimum water content of the sample. Basha et al. (2005) states that the addition of cement to a soil-rice husk ash mix increases the optimum water content but decreases the maximum dry density of the sample. However, during these experimentations, the water content was kept constant due to the comparative nature of the study. Had the samples all been compacted at their individual optimum water content, it would not only have been time consuming, but also would have imposed limitations on the different comparisons that have been made between samples.

However, as this method was uniform for all samples, then some comparisons are able to be made, and average dry densities may be used to compare the effect of adding wool to the sample. Every sample (other than batches D-L1 to D-L4) were included in calculations of dry density, meaning a minimum of 36 samples were used to calculate each average density value shown in Table 3.2, thereby mitigating the effect of cement altering the maximum dry density of the sample. It is noted, however, that this is expected to have a noticeable effect on the maximum dry density of the samples with high cement content, thereby causing the calculated average values in Table 3.2 to be lower than expected, as most samples would record a higher dry density if compacted at optimum water content. However, as the optimum water content is not expected to be affected by the addition of wool, then a comparison of values in the table may be be performed.

The decrease in peak shear stress (Figure 3.19) with increase in wool content could not be due solely to the decrease in dry density, as the dry density changes as a result of the addition of wool. One possible reason for this drop in strength could be due to the compressibility of the wool, as mentioned in Section 3.4.3. Application of general energy conservation laws implies that energy applied to the sample during compaction is absorbed either by the soil, the wool (if present) or the formwork containing the sample. Both the soil and the wool react to compressive force by compacting to relieve stress. While the

soil absorbs the energy through permanent deformation, the wool compacts through storing of potential elastic energy (as well as some irrecoverable deformation) in the fibres as they compress. Energy that cannot be contained through compaction of the soil or wool gets transferred into the formwork, which is then released as noise and motion, as the formwork is able to store negligible amounts of energy.

Potential energy stored in the wool will only have a physical effect on the RE when the potential energy in the wool is greater than the constraining forces in the RE preventing the wool from expanding. This can only happen through an increase in potential energy or through a decrease in constraining forces. As potential energy in a sample is fixed once the sample has been constructed, the potential energy will only affect the sample when the constraining forces are reduced. Energy stored in wool constrained on one by side by the formwork, for example, is released when the formwork is removed, and those wool fibres subsequently expand as mentioned in Section 3.4.3. The potential energy of wool fully contained in the sample, however, can only be released when the stored potential energy in the wool is greater than the constraining forces of the soil, which occurs once the sample has been weakened through application of shear forces during the direct shear test. Potential energy stored in this manner in the wool is assumed to be only small, as the wool strands can be easily manually compressed, but it is thought that this is the likely cause of any reduction of peak shear stress. It is therefore likely that hypothesis (a), mentioned at the start of this section, that wool creates areas of weakness not strength, is more likely than hypothesis (b). However, this is likely only the case when using compressible fibres.

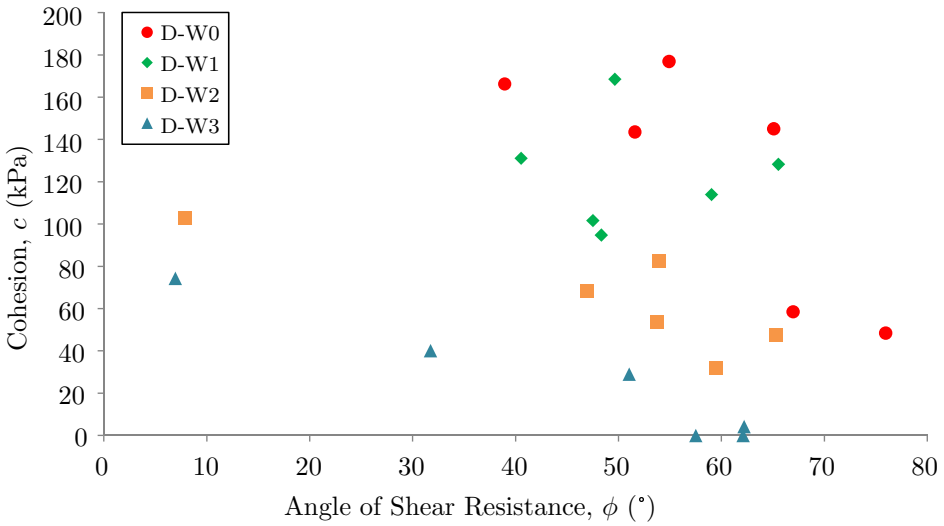

Figure 3.20: ϕ vs c of samples arranged by percentage wool content.

Angles of shear resistance (ϕ) and cohesion (c) are plotted against each other in Figure 3.20 as plotted in Section 3.4.5, but here arranged by wool content as opposed to cement content. Except for a couple of outliers with a low ϕ value of under 10° (which, as explained in Section 3.4.5, could lie at co-ordinates (ϕ = 23°, c = 65 kPa) and (ϕ = 33°, c = 86 kPa) for sample batches D-W2C0 and D-W3C4 respectively),

the figure shows that wool content has little effect on ϕ, as the variation and range is similar for each wool content group.

It is noted that there is a slight negative correlation in Figure 3.20, particularly evident in the batches with 1% and 1.5% wool, which appears to correspond neatly to a reduction in ϕ with a corresponding increase in c. However, there is considerable scatter around this relationship, implying that more samples should be tested in future in order to obtain a more reliable relationship. This is particularly relevant as the wool strands used this investigation are compressible, which has been discovered to be source of weakness in the sample. Considering that other investigations have found relatively small levels of scatter in their results (e.g. Maccarini (1993)), it is suggested that again, it is the wool that is the main cause of scatter issues. However, it appears rare that papers include data on result variability, which means that it cannot be stated with certainty that the results obtained in this thesis are more or less variable than the majority of other investigations into similar materials. However, if it is the case that the data presented in this thesis is more variable than the majority of other papers, this may be put down to the composition of these soil mixes.

It has previously been discussed that adding compressible fibres (waste carpet fibres, in this case) may add uncertainty about the sample behaviour due to the potential energy stored within the wool, however it is also possible that the variation in wool length plays a more significant role in the variability in the sample. Section 3.2.2 describes that the carpet fibres were provided in 'mats' which were then cut in strips of approximately 40mm width, which led to a variation in length of wool strands between 20 and 60mm. Considering that Aymerich et al. (2012) and Festugato et al. (2017) found that wool fibre length has a great effect on the behaviour of cemented and uncemented soils, it therefore must follow that the behaviour of the samples in this thesis also would be dependant on this variable. Considering the size and number of samples required, it was not practical to precisely control the length of each wool strand, it is assumed that the average sample had an even distribution of fibre lengths. As this cannot be confirmed, it is possible that some of the variation in the samples comes from this source.

However, this theory does not account for the variation seen in samples that do not contain wool. Considering that the samples were made in batches, it is possible that different samples have slightly different particle size distributions, which is known to affect sample behaviour (Hall and Djerbib, 2004b), however this is unlikely as the samples were well mixed and this is a standard method of making samples. It is more likely, therefore, that minor variations in sample size, compounded by the required construction method for the direct shear test, lead to larger variations in the results than expected. These variations might be expected to largely be removed through multiple sample testing, but the sample uncertainty remained as can be seen in the low R^2 values seen in Table 3.1

It is therefore recommended that, in future, tests on compressible fibres should use a larger number of

repeated samples, and should, if possible, control the fibres length in order that any random errors and experimental uncertainties in calculation of ϕ and c might be more easily identified and accounted for. A greater number of samples tested lead to a greater number of points plotted on the ϕ-c determination plot (Figure 3.9) and should place the plotted points on the ϕ-c comparison plot (Figure 3.20) in a closer region to each other, with particular emphasis on the proximity of values of ϕ.

Unstabilised SBCMs are known to source the majority of their compressive strength from water forming menisci between soil particles, which then shrink and add strength as the soil dries (Jaquin et al., 2009). Due to the substantial reduction in cohesion and maximum shear strength with the addition of wool (Figure 3.20), it follows that water does not attach to the wool with the same strength as it does to soil particles. This could be due to the wetting behaviour of wool, specifically that natural wool is slightly hydrophobic (Nakamura and Matsukawa, 1971). It is unknown, however, how the processing of the wool in preparation for carpet manufacturing might affect its hydrophobic qualities. Additionally, some carpets contain polyester and other plastic strands, which might affect the hydrophobic properties. Unfortunately, it was not possible to confirm with the supplier what other materials lay in the supplied carpet, and what the possible effect of this might be on the hydrophobic properties of the wool. Another potential contributing factor to the effect of wool, on drying rate in particular, is that if the wool is connected through to the surface of the sample, it is suggested that wool may wick away water from surrounding soil particles as the wool strands have air gaps between them, further weakening areas already weakened by the wool due to reduction in density. Moreover, the reduction in cohesion could be exacerbated by the expansive internal forces from the compression of the wool during construction (Section 3.4.3). Figure 3.20 shows a clear decrease in cohesion with increase in wool, while as the amount of wool in a sample increases, the amount of expansive internal force increases. This directly suggests that the wool is countering the cohesion of the soil in the sample, thereby reducing the recorded cohesion.

3.4.7 Discussion of the relationship between vertical and horizontal displacement at maximum shear force

The plots in Figure 3.21 compare the value of maximum shear force with the vertical and horizontal displacements measured at that maximum. Sample data is provided in Appendix B. Figures 3.21a, 3.21c and 3.21e display the results grouped by wool content, while Figures 3.21b, 3.21d and 3.21f display the results grouped by cement content. The figures are also paired such that Figures 3.21a and 3.21b display the same plot of maximum shear force against horizontal displacement, arranged by wool content and cement respectively. Likewise, Figures 3.21c and 3.21d plot maximum shear force against vertical displacement, and 3.21e and 3.21f compare horizontal with vertical displacement at maximum shear force, such that all variables are compared with each other in a way that any patterns might become clearer.

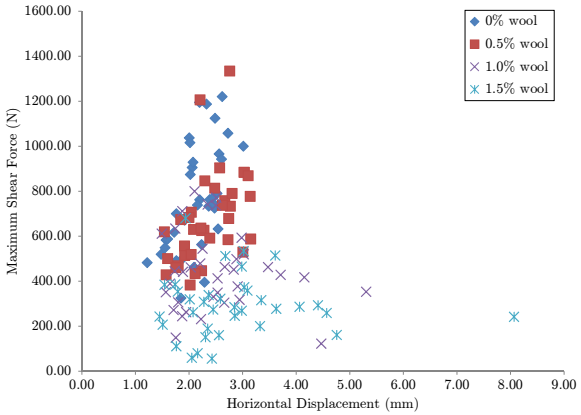

(a) The relationship between maximum shear force and horizontal displacement at maximum shear force, grouped by wool content.

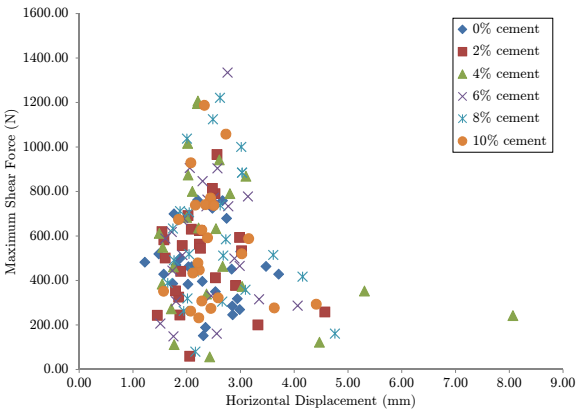

(b) The relationship between maximum shear force and horizontal displacement at maximum shear force, grouped by cement content.

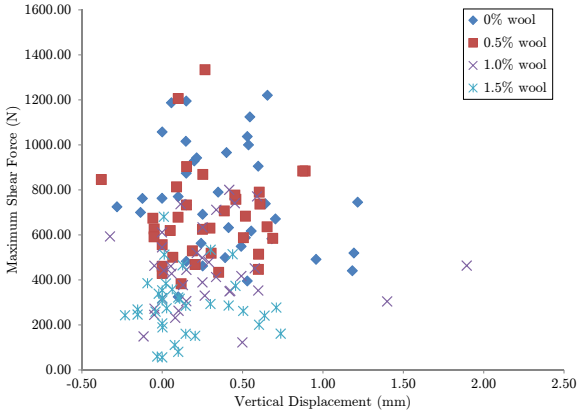

(c) The relationship between maximum shear force and vertical displacement at maximum shear force, grouped by wool content.

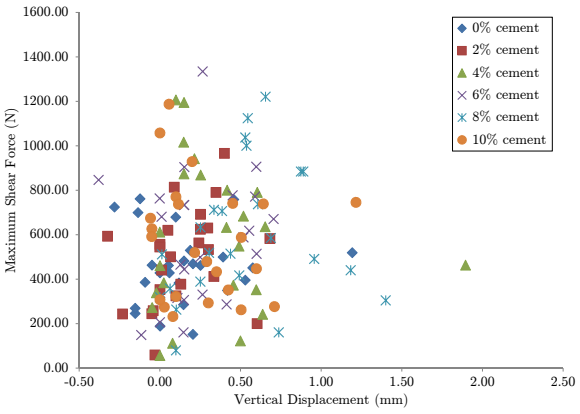

(d) The relationship between maximum shear force and vertical displacement at maximum shear force, grouped by cement content.

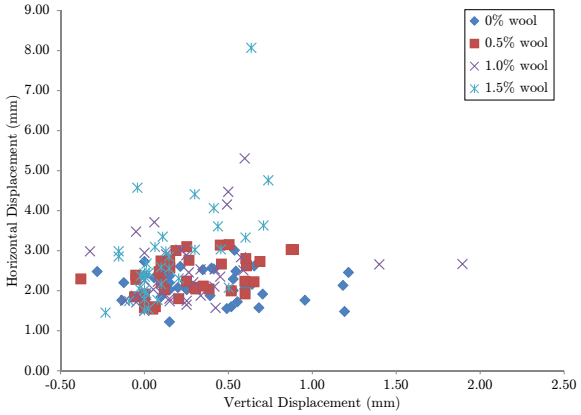

(e) The relationship between horizontal and vertical displacement at maximum shear force, grouped by wool content.

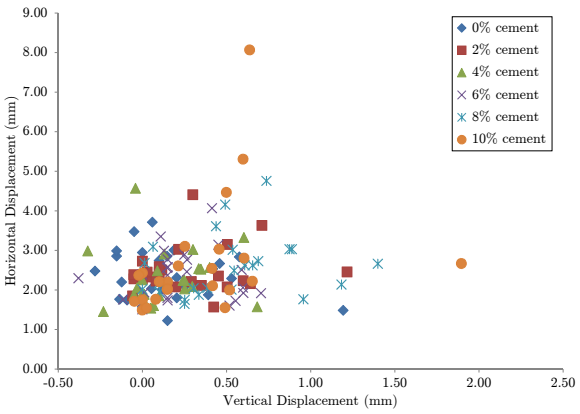

(f) The relationship between horizontal and vertical displacement at maximum shear force, grouped by cement content.

Figure 3.21: Figures showing the relationship between maximum shear force, horizontal and vertical displacement at maximum shear force, wool content and cement content in direct shear test samples.

Figure 3.21a shows a distinct inverse relationship between wool content and maximum shear force, supporting suggestions made about wool weakening the sample in Sections 3.4.3 and 3.4.6. The figure also implies a general increasing variation in horizontal displacement as percentage wool increases, marked by a spreading out of results closer to the x-axis. This shows that, in general, a higher wool content leads to a larger horizontal displacement at maximum shear force, therefore implying that adding wool to a rammed earth sample increases the plastic limit of the sample. No such pattern can be seen in Figure 3.21b, suggesting that adding cement does not appear to increase brittleness nor increase peak shear strength, which may seem contrary to the known behaviour of cement, that a cement-based material is brittle, but also agrees with the conclusions presented in Section 3.4.5, that cement was found to have no effect on the cohesion or angle of shear resistance of the material. It must be noted, however, that the results presented in Figure 3.18 in Section 3.4.5, which showed an increase in shear stress with an increase in cement content, did not contain any wool. Thus it may be reasoned that any increase in maximum shear force gained by adding cement is subsequently removed if wool is also added.

Figure 3.21c shows the same decrease in shear force with increase in wool as previously identified in Figure 3.21a, but it also shows that vertical displacements are more evenly distributed across the range of values for each different wool percentage rather than clustered around a more common displacement, i.e. the range of vertical displacements is much smaller than the range of horizontal displacements in Figure 3.21a (the majority of samples across all wool contents fall in a 1.5mm band) but the points are evenly distributed among them, marking little correlation between maximum shear force and vertical displacement with relation to wool content. Less still can be said about Figure 3.21d, as it shows no appparent correlation between maximum shear force, cement or vertical displacement.

Figures 3.21e and 3.21f show little that has not been previously observed and reported, but they do help to illustrate the variability in the results. Figure 3.21e further supports the observation made in Figure 3.21a, that as wool content increases, the variation in horizontal displacement at maximum shear force increases. There appears to be little correlation between wool content and vertical displacement. Figure 3.21f also shows no apparent correlation between cement content, horizontal and vertical displacement.

Thus it can be concluded that, while cement does affect the results in these experiments, wool is by far the most significant factor for determining shear strength, cohesion or angle of shear resistance. While it is generally due to the internal forces resulting from the compression of the wool, the fibres do play an active role in holding the sample together post-failure. It is therefore proposed that more predictable and beneficial effects might be achieved from adding the same amount of wool *fibre* by mass, as opposed to wool *strands*. While this is impractical for sourcing wool from a carpet waste stream, similar effects may be achieved from other, similar waste streams that do not come in strands.

3.4.8 Analysis of the effect of water content on sample behaviour

A separate set of direct shear test samples was made with varying initial water content, as stated in Section 3.4.2. These were used to investigate the effects of water content on shear behaviour. Each sample was compacted to the highest dry density for its water content, calculated using the same method detailed in Section 3.4.2, to maintain consistency of the compaction method. The samples were tested in the same manner as described for the other direct shear test samples as detailed in Section 3.4.2. Figure 3.22 plots the resultant values of ϕ and c against the water content.

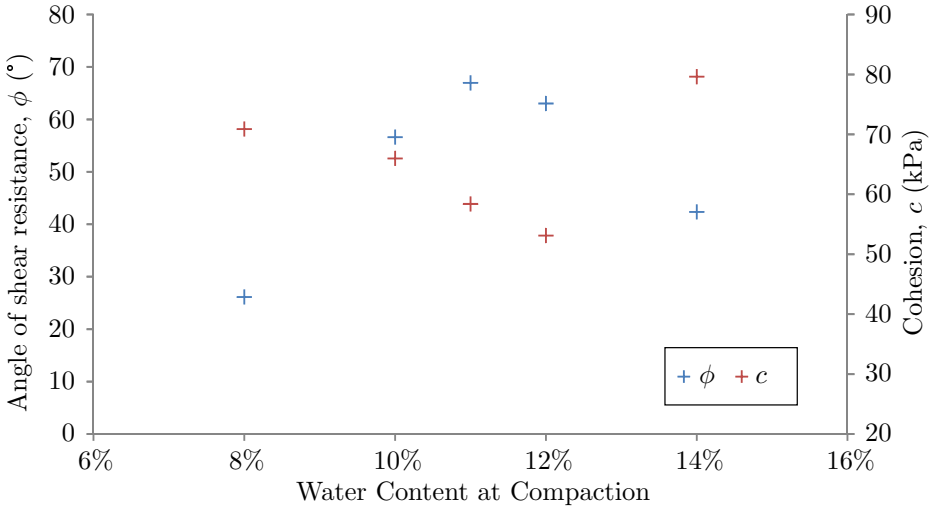

Figure 3.22: Change in ϕ and c relative to percentage water content.

Figure 3.22 shows clear variations in ϕ and c as the water content was increased. At the optimum water content (11% for this soil, see Section 3.2.1), ϕ reaches a maximum. In contrast, c decreases until 12% water content, after which it rises. However, as water content is not a property of the material, water content itself cannot affect the cohesion of shear resistance of the material. Instead, the water content affects compaction and hence the dry density, which in turn results in a higher cohesion due to particle interlock. It is therefore more appropriate to look at the effect of dry density on c and ϕ rather than looking directly at water content, as the same dry density can be obtained from two different water contents.

Figure 3.23 shows the same data as in Figure 3.22, but plotted according to dry density as opposed to water content. It can clearly be seen that as dry density increases, ϕ also increases while in contrast, c decreases. It is known that water content at compaction has a large effect on the dry density of the sample as seen in Figure 3.2, but Figure 3.23 shows that compaction amount also clearly has an effect on cohesion and angle of shear resistance of the sample. If a sample is compacted to a lesser degree, then the void ratio of the soil (that is the ratio of air : solids in the soil) would be larger, and would therefore offer

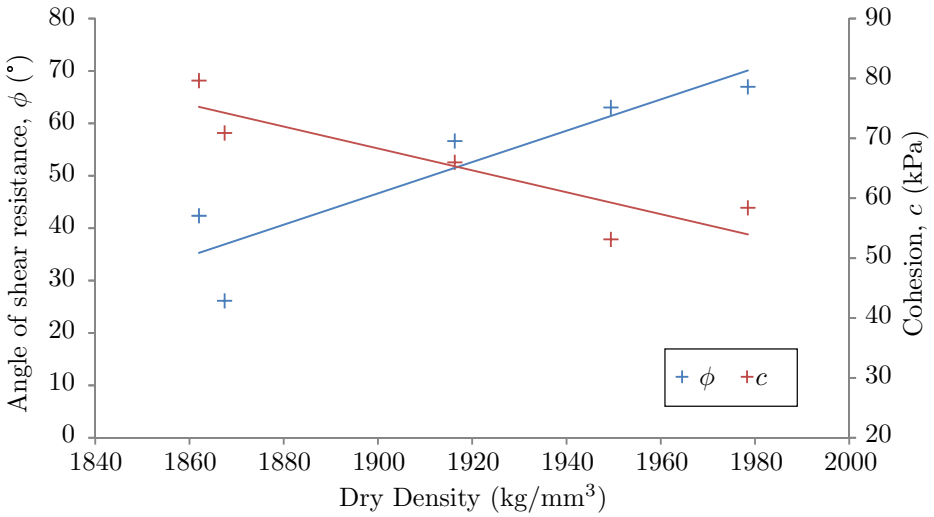

Figure 3.23: Change in ϕ and c relative to dry density.

decreased resistance to shearing and lower angle of shear resistance. Figure 3.24 shows in two simplified sketches how compaction might relate to the angle of shear resistance. Minimal compaction in Figure 3.24a results in a minimal force F required to shear the sample under vertical loading N. Figure 3.24b, in contrast, shows how greater compaction might lead to a greater shear force F to counter normal loading N, resulting in a larger angle of shear resistance ϕ.

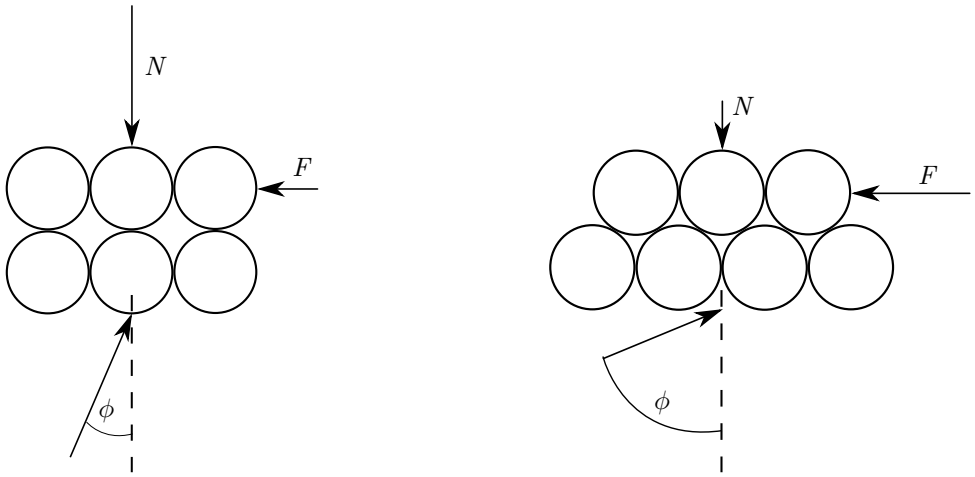

(a) Simplified sketch of forces resulting in a low ϕ value. (b) Simplified sketch of forces resulting in a high ϕ value.

Figure 3.24: Simplified sketches of the applied forces in a direct shear test to determine ϕ.

In summary, the DST is able to produce some reliable results, even though the reliability of some of those results is questionable. It is also to notice trends and patterns, if they are present, despite its disadvantages when compared with other tests. However, as the DST is a very simple and quick test to run, and the apparatus should be available in soil mechanics laboratories around the world, it is recommended that this test's use in SBCM is further investigated, in order to perform research into the reliability of the test when used on SBCMs, to further understand its limitations, and to discover if any

adaptations may be made to improve the reliability of the test.

3.5 Triaxial tests

The triaxial test is used to determine the shear strength of a soil sample and is a commonly used alternative to the direct shear test. Two advantages that the triaxial test has over the direct shear test are the ability to test undisturbed cored soil samples, which are often more easily obtained from site than shear box samples, and improved control testing conditions, including drainage and confining pressures. More importantly, however, the failure plane of a triaxial sample is not as well prescribed as in the DST, therefore allowing the sample to failure along a weaker plane. This means that triaxial tests are more conservative in their determination of shearing properties than the direct shear test. It is also able to measure volume change more accurately than the direct shear test and is less dependant on the accuracy of specimen dimensions. However, it is a slower test to perform and the equipment preparation is more complex. Two of the few experiments performed on SBCM samples using triaxial testing are reported in Jaquin et al. (2009) and Cheah et al. (2012). Jaquin et al. (2009) reports on tests which used tensiometers to measure suction in a sample tested in a triaxial rig and identified that suction in soil particles in RE is the source of its strength. Cheah et al. (2012) used the triaxial test to compare shear test methods with the triplet test, and found that triaxial test were more practical than triplet tests in many ways including test feasibility and apparatus availability. Low amounts of different fibres (0.05% and 0.1% by mass) were added to the samples, and found that fibres decrease cohesion and increase the angle of shear resistance (called the angle of internal friction).

This section presents an investigation into the triaxial testing of rammed earth samples and compares the results obtained with those gathered using the direct shear test in Section 3.4, and results reported from other investigations, in order both to verify the previous results and to determine whether the direct shear test is a suitable test method for determining the shearing properties of SBCMs.

3.5.1 Background to the triaxial test

The triaxial test, described in the British Standard BS1377-8, consists of placing a cylindrical soil sample, typically 38mm or 100mm in diameter and twice as tall, in a pressurised water cell. The sample is sheathed in a rubber membrane to prevent water from entering or exiting the sample via the sides of the sample. Caps on each end may be used to control and/or measure water leaving the sample, depending on the type of test required. Figure 3.25 shows a simplified schematic of the testing apparatus. A triaxial rig can be used to apply an evenly distributed cell pressure from the water in the perspex cell (σ_c) and applied vertical pressure from the piston (σ_v). A triaxial test usually involves two stages of testing. During the

'consolidation' stage, the cell pressure (σ_c) is increased to a desired value and drainage of the soil sample, if applicable, is allowed to a known back pressure. In the secondary stage, a vertical displacement is applied to the sample via a proving ring attached to the apparatus frame, and the corresponding vertical axial stress (usually compressive but can be tensile) is measured.

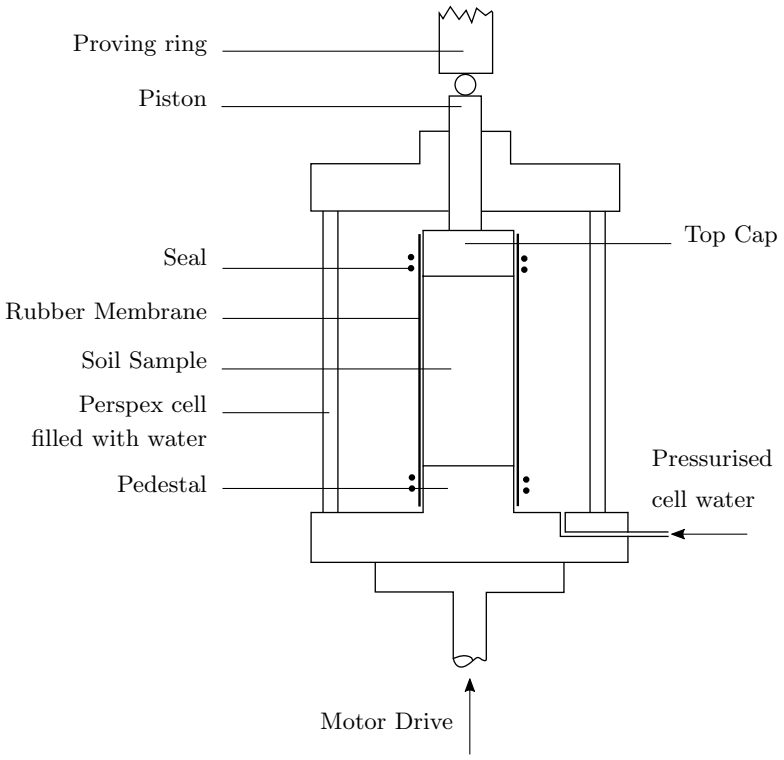

Figure 3.25: Schematic of triaxial test, adapted from Powrie (2013).

There are many options for the conditions under which triaxial tests are performed; these are described in full detail in Powrie (2013). A simple triaxial shearing test, called the conventional triaxial compression test, does not require consolidation or control of water flow into or out of the sample, and is generally the most appropriate test to use for SBCM samples. Conventional triaxial compression tests are performed *unconsolidated* and at *constant water content*.

In conventional soil mechanics investigations, triaxial samples are tested either fully saturated or partially saturated and typically involve investigations into the effects of water ingress or egress from the soil sample. As RE is a highly unsaturated and highly compacted material and this investigation does not require the ingress or egress of water during testing, this leads to a potentially unpredictable shearing behaviour and a different approach to triaxial testing is therefore required. Conventional unsaturated soil mechanics approaches also generally calculate the effective stress σ' of the soil as recommended in British Standard BS1377-8. Equation 3.6 is an alternative arrangement of Terzaghi's *principle of effective stress*, reported in Equation 3.5. σ is the total stress in the sample, u_w is the pore water pressure, S_r is the degree of saturation (volume of water V_w divided by the volume of voids V_v in a sample) and u_a

is the pore air pressure. Terzaghi's *principle of effective stress* is applicable only for saturated soils, and Equation 3.6 is applicable in unsaturated soils as well. Note that the equations converge if the degree of saturation S_r is 1, i.e. if the soil is completely saturated.

$$\sigma' = \sigma - u_w \tag{3.5}$$

$$\sigma' = (\sigma - u_a) + S_r(u_a - u_w) \tag{3.6}$$

However, as with the direct shear test samples in Section 3.4, the effective stress in the samples cannot be calculated as the internal structure of the soil, specifically regarding the pore water pressures, are not known. Therefore, as with the direct shear test samples, values of total stress σ were calculated and used in analysis.

3.5.2 Sample production and testing

12 triaxial samples were constructed in 4 batches of 3 samples, each 38mm in diameter and 76mm in height. Each sample batch contained either 0 or 4% cement by mass and either 0 or 0.5% wool by mass, and were mixed according to the procedure outlined in Section 3.2. These amounts of cement and wool were selected as they lie in the middle of the range of cement and wool contents used in the direct shear test samples. Sample IDs were assigned according to the procedure in Section 3.2.3, with the Test ID 'T'. The triaxial samples were, like the direct shear samples, statically compacted in a custom formwork, at the optimum water content of 11% and to a known dry density. Samples were constructed in two 38mm layers to ensure optimum compaction as samples compacted in one layer were found to be very granular at the base of the sample upon removal from the mould; a sample compacted in two equal layers produced a more homogenous sample. However, this method does create a potential weakness in the sample, as at the join between the two 'lifts' or layers of soil, there will be a slight, if minor, discontinuity. No soil particles will sit across this join due to a heavily compacted layer underneath, and neither will any wool cross the layer. This will result in a slight loss in cohesion along the compaction layer, which might result in an irregular failure pattern or a slight reduction in ϕ. It is noted that this layering is also present in RE construction, therefore is it not unreasonable for a layer boundary to be present within the test samples. No irregular failure patterns were observed during testing, however, although the potential effects of the reduction in ϕ are discussed in Section 3.5.3.

Triaxial samples were re-weighed and tested 7 days after construction, consistent with the procedure of testing the direct shear test samples. After 7 days, the average water content of the samples was 0.6%.

Each triaxial sample was placed in a triaxial rig before undergoing a conventional triaxial compression

test: unconsolidated and at constant water content. Consolidation was not required as the samples were unsaturated, and the sample was tested at constant water content in an attempt to replicate real-world conditions. This produced a positive side effect of reducing the time taken for each test compared to standard triaxial investigations. σ_c was set to a known pressure before an increasing vertical displacement was applied to the sample, which created a vertical force V_T, recorded on a data logger, from which the axial stress σ_a could be calculated. As with the direct shear test samples, the displacement-controlled vertical load was applied at a rate of 1mm/min. In each batch of three samples, one sample was tested at a cell pressure (σ_c) of 25kPa, one at 50kPa and at 75kPa as per the normal stresses in the direct shear test.

σ_c and σ_a were converted into the major and minor principal stresses, σ_1 and σ_3, using

$$\sigma_1 = \sigma_c + \sigma_a \tag{3.7}$$

$$\sigma_3 = \sigma_c \tag{3.8}$$

Figure 3.26 shows how the typical assembly of a plot to calculate the cohesion (c) and angle of shear resistance (ϕ) from a set of Mohr's circles. From the triaxial tests performed, and Equations 3.7 and 3.8, values of σ_a, σ_c, σ_1 and σ_3 can be used to plot similar circles. Once the Mohr's circles have been plotted, the tangential intercept of the circles can be calculated by using the method detailed in Craig (2004) and presented below.

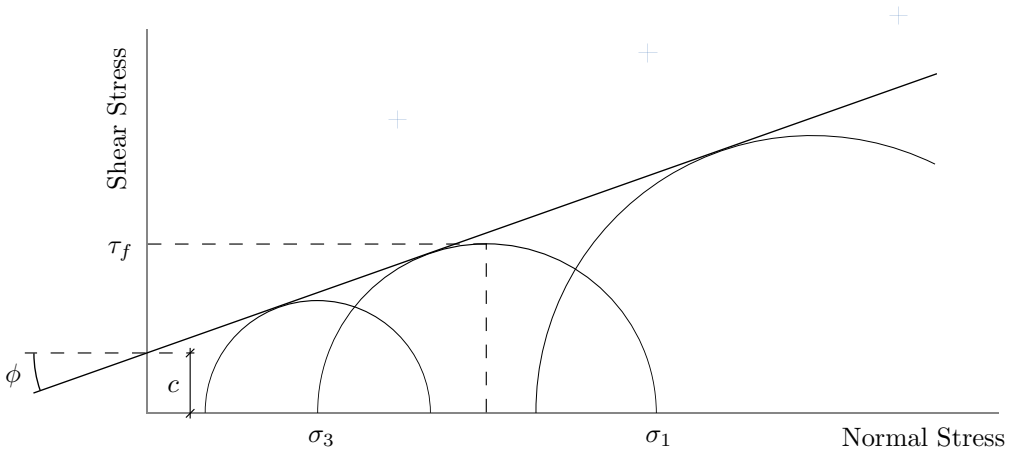

Figure 3.26: Example plot of the Mohr's circles for determination of c and ϕ.

Let the co-ordinates of the tangential intercept equal (σ_f, τ_f) where formulae for σ_f and τ_f are presented in equations 3.9 and 3.10 respectively and the value of θ is presented in equation 3.11.

$$\tau_f = \frac{1}{2}(\sigma_1 - \sigma_3)sin2\theta \tag{3.9}$$

$$\sigma_f = \frac{1}{2}(\sigma_1 + \sigma_3) + \frac{1}{2}(\sigma_1 - \sigma_3)sin2\theta \tag{3.10}$$

$$\theta = 45^\circ + \frac{\phi}{2} \tag{3.11}$$

The angle of shear resistance ϕ may be determined through trigonometrical analysis using

$$sin\phi = \frac{\frac{1}{2}(\sigma_1 - \sigma_3)}{c.cot\phi + \frac{1}{2}(\sigma_1 + \sigma_3)} \tag{3.12}$$

which may be arranged to give

$$2c.cos\phi = (\sigma_1 - \sigma_3) - (\sigma_1 + \sigma_3)sin\phi \tag{3.13}$$

Equation 3.13 was then used to calculate the value of ϕ (i.e. angle of the tangent) between two of the three Mohr's circles via simultaneous equations, after which c was calculated by inputting the ϕ value into equation 3.13.

Difficulties in calculating correct values of ϕ and c arose due to the constructed Mohr's circles not aligning, an example of which is shown in Figure 3.27. Each case was considered individually and slightly different approaches were used for different batches. In two cases, samples T-W0C0 and T-W1C0, a range of possible values of c and ϕ were calculated as it was unclear which pairing of two Mohr circles showed the 'true' properties of the soil. In these cases, three different possible values of c and ϕ (shown in Figure 3.27) were calculated using the method above and reported as as a range of likely values.

In the remaining two cases, batches T-W0C4 and T-W1C4, one of the set of three Mohr's circles was discounted as any calculations involving it produced unrealistic (i.e. negative) values of c or ϕ. Figure 3.28 shows one such example, for batch T-W1C4, where the Mohr's circle for the second sample (at 50kPa normal stress) lies completely in the Mohr's circle for the first sample (at 25kPa normal stress), thereby making a tangent between the two circles impossible. Additionally, the tangent between the second and third Mohr's circles (shown in blue in the Figure) resulted in a very high ϕ value (45°) and a very low c value (15kPa), lying outside the expected range obtained from analysing the other samples. Therefore this result was discounted and the tangent between Mohr's circles 1 and 3 was therefore used to calculate reported values of ϕ and c (shown in red).

When performing triaxial tests on soils, it is expected that sample variability is high if the water content varies between samples. Sample variability in these experiments are unlikely to have come from

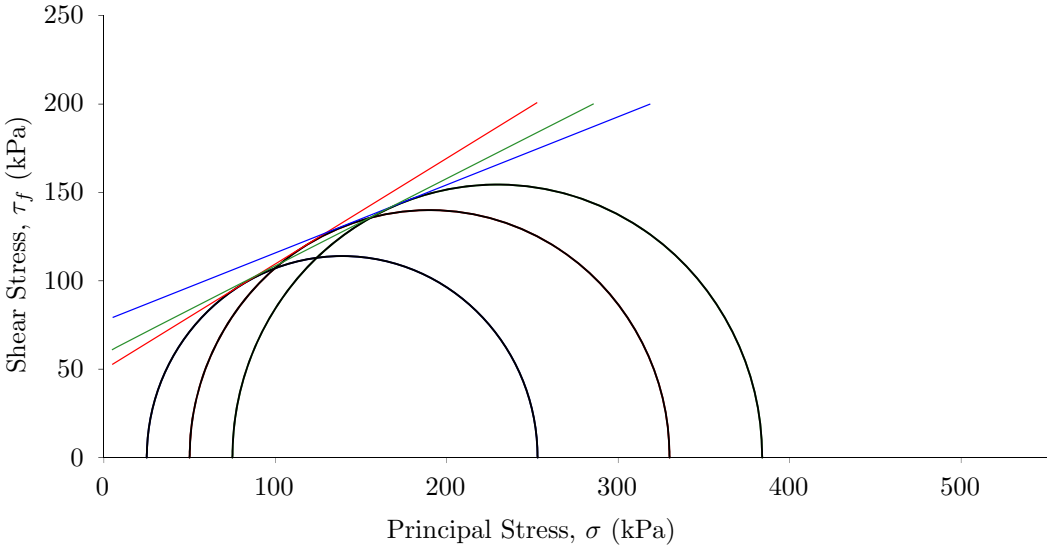

Figure 3.27: Example of possible variation in c and ϕ from tangential pairings.

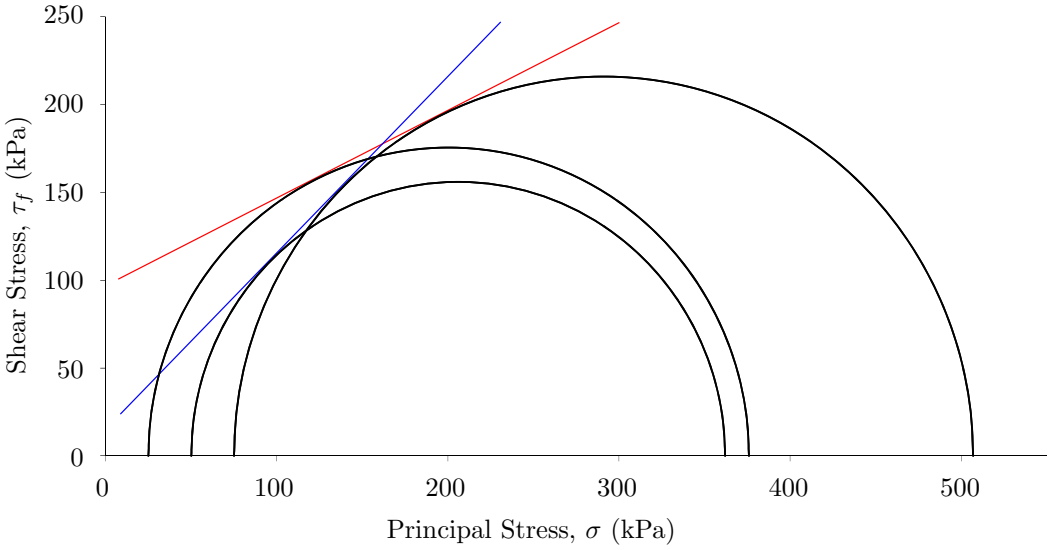

Figure 3.28: Example of discounted Mohr's circles.

this, however, as water content will play a negligible role in strength of a stabilised sample if the cement has fully hydrated (which these samples above may be assumed to be). Sample variability may be removed from the inclusion of UCS results in the graphs, as a UCS test is equivalent to a triaxial test without a confining pressure σ_3. The stress paths within each sample should be identical, and would be plotted similarly on a shear stress-normal stress graph, except that a plotted UCS test would show zero normal stress at zero shear stress. The results of the UCS test in Section 3.3 were not included, however, as the samples were of distinctly different size and shape, and are therefore expected to behave differently due to corner effects.

3.5.3 Results and discussion

During testing, it was observed that the triaxial tests were slower to perform than the direct shear tests, and the sample preparation was more complex. However, any minor inaccuracies in sample size were less problematic than those faced in the direct shear test, and it is also able to test more complex loading scenarios. Table 3.3 presents c and ϕ values from the performed triaxial tests, alongside equivalent values obtained from the Shear Box tests reported in Section 3.4. Some of the triaxial values of c are presented as ranges due to uncertainties in the calculation procedure as detailed in Section 3.5.2. It is noted that all samples failed in shear diagonally through the sample.

Table 3.3: c, ϕ and R^2 values for the triaxial test, including comparative values obtained from the direct shear test. Note that only Batch IDs are provided so that the results from different tests of the same soil batch may be presented side by side.

	Triaxial		Direct shear	
Batch ID	c **(kPa)**	ϕ (°)	c **(kPa)**	ϕ (°)
W0C0	72-101	13-23	58	67
W1C0	50-75	22-31	95	48
W0C4	140	22	133	53
W1C4	96	27	128	66

The triaxial results imply that adding wool reduces cohesion, while cement increases cohesion in the sample. Moreoever, neither wool nor cement appear to have a noticeable effect on the angle of shear resistance of the sample. There is a minor indication that wool increases ϕ by a small amount (around 5kPa), although not enough samples have been performed to be able to state this categorically. These results partially align with the conclusions drawn from the direct shear tests in Section 3.4: that wool reduces cohesion and that neither wool or cement appear to have a great effect on the angle of shear resistance of the sample. However, the direct shear tests found no evidence of the cement increasing cohesion in the sample, in fact clear evidence was seen showing that cement has no effect on the cohesion in the sample (Figure 3.15). The apparent increase in cohesion from cement in the triaxial samples (and, indeed, in the DST samples listed in Table 3.3) is likely chance due to high result scatter, as seen in Figure 3.15.

In comparing the values of c and ϕ determined from the triaxial tests with the values determined using the direct shear test (Table 3.3), that while there is some variation between the reported cohesion values, values of ϕ obtained from the triaxial test are roughly half of the values obtained from the direct shear test. Possible reasons for this behaviour are discussed later in the Section.

While no investigations are known to have been performed into SBCMs using the direct shear test, a few papers have been published detailing investigations into the behaviour of SBCMs and soils stabilised with cement and/or fibres using the triaxial test. Figure 3.29 plots the results of a couple of these

investigations - Diambra et al. (2010) and Maccarini (1993) - alongside the data provided in Table 3.3.

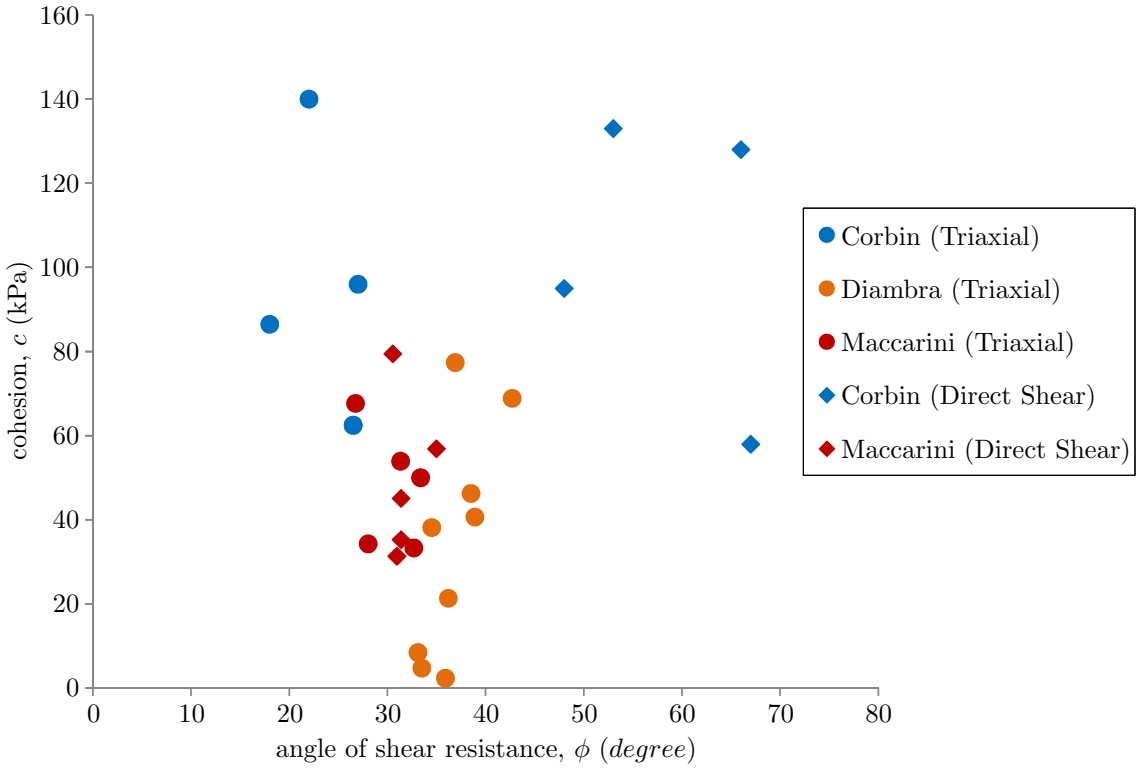

Figure 3.29: Comparison of DST and triaxial data, including data from Diambra et al. (2010) and Maccarini (1993)

Not only does Figure 3.29 highlight similarities and differences between the data sets presented in Table 3.3, but it also shows clear substantial differences between the calculated data sets and the data sets from other publications recorded in the figure, in both values of c and of ϕ. The 'Corbin (Triaxial)' and 'Corbin (Direct Shear)' data sets in the figure clearly show strong similarities between c values as identified in Table 3.3 and highlight the rough doubling of ϕ. It is noted that the ϕ values lie either side of the 'Diambra' and 'Maccarini' data sets. This indicates the possibility of two minor errors in the determination of ϕ - a slight undercalculation in the triaxial samples and a slight overcalculation in the direct shear samples - leading to a large difference between the two. It is unclear what might cause this difference, although possible reasons include the role of cement and wool in the samples which have already been found to either be problematic (wool in Section 3.4.6) or suspected to be (cement in Section 3.4.5). Additionally, while the values of c appear to be similar between the 'Corbin' data sets, it is clear that the 'Corbin' data sets report substantially higher cohesion values than those recorded by either Diambra et al. (2010) or Maccarini (1993). However, Diambra et al. (2010) reports the used of a sand for experimentation (i.e. therefore with a different particle size distribution), which is likely to result in lower cohesion than that of the soil used in this thesis, while Maccarini (1993) tested soil samples at 'natural' water content, which was recorded as a degree of saturation of between 32% or 67%.

Additionally, neither sample was heavily compacted, resulting in a difference in sample density between those samples and the ones details in this thesis. It would be expected that a higher density would lead to a higher angle of shear resistance, and Figure 3.29 suggests that this is the case - for triaxial samples and not direct shear samples. Soils are well known to be variable, and particularly when highly compacted in SBCMs, and therefore it is important to mention variability when presenting data. Considering that neither Maccarini (1993) nor Diambra et al. (2010) mention variability in the samples, it is possible that the variability exhibited in the samples in this thesis is not unusual, and that the results presented in Figure 3.29 are not as separate as it first appears.

The setup of the triaxial test and the direct shear test imply that there should be a noticeable difference in the strength of the sample between different tests, in that the direct shear test should report a higher shear strength, resulting in a higher cohesion but similar angle of shear resistance. This is because the direct shear test forces a failure plane along the centre of the sample, opposed to in the direct shear tests, whose failure plane follows a non-selected line of weakness. The triaxial test, therefore, should lead to a more conservative value of shear strength and hence of cohesion. However, Figure 3.29 suggests that cohesion between the two sample tests is similar while ϕ is different, contrary to the expected behaviour. While it is suspected that this might also be due to the expansive nature of the wool, it is also suggested that more work is needed in this area to confirm the relationship between the two different shear tests of fibre-reinforced samples.

Diambra et al. (2010) presents a study into the shear strength of fibre-reinforced sands using conventional drained triaxial tests. While the investigations focussed on the computational modelling of the sample and on the orientation of the short polypropylene fibres in the sample, it provides a useful comparison as both the 'Diambra' samples and the 'Corbin' samples are either entirely or mostly sand, and both used fibrous reinforcement. Figure 3.29 shows that the samples reported in Diambra et al. (2010) have a narrow range of ϕ values, with a large variation in c. It is noted, however, that the data suggests that fibrous reinforcement increases both ϕ and c (Diambra et al., 2010), contrary to the results found in this investigation, which found that cohesion decreases with fibre content. This difference, however, is likely due to the compressibility of the wool as discussed in Section 3.4.3, as polypropylene fibres are much less compressible than wool strands used in this investigation.

Maccarini (1993) reports on a comparison of the two tests on a residual soil, samples of which were taken from a slope and from a well. The paper reports on stress-strain data as well as calculating c and ϕ, and found that there seemed to be little difference between the obtained results. It is noted that these soils would not have been compacted to maximum dry density, unlike the samples tested in this investigation. A selection of results are plotted in Figure 3.29 and indicate that the triaxial data and the shear box data report similar values of both c and ϕ (Maccarini, 1993). It is also clear that, in comparison to the

results presented in this thesis, the variation in results is very small, although no fibrous reinforcement was used in Maccarini (1993) which is known to be one factor that alters the variation in the results.

While the data is not shown in Figure 3.29, Castellanos and Brandon (2013) reports on a different comparison between the triaxial and shear tests, performed on undisturbed and remoulded soils taken from alluvial and riverine deposits. Evidence was found that direct shear tests of natural deposits provided 'much lower' (2-5°) friction angles than triaxial tests of natural deposits, although the different tests on the remoulded samples were found to perform very similarly to each other, which was put down to the isotropy of the remoulded samples. The data in Castellanos and Brandon (2013) is not included in Figure 3.29 in order to clarify the distinctions between different data sets. Had the data been included, many data points would lie in similar positions to those already plotted in the Figure and would hence obscure the plotted data points.

Cheah et al. (2012) reports on a series of tests on triaxial and triplet specimens to investigate the effect of the addition of different fibres to the shear behaviour of RE. The results obtained were not included in Figure 3.29 as the paper reports values of cohesion between 550 and 760 kPa, more than three times the other data values plotted in Figure 3.29. Had these results been included in the figure, the remainder of the data values would have been more difficult to distinguish and interpret. While Cheah et al. (2012) appears to report on a set of experiments very similar to those performed in this thesis, it is noted that not only were large samples used, which might affect the behaviour of the samples due to size effect, but also a very limited range of fibre was added (either 0.05% or 0.1% by mass), and it is thought that is this, at least in part, contributes to the higher returned values of cohesion. Other differences between the tests, which could result in the large differences in cohesion values, include the range of confining pressures and the different size of samples. From the limited number of experiments performed, it was determined that wool reduces cohesion, whereas it does little to ϕ. This pattern of behaviour observed in Cheah et al. (2012) is similar to that observed during the tests performed in this Section, as both the direct shear test experiments performed in Section 3.4 and the triaxial tests in this Section show that wool reduces cohesion and either has no effect (DST) or little effect (triaxial) on the angle of shear resistance.

Consoli et al. (1998) presents the results from a set of triaxial tests on sandy-soil samples, reinforced with fibreglass fibres and cement stabilisation. However, samples were saturated before performing drained triaxial tests, thereby affecting the internal structure of the material. The unstabilised samples reported very low cohesion values (7 - 10 kPa) compared to the stabilised samples (57 - 67 kPa), which can clearly be put down to the saturation of the samples, and supports the findings that cohesion results from suction between particles and the saturation process would have increased the amount of internal water in the samples, thereby widening the inter-particle menisci, and reducing suction. In a saturated

sample, suction would be minimised, although it is unlikely that it would be completely removed. In this situation, it is considered possible that a portion of the strength may come from particle interlock, opposed to entirely from suction. However, when cement is present in the sample, or if the sample is unsaturated, the majority of sample strength is from suction or cement stabilisation. Obtained values of angle of shear resistance ranged from 35° to 46°, similar to those obtained in the tests described in Section 3.5.2, although spread across a narrower range. Fibres were observed to reduce cohesion in unstabilised soil but increase it in stabilised soil, while increasing ϕ in both stabilised and unstabilised samples. Differences in behaviour between those tests and other tests reported or discussed are likely to be caused either by sample saturation as previously discussed, or by the usage of the fibreglass fibres. Additionally, Consoli et al. (1998) reports that adding fibres to the samples affected the samples' failure mode from brittle to a more ductile failure.

All of these tests, those presented in Figure 3.29 and those described above, have presented values of c and/or ϕ, many of which have found different values and different ranges of values from different soils. The factor which has had the largest effect on the results is the properties of the fibrous reinforcement, more specifically whether the fibre is compressible or not. Following a review of all the data discussed, it is again suggested that the optimum properties of a sample will be obtained from a stabilised sample with incompressible wool. Amounts of chemical stabilisation, water content at compaction and raw soil properties and particle size distribution will all have an effect and will alter the optimal fibre content, and it is clear that more experiments are needed in order to determine the optimal combination of different materials to sufficiently enhance the properties of the raw (unstabilised) construction material.

3.6 Unconfined compression tests

The compressive strength of most SBCMs are usually determined using the UCS of cube samples, as per the investigation performed in Section 3.3. However, a few investigations have used prismatic or cylindrical samples as they have a few benefits over cube samples (Section 3.3.1). Maniatidis and Walker (2008), for example, presents tests on nine full-size prismatic columns involving the application of concentric and eccentric axial compression loads, and performed a series of unconfined cylinder compression tests for comparison. Unconfined cylinder compression tests have also been to calculate the compressive strength of rammed earth (Ciancio and Gibbings, 2012; Bui et al., 2014a) but only tests on short samples, with a slenderness ratio of 2, have been performed. To the author's knowledge, no investigations have been performed which study the compressive behaviour of rammed earth cylinders with a slenderness ratio greater than than 2, and it is for this purpose that this investigation was performed.

3.6.1 Sample production and testing

Two soil batches of six samples each (12 samples in total) were constructed to the soil ID 30*70:00 (Section 3.2.1). One batch used kaolinite clay, as per used in the previous experiments, while the other batch of the samples used bentonite clay. Bentonite clay is a highly expansive clay, and as such has generally been ignored in earthen construction research as it is generally suspected to be prone to cracking. Bentonite was used in this investigation to investigate whether this assumption is valid. In each batch of six, three samples were made with wool reinforcement and three without. Sample IDs were assigned according to batch constituents, and numerical antecedents identified the sample number in the batch (e.g. KW3 contained kaolinite clay (K) and wool (W) and is the 3rd sample in the KW batch).

The samples were originally constructed for use in an investigation into differing shrinkage of SBCMs when constructed with different clays. No shrinkage was observed in the large samples, however, and so the samples were repurposed for this investigation into unconfined compression tests on slender columns. As the samples were originally designed to be used in a shrinkage investigation, they were constructed to be proportional in size to the sample dimensions used in a shrinkage test as described in the British Standard BS1377-2. The samples were made 63mm in diameter and 353mm in length, giving a slenderness ratio of 22.4. Samples were constructed in six equal layers and compacted using a manual tamper to the previously calculated maximum dry density.

Samples were left to air dry in ambient conditions for 14 days, by which time their masses had stabilised. Samples were then placed vertically in an unconfined compressive test rig and a vertical displacement was applied to the upper face. The displacement was increased at a rate of 1mm/min until the sample failed. Each sample was fully constrained both at the top and the bottom of the sample.

3.6.2 Results and discussion

Due to a minor error in the alignment in the construction mould, the samples exhibited a slight eccentricity, accentuated by the length of the sample. Sample eccentricities, as measured immediately prior to testing, maximum compressive stress (MCS) and respective displacement are reported in Table 3.4. Sample B3 was damaged during the testing procedure and as a consequence its measurements and data were unable to be used in analysis.

Samples were observed to either fail through shear or through crushing, following failure patterns shown in Figure 3.30, and identified in Table 3.4 using ‘S’ or ‘C’ respectively. Samples also generally failed across two or more layers as seen in Figure 3.30b. As Figure 3.4 shows, the majority of kaolinite samples failed in crushing, while the majority of bentonite samples failed in shear. As the only common difference in these samples is the clay, it must be a property of the clay that defines the failure mechanism

Table 3.4: Results for unconfined cylinder samples: Load eccentricity, maximum compressive stress and respective displacement, and failure location. Eccentricities are also presented in percentage of the diameter.

Sample ID	Eccentricity (mm)	MCS (N/mm2)	Displacement at MCS (mm)	Failure Type	Layer No. of Failure
K1	4.90 (7.8%)	1.068	1.44	C	4/5
K2	7.29 (11.6%)	0.880	1.92	C	5/6
K3	2.93 (4.7%)	1.167	3.62	C	4/5
KW1	0.65 (1.0%)	1.112	3.38	C	4/5
KW2	5.86 (9.3%)	1.036	4.18	C	4
KW3	3.64 (5.7%)	1.255	4.56	S	4
B1	2.11 (3.3%)	0.506	5.18	C	4/5/6
B2	2.85 (4.5%)	0.442	5.87	S	5/6
B3	-	-	-	-	-
BW1	1.60 (2.5%)	0.591	6.65	S	4/5
BW2	0.55 (0.9%)	1.014	11.38	S	4/5
BW3	2.91 (4.6%)	0.959	10.08	S	4

in this test. Bentonite is highly water absorbant, and as such is highly expansive (Grim, 1962). It is possible that the shrinkage that occurs during drying affects the bonds between soil particles, making a shear failure more likely than a crush failure.

Additionally, all samples failed in the uppermost half of the sample, in the compaction layer identified in Table 3.4, whereby layer number 1 is at the bottom of the sample. Considering that each soil layer was of an equal size, the pattern of failure locations suggest that adding wool to a sample moves the point of failure closer to column midheight. It has been previously found that this effect can also be achieved by increasing the slenderness of the column or by reducing the eccentricity (Maniatidis and Walker, 2008). Tests performed during this investigation also appear to confirm a general link between eccentricity and height of failure as sample K2 had the highest eccentricity by a considerably margin and the failure point was higher in this sample than any other (Table 3.4).

Figure 3.31 plots the average values of maximum stress against displacement at maximum stress, with error bars indicating variation in results. It clearly shows that, with or without wool reinforcement, the bentonite samples failed at a lower stress than the kaolinite soil. It also shows that wool reinforcement increases the ultimate stress of the sample, although the amount of improvement in ultimate stress varies between the samples. Addition of wool clearly improves the shear resistance of the bentonite samples more than the kaolinite samples, and it is thought that this is likely due to the wool fibres providing an internal force holding the sample together.

The Figure also shows that the displacement at maximum force varies between the different sample mixes too. As seen previously in Figure 3.21 (Section 3.4.7), the addition of wool increases the displacement at maximum stress. The effect of wool was also discussed in Section 3.4.6, where it was concluded that wool increasing displacement is likely in part due to the compressibility of the wool, but also likely

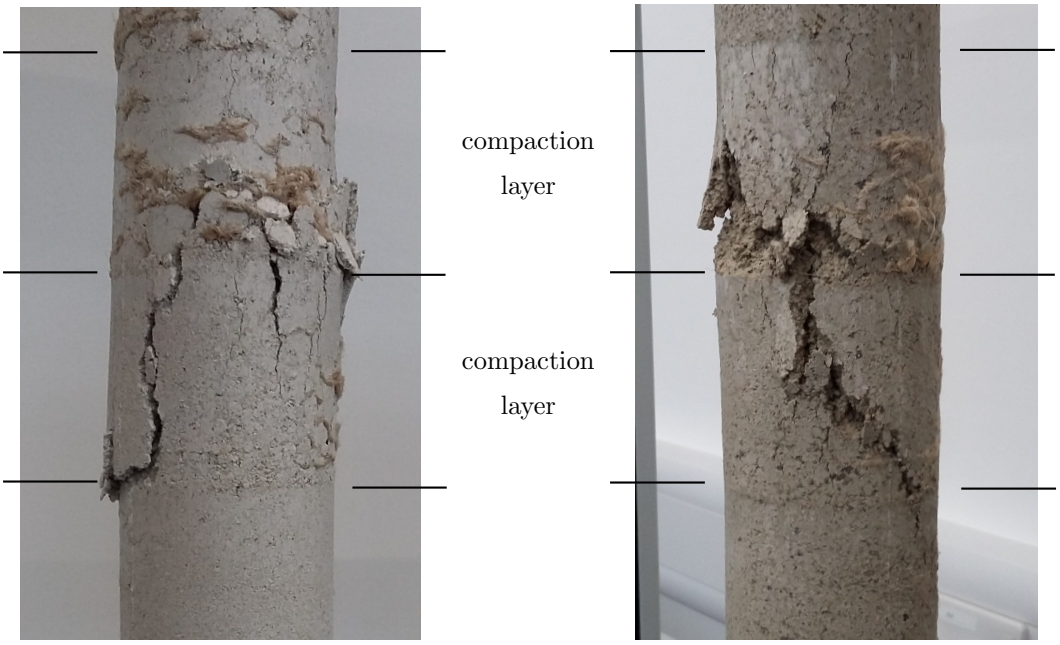

(a) Example of crushing failure. (b) Example of shearing failure.

Figure 3.30: Examples of sample failure during unconfined cylinder test.

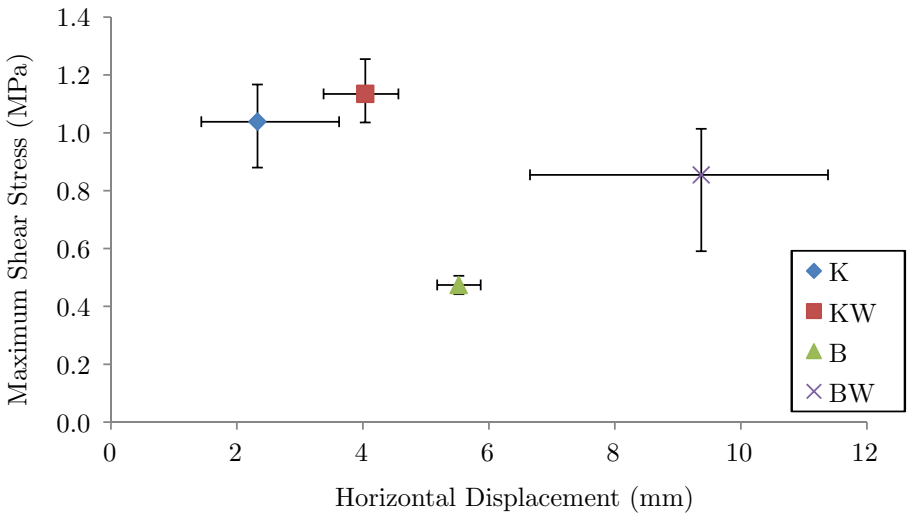

Figure 3.31: Relationship between maximum shear stress and respective horizontal displacement according to sample type.

due to any compressibility in the soil itself, which is confirmed by the results above. As a highly expansive soil, it is likely that bentonite samples would retain a degree of flexibility, even when the sample has naturally dried. It is unknown if any other investigations have been performed as to the unconfined compressive strength of rammed earth in relation to clay type. The use of bentonite in earthen construction is further studied in Chapter 5.

3.7 Scanning electron microscopy

During the direct shear test investigation (Section 3.4), it became apparent that the two halves of any sample containing wool remained attached to each other after sample failure (Section 3.4.3). This was found to be due to the presence of wool fibres bridging the failure plane. Once these fibres had been identified, further investigation was prompted involving closer examination using microscopes to investigate the role that the fibres play in the strength of the samples tested. A Scanning Electron Microscope (SEM) was used to examine these fibres as they have a greater depth of field (up to 1000 μm) compared to conventional light microscopes (up to 20μm) (Wetzig and Schulze, 1995), and the quality of the returned images is greater than when using a tabletop light microscope.

3.7.1 Introduction to scanning electron microscopy

A SEM can be used to produce direct, high-resolution imaging of solid surfaces. A beam of electrons is emitted from a source and focused to form a very fine point a few nanometres in diameter. This beam travels through a vacuum to hit the sample, after which reflection readings are taken using detectors. The electron beam is moved across the sample using magnetic deflection coils, scanning the sample point by point. Simultaneously, another electron beam moves over a TV monitor screen, displaying the scanned output. Magnification is controlled by aspects of the beam deviation. A schematic view of its primary mode of operation, from Wetzig and Schulze (1995), is provided in Figure 3.32.

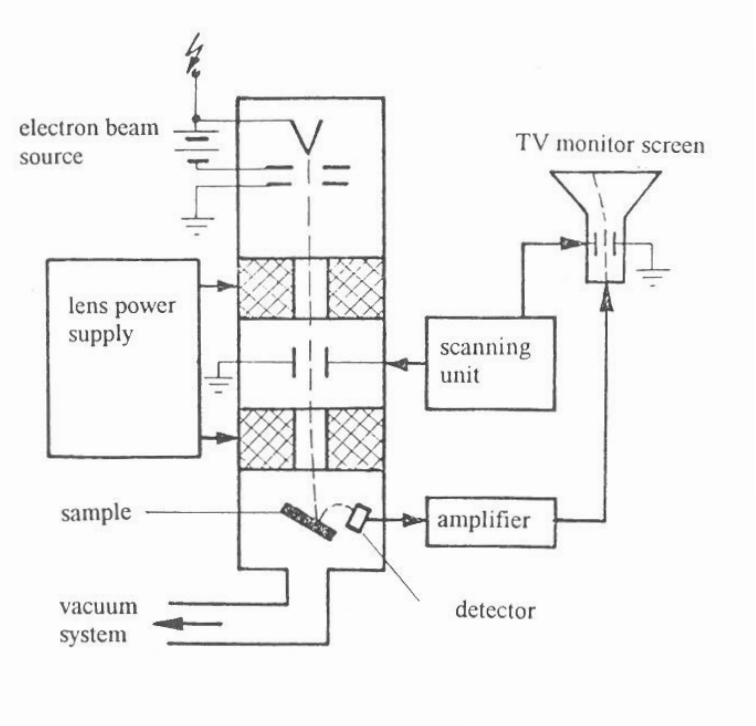

Figure 3.32: Schematic view of the operation of a basic SEM, from Wetzig and Schulze (1995).

It is generally recommended that samples are coated in an ultra-fine layer of gold or carbon before scanning (Wetzig and Schulze, 1995), as an adequate layer of a conductive material, such as gold, will prevent the electrons used in the scanning beam from attaching to the sample, thereby charging it and causing a distortion of the resultant image.

3.7.2 Sample testing

Two direct shear test samples were used for this investigation - one containing wool (D-W3C0-2) and one with wool and cement (D-W1C2-1). A suitable section of each sample was selected, one with plenty of wool fibres and both with a roughly level crack face, before being broken into an approximate 15mm x 15mm square in plan view. They were then mounted on specimen stubs using epoxy resin. The samples were coated in an ultra-thin layer of gold, as preliminary scans indicated that the sample was unable to discharge electrons and subsequently produced poor quality images (Section 3.7.1). Samples were scanned using a Hitachi S2400 tungsten filament SEM before the scans were visually analysed.

3.7.3 Results and discussion

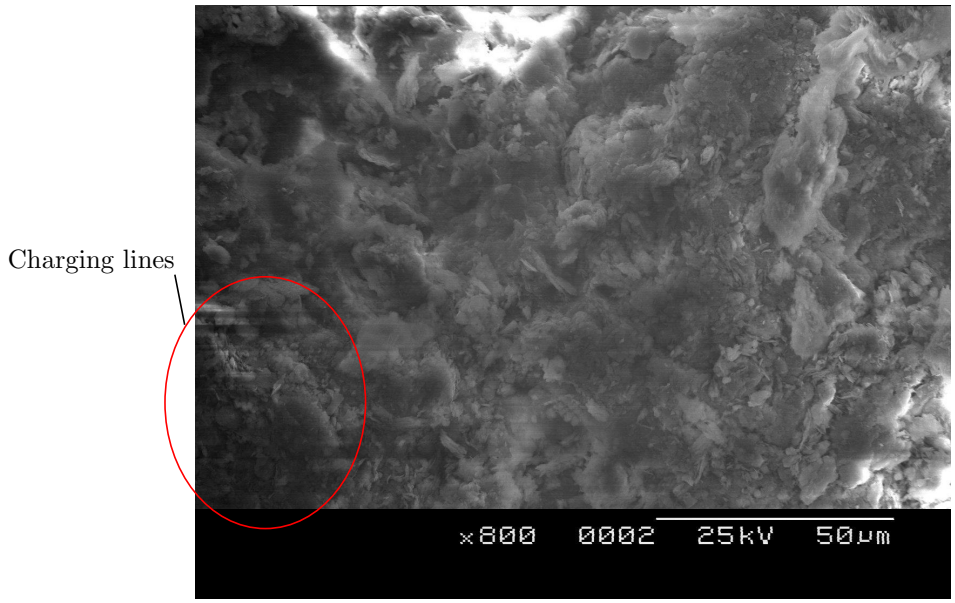

Figure 3.33: SEM scan of an unstabilised sample.

Figures 3.33 and 3.34 show SEM scans of the two samples, unstabilised (Figure 3.33) and stabilised (Figure 3.34). Both samples were scanned at the same voltage and scale. Horizontal lines in Figure 3.33 (seen on the left hand side of the image) are a result of charging in the sample, likely due to an insufficient coating of gold due to surface variation on the sample. Repeated attempts to improve the image and remove the lines were unsuccessful, however the detail in the remainder of the image is judged sufficient to continue visual analysis and interpretation. Attempts were also made to examine the samples at a higher

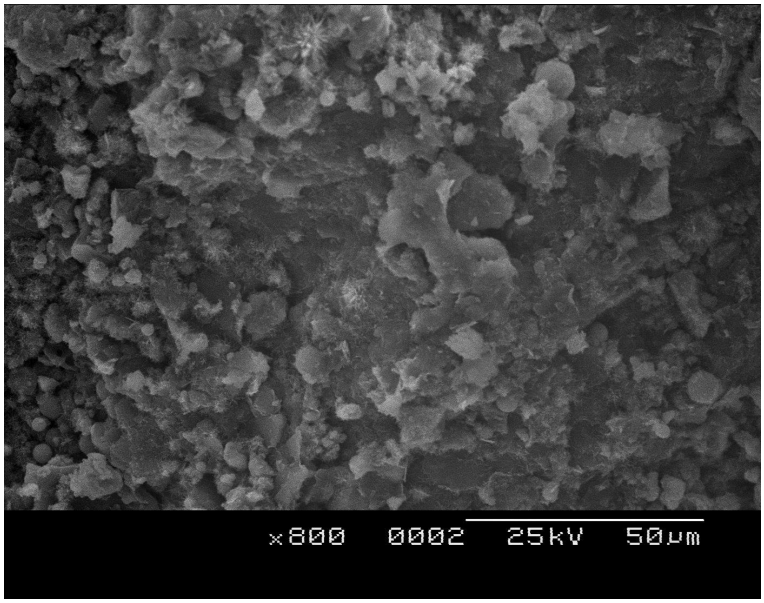

Figure 3.34: SEM scan of a cement-stabilised sample.

scale, however the poor discharging of the material prevented clear images being taken, and therefore no comments or observations regarding the microstructure can be made.

Despite this, it is clear that the unstabilised sample (Figure 3.33) appears smoother in the image, likely due to the lack of cement in the sample. When the cement was added to the mix, as detailed in Section 3.4.2, the cement coated all the small clumps of the sand-clay-water mix. When compacted, this creates a three-dimensional cell-like cementitious structure, as opposed to an even distribution of cement throughout the entire sample. Smoothness of the crack plane suggests a shorter, more direct crack path through the sample, which should relate to a lower peak shear strength, as it is known that a longer crack path in all conventional brittle materials results in a larger force required for failure (Section 2.4). It is proposed that the addition of cement increases the length of the crack path by reinforcing areas of soil in the crack path, forcing the crack to divert to a weaker area of soil structure. It therefore follows that samples with greater amounts of cement would provide a greater peak shear stress. This was confirmed with the results shown in Figure 3.18 in Section 3.4.5.

Figure 3.35 shows a wool fibre emerging from in the stabilised RE sample (D-W1C4-1) at the bottom of the image. The image appears to show little or no cementitious or menisci bonding between the wool and the RE, as was seen in Jaquin (2008). This implies that the bonds were either absent before the sample was scanned, removed during the scanning process, or are unable to be identified with the apparatus used. If the bonds were absent prior to being tested, this implies that any additional strength recorded in samples that contain wool is a result of pull-out friction or tensile strength of the fibres, as opposed to suction attaching the fibres to the soil. Alternatively, if the bonds were present during DST testing but not during SEM observation, they must have been removed either in the vacuum of the

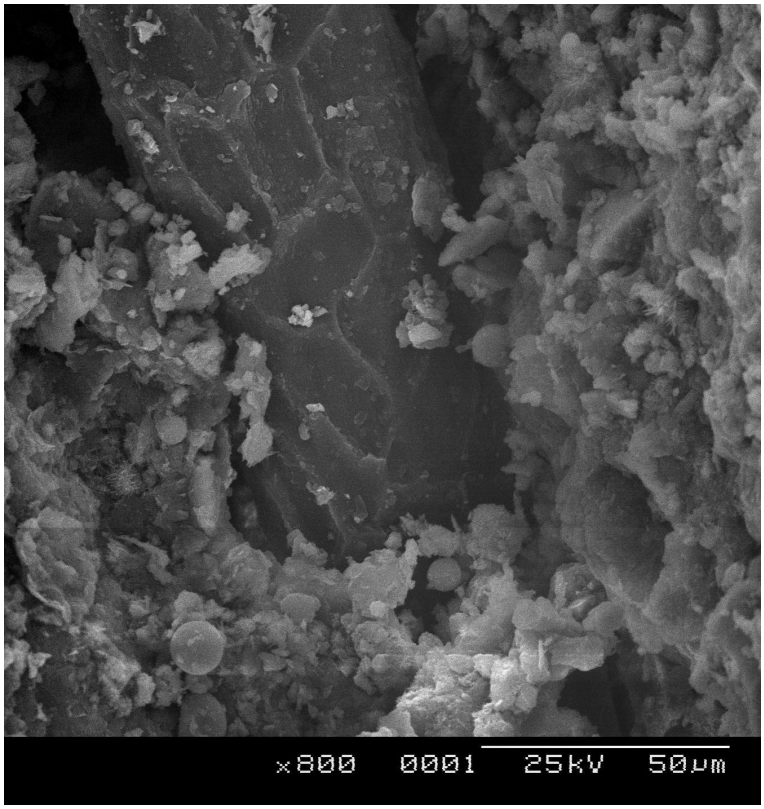

Figure 3.35: Composite image of a SEM scan of a wool fibre embedded in a stabilised RE sample.

gold-coating process, or during the vacuum present in the SEM chamber. Finally, if the bonds do exist but could not be observed with the apparatus, this could be due to the scale of the images or could be due to the gold coating needed for the imaging to be successful. It is uncertain whether a gold particle, if it comes into contact with a water droplet, would sink 'through' the droplet, hence the impression that no droplet exists. There would therefore be little distinction between the menisci and the soil particles if both coated in gold. Hence it is suggested that any future investigations use an environmental scanning electron microscope (ESEM) as that apparatus is able to produce scans without a vacuum (and potentially without the coating of gold) and hence examine samples without risking altering the presence of water.

3.8 Summary of results, discussions and conclusions

This chapter has presented results from four different experimental investigations, involving many separate programs of testing and some microscopic analysis using a SEM. The results in this chapter may be summarised as follows:

- Stabilising a rammed earth soil mix with cement has been shown to improve UCS of the sample,
- Stabilising a rammed earth soil mix with wool has also been found to improve the UCS of the sample,

- A proportion of cement can be replaced with wool to achieve a desired UCS while reducing the cost and environmental impact of the material,
- Adding cement to a mix after a period of equilibration does not enable the cement to mix completely evenly through the soil. It is currently unknown how much this, or the process of equilibration, actually affects the strength of the material,
- Reinforcing a rammed earth soil using wool fibres has little effect on the angle of shear resistance of the soil,
- The addition of fibres decrease cohesion in the sample in proportion to the mass of added fibre,
- No relationship has been found between cement content and the angle of shear resistance or cohesion of the sample,
- Wool fibres have also been found to increase the sample ductility at failure, by reducing maximum shear load but increasing displacement at maximum load,
- RE has been observed at a small scale, and it has been shown that wool does not appear to bind to RE, instead appearing to gets its strength from friction and interlocking around the soil particles, although more work is needed to confirm this,
- The fracture planes of unstabilised RE appear to be microscopically (and macroscopically) smoother than fracture planes of stabilised RE, which may contribute to an increase in shear strength with stabilisation.

Chapter 4

Fracture behaviour

Understanding the fracture properties of any material is crucial to determining its behaviour under different loading conditions. This is particularly crucial when considering limit-state scenarios and investigating how materials behave pre- and post- critical loading. A common way that quasi-brittle construction materials like rammed earth (RE) and concrete fail is through tensile fracture. Understanding the processes of fracture initiation and progression is, therefore, crucial to the continued study of RE.

This chapter presents an investigation into the fracture energy of rammed earth using the wedge splitting test, which was developed for the calculation of fracture energy of concrete. This test has not been used previously for rammed earth despite clear benefits of the test over alternatives such as the three-point bending test. This investigation focussed on the effect of two different stabilisers - cement and wool - on the fracture energy and fracture behaviour of RE. A range of wool (0-2%) and cement (0-10%) portions were used for the sample batches. The advantages of the wedge splitting test are presented, and a discussion on the effect of fibrous reinforcement and cement stabilisation of the fracture energy of rammed earth is made. Recommendations for the use of wool stabilisation in RE are made, which build on recommendations made in Chapter 3. This chapter finishes with a summary of the discussions and a selection of suggestions about where this research could be built upon and continued.

4.1 Introduction

This section details a brief overview of the science of fracture in quasi-brittle construction materials and provides details of the wedge splitting test and the three point bending test, the two most commonly used tests in concrete research for determining fracture energy. Benefits of each are discussed and the reasons behind test selection is made. For a more detailed explanation of the history and development of fracture theory, the reader is referred to Section 2.4.

4.1.1 Background to fracture energy

Fracture energy is the amount of energy needed to generate and propagate a crack through a material, and is a measure of how resistant a material is to crack formation. It is therefore used as an indicator of flexural strength in a brittle material. The amount of work done, $\mathcal{W}$, to extend a crack by length δa in a material of thickness b and resisted by an internal force $\mathcal{R}$, can be expressed as in equation 4.1.

$$\mathcal{W} = \mathcal{R} \times b \times \delta a \tag{4.1}$$

As RE is a very brittle material, the elastic energy is negligible and therefore it may be assumed that the crack growth resistance $\mathcal{R}$ is equal to the specific fracture energy, G_f (Bazant and Planas, 1998). Therefore, for RE, as for concrete, the fracture energy equals the work $\mathcal{W}$ divided by the crack area ($b \times \delta a$). The work $\mathcal{W}$ is defined by the area under a force-displacement plot generated through experimental or analytical investigation.

For a more detailed breakdown of formula derivation and explanation, and details of fracture theory, the reader is referred to Section 2.4.

4.1.2 Fracture energy determination methods

The study of fracture and of fracture energy in concrete has been a research area of interest since the 1980s, and as such a number of tests have been designed to calculated the fracture energy of the material (e.g. Petersson (1980); Linsbauer and Tschegg (1986)). However, it is a relatively new area of research in RE, therefore it is appropriate for pre-established tests from concrete research to be adapted for investigations into RE. The test primarily used in concrete literature for calculating fracture energy is the three point bending test, which has subsequently been used in RE research. The wedge splitting test, however, has so far been overlooked as a potentially more suitable alternative.

Three point bending test

The three point bending test, first proposed in Hillerborg et al. (1976) and described in detail in a 1985 RILEM technical report, has been widely used for the determination of fracture properties. Figure 4.1 shows the simple test and loading arrangement. An increasing displacement δ is applied at the centre of the beam, and the reaction force F is continuously measured.

This very simple method has a number of substantial drawbacks, however. The self-weight of the sample has a large effect on the recorded fracture energy as it pre-loads the beam, increasing the initial stresses around the notch, resulting in a lower recorded fracture energy. This is particular issue in weaker materials, where the self-weight will be greater proportion of the total measurements. The three point

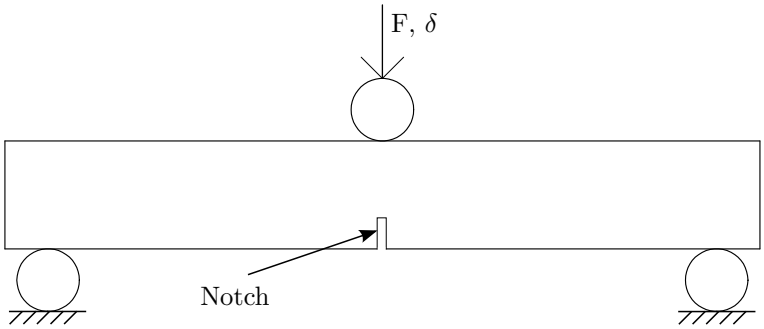

Figure 4.1: Experimental arrangement of the three point bending test.

bending test is, therefore, a conservative method of calculating the fracture energy. However, in order to compare different materials and different material properties, the effects of self weight need to be carefully considered as different densities and dimensions would affect the self weight in different ways and hence the calculated fracture energy. Thus, the self-weight must be carefully measured and analysed before fracture properties can be correctly determined.

Three point bending test samples are often created to be very large (1m in length), in order to minimise the risk of being unrepresentative of the material undergoing investigation. The increased size, however, increases the effect of self-weight on the results, which is often considered in concrete research. The smaller a sample gets, however, the more the results are affected by the 'size effect', a term which includes the edge effects and maximum particle size percentage (i.e. the size of the largest particle in the material compared to the minimum width of the material). In concrete research, the effect of self weight can be calculated and accounted for, and size effect is a large research area still undergoing investigation (Bazant and Planas, 1998).

The three point bending test has been used for determining the fracture behaviour of RE on a few occasions with different focusses and different outcomes. Aymerich et al. (2016) reports on a series of three point bending tests investigating the effect of adding hemp fibres to a RE mix, measuring fracture resistance, energy absorption and maximum load capacity of the samples. It was found that the fibres used increased the fracture resistance of the samples, and that the bridging of fibres across cracked surfaces improved the post-cracking performance. However, no account was taken of self-weight of the samples nor of size effect, both of which should have a large effect on the results as the samples were long and narrow and of generally small dimensions (70x70x160mm). Lenci et al. (2012) presents a limited set of experiments on 'unfired dry earth', similar to RE except with a greater proportion of silt and clay, and compacted with reduced compaction effort. Linear elastic fracture mechanics (LEFM) was applied and a two parameter model was used to obtain the R-curve. The paper presented the first application of classical fracture mechanics theory to RE and other soil-based construction materials (SBCMs) to the author's knowledge, however doing so several assumptions had to be made. As in Aymerich et al. (2016),

it was assumed that the self-weight was negligible and the size effect of the samples was not considered. Additionally, it was assumed that RE is a brittle material in order to apply LEFM. The exact nature of RE is uncertain, and as RE is similar in structure and properties to concrete, a brittle approach to fracture seems the most appropriate, at least until a new approach is deemed more so.

The three point bending test has been used to investigate the fracture properties of SBCMs on a number of occasions, the use of which has been reported in Aymerich et al. (2012), Wang et al. (2007), Aymerich et al. (2015), Clementi et al. (2008) and Guinea et al. (1992) among others. No investigations have been found that address the issue of size effect in RE and only Wang et al. (2007) has been found to take account of self weight by performing the test laterally such that the applied displacement was horizontal rather than vertical. Also, the majority of the investigations have been performed on sandy-clays, opposed to more traditional soils which include gravel. While this would make size effect less of an issue as the maximum particle size is smaller, it is unknown what effect this has on the calculation of fracture energy compared to the real fracture energy of a traditional soil mix containing gravel.

Wedge splitting test

Linsbauer and Tschegg (1986) first proposed the wedge splitting test, which was later extended in Brühwiler and Wittmann (1990), as an alternative method to the three point bending test for calculating the fracture energy of concrete. Advantages of the wedge splitting test include a large fracture area compared to sample mass, resulting in less redundant material, and less risk of sample breaking during construction or handling due to a less vulnerable shape (i.e. a cube or cylinder opposed to a thin rectangular prism.) Brühwiler and Wittmann (1990) recommends that this test maybe used on cubic or cylindrical samples, although a cylindrical sample shape was chosen for this investigation due to ease of sample construction. A schematic diagram of the sample shape and testing apparatus is shown in Figure 4.2, alongside images showing the test apparatus assembly in 3 stages. The notch is needed to guide the location of crack formation. An increasing vertical displacement is applied to the wedge plate, which is resisted by the force F_v. This force originates from the sample's resistance to splitting, otherwise called the splitting force F_s, and is transferred from the sample to the resistance F_v through the wedge-shaped loading plate and the bearings. The crack opening displacement δ is measured at the crack mouth. The test details and procedures were obtained from Brühwiler and Wittmann (1990) and Rossi et al. (1991).

A wedge splitting test sample can be considered to be a cylindrical section of a three point bending test sample surrounding the notch, inverted such that the crack lies at the top of the sample as opposed to at the bottom of the sample. This arrangement means that the sample area is similar in size to the affected cracking area, resulting in the self-weight of the sample having negligible effect on the results of the test (Rossi et al., 1991). A positive side-effect of this is that the samples can be made considerably

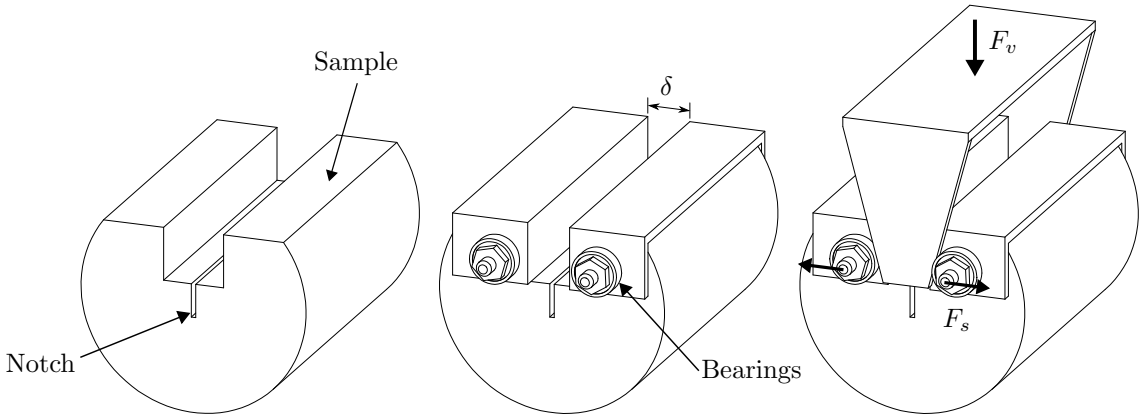

Figure 4.2: Wedge splitting test arrangement.

smaller (depending on the size of the three point bending test sample) and are subsequently less resource-intensive and easier to manoeuver in a laboratory environment. The main disadvantage of this test is the irregular shape of the sample, which complicates construction when using RE due to the need for good compaction quality. When the wedge splitting test is used in concrete literature, the shape is generally created using either a specially-created mould or, more simply, cut out of a cylindrical sample, around around 28 days after construction. This is not possible in earthen construction samples, particularly if not chemically stabilised, as any sawing is likely to affect the structural integrity of the sample. Thus the RE samples (Figure 4.2) were constructed using a sample insert in a cylindrical mould, such that the sample would be constructed to the required dimensions.

4.2 Method

Of the two tests described in Section 4.1.2 for calculating the fracture energy of a sample, the three point bending test and the wedge splitting test, the latter was chosen in this study for the advantages that the test has over the former as described in section 4.1.2. Such advantages include not having to consider self-weight of the samples and the subsequent effect this has on fracture energy, and the relatively large size of the crack zone with respect to the mass of the sample.

4.2.1 Materials

The soil mix used in all tests was specified as 30*:60:10[2.1], and Speswhite was used for the clay fraction of the mix (Section 3.2.1). The particle size distribution of the soil is shown in Figure 4.3, while the optimum water content was determined to be 12%, obtained using a series of vibrating hammer tests as detailed in the British Standard BS1377-4. The soil was mixed in 8.4kg 'lots' in a Hobart planetary mixer before 5 'lots' were combined in a Croker rotating pan mixer to produce one soil batch of 42kg. A

1kg sample of each soil batch was oven-dried at 105° for the calculation of water content before performing wet sieve, dry sieve and sedimentation tests.

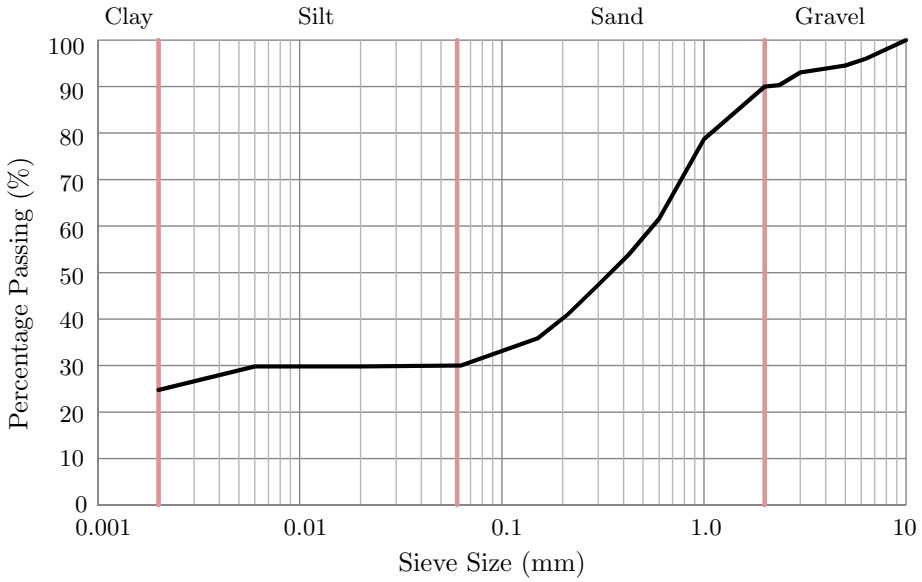

Figure 4.3: Particle size distribution curve for soil 30*:60:10[2.1].

4.2.2 Sample production and testing

From each 42kg soil batch, 6 cube samples were constructed to investigate unconfined compressive strength (see Section 3.3) and 6 cylindrical samples for determination of fracture energy as presented in this chapter. Sample mixes were constructed and given identification codes according to the method detailed in Section 3.2.3, and the unique 'Test ID' for the wedge splitting test samples presented in this Chapter is 'S'. As per construction of the samples presented in Chapter 3, cement and wool fractions were added to the mix immediately prior to sample construction to minimise hydration of the cement in the sample before compaction could occur, along with extra water where appropriate to keep the water content constant at 12% by mass according to the inclusion of the additional mass of the cement and wool.

The wedge splitting test samples were constructed using a concrete cylinder mould and a specially designed insert to produce samples with the shape and dimensions as identified in Figure 4.4. Samples were compacted in 5 layers, each 30-40mm deep, and compacted using a pneumatic hammer for 60s per layer. This method was determined from previous experience while ensuring that the samples were fully compacted. All samples were removed from their mould immediately after compaction and left to dry in an indoor, open environment for 14 days. The lengths of the samples varied between 150mm and 208mm, with the average sample length at 175mm and the standard deviation at 12.25. The samples were tested in a displacement-controlled triaxial test rig, which was set to move vertically at a rate of 0.1

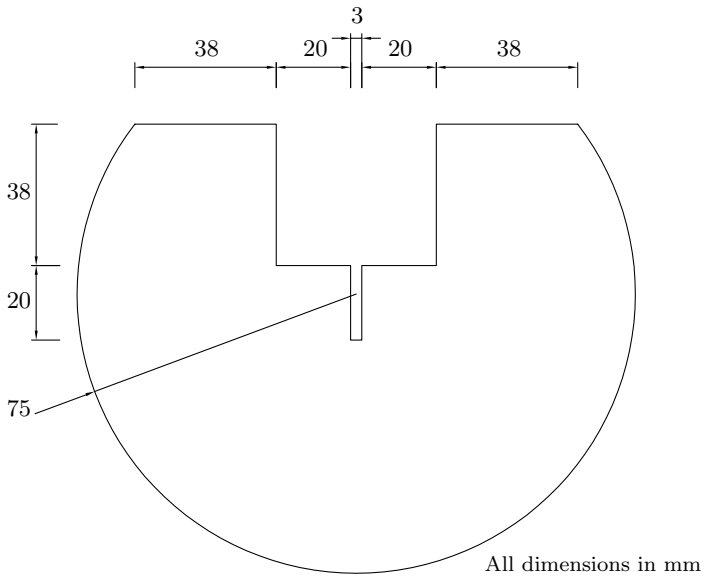

Figure 4.4: Sample dimensions for the wedge splitting test.

mm/min. The test setup and arrangement was shown in Figure 4.2. The crack opening displacement, δ, was measured using a pair of linearly variable differential transducers (LVDTs) while the vertical reaction force, F_v, was measured using a load cell attached to the loading frame. The wedge angle α (Figure 4.5) is generally recommended to be 15° (Rossi et al., 1991; Brühwiler and Wittmann, 1990), as a compromise between rig height limitations and limiting vertical stress, and was therefore used in the experiments presented.

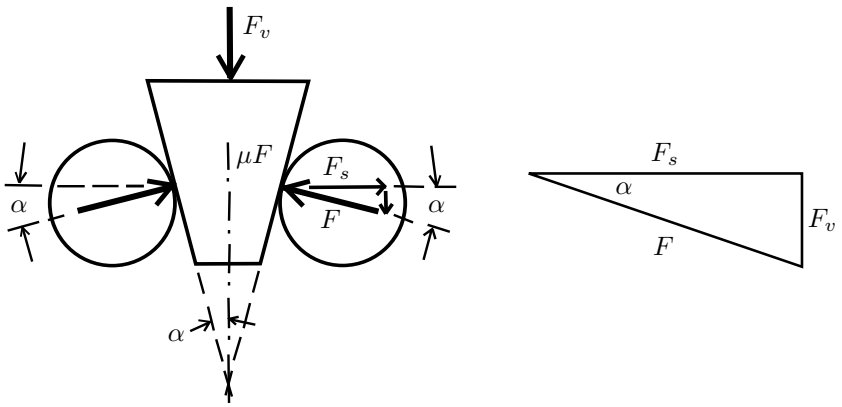

Figure 4.5: Force equilibrium in the wedge splitting test.

4.2.3 Procedure for calculation and analysis

The readings taken from the test rig were imported into Matlab. Through trigonometrical principles and force equilibrium (Figure 4.5), the reaction force F_v measured at the load cell was converted into the splitting force F_s at the bearings, and hence at the crack tip, using equation 4.2. It is noted that F_s is

the total horizontal splitting force applied to the sample, opposed to the force applied to one bearing as implied in Figure 4.5.

$$F_s = F_v/2tan\alpha \tag{4.2}$$

A plot of F_s vs δ (splitting force vs crack opening displacement) was made for each sample, an example of which is given in Figure 4.6. East test was halted at around 5% of peak load to avoid damage to the apparatus. A tangent was taken at the end of‘ the loading curve and extended to the x-axis in order to obtain an approximate value as recommended by Rossi et al. (1991). Each curve was analysed using Matlab to produce a unique equation for the curve. Curve equations determined from Matlab were compared with the original F_s-δ curves, and only equations with an R^2 value of 0.99 were accepted, in order to minimise any calculation error. Matlab was subsequently used to calculate the area under each curve, which was then divided by the sample length to obtain the *specific fracture energy* G_f of the material as per described in Bazant and Planas (1998).

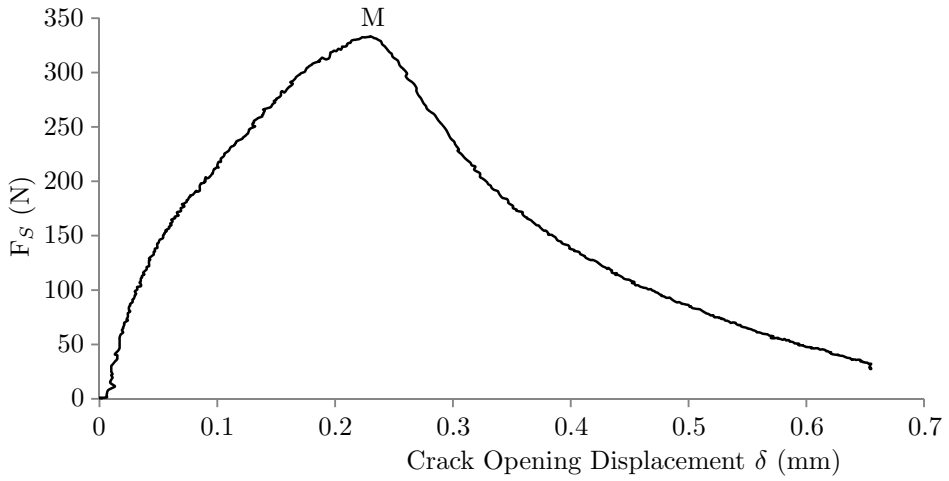

Figure 4.6: Example of an F_s vs δ plot.

4.3 Results and discussion

This section presents the results from the wedge splitting tests as previously described in Chapter 4.2 and presents a discussion on the effect of wool content and cement content on the fracture energy of rammed earth. Test observations are also presented, and comments are made about the effect of cement and wool on the drying rate and crack initiation and progression in the RE samples.

4.3.1 Experimental observations

One of the greatest challenges faced during construction of these samples was ensuring the even distribution of wool in the sample. Mixing for a longer amount of time should imply a reduction in wool clumps forming, however it was observed during sample mixing that the wool tended to attach to other wool strands in preference to the soil, often resulting in large clumps which had to be separated and then mixed by hand. This preference is likely due to three different combining factors. Firstly, the wool was slightly static, which meant that the wool had a preference to stick to itself over the natural, unconductive, soil. Secondly, the microfibres, previously observed in Section 3.4, spreading out from the wool strands, would be more likely to tangle with other wool microfibres than relatively large clumps of soil. Finally, the difference in density between the soil and the wool meant that the soil naturally sank to the bottom during mixing, whereas the wool naturally rose to the top, creating an inherent separation in the mix, which exacerbated the first two effects, creating large clumps of wool with no soil. This was largely overcome by checking the soil and separating any larger areas of wool and subsequently dispersing that wool through the soil mix.

Not all attempts were successful, however, as it was observed during sample construction that the quality of the samples varied between mixes. It was observed that some of the samples containing high amounts of wool were prone to full or partial collapse after their removal from the mould. The most likely explanation of this behaviour is the compression and subsequent expansion of the wool strands as previously observed and discussed in Chapter 3. This action loosened the areas of the soil around the wool, resulting in a less dense and structurally weaker area of the sample, the effect of which is amplified in areas of high wool concentration resulting from poor mixing. An example of the result of uneven mixing is shown in Figure 4.7, in which the area of high wool concentration is indicated in the crack zone of a broken sample. It is noted that the highlighted area was not as solid wool as the image appears as large amounts of loose soil fell out of that area of the sample after testing, likely due to the reduction in cohesion seen resulting from wool as previously discussed in Sections 3.4.6 and 3.5.3. While some samples with uneven distribution of wool were unable to be tested, the majority of samples were successful and are hence included in the presented data.

Additionally, the variability of compaction quality could be due, at least in part, to the addition of large amounts of cement, which altered the particle size distribution. It is assumed that increasing the percentage of particles less than 50µm, and hence changing the particle size distribution (Figure 4.3) by increasing the percentage in the 'silty-clay' region, would change the maximum density and optimum water content. However, work is needed to investigate how the addition of the cement particles affects the optimum water content, particularly when considering the requirement of enough water in the sample to allow complete cement hydration.

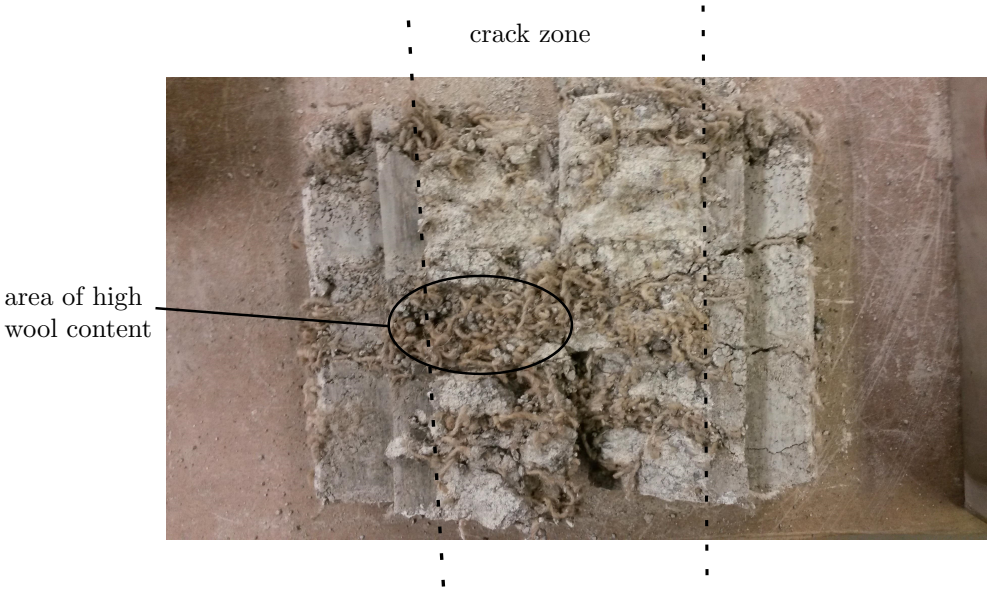

Figure 4.7: View of crack zone and example of uneven wool distribution in sample S-W4C2-S2 after testing.

4.3.2 Discussion on drying rate of samples

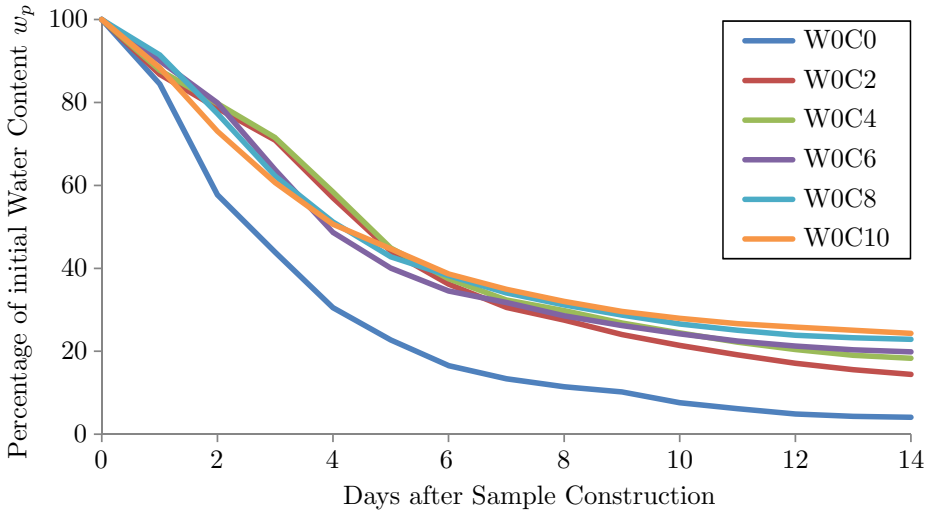

Figure 4.8: Drying curves for the cylindrical samples without wool stabilisation.

Figure 4.8 shows the average drying curves for all the cement-stabilised samples not containing wool. Water contents are reported as percentage of initial water content w_p whereby 100% corresponds to the 12% optimum water content as added to each sample and 0% represents the theoretical dry mass as calculated from the wet mass and the percentage added water content of each sample. It is noted that the steepest initial drying curve of all the samples is that of the unstabilised sample. This was to be expected as the the chemical cementation process retains water, resulting in a slower drying rate and ultimately a higher final 'water content'. Due to the cementation process, and due to the water content being measured by mass, the recorded 'water content' of stabilised samples is, at least partially, not water

but in fact hydrated cement particles.

Figure 4.9 further confirms that the apparent water content relates to the amount of cement in the sample. The clear positive linear relationship between cement and water content implies a straightforward relationship between water content on day 14 and cement content in the sample, however the sample containing no cement must be considered as it does not lie on the straight line linking the other samples. However, this point simply confirms that hydration is taking place in the stabilised samples, as the lower water content in the unstabilised sample must arise from more water leaving the sample naturally due to air drying.

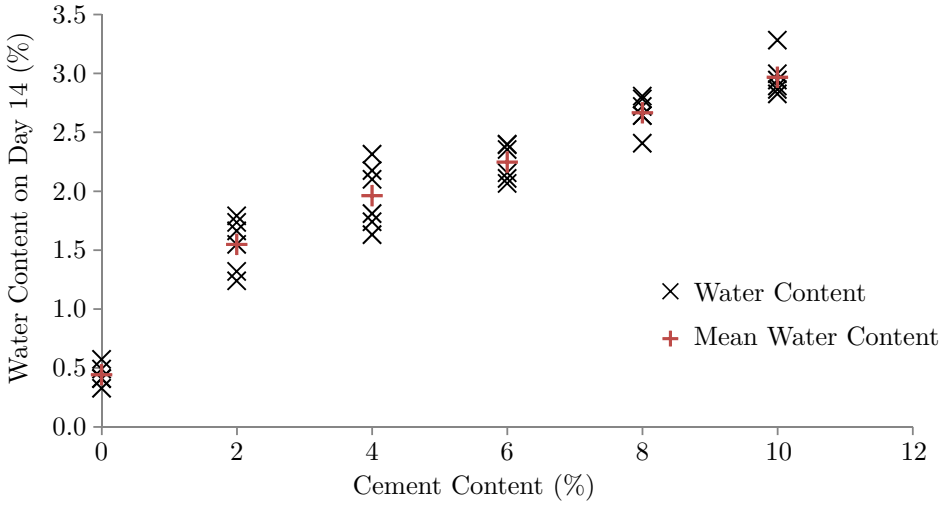

Figure 4.9: Percentage water content on day 14 after sample construction.

Jones (2015) demonstrates that 4.2g of cement needs 1g of water (or 1g cement needs 0.24g water). Considering this proportion, the assumed water content in each sample can be calculated. Figure 4.10 shows the same data with the water content assumed to used in hydration removed, thereby leaving only the 'true' cement content of each sample.

Calculated drying rates in Figure 4.10 show considerable variation between the drying rates of different samples, although it is clear that the large difference in final water content between sample batch W0C0 and the other batches in Figure 4.8 has been removed. Instead, sample batches W0C2 and W0C4 are the most different to the other batches, as the drop in water content between days 2 and 4 is significantly smaller than for other samples. After day 4, the drop in sample mass continued on its expected trajectory, albeit at a higher value, therefore the final water content at day 14 is higher than the others. It is noted that sample batches W0C2 and W0C4 were constructed on the same day, and also that no other samples were being dried during days 3 and 4 of those samples' drying period, which is why the reducing in drying rate does not appear in any other sample batches. This difference is likely due to environmental conditions within the lab during the drying period, which could not be controlled.

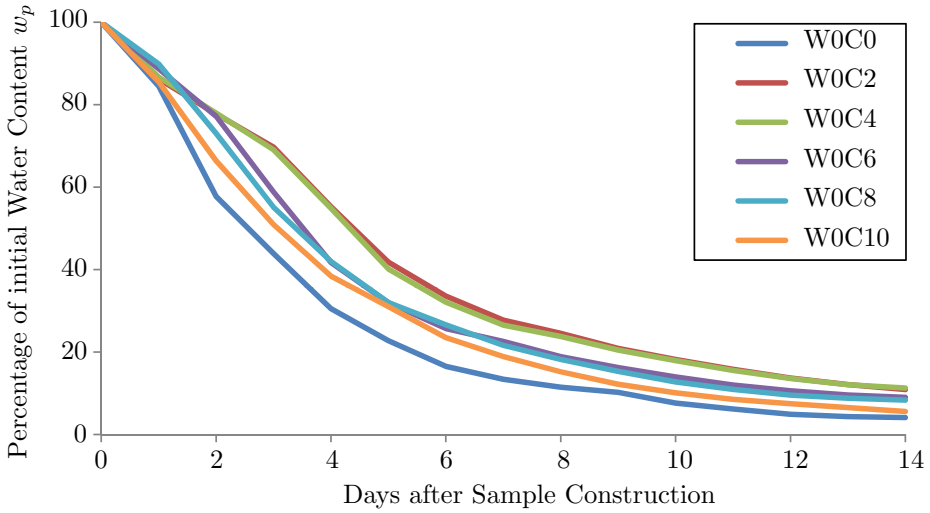

Figure 4.10: Drying curves for the cylindrical samples without wool stabilisation, reporting calculated water contents.

Drying rates for samples containing wool but not cement were found to be almost identical, and as such any differences were undiscernible when presented graphically. This further supports the conclusion in Section 4.3.2 that the addition of wool fibres does not affect the drying rate of the samples. However, these calculations were performed under the assumption that the cement has fully hydrated - which is not necessarily the case. Irrespective of the amount of time needed for stabilisation to occur, sufficient water is needed in proximity to the cement to enable complete hydration. The samples were allowed to equilibrate before cement was added, meaning that water should be evenly mixed throughout the soil, but this will only be the case if the water can move freely through the soil to areas of high low pore water pressure. Hydration of the cement is also likely to be improved if water mobilisation is high, as this means that water can move more freely around the soil particles to access the cement where required.

4.3.3 Crack initiation and progression

It was observed that after the peak load in each sample had been reached, a crack formed at the notch tip (Figure 4.2) and began propagating through the sample. Examination of the crack zone after sample failure showed that the percentage of cement affected the length of the crack path. Samples with little or no cement generally created slightly longer crack paths, preferring to extend around some soil areas, which is seemingly contrary to crack theory which implies that longer crack paths create higher fracture energies. (Theory states that fracture energy is the energy needed to create and extend a crack; a longer crack therefore means a greater fracture energy.) However, the properties of the cement must be considered when comparing the crack paths. It can be assumed that the areas of soil that the crack moved around, opposed to through, offered greater crack resistance compared to the surrounding area, due to a greater density caused by the presence of larger soil particles or a higher degree of suction. It is expected,

therefore, that the cement is not perfectly mixed through the sample, resulting in an even longer crack path as the crack found its way around very high strength areas of soil. Samples with higher cement content, however, generally formed straighter crack paths extending directly to the edge of the sample, occasionally breaking through some larger pieces of gravel in the soil mix. It is therefore evident that the cement bonding between particles was greater than the strength of the pieces of gravel. Although the increased crack path length in the unstabilised soil should result in a higher fracture energy, the addition of cement alters the structure of the soil, meaning that the effect of crack path length is not able to be discussed in detail in this investigation.

It was also observed that as the crack progressed, the output force-displacement curves (such as those shown in Figure 4.11) greatly varied between samples with and without wool. In the samples without any wool, F_v dropped steadily until the test was halted at approximately 5% of peak load (Figure 4.11a), whereas samples with wool reached a residual strength of between 60% and 80% of the maximum load and maintained that load (±20%) until the test was halted due to spatial limitations of the testing apparatus (Figure 4.11b). It is clear from Figure 4.11 that Samples S-W0C8-S6 and S-W4C10-S6 shared a similar shape up to maximum load and for a short while afterwards, during the reducing load period. At around 0.7mm crack opening displacement in Figure 4.11b, however, the two plots look very different as Sample S-W4C10-S6 levels off at around 360N. From this point onwards, the majority of the residual strength of the soil results from the wool in the sample, as the applied force is transferred from the RE onto the wool. Instead of breaking, however, the wool was pulled out of the sample, resulting in the sustained residual strength. This also indicates that the bond strength between the RE and the wool was weaker than the tensile strength of the wool alone.

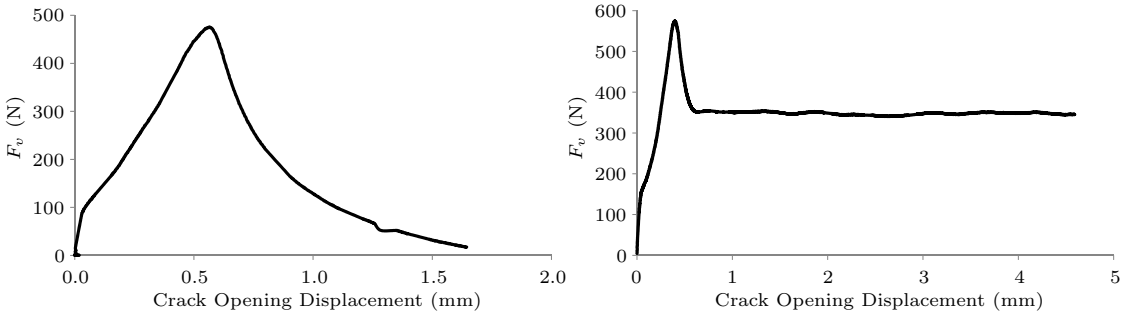

(a) Sample S-W0C8-S6. (b) Sample S-W4C10-S6.

Figure 4.11: Example force-displacement curves.

It is proposed that the role of wool and similar fibrous reinforcement might be further investigated using a comparison of similar test loading response curves. If suitably similar samples, with and without wool, are created, it is suggested that the forces applied to the wool might be directly calculated from the difference between the two curves. Unfortunately, no samples in this investigation were found to be

suitable to check this. Such a pair of response curves would be expected to look similar to the red and blue lines shown in Figure 4.12. As you can see, the red 'with wool' and the blue 'without wool' curves are identical until the load drops to around 70% of the peak load. At this point, the wool starts to take a proportion of the load and the response curve levels out and remains constant. From this, the wool contribution can be determined, shown by the green line, calculated as the difference between the 'with' and 'without' wool response curves. It can also be suggested that the more wool fibres there are crossing the crack then the higher residual strength there will be. This is not necessarily the entire picture of the relationship, however. Readle et al. (2015) reports on a series of pull-out tests on fibres imbedded in rammed earth. It was found that the water content and the fibre length were the most important factors of material bond strength. Therefore it is not only the number of fibres but also the length of fibres that are critical. In the tests performed above, average length and number of fibres were not calculated, therefore firm conclusions cannot be drawn. It is currently unknown whether the optimum benefit of fibres results from an even length of fibres or from an even distribution from fibre lengths, which is recommended as an area of further research.

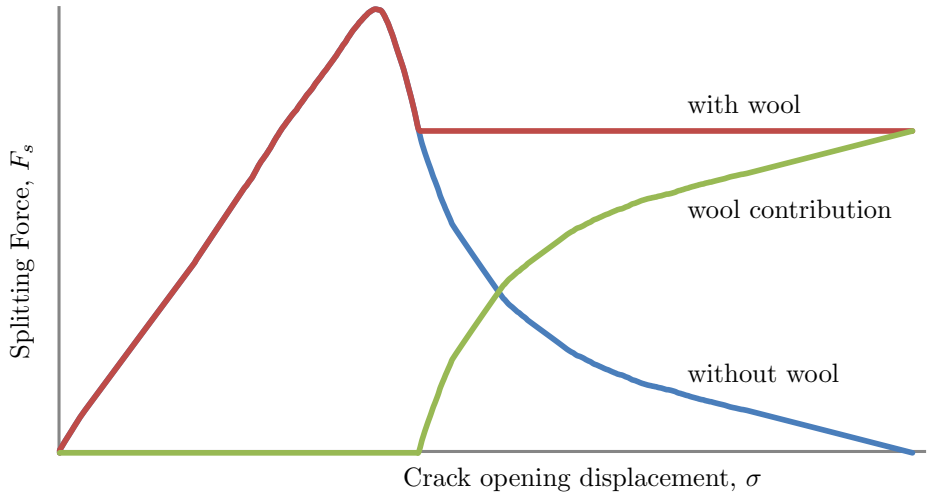

Figure 4.12: Idealised loading response curves for samples with and without wool, plus highlighting of the wool contribution.

The load response behaviour of the samples with wool necessitated a slightly different approach to calculating the fracture energy, as the sustained load resulting from the wool would contribute to the calculation of fracture energy without any fracture taking place. The area under the loading response curve (see Figure 4.6) can be divided into two areas: that of increasing load before the creation of a crack (before point M), and that of decreasing load once the crack is formed (after point M). As the decreasing load curve portion of the plot could not be used in analysis due to the influence of wool pull-out effects discussed above, it was hypothesised that the fracture energy used to create the initial crack (i.e. before point M) would be an appropriate alternative to calculating the fracture energy of the entire loading

curve. Although the fracture energy by definition is the energy needed to create and propagate a crack, the energy used to create the crack in the material must be linked to the energy required to propagate a crack, therefore a loading fracture energy $G_{f,L}$ is proposed, which equals the fracture energy of the sample up to maximum load, which is the point at which the macrocrack first starts to form. To verify that $G_{f,L}$ is related to the full fracture energy G_f, the response curves of all the samples with no wool were analysed and areas under the plot were calculated. Figure 4.13 shows a comparison of the areas under the increasing load portion of each sample plot with the area under the full response curve, and shows a clear positive linear relationship between the two. Therefore $G_{f,L}$ may be calculated and used instead of G_f when there is reason to doubt the accuracy of calculations involving the curve after the maximum load point, such as in samples where pull-out effects are likely to skew the results. In the case of the investigation presented above, G_f may be calculated from $G_{f,L}$ by multiplying it by a factor of 1.3, as calculated from the gradient of the line of best fit in Figure 4.13, in order to obtain a rough value for comparison with other investigations. This factor, however, is fully dependant on the size and shape of the response curve which itself is dependant on the material properties and it is therefore recommended that a comparison is obtained for each new set of tests with each material. Such material properties that would affect the multiplication factor would include, but not be limited to, elasticity in the soil matrix arising from the clay and the overall bonding strength of the material.

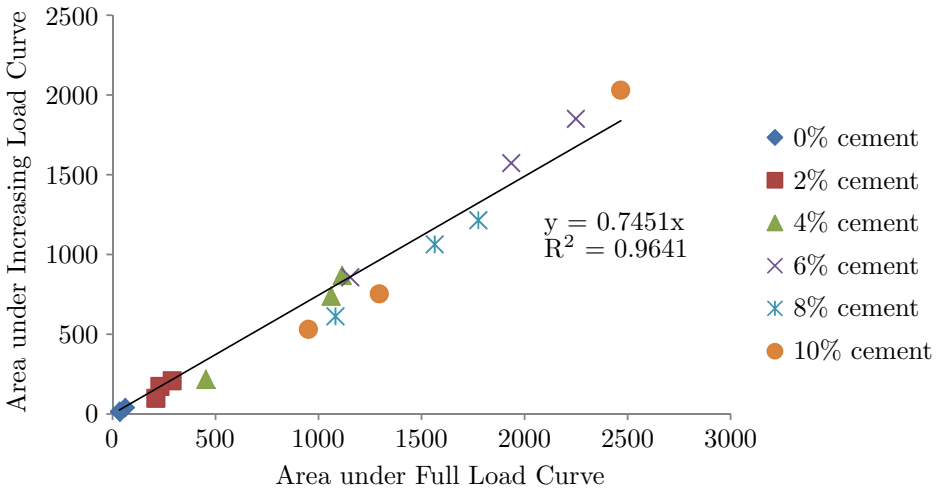

Figure 4.13: Comparison of areas under the increasing loading curve and the full curve of samples without wool.

4.3.4 Analysis of fracture energy

Average values of $G_{f,L}$ from this investigation and unconfined compressive strength (UCS) from Section 3.3 are given in Table 4.1, alongside the variability of the results around the average values and the standard deviation, s. Percentage variability var is presented as a maximum and minimum value, as

calculated using Equation 4.3.

$$var = max\left(\frac{x_i - \bar{x}}{\bar{x}} \times 100\right)\% \ , \ min\left(\frac{x_i - \bar{x}}{\bar{x}} \times 100\right)\% \tag{4.3}$$

where x represents UCS or $G_{f,L}$, x_i is the sample's value of x and $\bar{x}$ is the average value of x across all samples in the same batch.

It is clear from the table that samples without wool have a much greater percentage variability in UCS than those with wool, with an average variability of ±27% opposed to ±6% or ±8% for 1% and 2% wool respectively. This suggests that wool homogenises and unifies the sample, making different parts of the sample fail at the same time, thereby also increasing the UCS, but this is independent of the amount of wool added - that is, the amount of wool does not change the variability in the sample. Variability in $G_{f,L}$ follows the opposite pattern where samples with 0% wool have a ±50% average variability, whereas samples with 1% and 2% wool have variability of ±74% and ±71% respectively. Variability of UCS with respect to cement content, however, is negligible.

Table 4.1: Average values of UCS and $G_{f,L}$ from all WST samples. Numbers in brackets indicate the number of samples tested. Where fewer than 6 samples have been tested, this was due to substandard sample quality.

Batch ID	UCS (N/mm^2)	$G_{f,L}$ (N/m)	Variability in UCS	s (%)	Variability in $G_{f,L}$	s (%)
S-W0C0	0.45 (5)	2.96 (6)	+13%, -21%	15.8	+89%, -73%	55.4
S-W0C2	0.96 (6)	12.78 (5)	+29%, -42%	31.1	+31%, -59%	38.5
S-W0C4	1.48 (6)	15.85 (4)	+25%, -33%	25.6	+11%, -18%	13.3
S-W0C6	2.07 (6)	49.73 (5)	+30%, -35%	26.5	+65%, -59%	51.6
S-W0C8	2.50 (6)	44.32 (6)	+21%, -21%	19.7	+38%, -32%	32.4
S-W0C10	3.58 (6)	69.26 (6)	+25%, -28%	26.5	+65%, -60%	54.4
S-W2C0	0.86 (6)	1.38 (4)	+5%, -8%	5.2	+69%, -46%	49.2
S-W2C2	1.89 (6)	12.66 (6)	+4%, -2%	2.1	+107%, -71%	80.8
S-W2C4	2.68 (6)	14.88 (5)	+7%, -7%	4.9	+95%, -37%	54.3
S-W2C6	2.92 (6)	15.83 (5)	+9%, -12%	6.7	+73%, -79%	59.0
S-W2C8	3.56 (6)	21.90 (6)	+5%, -3%	3.0	+59%, -82%	50.6
S-W2C10	4.24 (6)	23.29 (2)	+7%, -4%	3.7	+4%, -4%	5.5
S-W4C0	0.94 (4)	1.31 (5)	+8%, -5%	5.3	+80%, -64%	59.6
S-W4C2	1.68 (5)	16.53 (5)	+10%, -9%	7.1	+133%, -83%	80.0
S-W4C4	2.41 (6)	15.75 (5)	+7%, -9%	5.6	+47%, -41%	96.8
S-W4C6	3.41 (6)	52.03 (6)	+12%, -9%	7.9	+149%, -78%	31.6
S-W4C8	3.10 (6)	20.37 (5)	+5%, -9%	4.7	+48%, -48%	43.0
S-W4C10	4.30 (6)	35.46 (6)	+8%, -5%	4.9	+47%, -39%	30.7

Rossi et al. (1991) presents values of $G_{f,L}$ of concrete of between 42.4 and 75.6 N/m; the average value for each test ranging between 48.8 and 68.7 N/m. Average percentage variability for each test was between -25% and +21%, while standard deviation s ranged between 7.8% and 18.8%. Comparison of those results with the results of the tests performed in this investigation indicate that the fracture energy of RE varies between 4% (W0-C0) and 101% (W0-C10) of that of concrete, depending on cement content.

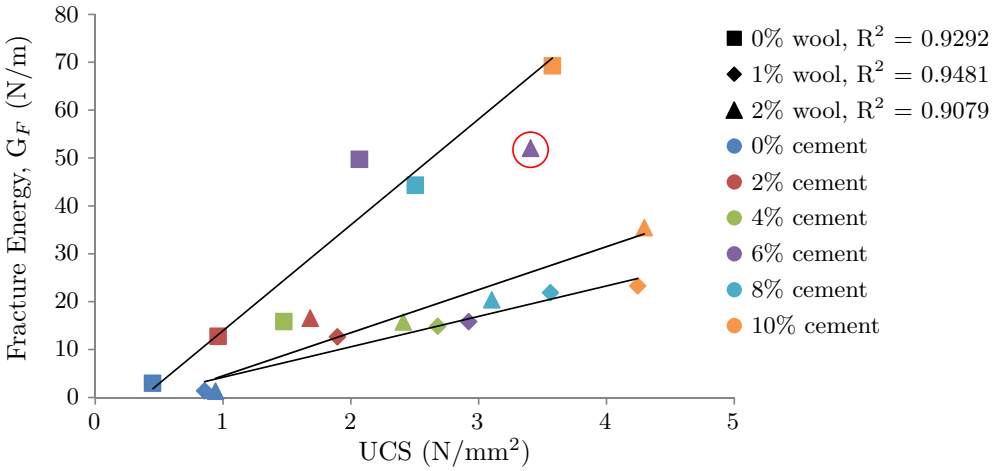

Figure 4.14: Results of fracture energy and UCS.

Figure 4.14 shows a plot of average $G_{f,L}$ values against average UCS for all samples as reported in Table 4.1. Lines of best fit were drawn between samples with the same wool content. Respective R^2 values were calculated and are presented in the figure. For the wool reinforced samples, in the majority of samples, the amount of wool present in the sample makes negligible difference to the fracture energy, but does affect the UCS as described in Section 3.3. An exception to this, sample batch S-W4C6, is circled in the Figure. This sample was not included in the calculation of the line of best fit as it is a clear outlier - the average fracture energy equals more than double that of the sample containing the same amount of cement and 1% wool. The result is also around $1\frac{1}{2}$ times the second highest value of fracture energy (10% cement) whereas in all other cases the samples with different amounts of wool but the same amount of cement produced similar fracture energies ($\pm$20%), therefore this data point must be considered to be unrepresentative of the material. It is noted that of the 6 samples tested in this batch (S-W4C0), 2 of the samples produced a fracture energy around 5 to 6 times the average of the other 4 samples, therefore skewing the mean average to much higher than the median, casting doubt on the validity of using the mean as the actual value in this case. The maximum F_s of the samples, however, showed a similar variation between them as between the samples in other batches, therefore the large disparity in the results must arise from the crack opening displacement portion of the plot, as a larger crack opening displacement at the same maximum F_s would produce a higher calculated fracture energy $G_{f,L}$. Figure 4.15 shows the force-displacement response curves for samples S-W2C6-2 and S-W4C6-3, which reported the highest and lowest fracture energies respectively. Sample S-W4C6-3 produced a fracture energy of 10.48 N/m, while sample S-W4C6-2 produced a fracture energy of 129.52 N/m, more than 12 times that of sample S-W4C6-3.

It is suspected that this disparity between the plots was due to a difference in the wool arrangement in the sample, whereby a crack formed and opened prior to the sample reaching maximum load, meaning

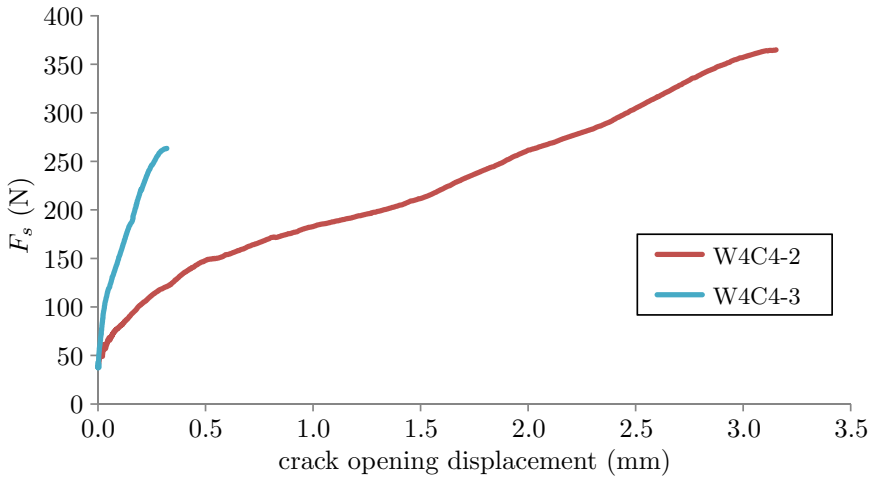

Figure 4.15: Comparison of crack development with increasing F_s for samples S-W4C4-2 and S-W4C4S-3.

that wool had started to pull out of the sample before the maximum load. If the two results with very high fracture energies (S-W4C4-1 and S-W4C4-2) are disregarded, the average fracture energy is reduced to 20.3 N/m, with the point lying below the line of best fit, adjacent to the W2C8 data point. it is recognised, however, that discounting those two results increases the uncertainty in the resulting value as only 4 samples would be considered to obtain this result. It is also noted that, due to multiple sample failure in 4 of the 6 samples in batch S-W2C10 resulting from high wool content, the result plotted in Figure 4.14 has a higher degree of uncertainty than the other points on the plot. The point still lies in the expected region, however, and can therefore be included in calculations for the line of best fit, albeit with less certainty considering the high variability between the results of other sample batches. However, the uncertainty in this point lends more credibility to the consideration that the amount of wool (either 1% or 2%) makes little difference to the fracture energy. This idea was previously discussed in Section 3.3, however in that situation the wool increased the UCS of the material.

Figure 4.14 also shows a difference in behaviour when wool is added between samples with low cement content (0%-4%) and high cement content (6%-10%). The inclusion of wool increases the UCS as has been previously stated, but it makes negligible difference to the fracture energy of the samples with low cement content. In these cases, therefore, the area under the loading half of the curve must be very similar in the samples with or without wool. For the high cement content samples, this relationship changes, as the inclusion of wool actively reduces the fracture energy of the sample. Any increase in wool content would increase the likelihood of any wool strands lying in, but not across, the crack zone, and a larger increase in wool content results in a larger likelihood of this occurring. Any such wool would not only create an area of weakness in the crack zone due to the expansive nature of the wool, as previously identified and discussed in Section 3.4.6, but also decrease the area of effective soil-soil bonding in the crack zone. It is also noted that when subjected to tensile tests to determine maximum strain, the wool

strands increased in length by approximately 35% before they failed. This means that if any wool strands were lying across the crack zone, they would have been very unlikely to contribute to the strength of the RE as while the RE would have broken as it is a brittle material, the wool would have stretched and hence taken a negligible fraction of the load before sample failure.

While this might explain the reduction in fracture energy when wool is added to the high cement samples, it does not explain why the wool reinforcement has a different effect on samples with low cement compared to high cement content. It was observed during sample construction that the samples with high cement content felt drier that the samples with low cement content. This suggests that there was less free water available for bonding to form between the wool and the fibres. In other words, a high cement content accentuates the soil/cement - fibre bonding issues previously identified in this section. Thus adding wool to high cement content samples weakens the sample to a greater degree than adding wool to low cement content samples. This is supported by the development of strength of cement-based materials as it is commonly known that cement does not add immediate strength to a sample, but instead the strength increases as cementation occurs, typically requiring an assumed 28 days to fully develop material strength.

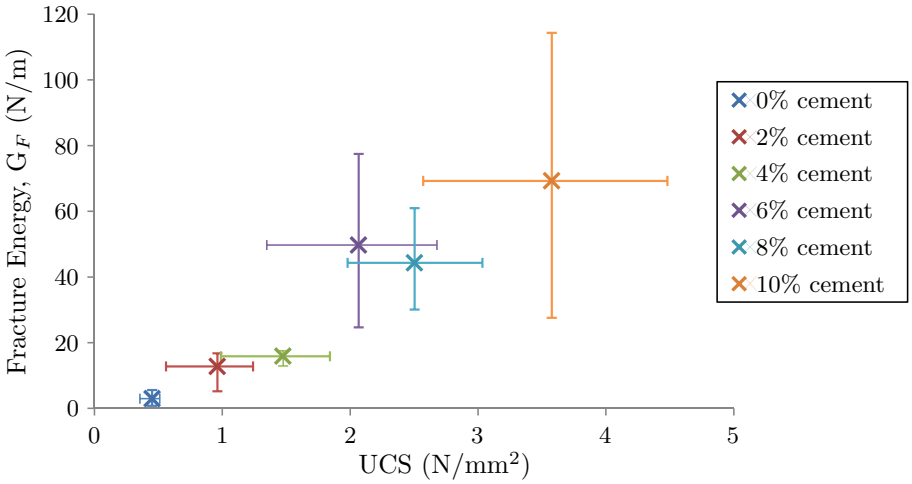

Figure 4.16: Plot showing the relationship between $G_{f,L}$ and cube strength.

Figure 4.16 shows average values of fracture energy of the samples without wool, plotted against average UCS, along with sample variation as reported in Table 4.1. Each 'region' defined by sample variation is a different shape and size, suggesting that there is no common factor that affects the variability of the results. There is a general positive correlation between $G_{f,L}$ and UCS, although it appears that as $G_{f,L}$ and UCS increase, the variability of each increases also. There is a slight anomaly considering the samples with 8% cement, as the variability of these samples is very small compared to those with 6% and 10% cement. It is unclear what caused this, but it is likely that it is either due to an inconsistency in construction technique or that too few samples were tested to generate the large sample variation as

exhibited in other sample batches.

4.4 Conclusions

In this chapter, the fracture energy of RE, that is the amount of energy needed to generate and propagate a crack through a material, was calculated and the effects of two different stabilisation materials, cement and wool, were assessed. It has been found that wool strands in a compacted soil affect the response curve to such a degree that the post-peak curve may not, and indeed should not, be considered in the calculation of fracture energy of this soil. This is because the measured fracture energy from the response curve would not be representative of the material due to pull-out forces artificially enhancing the latter half of the curve after peak load has been reached. It has also been suggested that the pre-peak curve is a sufficiently equal portion of the full response curve of samples without wool reinforcement, such that the pre-peak curve alone may be considered as a suitable alternative for calculating fracture energy. An alternative fracture energy $G_{f,L}$ has been proposed for situation such as this where the full curve cannot be used and recommendations for comparison of this value with other fracture energies reported in literature has been proposed. It has been acknowledged that this may be a feature of this particular fibrous reinforcement, and that individual fibres, or microfibres, may provide a more favourable response than the fibre strands of wool used in these investigations. It is likely that as they might provide a similar or greater fracture energy improvement than wool fibres, as fibres not bunched in strands would not compact and expand in the same manner that the strands have been found to do.

This chapter has confirmed that a higher UCS generally leads to a higher fracture energy, likely due to the same increased bonding between the material particles. It was also found and discussed that wool decreases the fracture energy, likely, at least in part, due to weaker bond strength between wool and soil particles than between two soil particles, while the effect of wool on the drying rate of the samples has been discussed.

Chapter 5

Hydraulic behaviour

Water plays a crucial role in rammed earth and other earthen construction materials, whether stabilised or unstabilised. In a chemically stabilised soil-based construction material (SBCM) using cement or lime, to mention the two most commonly used methods of chemical soil stabilisation, water is required for the hydration processes which gives the material strength. In cement-stabilised soils, water enables the cement to hydrate, forming cementitous bonds between soil particles, while in lime-based soil mixes, water initiates cation exchange and starts the cementation process (Ciancio et al., 2014). In unstabilised earthen construction, water is crucial because it aids compaction and provides suction to give the material strength (Jaquin et al., 2008b). Many studies have been performed to study the role of water content in the construction and strength of SBCMs and a few studies have investigated the effect of water on SBCMs, post-construction. Examples of research performed to understand the material pre- and mid-construction include investigations into strength development (Schroeder, 2011), suction development due to compaction water content (Jaquin et al., 2009) and the effect of water content on the material characteristics (Bui et al., 2014a; Beckett and Augarde, 2012). Examples of research performed to study the material post-construction include investigations into water absorption in unstabilised samples (Hall and Djerbib, 2006), submersion of stabilised samples (Bahar et al., 2004; Kenai et al., 2006), the effect of humidity on compressive strength and suction (Gerard et al., 2015) and assessing the effect of climatic simulations on moisture penetration (Hall, 2007).

Water is also known to be the main cause of shrinkage in clays, particularly in expansive montmorillonite or illite based clays, when water removal through natural or forced drying is known to often result in the creation of shrinkage cracks through the clay. As water has such a crucial effect on unstabilised soils, it is therefore likely to play a significant role in a physically stabilised (e.g. fibre reinforced) SBCM also, the specifics of which will depend on the material and are currently unknown.

In this chapter, the effect of wool stabilisation on the formation and development of cracks in soil is

studied. Two different clays (kaolinite and bentonite) are mixed with sand and/or wool and the effect on drying rate and crack development is discussed. As no pre-existing tests recommended in the British Standards were suitable for the analysis required, a test is performed which uses image analysis to track crack initiation and development. In order to accentuate shrinkage and hence facilitate the study of crack development, soil with a high water content was used, in contrast with the low water contents typically used in SBCMs.

5.1 Introduction to shrinkage in SBCMs

Cracking in SBCMs is undesirable as cracks allow water ingress leading to potentially catastrophic failure, particularly in unstabilised rammed earth (Jaquin et al., 2008b). Therefore, understanding the processes of crack initiation and propagation in earthen construction materials is essential in order to create solutions and to adapt the soil mixture to prevent it. Of the main four components of earthen construction (gravel, sand, silt and clay), clay is the only portion that provides any level of shrinkage due to small particle size and the electrostatic effects not present in other materials (Section 2.2.3). Therefore the shrinkage of clay must be studied and investigated in order to understand, control, and hence minimise, the formation of shrinkage cracks in SBCMs. As SBCMs are not pure clay materials, the variation in the amount of shrinkage of clay when mixed with sand or gravel is of particular interest.

Shrinkage of different clays has been explored in traditional soil mechanics, as well as how crack development is affected by the presence of other materials, but few investigations, however, have been performed specifically on shrinkage in SBCMs. In soil mechanics, Wei et al. (2016) investigated crack formation and propagation mechanisms in pure clays and found, amongst other conclusions, that the first cracks form when the soil is saturated and confirmed that large cracks in clays originate from smaller cracks (or microcracks) joining together. It is suggested that this mechanism is present in rammed earth (RE) also. In SBCM research, Du et al. (1999) found that clay shrinkage can be reduced by the addition of lime, indeed it is recommended that clayey soils use lime stabilisation as opposed to cement stabilisation as the cementation reactions are less favourable than the ionic exchange reactions present during lime construction (Sherwood, 1993). Little research has been performed, however, on the effect of fibrous reinforcement on shrinkage in soils, and how the addition of fibres might help to reduce it.

5.2 Method

It is theorised that fibres in a soil mix would help to reduce cracking in the soil as fibres might help to dissipate the energy that would otherwise be used for crack extension. A test was therefore needed which could study the shrinkage of earthen materials in a quantitative way. In soil mechanics, the standard

test is the linear shrinkage test, details of which are given in the British Standard BS1377-2. The test calls for a very small sample (less than 150g) in a half-cylindrical mould 140mm in length and 25mm in diameter. This was judged to be too small for the addition of any wool fibres, and so an initial test was performed using this method, scaled up to 353mm in length and 63mm in diameter, and using a full cylinder. However, these samples did not exhibit any shrinkage, partly, it is thought, because the samples had to be constructed at optimum water content in order for the sample to maintain integrity. Those samples were subsequently used for the unconfined cylindrical shear tests detailed in Section 3.6. Therefore an alternative test was needed, one that would allow observations of shrinkage while also allowing the inclusion of wool fibres without the fibres dominating the sample.

An experimental program was devised whereby two different clays, a highly expansive sodium-bentonite clay and an unexpansive kaolinite clay, would be mixed with different combinations of sand and wool strands. These soil mixes would be mixed with water and lightly compacted into petri dishes and naturally dried to observe crack formation and propagation and drying rate. Although this test is not representative of real-world conditions, due to the difference in water content and soil composition (see Section 5.2.1), the scope of this experiment is to compare the effects of adding different materials, rather than to measure actual values. The following sections provide details of the performed investigation.

5.2.1 Materials

Two different clays were used to make a comparison of shrinkage characteristics of different soil mixes, both of which needed to be readily available in dry, powdered form for ease of soil mixing and sample repeatability. The kaolinite used in Chapters 3 and 4 was used, as well as sodium bentonite, a montmorillonite clay. Sand was added to half of the samples to investigate the role of particle size distribution on shrinkage cracking.

Four different soil mixes were constructed, two for the different pure clays, plus two for the different clays with added sand. Where used, sand was mixed into the clay at a ratio of 2:1 by mass, to approximate the soil mixture used for the samples tested in Chapters 3 and 4. The samples were constructed at or near to the soil's liquid limit in order to maximise the shrinkage cracking. Although this method is not representative of RE construction, the scope of this experiment was to investigate the relative effects of adding wool fibres to different clay mixes. Liquid limits were determined using the cone penetrometer test as described in the British Standard BS1377-2. The pure kaolinite (K) and kaolinite plus sand (KS) mixes were found to have liquid limits of 69% and 26% respectively, however the liquid limits of the bentonite (B) and bentonite plus sand (BS) soil mixes were higher due to the properties of the clay and subsequently much more difficult to obtain. Difficulty in obtaining a reliable liquid limit value for bentonite is well known and the liquid limits of different sodium bentonite clays typically range between

550% and 750% (Inglethorpe et al., 1993). While the bentonite plus sand (BS) soil mix returned a liquid limit of 103%, adding enough water to the bentonite (B) soil proved difficult in the time available. The bentonite samples were ultimately constructed at 245% water content, less than half the expected liquid limit of over 500%. Despite the large disparity between the expected and constructed values, the clay greatly increased in size when water was added, so it was concluded that shrinkage cracks would still form such that sufficient comparisons regarding the role of fibrous reinforcement could be made.

5.2.2 Sample production and testing

A small amount of wool, identical to the material used in samples in Chapters 3 and 4, was mixed into half the samples of each soil in order to investigate the effect of wool content on drying rate and crack initiation and propagation. In total, 24 samples were constructed; 3 samples with wool and 3 samples without, for each of the 4 different soil mixes. Sample IDs were assigned according to the constituents of the sample concerned, followed by a number indicating the individual sample. For example, sample KW3 contains kaolinite clay (K), wool (W) and is the 3rd of the KW samples. Additionally, sample BS1 contains bentonite clay (B), sand (S) and is the 1st of the BS samples.

Plastic petri dishes, hereafter referred to as sample trays, 92mm in diameter and 7mm in height, were used to construct and hold the samples. The samples were constructed by pushing the clay mix into the sample trays, ensuring that no air was trapped in the soil, and levelling the samples to the top of the sample tray using a spatula. They were then left to dry at in a temperature controlled room at 19.7 $\pm$0.2°C and 50 $\pm$4% relative humidity. Samples were photographed and weighed once every 24 hours for 10 days, after which all sample masses had stabilised which allowed further analysis to be performed.

5.2.3 Image manipulation

In order to obtain quantitative data from the daily photographic record of the changes in the samples, it was decided to manipulate the images using digital processing tools in order to visually enhance the cracks such that the images could be assessed by a computer to detect cracks and hence calculate the crack area. Advantages of this method over visually comparing the images include obtaining quantitative data, and the ability to process large numbers of images in a short period of time. The main potential problem with this method is that of correct determination of the crack area. Methods to minimise the potential errors in the calculation are included in the relevant part of the experimental procedure detailed below.

Each photograph was digitally manipulated in order to accentuate the cracks by turning the cracks and soil into black and white areas respectively. Each initial image (such as that shown in Figure 5.1a) was made monochrome and inverted in colour, followed by minimising the image 'fill' and maximising

the image 'shadow' using a simple photo editing software. The effect of this was to turn the cracks black and the soil and background white in order to maximise the contrast between the two parts of the image, which minimised potential internal thresholding errors during the digital analysis.

Images were then re-inverted to form images similar to that shown in Figure 5.1b. The sample images were then processed using Matlab using the 'binaryImage' function and subsequently summing the number of dark pixels to calculate the crack area in the image. An unprocessed image was used in Matlab to calculate the number of pixels across the sample, from which the area of the sample in pixels could be determined and the percentage crack area was then calculated. The crack area could then be used to track crack development and compare final crack sizes between different samples. Figure 5.1 shows an example comparison of sample BSW2 (containing bentonite clay, sand and wool), showing the sample photograph before (5.1a) and after (5.1b) digital manipulation for crack area calculation in Matlab. The post-manipulation photo clearly shows a few white 'crack' areas in the sample (such as those highlighted in Figure 5.1b) which do not show as cracks in the pre-manipulation image, and are likely due to shadows in the soil due to the lighting conditions under which the photographs were taken. All post-processing images were observed to contain similar small regions, which appeared to be approximately proportional to the amount of cracking in the sample. In order to calculate the effect of these imaginary cracks on the calculated crack area, one image was altered such that the imaginary crack were removed from the image. This doctored photo was then processed using the same method as the undoctored images, and the difference between the two images was calculated to be less than 2% of the total crack area. Therefore it was decided that the extra black pixels (from the imaginary cracks) did not need to be removed from the images and were hence subsequently included in the crack area calculation.

It is recognised that there is a level of uncertainty in the image manipulation that is difficult to remove in its entirety. Whilst a trial image was used to confirm that Matlab calculated the black and white areas correctly ($\pm$<1%), the process of obtaining a black and white image was subject to the user's input on selection of different lighting levels. Although the levels selected for each image used was the same, and that all photos were taken in the same lighting conditions by the same camera at the same distance, there is no way to guarantee that the black and white image corresponded exactly with the location, size and shape of all the different cracks present in the sample. Errors were minimised by using the same manipulation for each image as this reduced random error which left a minor systematic error in the images as previously discussed. One example of this systematic error is the shrinkage of the sample from the edge of the dish. Whilst in the majority of cases, the samples only shrank from the edge of the casing by a small amount, in some cases the change was large which resulted in some of the white paper under the clear tray shining through. This extra light area ultimately registered as soil in digital processing, with a line crack around the edge of the area, clearly underestimating the amount of shrinkage cracking

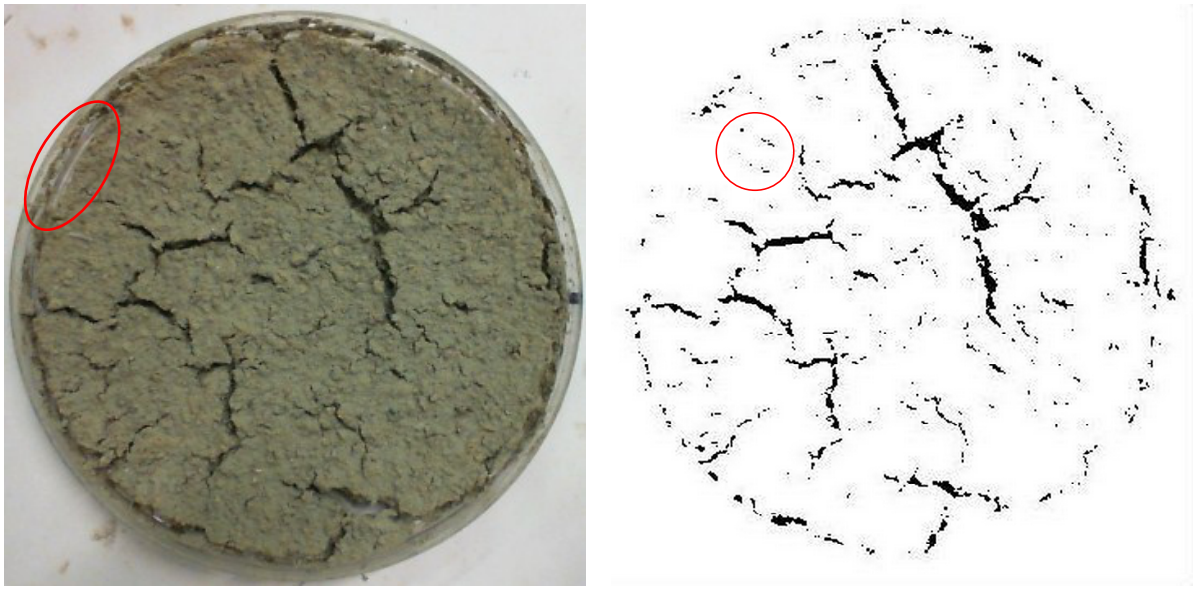

(a) Photograph of sample BSW2 on day 10 of drying, pre-digital manipulation.

(b) Photograph of sample BSW2 on day 10 of drying, post-digital manipulation.

Figure 5.1: Comparison photographs of shrinkage sample BSW2 on day 11 of drying, pre- and post-digital manipulation.

in the sample. A small example of this effect can be seen in the upper left hand corner of Figure 5.1. It can be clearly seen in the pre-manipulation image that the sample has detached from the edge of the sample tray and the white paper can be seen through the bottom (highlighted in Figure 5.1a), but the post-manipulation image just shows an area of white, implying that no cracks are present in this region. Whilst fairly common, as this appeared as a minor feature in around 30% of samples, it was judged that error had little effect on the overall readings as the large area of cracking in the central region of the sample was of most interest. The samples most affected by this underestimation were the samples with pure bentonite and no wool. It is estimated that cracking in these samples is underestimated by around 10%, obtained from a comparison of images of the sample before and after digital manipulation, and calculating rough the error margins.

Attempts were made to include crack depth in analysis, however all attempts were unsuccessful. Stereo-photogrammetry has been used successfully in other investigations (Bui et al., 2009), however this was not possible due to equipment availability and time constraints.

In addition to the built-in uncertainty from the image analysis, it must be also stated that the method used does not take account of microcracks in the material, as these were too small to be observed either visually or with the photographic equipment. Considering standard crack theory, that a bigger crack has a greater buildup of stress and is therefore more likely to propagate, it may be reasoned that macrocracks are more critical to the behaviour of the material. Macrocracks are also more vulnerable to massive water ingress and subsequent catastrophic failure than microcracks, therefore the change in amount of

macrocracking in the material when mixed with wool fibre is crucial to understand in order to optimise material behaviour, for if cracking is reduced, then the overall strength of the material is likely to be increased. For this reason, the study of microcracks did not lie within the scope of this research, and hence discussions regarding the role or effect of microcracks in the material are not presented.

5.3 Results and discussion

This section presents and discusses observations regarding sample drying rate and crack development, made during the sample production and sample drying processes. Observations are compared with the relevant results in order to confirm the theories made during sample observation. The results of the analysis detailed in Section 5.2.3 are also presented. Discussions are focussed on the effects of the addition of sand or wool, as well as their differing effects on the clay type. It was highlighted in Section 5.2 that these tests were performed for comparative purposes only, and this is particularly relevant considering the constraining forces applied on the samples. Internal and external constraints, either from differing shrinkage rates or from friction against the sample tray respectively, dictate where the cracks within the material occur, and these cannot be removed completely from the considerations. However, considering that the constraints apply to all samples, it is appropriate to use these tests for comparing the effects of different soil compositions and the addition of wool fibres on shrinkage cracking.

It is acknowledged that these samples are not representative of RE due to particle size distribution and water content, and also the sample size is very different to that usually used for experimentation. Additionally, the void ratios for these samples are likely to be very different due to the different compositions of the clays chosen for this investigation. However, this does not negate the outcomes of this test. Considering that RE is unlikely to be completely homogenous, it is likely that there will be pockets of 'pure' clay within the mix, and these areas will be particularly vulnerable to cracking. Additionally, fibres have been found to increase compressive strength of the material (Section 3.3), and it is of interest if compressible fibres help to prevent cracks forming or growing as incompressible ones have been found to do in SBCMs (Galán Marín et al., 2010). Finally, throughout the experiments presented in this thesis, it has been observed than very few cracks have been observed, and therefore a test was required to emphasise any cracks in the material in order to investigate how to minimise microcracks that could not otherwise be observed.

5.3.1 Sample drying rate

Figure 5.2 shows the average drying curves for all samples up to day 6 after construction, after which no further drop in mass was recorded. It initially appears that the Figure only shows plots the samples

containing wool, but in fact the difference between the drying curve of samples with wool and samples without is negligible and so the lines occupy the same space in the plot. This clearly shows that wool fibres have no effect on the drying rate of these samples. The Figure also shows that the samples containing kaolinite dry quicker than the bentonite samples, and that sand also increases the rate of drying. However, as the plots start at different water contents, it is more difficult to draw conclusions from the drying rates at any point other than at the end of the plot, when the percentage water content is constant.

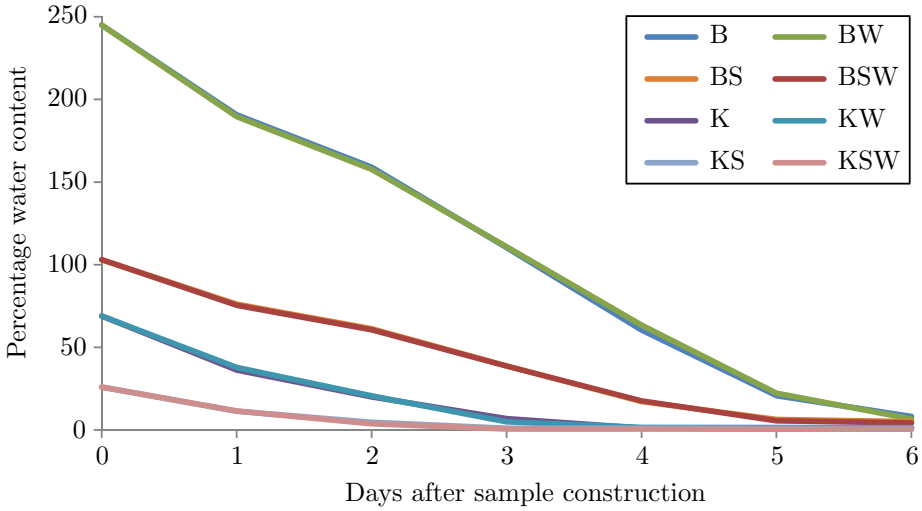

Figure 5.2: Average drying curves for shrinkage samples.

The water contents of all samples, measured daily during the drying period, were therefore converted into percentage of initial water content w_p according to equations 5.1 and 5.2.

$$w_t = \left(\frac{m_t - m_d}{m_d} \right) \tag{5.1}$$

$$w_p = \frac{w_t}{w_i} \times 100 \tag{5.2}$$

where w_t and m_t are the water content and mass of the sample respectively at time t, m_d is the dry mass of the sample, measured from drying the sample in the oven after natural drying, and w_i is the initial water content of the sample. Values of w_p were used in order to compare the drying rates of different samples with different initial water contents on the same figure.

Figure 5.3 shows the average drying curves of all samples plotted against w_p, together with error bars showing the maximum and minimum values of each triplicated result. Figure 5.3 shows little difference between the drying curves of the samples with and without wool, as was previously seen in Figure 5.2, therefore confirming that wool has a negligible effect on the drying rate of these samples. However, the type of clay used and the soil composition both have a clear effect on the drying rate. The variation in the behaviour of the samples with different clays is a result of the behaviour of the different clays upon interaction with water. As detailed in Section 2.2.3, kaolinite clays are hydrophobic while bentonite clays

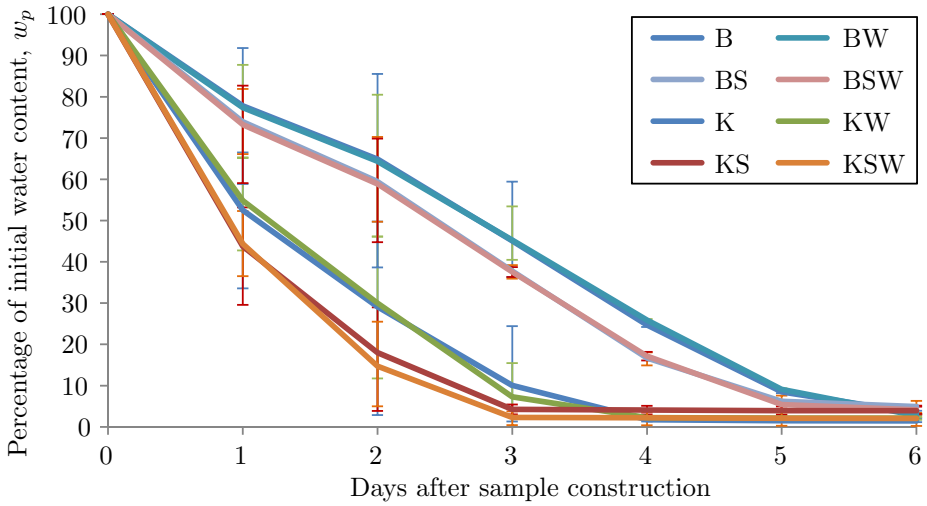

Figure 5.3: Average drying curves of shrinkage samples, presented as values of percentage of initial water content w_p, together with error margins.

are hydrophilic, due to the ions contained between the individual particles. A hydrophilic clay such as bentonite would not only absorb more water, as shown by the clay's higher liquid limit compared to kaolinite, but would also be more resistant to water removal. This would result in a bentonite sample recording a shallower initial part of the drying curve than a kaolinite sample, which is clearly seen in Figure 5.3. While the error bars display a wide variation between similar samples, particularly before 3 days after sample construction, it is noted that the extreme values of each sample set remained the extreme sample for each data point (i.e. the sample with the highest mass on day 1 after construction also had the highest mass on days 2 and 3 after construction, and likewise for the sample with the lowest mass). Therefore it may be noted that while there is a large amount of variation, the average values may still be used for comparison. It is noted that the different samples have very different initial water contents (Section 5.2.1), which may affect the drying rate of samples, and the difference in drying rate may be simply due to the fact that the B and BS samples take longer to dry as they contain more water. If this was the case, through, it would be expected that the water content would be directly related to the length of time needed for the sample to fully dry. The bentonite (B) samples were constructed with a water content of 245%, while the BS samples were constructed at 103% water content. If drying time was entirely related to the initial water content, then the B samples would take longer (but not necessarily twice as long) as the BS samples. However, Figure 5.3 clearly shows that B and BS samples both finished drying on day 6, and only had a minor difference between the samples on their drying curves - indeed, around half the drying takes place between days 2 and 4, during which the drying curves for samples B and BS are running approximately parallel. If the drying rate was linked to the amount of initial water content, the B samples would be expected to report a much shallower drying curve.

Figure 5.3 also shows that the addition of sand increases the drying rate of the sample. The inclusion

of sand primarily changes two properties of the soil - it reduces the amount of clay in the sample, and it also changes the particle size distribution of the soil. Although these properties are linked as they result from the same action, they may be considered to produce two different effects. A reduction in the amount of clay would also have different effects depending on the type of clay concerned. While water is understood to be held in both clays in menisci between particles, water is also stored in the bentonite clay microstructure between the layers (Section 2.2.3), resulting in a greater amount of water capacity in the soil. Therefore, if the amount of kaolinite clay is reduced then only the potential water stored by the clay particles' connecting menisci will be lost, whereas if the amount of bentonite in a sample is reduced, then a larger proportion of potential water storage would be lost as the water stored interally between the layers of clay, plus water stored as menisci would both be lost. Therefore, there would naturally be a considerable difference between the percentage change in drying curves comparing the bentonite and the kaolinite samples, which is seen in Figure 5.3. However, as both samples exhibit a decrease in the liquid limit by approximately 60%, it is not the reduction in clay that affects the drying rate, assuming that the water held in each clay by menisci is approximately equal. If reduction in clay did affect the drying rate, then the liquid limit of the bentonite mix should display a greater drop in liquid limit. Alternatively, as the percentage changes in liquid limit are identical, this is likely due to the change in particle size distribution of the soil, specifically regarding the addition of sand opposed to the removal of clay. It has already been seen that the samples with sand are able to contain less water than their pure clay counterparts (Section 5.2.1), which implies that the water is less able to form bonds with sand particles than with clay particles. This implies that a matrix of large and small particles is able to contain less water in the soil matrix than a sample with all small particles.

While the inclusion of wool does not appear to affect the drying rate of the sample as previously discussed, it is possible that the dimensions of the samples used in this investigation may have affected this apparent lack of difference. A thin sample, with high surface area to volume ratio, like the samples tested in this investigation (approximately 1:3), would naturally dry much quicker and more evenly through the cross-section of the sample compared to a sample with a smaller surface area to volume ratio, such as the majority of samples previously investigated (e.g. unconfined compressive strength (UCS) (Section 3.3) surface area to volume ratio = 1:17, direct shear test (DST) (Section 3.4) surface area to volume ratio = 1:6). As the shrinkage samples are thin, 90% of total water loss occurred in 3 - 5 days, compared to around 14 days for the UCS and DST samples (see Sections 3.3 and 3.4). A slower drying time would result also in a greater hydraulic gradient between the innermost section of sample and the surface, which might result in the wool creating a path by which the water in the middle of the sample may travel to the surface easier than by having to pass between soil particles. This would need to be investigated through the construction a variety of samples of the same volume but with different surface areas, some of which

contain different amounts of wool. It is widely known that a greater surface area to volume ratio will improve rate of drying in the majority of materials, but it is only with the same investigation including wool, that the effect of wool or other fibrous reinforcement on the drying rate of a SBCM sample might be known and understood.

Table 5.1: Final water contents of shrinkage samples, including average final water content (AFWC) and percentage final water content compared to the original water content (w_p).

Batch ID	Final Water Content (%) 1	2	3	AFWC (%)	w_p (%)
K	0.67	0.67	0.65	0.66	0.96
KW	0.75	0.83	0.72	0.77	1.12
KS	0.36	0.36	0.11	0.28	1.08
KSW	0.41	0.36	0.36	0.38	1.45
B	8.99	9.12	8.98	9.03	3.69
BW	9.08	9.04	9.17	9.10	3.71
BS	0.00	2.33	2.28	2.31	2.24
BSW	0.00	2.44	2.45	2.44	2.37

Table 5.1 shows final water contents of each sample, alongside the average final water content (AFWC) and w_p from Equation 5.2. All samples reported a w_p value of between 0.9% and 4%, likely, at least in part, held in the soil matrix as menisci bonding between particles. Additionally, it can be assumed that in the bentonite samples, a proportion of the withheld water is stored in the expansive layer of the bentonite clay. It has been previously stated that adding sand to either kaolinite or bentonite samples reduces the final water content of the sample, however the w_p values suggest that the sand does not greatly affect the percentage of water retained in the kaolin samples (Table 5.1). This suggests that the difference in final water content between the K and KS samples is primarily due to the difference in original water content. This also suggests that there is little difference between the water retaining properties of the sand particles and the kaolinite particles. This is expected as kaolin clay, like sand, is unexpansive and unreactive (Section 2.2.3). The bentonite samples, however, show a slight reduction in w_p (3.69% (B) to 2.24% (BS)) when sand is added, suggesting that bentonite is better at retaining water in the sample than sand. This is also expected due to the properties of bentonite, as water is retained between the clay layers that make up its microstructure (Section 2.2.3).

Wool appears to have the same small effect on the water retention properties of the samples, as all samples exhibited an average increase of 0.1% in AFWC. However, this equal apparent increase in water content, rather than being due to the wool increasing the water retention properties of the material, is more likely due to the mass of the wool itself, as the amount of wool added to each sample was included in the calculations of AFWC. It is therefore likely that the difference between final 'water content' of the samples is actually mass of wool rather than water. This minor inconsistency is negligible, however, due to its size, and has limited implications for further analysis and discussion, considering that wool has

repeatedly been found to have no effect on the drying rate of the samples tested in these investigations.

5.3.2 Crack development

During the drying period, the kaolinite samples did not appear to produce any cracks across the sample surface that were visible to the naked eye, which meant that the computer visual analysis as described in Section 5.2.3 was unable to be performed. However, the samples were not uniform as a very small ($\leq$1mm) amount of shrinkage was observed by eye in a small number of pure kaolinite samples, shown through a very minor detachment of the sample from the edge of the sample dish. Some samples were also observed to reduce in height, particularly towards the centre of the sample, producing a slightly concave surface. Lack of substantial shrinkage was expected as Kaolin is an unexpansive, unreactive clay (Grim, 1962) and hence does not expand upon contact with water, nor react to its continued presence, and therefore does not shrink once water is removed from it.

The small amount of shrinkage at the sample edges that did occur is likely due to suction in the material. As the samples were constructed at the soil's liquid limit, the samples would have been fully saturated. As a saturated sample dries, menisci form between the soil particles (Lourenço et al., 2012), which then shrink as the sample dries further. Reduction in the size of the menisci through sample drying increases suction in the sample, which results in forces pulling the sample towards the centre of the sample. The minor amounts of sample shrinkage is therefore likely as a result of the increase in suction in the soil mix. As suction is an internal force pulling the sample together, an increase in suction may result in shrinkage, which is magnified at the edge of the sample resulting in small gaps between the sample and the tray as observed in Figure 5.1 in Section 5.2.3. It is suggested that a larger sample might distribute the suction forces differently such that cracks may appear in the central region of a sample, similar to the cracks observed in tests on shrinkage of kaolin clay reported in Wei et al. (2016), when samples 300mm by 200mm in size were used.

In contrast to the kaolinite samples, all of the bentonite samples exhibited shrinkage through cracking as well as significant shrinkage at the edge of the sample. The notable expansion upon continued contact with water results in a subsequent substantial contraction if water is removed from the clay. This was confirmed as extensive shrinkage was observed, despite the samples being constructed at under liquid limit (Section 5.2.1). Therefore a greater water content (i.e. at liquid limit) would have resulted in an even greater shrinkage resulting from a greater expansion during mixing the water into the clay.

Figure 5.4 shows an array of photographs of sample BS2 taken on each of the first 9 days of drying. Photographs of the sample taken after day 9 are not shown as they were visually identical to the sample on day 9, and no further decrease in mass was observed after this point. Figure 5.4 shows that the first small cracks in sample BS2 were observed on day 2. At the same time, the pure bentonite samples were

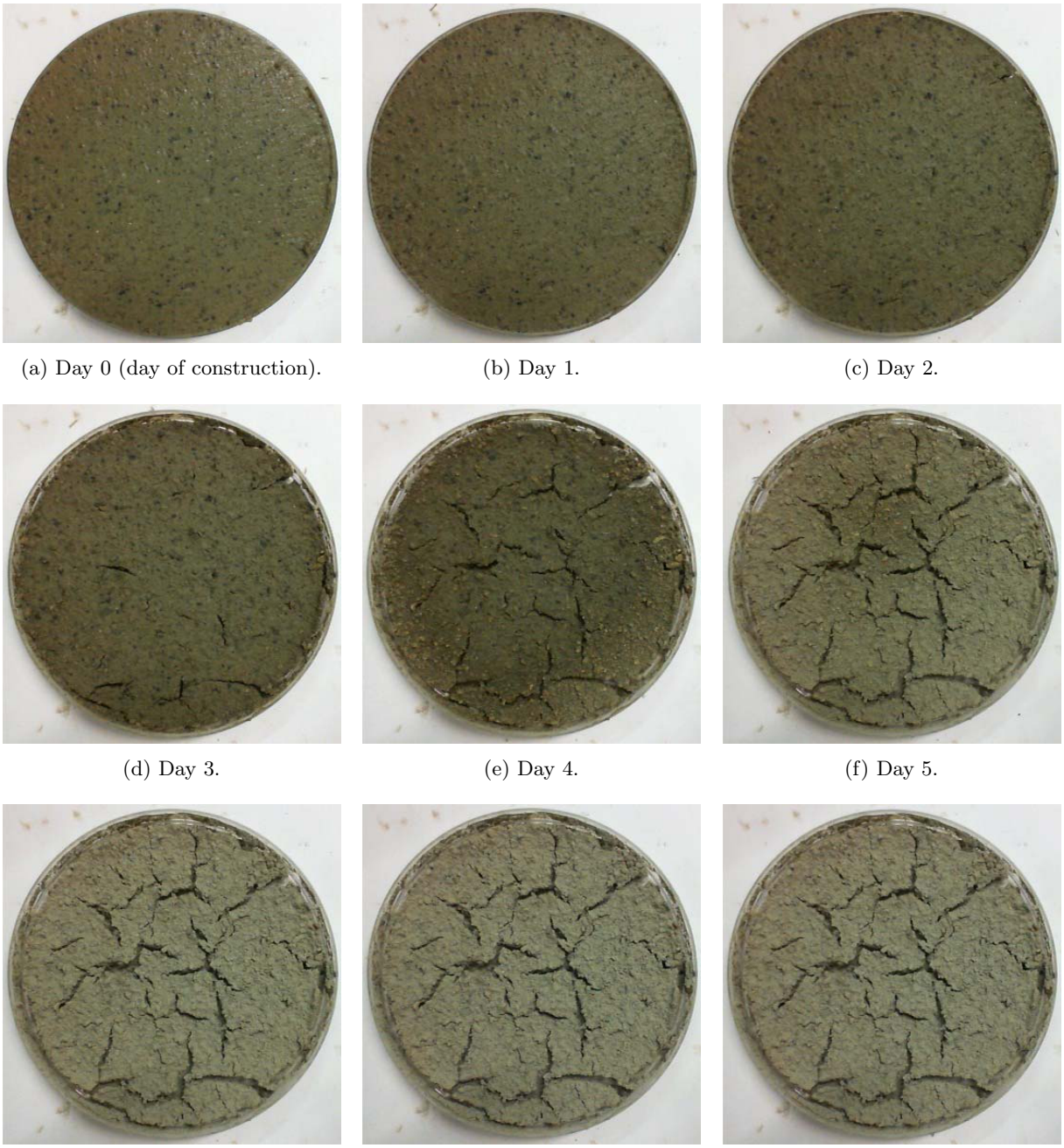

(a) Day 0 (day of construction). (b) Day 1. (c) Day 2.

(d) Day 3. (e) Day 4. (f) Day 5.

(g) Day 6. (h) Day 7. (i) Day 8.

Figure 5.4: Photographs of crack development in shrinkage sample BS2.

beginning to show signs of shrinkage from the edge of the sample tray. Day 3 shows the first large main cracks appearing in sample BS2, while the majority of cracks had appeared by day 4. Also on day 4 the first noticeable colour change due to reduction of water was visible at the edge of the sample. The image on day 5 shows few additional cracks to day 4, although each existing crack has noticeably expanded and the sample has mostly changed to a final, pale, colour and looks 'dry'. This drying pattern shows that, despite the thin cross-section of the sample, crying clearly occurs from the outside towards the centre. By day 6, the sample is almost dry and there is no further visible-by-eye change in crack growth.

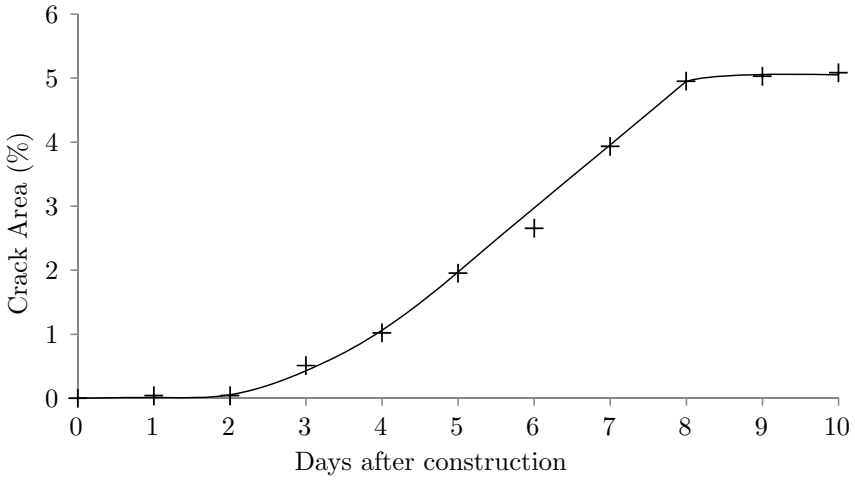

Figure 5.5: Crack development in sample BS2.

The photographs of sample BS2 were analysed according to the process detailed in Section 5.2.3 and Figure 5.5 plots the crack area development of the same sample. It clearly shows that substantial crack development begins to show on day 3, and proceeds at a steady rate until it peaks and levels out on day 8. It is noted that there is a difference between the perceived and the measured halts to crack growth. The images in Figure 5.4 imply a halt to crack growth on day 6, while Figure 5.5 shows a measured halt to crack growth on day 8. This suggests that between days 7 and 8, crack growth is very evenly distributed among the cracks, giving the impression to the human eye that the cracks have not changed in size. Figure 5.5 also shows that the crack area growth is very even in the central portion of the plot, at around 1% per day. It is unclear what causes this regularity, although it is likely linked to the drying rate shown in Figure 5.3. Applying the basic principles of crack growth, such as that a crack will grow if the applied stress is greater than the material capacity (Section 2.4), the fact that crack growth appears to be evenly spread across the sample suggests that buildup of stress in the material is similarly evenly distributed. As an increase in stress in the drying samples could only be related to the increase in suction in the sample resulting from the drop in water content, then the crack growth must inherently be related to the decrease in water content.

Additionally, it was previously noted from Figure 5.3 (Section 5.3.1) that sample BS2 lost negligible mass after day 6 (0.2g or 0.7% of the total water loss). It has also been shown that cracks in the sample continued expanding for a further 2 days until day 8 (Figure 5.4), suggesting that on day 6 there were still considerable residual stresses contained in the soil matrix to continue crack formation for 48 hours after the water had been removed from the sample, which proves that continued crack growth is due to the stresses in the material, and not as a direct result of the removal of water in the sample. This likely originates from a small amount of elasticity in the bentonite clay, which would also contribute to the crack growth during the drying process. This might also help to explain the discrepancy between the immediate

start to the drop in sample mass at the start of sample drying (Figure 5.3) and the slow start to crack formation in Figure 5.5. The elasticity of the clay would absorb the majority of the initial stresses, and, according to general fracture theory (Section 2.4.2), cracks would only form once the plastic limit of the clay has been reached. After this point, any increase in stress would be transferred into sample fracture, as microcracks will start to form and eventually form macrocracks in the sample. As buildup of stress cannot be directly observed using the apparatus in this test, the evidence must be considered for this expected behaviour, which can be seen in the Figures above as explained.

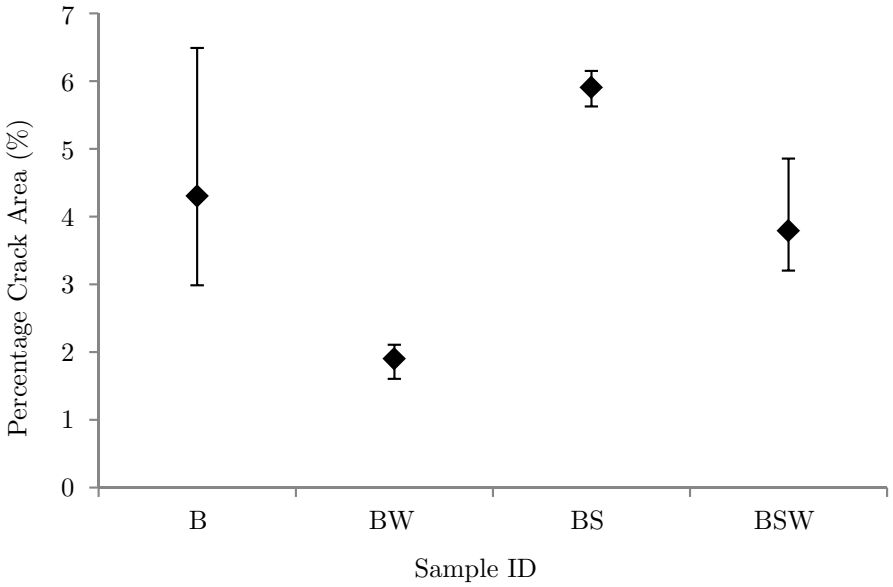

Figure 5.6: Final crack area for all bentonite samples, with and without sand and wool.

Figure 5.6 shows the final crack areas according to sample contents for all bentonite samples. It is clear that adding wool to either the B or BS mix reduces the final crack area in the sample, while adding sand to the B or BW mix slightly increases the final crack area. The variation in the B samples is likely due to analytical errors in the visual computational analysis. The cracks appeared to have similar areas, but some samples were heavily domed in appearance, the centre lying around 8mm above the top of the sample tray, which were therefore much more difficult for the computer to analyse visually. This was rectified by lightly breaking the samples into flat pieces around 4cm^2 which were kept in the sample tray before analysing the broken pieces in the usual way. Any errors introduced using this method may be justified as accurate analysis of the samples would have been impossible if the samples had remained their domed appearance. Despite any errors added through this method, however, it is still thought that the average crack area value obtained is still representative such that a comparative value may be obtained, due to the area-based method used (Section 5.2.3).

There was no apparent correlation between the location of the wool strands and the cracking pattern, i.e. the cracks did not lie along the lines of wool on the surface of the sample, therefore further supporting

the rejection of the hypothesis presented and rejected in Section 3.4.6, which proposed that wool creates areas of weakness in the sample. However, evidence was seen of wool strands halting the growth of some cracks. Figure 5.7 shows a close-up view of a crack, clearly showing wool fibres bridging the crack near the crack tip. These strands were stretched tight across the crack, implying that the fibres had been pulled out of the soil. This not only implies that soil forms very strong bonds with the wool fibres, but also that the fibres add to the tensile strength of the sample. A higher tensile strength results in fewer shrinkage cracks (formed by tensile forces overcoming the suction bonds) across the sample. Furthermore, as the wool strands did not cross any crack paths, they could not have enhanced the strength of the samples alone, thereby further supporting the proposal set out in Section 3.7: that it is the wool fibres, not the compressible wool strands that are the main cause of increase in structural properties of the soil resulting from this investigation into the effect of fibrous reinforcement.

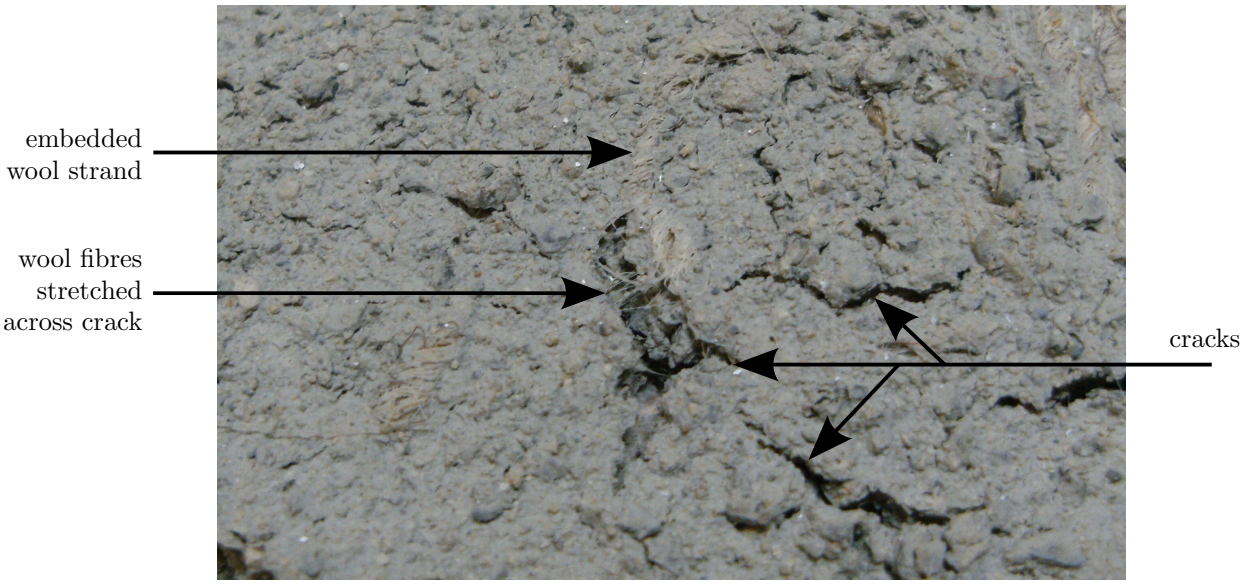

Figure 5.7: Close-up view of sample BSW2, showing shrinkage cracks, embedded wool strands and wool fibres stretched across a crack.

It was previously observed in this section that the inclusion of sand increased the shrinkage crack area of the sample. This leads to two different hypotheses:

1. That larger soil particles result in a few number of meniscus bonds in the sample, therefore reducing the tensile strength of the sample, or

2. That the addition of sand creates a more brittle soil, as adding a brittle sand to a ductile clay would reduce the overall plasticity of the sample.

An easy way to prove hypothesis 1 would be if that individual suction bonds in a soil create the same suction between particles, considering that, logically, a greater number of larger sand particles with a set volume would result in a fewer total number of particles overall. Gens (2010) reports that the

force between two spherical particles, due to suction, depends on the surface tension and diameter of the particles, as calculated by Fisher (1926), and while Gens (2010) also notes that soil particles are not spherical, it may be reasoned that the suction still depends on the surface tension and the diameter of the soil particles concerned. Assuming that this is the case, and also assuming that surface tension is equal, based on the reasonable assumption that pore water pressure throughout the sample is also equal, this means that the particle size is therefore linked to suction. As the particle sizes are not equal, this means that the suction bonds are likely to be unequal. However, this does not prove that hypothesis 1 is incorrect - it merely shows that it is not simple to confirm. Proof via direct measurement of individual suction bonds would be near-impossible, particularly considering the microscopic dimensions and measurements concerned. It is possible that different carefully-selected and mixed soil samples, analysed using an environmental scanning electron microscope, may be an alternative method to verify this hypothesis.

Hypothesis 2 requires the natural plasticity of bentonite to remain present in the material when water is removed from the samples, as if the bentonite clay has no plastic component to its strength when dry, then the soil would be no less brittle either with or without sand. Thus the bentonite clay must not only be plastic when very wet, but also maintain a small amount of plasticity when dry. Grim (1962) states that 'Clay materials ... develop plasticity when they are mixed with relatively small amounts of water,' thereby implying that clay without water cannot have any plasticity. However, the 'small amount[s] of water' will naturally depend on the type of clay concerned. Considering that it is highly unlikely that all the water in a bentonite sample will dry out naturally, without oven drying, it may be assumed that there is a very small amount of plasticity remaining in the clay after 'drying'. However, considering that the samples were very brittle to the touch, it is unlikely that the amount of plasticity left in the sample is significant.

Therefore, as neither hypothesis 1 nor hypothesis 2 may be completely confirmed or proved incorrect, it suggested that both factors may contribute to the sand increasing the crack area of the sample.

5.4 Conclusions

Cracking and shrinkage in unstabilised RE is a known concern as it can lead to catastrophic failure. In this chapter, an experimental procedure to analyse the differing effects on shrinkage and cracking generation of adding sand and wool to different types of clay has been performed and the results and implications discussed.

As expected, the kaolinite clay samples, either pure, with or without sand, and with or without wool, did not exhibit any levels of cracking, although a small amount of shrinkage from the edges of some samples was observed. In contrast to the kaolinite samples, the bentonite clay samples exhibited a much

larger degree of shrinkage and cracking. While wool was found to reduce the cracking in any sample, sand was conversely found to increase crack area. It was suggested that wool microfibres resist crack growth, slowing down and occasionally halting the cracks which happened to cross their path. Sand increases cracking, likely in part due to a reduction in forces holding the samples together. These forces were proposed to originate from the plasticity of the bentonite clay, coupled with the water menisci between the particles, together forming a tight suction bond between the particles. Plasticity in the bentonite was further supported through observations of continued crack extension after the sample mass had stabilised and subsequent discussions.

The bentonite samples were also found to dry considerably slower than the kaolinite samples. It was discussed that this was likely due to a combination of the higher initial water content and also water storage in the expansive bentonite samples, which was withheld by the clay for longer than the water contained in menisci. Results showed that wool did not affect the drying rate of any samples, neither bentonite nor kaolinite, while sand was shown to increase the drying rate. It was discussed that this is likely due to the size of particles, creating fewer menisci between particles, allowing more water to be removed from the sample more quickly. It is suggested that wool would have an effect on the drying rate of larger samples, but that effect was not observed in these samples presented due to their limited size. A set of experiments varying sample volume with surface area and wool content would be able to reach firm conclusions about wool strands creating a hydraulic path through the samples, allowing for a quicker drying curve. Investigations involving forced drying or wetting on one end of the sample could also be included to exacerbate any effects.

In this Chapter and in Section 3.6, bentonite has been shown to be less appropriate for use in SBCMs, although if a bentonite-bearing natural on-site soil is desired for use in a RE construction, fibres may be added to improve the shearing properties of the material. However, if the soil is being brought from off-site or being used for scientific investigations, kaolinite is the more appropriate clay to use for the reasons explained in this Chapter.

Chapter 6

Thesis Discussion

This chapter combines the research described in the previous chapters in this thesis into a series of principal themes spanning all the experimental programs. These principal themes link directly to the research aims of this thesis presented in Section 1.1. These research aims are centered around how the addition of cement and waste carpet fibre affect three key material properties: unconfined compressive strength (UCS), shear strength, and fracture energy. This chapter presents discussions showing how these aims have been achieved.

6.1 Effect of cement stabilisation on the properties of RE

Cement stabilisation of rammed earth (RE) and other soil-based construction materials (SBCMs) is common in order to improve the compressive strength of the material (Burroughs, 2008). The effect of cement stabilisation on other material properties, such as shear strength and fracture behaviour, have received less attention, and this research aims to contribute to the limited knowledge in this area.

6.1.1 Effect of cement stabilisation on UCS

As described in Section 3.3, the compressive strength of a sample is commonly measured in concrete construction in order to determine whether the material is of sufficient quality to be used. In this capacity, it can also used for assessment of RE mix suitability for construction purposes (Burroughs, 2008). Cement is known to increase the UCS of SBCMs, previously found in many investigations (e.g. Jayasinghe and Kamaladasa (2007); Burroughs (2006); Venkatarama Reddy et al. (2016)), and the results of the tests performed in Section 3.3 are consistent with these previous conclusions. Cement has been found to increase UCS linearly in proportion to the amount of added cement (Section 3.3), at a rate of approximately 0.4N/mm^2 per % cement added (Figure 3.5). This concurrence with previous data sets

confirms that the mixes used for experimentation do not behave in a significantly different manner to those tested in other investigations, and therefore validates comparison between the investigations in this thesis and other published research.

When comparing different data sets for cement-containing samples, either from investigations using concrete or stabilised RE, it must be noted that not all data sets can be directly compared as the experiments in this thesis use a range of cement contents from 2% to 10%. This range is lower than that typically used in concrete (general purpose concrete typically being mixed at 1:2:3 ratio of cement:sand:gravel, resulting in a 17% cement content), and is also higher than is often used in soil stabilisation in soil mechanics (generally 0-4% in the papers found during this research). It is important, therefore, that the cement content of the samples is considered when making comparisons between the research presented here and other research papers.

6.1.2 Effect of cement stabilisation on shear strength

Shear behaviour has been studied extensively in the soil mechanics field of study, and the shear behaviour of soils with fibrous reinforcement has also received attention. However, soil mechanics investigations typically do not investigate samples with high levels of compaction similar to that in SBCM research, and so while some comparisons may be made between shearing behaviour in soils and RE, the limitations of such comparisons must be considered. To the author's knowledge, shear behaviour in SBCMs has not been extensively studied, and Cheah et al. (2012) is one of few previous investigations which specifically look into the shear strength of *stabilised* rammed earth. It presents the results of a triaxial test and triplet test performed on cement-stabilised soil. The main purpose of the study was to compare the two tests and so no measurements from unstabilised samples were reported in the paper, limiting the potential opportunities for comparing change in strength or initial soil strength. However, the authors do report values of cohesion and angle of shear resistance ϕ of 724kPa and 48˚ - 56˚ respectively (for stabilised, unreinforced triaxial samples). Consoli et al. (1998) performed a triaxial investigation on stabilised sand samples, and reports a marked increase in cohesion (9.9kPa to 56.7kPa) and a smaller increase in angle of shear resistance (35˚ to 41˚) when 1% cement was added to a sandy soil (Soil ID 8:31:61:00 or 39*:61:00 following the soil identification system presented in Section 3.2.1).

The experiments performed in this thesis report comparative values of cohesion of 48kPa - 177kPa (mean 129kPa) and values of angle of shear resistance of 52˚ - 76˚ (mean 60˚) (Table 3.1). These values are higher than the values reported in Consoli et al. (1998), although any patterns between factors in Consoli et al. (1998) are harder to identify. This is because the variation between samples was limited (0%/1% cement, 0%/3% fibre) and no repeat tests appear to have been performed, leading to no data on sample variation. Also, considering that only two different cement and fibre contents were used, no relationship

between increase in cement/fibre content and sample behaviour could be identified. Additionally, the differences between the results might also be due to the different material composition - the samples used in Consoli et al. (1998) had a high sand content and very little clay, resulting in a significantly different material being tested.

Adding cement appears to have little effect on angle of shear resistance (Table 3.1), although the results do suggest an increase in cohesion with an increase in cement, except for the sample with 6% cement, where cohesion is reported as lower than the unstabilised samples. Additionally, Figure 3.16 plots values of cohesion against angle of shear resistance, which shows that there appears to be no clear link between cement content and either angle of shear resistance or cohesion, although it does suggest that an increase in angle of shear resistance will result in a lower recorded value of cohesion, and vice versa.

6.1.3 Effect of cement stabilisation on fracture energy

As fracture tests were developed for concrete, the author has found limited previous studies to compare the fracture behaviour and properties of materials such as RE before and after cement stabilisation. Lenci et al. (2012) investigated the fracture properties of unfired dry earth, similar to RE but with a different particle size distribution to 'typical' RE construction. A series of three-point bending tests were performed and subsequently analysed using linear elastic fracture mechanics (LEFM) to model crack tip opening rate according to fracture theory (Section 2.4.1), although the fracture energy of the material was not presented in the paper. Similarly, Hallett and Newson (2005) modelled crack growth in soil using elasto-plastic fracture mechanics, but the authors predominantly investigated crack growth rather than the fracture energy of the material. Both papers are predominately focussed on fracture behaviour rather than fracture energy, and so there are minimal opportunities for comparison. Therefore, more similar tests that may be used for comparison can be found in the concrete literature.

The results presented in this thesis suggest that cement stabilisation greatly increases the fracture energy of RE (Table 4.1), but has little effect on the variability between the samples. Section 4.3.4 presented a discussion on fracture energy in comparison with concrete, and found that the fracture energy of RE varies between 6% (W0-C0) and 185% (W0-C10) of that of concrete as reported in Rossi et al. (1991), depending on cement content and to which sample in Rossi et al. (1991) it is being compared. Addition of cement has been found to increase the fracture energy of RE, and it is proposed that this is due to the cementitous bonding between particles being stronger than suction bonds in unstabilised RE, leading to a higher bond force between particles, thereby increasing the fracture energy of the sample.

6.1.4 Summary of cement stabilisation findings

In the experiments presented in this thesis, cement has been shown to increase UCS and fracture energy. In contrast, the addition of cement has been shown to have little effect on angle of shear resistance or cohesion. Therefore, addition of cement has been found to have a positive or neutral effect on all material properties measured in this thesis.

6.2 Effects of wool reinforcement on the properties of RE

Mechanical stabilisers such as plastic (Binici et al., 2005), straw (Schroeder, 2011) and wool fibres (Aymerich et al., 2012) have been used, on occasion, to reinforce soils to improve material properties. In this thesis, the use of waste carpet fibres (called wool throughout this thesis) from the manufacturing industry has been investigated as a potentially viable method of strengthening SBCMs.

6.2.1 Effect of wool reinforcement on UCS

It was observed in Section 3.3.3 that wool increases UCS, however the experiments performed did not show a significant difference between UCS values when either 1% or 2% wool was added. It was found that wool increases UCS from 0.45N/mm^2 to 0.86N/mm^2 for 1% added fibre and to 0.94 for 2% added fibre, a difference on only 0.08N/mm^2. The existence of an *optimum fibre content*, where UCS is at a maximum and also higher than measured during experimentation, was discussed in Section 3.3.3. An *optimum fibre content* between 1% and 2% fibre would lead to a situation where two different fibre contents either side of optimum have the same UCS, and it is proposed that this is the cause of the apparently similar UCS values on this occasion.

Galán Marín et al. (2010) concurs that adding wool fibres to a 'clay composite' earthen material increases the UCS of the material, albeit an increase of a lower percentage and from a higher unreinforced UCS - an increase in UCS of 37%, from 2.23 MPa to 3.05 MPa (compared to the 91% increase from 0.45MPa to 0.86MPa observed). The soil ID, translated to the system used in this thesis, is 32:45:23:00 (or 77*:23:00), which has a significantly higher silt content than the soil used in this thesis. This difference in particle size distribution is likely to be a significant cause of the difference in compressive strength, although it is likely that the addition of Lignum, a resin, included to 'improve the workability' of the soil, has also increased the strength of the material by acting as a stabiliser and binding the material together beyond that expected from suction. Wool was added at 0.3% by mass and water at 24.8% by mass - a very high optimum water content for a SBCM, again suggesting that the Lignum had a large effect on the material which was not considered within the work. Despite the difference in soil composition, however,

Galán Marín et al. (2010) does support the findings in this thesis - that adding wool to RE increases the UCS of the material.

6.2.2 Effect of wool reinforcement on shear strength

Section 3.4.6 presents a discussion on how adding waste carpet fibre to a RE sample affects its behaviour under shearing loading conditions. It has been found that it reduces peak shear stress (Figures 3.19 and 3.21a), and decreases density (Table 3.2), which is expected as carpet fibres are less dense than compacted soil. Table 3.1 shows a reduction in angle of shear resistance when wool is added to an unstabilised soil (i.e. sample W0C0 reported an angle of shear resistance of 67°, W1C0 - 48°, W2C0 - 8° and W3C0 - 32°). Note that the 8° reported for W2 (1.0% wool content) is more likely to be 23° in reality, due to the result variation shown in Figure 3.17 and surrounding discussion in Section 3.4.5. This would fit more closely with the trend of decrease in shear strength with increase in wool content. An increase in wool content affects the shear samples in two ways - firstly, it decreases the density, therefore reducing the number of soil particles that resist the shear forces, and secondly, it also adds an internal weakening force resulting from the compression of the wool particles during construction, as discussed in Section 3.4.3. Table 3.1 also reports values of cohesion for these samples, but no pattern can be seen with regards to the wool content and the values range from 40kPa to 103kPa (Section 3.4.6).

Bouhicha et al. (2005) reports on a series of experiments on different soils with added straw fibres. Shear box tests found that, in the majority of cases, adding either 1.5% or 3.5% fibre significantly reduced T, which is assumed to be the maximum shear pressure (measured in bar), although this is not clearly stated. Bouhicha et al. (2005) implies that T is a measure of the samples' strength measured during a shear box test (although it is strangely not specified what T measures), therefore allowing limited comparison with the data reported in Section 3.4. Both data sets agree that adding wool reduces the shear strength of the material, although the difference in additional strength is difficult to analyse as Bouhicha et al. (2005) used a different range of fibre contents (1.5%/3.5% as opposed to 0%/2%/4%/6%/8%/10%) and a different soil composition (various, see Bouhicha et al. (2005), as opposed to 30*:70:00) to that used in this thesis.

Additionally, Consoli et al. (2004) performed a series of tests on uncemented soil matrices, adding different types of fibre at 0.5% by mass and also investigating the effect of change in fibre length. Consoli et al. (2004) reports that adding plastic fibres to an uncemented soil increases the angle of shear resistance ϕ by around 20% (from 37° to 40° - 44° depending on plastic type and fibre length), and found that the cohesion is unchanged from 0kPa for polyester fibre, but increases to 12kPa or 32kPa when polypropylene fibres are used. The soil used is very different to that used in this thesis (100% fine sand), which accounts for the lower reported values of cohesion, as a uniform sand will have less cohesion than if clay is present

with the sand. Clay in the sand mix will help the formation of suction bonding between sand particles, whereas sand alone will produce much fewer due to the size of the particles (Section 2.2.3). The angles of shear resistance (43˚- 44˚ for the most similar fibre length) lie within a similar region to those determined in the experiments presented in this thesis (48˚ for 0.5% fibre - W1C0), therefore supporting the work presented in this thesis. Consoli et al. (2004) tested samples with fibre lengths of 12mm or 36mm only, and found that increasing the fibre length increased the angle of shear resistance, therefore increasing it further to 40mm or longer, as per the length used in this thesis, would be expected to further increase the angle of shear resistance, as the experiments in Section 3.4 show. A longer fibre length is likely to cross more stress planes, bonding particles together and therefore increasing angle of shear resistance.

Comparing values of cohesion in this thesis with those in Consoli et al. (2004), it suggests that cohesion is linked to suction in the material, because the soil with lower suction (i.e. compacted sand in Consoli et al. (2004)) produces a lower cohesion than that in compacted soil (in this thesis). Vanapalli et al. (1996) reports that a higher suction will result in a higher shear strength, which supports this hypothesis - a higher shear strength τ would result in a higher y-intercept and hence higher cohesion. This will not lead to a large change in angle of shear resistance ϕ, however, as a change in ϕ would need a different change in shear strength with normal stress.

6.2.3 Effect of wool reinforcement on fracture energy

In Section 4.3.4, the fracture energy of RE samples were calculated using the wedge splitting test. It was identified during testing that the measured fracture energy was being artifically enhanced by pull-out effects, and an alternative *loading* fracture energy $G_{f,L}$ was proposed, as described in Section 4.3.3. $G_{f,L}$ could be converted into the 'full' fracture energy G_f for comparative purposes by multiplying it by a factor of 1.3 as described in Section 4.3.3. By analysing this new measure of fracture energy $G_{f,L}$, it was shown in Table 4.1 that adding either 1% or 2% wool to the soil mix approximately halved the measured fracture energy from 2.96 N/m to 1.38 N/m or 1.31 N/m respectively. This is likely due to the wool reducing the number of strong particle bonds within the fracture zone, thereby reducing the measured fracture energy. Table 4.1 also shows that adding wool decreases the variability in the samples by approximately two-thirds - the standard deviation s of the samples is reduced from 15.8% to 5.2% or 5.3% for samples S-W2C0 and S-W4C0 respectively. It is not known why the deviation is reduced when wool is added, although it is possible that it is due to the effect of the wool binding different section of the soil mix together, transferring forces from weaker areas of soil to stronger areas, making a more homogenous sample overall.

To the author's knowledge, the experimental program described in Chapter 4 is the first within SBCMs research to use the wedge splitting test, therefore direct comparisons with other research are not possible.

However, some research has been performed analysing the fracture energy of compacted soils calculated using a different industry-standard test. Aymerich et al. (2012) describes a set of three point bending tests on a fibre-reinforced earthen material, finding that increasing the fibre length (from 1cm to 3cm) or content (from 2% to 3% by mass) increased the peak load, although the increase in fibre length appeared to have a greater effect than the increase in fibre content. The author has been unable to find other papers that present specific investigations into the fracture energy of unstabilised earthen materials, other than another paper by the same authors (Aymerich et al., 2016) that reached similar conclusions to those reported in Aymerich et al. (2012) regarding the effect of change in fibre length and its effect on peak load or absorbed energy.

6.2.4 Summary of wool reinforcement findings

In summary, adding waste carpet fibre to unstabilised RE has been found to negatively affect many material properties, which is likely due to the compressibility of the wool. It decreases dry density, peak shear strength and fracture energy of the material, although it has also been shown to improve the UCS. It has also been found to reduce angle of shear resistance, and have little effect on cohesion. Considering these results alone, it is suggested that waste carpet fibre is not used within SBCMs. As these experiments have been shown to be contrary to other investigation on fibrous reinforcement in both RE and in concrete, it is suggested that this is due to the compressible nature of the fibres, and that incompressible fibres might be more beneficial to material properties.

6.3 Effects of combined wool reinforcement and cement stabilisation on the properties of RE

While adding wool and adding cement have been investigated separately, and the findings summarised in the previous sections, the combined effect of adding cement and wool to RE is of particular interest as each was likely to have an effect on the other. It has been found that adding one material may negate the positive effects of the other in some cases, and that positive effects have been improved further in others.

6.3.1 Effect of wool reinforcement and cement stabilisation on UCS

Section 6.1.1 and 6.2.1 presented discussions that show that adding cement or wool fibres to a RE mix improves the UCS of a RE sample independently, and therefore it may be assumed that adding both to one sample also provides a positive effect. Figure 3.5 clearly shows that the positive effects of adding

cement or wool are neither inhibited nor enhanced by the presence of the other - that is, the effects are added rather than multiplied. Adding wool to unstabilised samples increases the UCS by a similar amount for each wool percentage (Section 6.2.1), and this behaviour does not only occur in unstabilised samples (Figure 3.5). Indeed, it is clearly shown that the UCS increases by a similar amount ($0.8N/mm^2$) when either 1% or 2% wool is added, regardless of the cement content. This apparently consistent increase of UCS with wool content, combined with the increase in UCS with increasing cement content, gave rise to the hypothesis that the same target UCS of a RE soil mix may be obtained either by stabilisation alone or by reduction in cement content combined with inclusion of a pre-determined proportion of wool. This would reduce the environmental impact of construction, and also potentially reduce material and construction costs without compromising material strength (Section 3.3.3).

Including both wool and cement in SBCMs has been found to increase UCS in other investigations, such as in Festugato et al. (2017), where strength of a cemented soil was found to increase with the addition of polypropylene fibres. Wang et al. (1994) investigated how the properties of concrete are changed when mixed with waste carpet fibres, testing samples with 1% and 2% fibre by volume. Cylindrical samples were used to calculate UCS, and tests found that adding 1% wool by volume increased the UCS by 15%, however adding 2% wool by volume decreased UCS by 24%. However, wool was added to the sample by volume as opposed to by mass, making comparisons difficult as mass and volume cannot be converted without knowledge of material density, which is not provided. However, Wang et al. (1994) showed that adding waste carpet fibre "..significant increases... shatter resistance, energy absorption and ductility.." and produced a "reduction in drying shrinkage" in the samples. Adding carpet fibres to unstabilised RE, as presented in Section 3.3, resulted in an average UCS increase from $0.45N/mm^2$ to $0.86N/mm^2$ for 1% fibre (a 90% increase) or to $0.94N/mm^2$ for 2% fibre (a 109% increase). This significantly larger increase that reported in this thesis is likely due to the difference in initial UCS between the concrete used in Wang et al. (1994) (52.6MPa) and the RE used in the investigations in this thesis (0.45MPa).

6.3.2 Effect of wool reinforcement and cement stabilisation on shear strength

When studying the combined effect of wool and cement on shear strength of RE, wool has a significantly greater effect on cohesion than on angle of shear resistance (Figure 3.20), and cement has been found to have no significant effect on either of the measured properties (Figure 3.15). It was discussed in Section 6.2.2 that adding wool to the samples reduces the maximum shear force and decreases the measured cohesion, and this effect is present in samples containing any amount of cement (Figure 3.20). Additionally, wool decreases maximum shear force independent of cement content (Section 6.2.2), but an increase in wool content also increases the likelihood of a large horizontal displacement at maximum shear force, as shown by the increasing x-variation towards the lower half of Figure 3.21a.

Consoli et al. (1998) performed one of the most comparable investigations to the research described in this thesis, but on a slightly smaller scale and using a different soil composition. However, the findings were different, particularly those surrounding the effect of cement on the samples. It has been previously found that adding cement increases cohesion and also increases the angle of shear resistance of the uncemented soil (Consoli et al., 1998), while no evidence of this was found in this thesis (Figure 3.15). This could be due to the difference in soil composition, as Consoli et al. (1998) reports using a soil with ID 8:31:61:00 (or 39:61:00). Soil composition is known to affect soil properties such as UCS and dry density (Hall and Djerbib, 2004b) and is suggested to have an effect on other soil properties such as shearing behaviour, although this was outside the scope of this thesis. However, as the soil is only slightly different to that used in this thesis, it is likely to be due to the compressible nature of the wool affecting the behaviour of cement in the material, by minimising cementitious bonds and possibly wicking away moisture from where it is needed for hydration. The addition of wool was found to reduce the cohesion in the uncemented soil, which is in agreement with this thesis, but actually increase it in the cemented sample, contrary to this thesis. This is likely due to the differing nature of the fibres (incompressible fiberglass compared to highly compressible wool strands) as the compressibility of the wool fibres has been found to negatively affected the shearing behaviour of RE (Sections 6.2.2 and 6.3.2) and is likely to have affected the fracture energy for similar reasons (wool fibres were compressed during sample construction, storing potential energy in the sample which was then released when an external load was applied to the sample).

6.3.3 Effect of wool reinforcement and cement stabilisation on fracture energy

As in unstabilised samples, addition of wool was found to decrease the fracture energy of cement-stabilised samples. Likewise, as cement was found to increase the fracture energy of unreinforced RE, it was also found to increase the fracture energy of reinforced samples. Figure 4.14 highlights this relationship, and also suggests that wool reduces the fracture energy of all samples by approximately 50%, regardless of cement content, which is consistent with the conclusions in Section 6.2.3 - that adding either 1% or 2% wool to an unstabilised soil mix reduces the measured fracture energy by approximately 50%. However, Figure 4.14 shows that this might not be the case for samples with *any* amount of cement. While the general relationships between fracture energy, wool content and cement content in Figure 4.14 is clear, Table 4.1 shows that the presence of wool in samples with low cement content (0%-4%) has minimal effect on the measured fracture energy $G_{f,L}$, while samples with high cement content (6%-10%) were shown to approximately halve the fracture energy $G_{f,L}$. This apparent change in relationship at 6% cement is likely instead due to a low fracture energy recorded for sample W0C4, resulting in an apparent

'gap' between samples W0C2 and W0C6.

In Section 6.2.3 it was discussed that adding wool reduced the variability between the samples by approximately two-thirds. This improvement in variability is not limited to samples without cement, and Table 4.1 displays a consistently lower variability and standard deviation s for all samples containing wool compared to those without. Similarly, in Section 6.1.3 it was mentioned that there appeared to be no change in variation when cement is added to the samples, and this pattern is seen across all samples, also in Table 4.1.

6.3.4 Summary of wool reinforcement and cement stabilisation findings

In summary of the experiments performed on samples containing both cement *and* wool, wool has consistently been found to reduce the shear and fracture properties of RE, often negating any benefits of adding cement. It was found, however, that wool enhances the compressive strength of stabilised RE as well as unstabilised RE, and therefore it has been proposed that some wool may be added into a mix in replacement for some cement in order to reduce the carbon footprint of the construction but maintaining the desired UCS. Cement has been found to have no common influence on samples as it was shown to negatively affect some material properties and enhance others, with the exception of UCS when cement was confirmed to increase the UCS of RE samples. Additionally, variation in the stabilised samples has also been shown to be generally higher than those of unstabilised.

Wool has been found to increase UCS (Section 3.3), but decrease both shear strength (Section 3.4) and fracture energy (4.3.4). During UCS testing, wool helps to bond the soil together, increasing it's compressive strength, but during direct shear testing or wedge splitting testing, wool decreases the shear or fracture 'strength' of the soil. This initially appears contradictory, as it implies that wool behaves differently under different test conditions. This is not the case, however, as the different tests apply different load conditions and have different failure mechanisms. During UCS testing, the failure zone consists of the entire sample, as a classic failure pattern, such as that shown in Hughes and Bahramian (1965), is spread over the entire cube specimen. During wedge splitting and direct shear testing however, the failure zone is prescribed by the testing apparatus and directly tested, implying that wool improves the behaviour of samples as a whole but weakens specific failure planes within the material, possibly as a result of the compressibility of the fibres. Therefore, while the different tests imply different wool-soil behaviour, it may be instead that the wool-soil behaviour is similar in each test, but responds differently to different applied forces.

Chapter 7

Concluding remarks

7.1 Thesis summary

This thesis has presented a number of detailed investigations into a variety of different aspects of rammed earth (RE) construction, including shear behaviour and fracture, with a primary focus on investigating the effect of cement and wool stabilisation on the behaviour of the material.

A background and brief history of the use of and research into soil-based construction materials (SBCMs) was presented in Chapter 2, as well as a brief exploration of current fracture mechanics theory and its development. Recent research into SBCMs has produced an increasing number of scientifically rigorous investigations into their behaviour and performance. One particularly good example of a rigorous investigation into RE is the study by Hall and Djerbib (2004b), which has set the standard for good quality papers since. Some investigations have focussed on assessing the validity of current research practises and found them scientifically unsound (e.g. Smith et al. (2014)), others have sought to advance understanding of the internal processes which give SBCMs their strength, such as Jaquin et al. (2009) and Schroeder (2011), while others have proposed new ways to enhance material strength by adding foreign materials (e.g. Cristelo et al. (2012)). Recent publications (Jaquin and Augarde, 2012) have attempted to bring research into RE to a wider community, while new conferences, namely the 1st International Conference on Bio-Based Building Materials (ICBBM2015) and the 1st International Conference on Rammed Earth Construction (ICREC2015), have improved collaboration within the scientific community and raised the international awareness of SBCM research and construction. It is hoped that further collaboration and public engagement through publications and conferences will continue to extend current research into sustainable construction methods and materials like SBCMs.

Chapter 3 described the experimental programmes and results of 5 investigations into the effects of wool and cement stabilisation on RE. Tests to measure cube strength, shear strength, and cylinder

strength were performed using unconfined cube strength tests (Section 3.3), direct shear tests (Section 3.4), triaxial tests (Section 3.5), and unconfined cylinder strength tests (Section 3.6). Cement was found to be universally beneficial or neutral, increasing both unconfined compressive strength (UCS) and shear strength. However, when high percentages of cement were combined with high percentages of wool, shear strength of the samples fell dramatically.

While cement was consistently beneficial, wool was found to have different effects on the material depending on the type of test performed. For example, it was found that the addition of wool increases the cube strength (Section 3.3) but wool was also found to decrease the shear strength (Sections 3.4 and 3.5) of RE. The decrease in shear strength is due to the expansive nature of wool counteracting the compaction required to develop strength in RE. However, scans of samples using a Scanning Electron Microscope confirmed that wool fibres form a crucial part of wool stabilisation (Section 3.7), therefore suggesting that an optimal reinforcement material might be wool fibres without the (compressible) strand component.

Fracture is a relatively recent research area within SBCMs, as theories behind its importance have only recently been suggested (Ciancio and Augarde, 2013). In Chapter 4, the advantages and disadvantages of two different industry tests were discussed; the three point bending test and the wedge splitting test. Both were developed for, and are commonly used in, fracture investigations of concrete. The wedge splitting test was adapted for use in the experimental programme into the fracture behaviour of RE. 108 samples were tested using the wedge splitting test, investigating the differing effects of cement and wool fibre stabilisation and the combined effect of both. Wool was initially found to artificially increase the fracture energy of the samples through pull-out forces showing slow sample deterioration, opposed to more immediate failure observed in typical wedge splitting test investigations. Therefore, a loading fracture energy $G_{f,L}$ was proposed, to be determined from the pre-peak loading curve only (Section 4.3.3). $G_{f,L}$ was found to be suitable and therefore suggested for any wedge splitting test investigations in which the full test curve cannot be obtained. Addition of wool was found to approximately halve the fracture energy of samples, with not apparent variation according to percentage wool content, the implications of which were discussed in Section 4.3.4. Cement was generally found to increase the fracture energy of the soil, the effect of which was lessened when wool was also added.

Chapter 5 presented a study into the shrinkage behaviour of clay used for RE, with specific focus on its behaviour when mixed with other sized soil particles (i.e. sand) or wool. Clay samples, mixed at liquid limit and made in petri dishes, were produced in triplicate in all different combinations of the following: bentonite or kaolinite clay, with or without sand, and with or without wool. As expected, samples containing kaolinite clay did not noticeably shrink to any noticeable degree, as kaolinite is known to be inexpansive. Shrinkage was observed, however, in all of the samples containing bentonite, and

different samples shrank different amounts according to soil composition. The inclusion of sand was found to increase the crack area of samples, while wool conversely decreased the cracking area in the sample due to the fibres binding the soil together. Sand was also found to increase the drying rate of the samples, likely due to the internal structure and water-retaining properties of the clay (Section 5.3.2). It was also discovered that cracks continued to grow after water had ceased to leave these samples.

7.2 Thesis conclusions

There are many different SBCMs, as detailed in Section 2.1, and while the experiments described in this thesis were primarily focussed on the investigation of RE, it is suggested that the majority of the conclusions in this thesis are applicable to other SBCMs, particularly those in the *compacted earth* group of construction methods (Section 2.1).

In Chapter 1, the aim of this thesis was identified as studying the behaviour of earthen materials when stabilised with wool or cement, with a focus on determining the suitability of wool (in this case, waste carpet fibres) for inclusion in earthen construction. With respect to these aims, the main conclusions regarding the addition of wool into SBCMs are:

- Wool increases UCS (Section 3.3.3);
- Wool may be used to replace a portion of cement to obtain the same UCS while reducing the carbon footprint of the construction (Section 3.3.3);
- Wool decreases the peak shear stress of the soil mix, and has little effect on the angle of shear resistance. An increase in wool, however, reduces the cohesion of the sample (Sections 3.4.6 and 3.5.3);
- An increase in wool leads to an increase in displacement at peak shear stress (Section 3.4.7);
- Wool improves the shear resistance of soils containing kaolinite or bentonite clays, although the effect was more prominent in bentonite samples (Section 3.6.2);
- Wool increases displacement at maximum shear force (Section 3.6.2);
- Wool stands act as a carrier for wool fibres, which are the important part of the wool stabilisation (Section 3.4.4);
- Wool fibres were observed to bind with the soil particles (Section 3.7), providing evidence of the advantages of fibres over strands as seen in previous conclusions;
- Wool halves the fracture energy (Section 4.3.4); and

- Wool does not affect the drying rate of RE and reduces cracking (Section 5.3.1.

In summary, waste carpet fibre has been found to be beneficial in compression but either neutral or detrimental in tension. This has generally been due to the compressibility of the fibres acting against the internal forces in the soil. It is therefore proposed that similar advances but fewer disadvantages may be obtained using the incompressible part of the fibres alone,

Alongside the above conclusions regarding the role of wool reinforcement in SBCMs, the following conclusions regarding other aspects of this research have been made:

- Cement mixes unevenly into wetted soil, coating soil clumps with a thin layer of cement (Section 3.4.3);
- Cement increases the peak shear stress of the soil, but has little effect on cohesion or angle of shear resistance (Section 3.4.5);
- Cement stabilisation increases the fracture energy of RE (Section 4.3.4);
- An increase in sample dry density increases cohesion but decreases the angle of shear resistance (Section 3.4.8);
- A loading fracture energy ($G_{f,L}$) has been proposed, equal to the fracture energy of the sample up to maximum load (Section 4.3.4); and
- Sand increases the drying rate of RE and increases cracking (Section 5.3.1).

7.3 Implications for the SBCM industry

This thesis has discussed the advantages and disadvantages of adding wool to SBCMs, and the following advice on the application of this research is given:

- An *optimal fibre content* should be determined prior to construction, which equals the fibre content at the point at which UCS is at a maximum (Section 3.3.3); and
- When using fibrous reinforcement, the fibres used should be incompressible where possible, to avoid any detrimental effects of adding compressible fibrous reinforcement (Section 3.5.3).

7.4 Suggestions for new and expanded areas of research

During the experimental work and discussions presented in this thesis it has been increasingly clear that there is considerable research that may be performed to improve understanding of SBCMs. A

number of new potential research areas were identified, as well as other areas of research that need further attention.

7.4.1 Water content

While the relationship between water content and dry density has been established in earthen construction, the importance of suction is only just being realised. As water content is essential to the strength of unstabilised SBCMs, the contribution to strength of the different types of suction (matric and osmotic) must be identified. The contributions of capillary and absorptive suction must also be determined in order to further enhance our understanding of the material such that it is possible to efficiently maximise the strength of the material.

7.4.2 Fibrous reinforcement

Further research is needed into the effectiveness of different fibrous reinforcements, and it is recommended that further research is focussed on incompressible fibres. Also, the idea of an optimum fibre content should be further explored. The length and number of fibres should be investigated with the aim of obtaining an optimum length of fibre, much may depend on the fibre, for fibrous reinforcement of RE.

7.4.3 Chemical stabilisation

While chemical stabilisation is commonly used within earthen construction, the author has not found any research into balancing the priorities of simplicity in construction versus accuracy of optimum water content - i.e. whether a sample should be compacted at optimum water content of the soil regardless of cement content, or whether the amount of cement added should then affect the amount of water added to the mix as the optimum water content of the soil would change. It is proposed that a greater strength would be achieved from a sample compacted at optimum when the cement content is considered. To determine the optimum water content of a sample including cement, the procedure outlined in British Standard BS1377-2 (1990) must be adapted to account for hydration. An artificial additive must be used in place of cement in order to prevent hydration of the cement altering the measured water content in the sample.

Additionally, research should be performed into the importance of equilibration, for if it is not required for stabilised soils prior to the stabiliser being added, then the stabiliser may be mixed more evenly into the soil by mixing the cement into the soil mix before water is added. Also, the importance of obtaining the optimum water content of a *stabilised* soil mix is not yet fully understood. It is also unknown whether it is important to compact a stabilised soil at optimum water content (which is essential for unstabilised soils) or whether it is more important to compact with enough water to ensure complete hydration occurs,

although some investigations have begun to look at this crucial research area (e.g. Beckett and Ciancio (2014a)).

Alternative stabilisers to cement and lime must also be investigated in order to find a more environmentally-friendly and sustainable stabiliser, such as fly ash (Cristelo et al., 2012).

7.4.4 Fracture

Research is needed to quantify fracture failure stresses and mechanisms within RE as the research in this thesis has shown that there is a high degree of variability in the results. It is recognised that some of this variability, however, may be due to the compressibility of the wool fibres used during experimentation. It is recommended that further tests are performed using some of the tests used and devised in this thesis to further investigate the shear, splitting and crushing failure modes of RE and other SBCMs.

The way that fibres affect the calculation of fracture energy also needs to be further explored, particularly with regard to how different fibres (e.g. microfibres) affect the calculation of fracture energy in different ways.

7.4.5 Scanning Electron Microscopy

During future investigations into the microscopy of SBCMs, it is advised that an Environmental Scanning Electron Microscope (ESEM) is used opposed to a Scanning Electron Microscope (SEM) used in this thesis. An ESEM allows water present in a sample to be viewed clearly unlike in an SEM where is is usually impossible to identify on the output images (Section 3.7.3).

References

Achenza, M. and Fenu, L. (2006). On earth stabilization with natural polymers for earth masonry construction. *Materials and Structures*, 39(1):21–27.

Al Shayea, N. (2001). The combined effect of clay and moisture content on the behavior of remolded unsaturated soils. *Engineering Geology*, 62(4):319–342.

Augarde, C. (2012). Soil mechanics and earthen construction: strength and mechanical behaviour. In Hall, M., Lindsay, R., and Krayenhoff, M., editors, *Modern earth buildings*, chapter 8, pages 204–221. Woodhead Publishing Limited, Philadelphia.

Aymerich, F., Fenu, L., Francesconi, L., and Guanzhe, F. (2015). Evaluation of the fracture behaviour of a fibre reinforced earthen material using digital image correlation. In *Proceedings of the 23rd international conference on composites and nano engineering (ICCE-23)*.

Aymerich, F., Fenu, L., Francesconi, L., and Meloni, P. (2016). Fracture behaviour of a fibre reinforced earthen material under static and impact flexural loading. *Construction and Building Materials*, 109:109 – 119.

Aymerich, F., Fenu, L., and Meloni, P. (2012). Effect of reinforcing wool fibres on fracture and energy absorption properties of an earthen material. *Construction and Building Materials*, 27(1):66–72.

Bahar, R., Benazzoug, M., and Kenai, S. (2004). Performance of compacted cement-stabilised soil. *Cement and Concrete Composites*, 26(7):811–820.

Bailey, S. (1971). Summary of national and international recommendations on clay mineral nomenclature. *Clays and Clay Minerals*, 19:129–132.

Barenblatt, G. (1959). The formation of equilibrium cracks during brittle fracture. General ideas and hypotheses. Axially-symmetric cracks. *Journal of Applied Mathematics and Mechanics*, 23(3):622–636.

Barenblatt, G. (1962). The mathematical theory of equilibrium cracks in brittle fracture. *Advances in Applied Mechanics*, 7:55–129.

Basha, E., Hashim, R., Mahmud, H., and Muntohar, A. (2005). Stabilization of residual soil with rice husk ash and cement. *Construction and Building Materials*, 19(6):448–453.

Bazant, Z. P. (1984). Size effect in blunt fracture: concrete, rock, metal. *Journal of Engineering Mechanics*, 110(4):518–535.

Bazant, Z. P. and Planas, J. (1998). *Fracture and Size Effect in Concrete and Other Quasibrittle Materials*. CRC Press, Florida.

Beckett, C. (2011). *The role of material structure in compacted earthen building materials*. PhD thesis, University of Durham, United Kingdom.

Beckett, C. and Augarde, C. (2012). The effect of relative humidity and temperature on the unconfined compressive strength of rammed earth. In Mancuso, C., Jommi, C., and D'Onza, F., editors, *Unsaturated Soils: Research and Applications*, volume 1, pages 287–292, Berlin. Springer.

Beckett, C. and Ciancio, D. (2014a). Effect of compaction water content on the strength of cement-stabilized rammed earth materials. *Canadian Geotechnical Journal*, 51(5):583–590.

Beckett, C. and Ciancio, D. (2014b). Effect of microstructure on heat transfer through compacted cement-stabilised soils. In *International Symposium on Geomechanics from Micro to Macro (IS-Cambridge)*.

Beckett, C., Ciancio, D., Manzi, S., and Bignozzi, C. (2015a). Strengthening mechanisms in cement-stabilised rammed earth. In *Proceedings of the First International Conference on Rammed Earth Construction*, pages 41–45, London. Taylor & Francis Group.

Beckett, C., Hall, M., and Augarde, C. (2013). Macrostructural changes in compacted earthen construction materials under loading. *Acta Geotechnica*, 8:423–438.

Beckett, C., Smith, J., Ciancio, D., and Augarde, C. (2015b). Tensile strengths of flocculated compacted unsaturated soils. *Géotechnique Letters*, 5(4):254–260.

Binici, H., Aksogan, O., Bodur, M., Akca, E., and Kapur, S. (2007). Thermal isolation and mechanical properties of fibre reinforced mud bricks as wall materials. *Construction and Building Materials*, 21(4):901–906.

Binici, H., Aksogan, O., and Shah, T. (2005). Investigation of fibre reinforced mud brick as a building material. *Construction and Building Materials*, 19(4):313–318.

Bolton, M. (1991). *A Guide to Soil Mechanics*. Macmillan Education Ltd, London.

Boominathan, S., Senathipathi, K., and Jayaprakasam, V. (1991). Field studies on dynamic properties of reinforced earth. *Soil Dynamics and Earthquake Engineering*, 10(8):402–406.

Bouhicha, M., Aouissi, F., and Kenai, S. (2005). Performance of composite soil reinforced with barley straw. *Cement and Concrete Composites*, 27(5):617–621.

Brink, F. and Rush, P. (1966). Bamboo Reinforced Concrete Construction. Technical report, U.S. Naval Civil Engineering Labaoratory, California.

British Standard BS1377-2 (1990). *Methods of test for soil for civil engineering purposes - part 2: Classification tests*. British Standard Institution.

British Standard BS1377-4 (1990). *Methods of test for soil for civil engineering purposes - part 4: Compaction-related tests*. British Standard Institution.

British Standard BS1377-7 (1990). *Methods of test for soil for civil engineering purposes - part 7: Shear strength tests (total stress)*. British Standard Institution.

British Standard BS1377-8 (1990). *Methods of test for soil for civil engineering purposes - part 8: Shear strength tests (effective stress)*. British Standard Institution.

Broek, D. (1974). *Elementary Engineering Fracture Mechanics*. Noordhoff International Publishing, Leyden.

Brühwiler, E. and Wittmann, F. (1990). The wedge splitting test, a new method of performing stable fracture mechanics tests. *Engineering Fracture Mechanics*, 35(1):117–125.

Bui, Q., Hans, S., Morel, J., and Do, A. (2011). First exploratory study on dynamic characteristics of rammed earth buildings. *Engineering Structures*, 33(12):3690–3695.

Bui, Q.-B., Morel, J.-C., Hans, S., and Walker, P. (2014a). Effect of moisture content on the mechanical characteristics of rammed earth. *Construction and Building Materials*, 54:163–169.

Bui, Q.-B., Morel, J.-C., Venkatarama Reddy, B., and Ghayad, W. (2009). Durability of rammed earth walls exposed for 20 years to natural weathering. *Building and Environment*, 44(5):912–919.

Bui, T.-T., Bui, Q.-B., Limam, A., and Maximilien, S. (2014b). Failure of rammed earth walls: From observations to quantifications. *Construction and Building Materials*, 51:295–302.

Burroughs, S. (2006). Strength of compacted earth: linking soil properties to stabilizers. *Building Research and Information*, 34(1):55–65.

Burroughs, S. (2008). Soil property criteria for rammed earth stabilization. *Journal of Materials in Civil Engineering*, 20(3):264–273.

Caporale, A., Parisi, F., Asprone, D., Luciano, R., and Prota, A. (2014). Micromechanical analysis of adobe masonry as two-component composite: Influence of bond and loading schemes. *Composite Structures*, 112:254–263.

Castellanos, B. and Brandon, T. (2013). A comparison between the shear strength measured with direct shear and triaxial devices on undisturbed and remolded soils. In *Proceedings of the 18th International Conference on Soil Mechanics and Geotechnical Engineering*, volume 1, pages 317–320, Paris.

Cheah, J. (2014). *Development of a flax-fibre reinforced, cement-stabilized rammed earth housing solution (Uku) for rural Māori communities*. PhD thesis, ResearchSpace@ Auckland.

Cheah, J., Walker, P., Heath, A., and Morgan, T. (2012). Evaluating shear test methods for stabilised rammed earth. *Proceedings of the ICE - Construction Materials*, 165:325 – 334.

Ciancio, D. (2011). Use of rammed earth in aboriginal remote communities of western australia: a case study on sustainability and thermal properties. In *International Workshop on Rammed Earth Materials and Sustainable Structures*.

Ciancio, D. and Augarde, C. (2013). Capacity of unreinforced rammed earth walls subject to lateral wind force: elastic analysis vs. ultimate strength analysis. *Materials & Structures*, 46:1–17.

Ciancio, D., Beckett, C., and Carraro, J. (2014). Optimum lime content identification for lime-stabilised rammed earth. *Construction and Building Materials*, 53:59–65.

Ciancio, D. and Gibbings, J. (2012). Experimental investigation on the compressive strength of cored and molded cement-stabilized rammed earth samples. *Construction and Building Materials*, 28(1):294–304.

Ciancio, D., Jaquin, P., and Walker, P. (2013). Advances on the assessment of soil suitability for rammed earth. *Construction and Building Materials*, 42:40–47.

Ciancio, D. and Robinson, S. (2010). Use of the strut-and-tie model in the analysis of reinforced cement-stabilized rammed earth lintels. *Journal of Materials in Civil Engineering*, 23(5):587–596.

Clementi, F., Lenci, S., and Sadowski, T. (2008). Fracture characteristics of unfired earth. *International Journal of Fracture*, 149(2):193–198.

Consoli, N., Montardo, J., Donato, M., and Prietto, P. (2004). Effect of material properties on the behaviour of sand-cement-fibre composites. *Ground Improvement*, 8(2):77–90.

Consoli, N., Prietto, P., and Ulbrich, L. (1998). Influence of fiber and cement addition on behavior of sandy soil. *Journal of Geotechnical and Geoenvironmental Engineering*, 124(12):1211–1214.

Corbin, A. (2012). Design and testing of flexural members in rammed earth. Undergraduate Masters Research Project, Durham University.

Craig, R. (2004). *Craig's Soil Mechanics*. Taylor & Francis, New York.

Cristelo, R., Roma, R., Fernandes, L., Miranda, T., Oliveira, D., and da Silva, R. (2012). Residual granitic soil improvement for rammed earth construction. In *13° Congresso Nacional de Geotecnia*. Sociedade Portuguesa de Geotecnia.

da Silva, R., Oliveira, D., Miranda, T., Escobar, C., and Cristelo, N. (2012). Rammed earth: feasibility of a global concept applied locally. In *13th Congresso Nacional de Geotécnia*, Lisbon. Sociedade Portuguesa de Geotecnia.

Danso, H., Martinson, B., Ali, M., and Mant, C. (2015). Performance characteristics of enhanced soil blocks: a quantitative review. *Building Research & Information*, 43(2):253–262.

Diambra, A., Ibraim, E., Wood, D., and Russell, A. (2010). Fibre reinforced sands: Experiments and modelling. *Geotextiles and Geomembranes*, 28(3):238–250.

Du, Y., Li, S., and Hayashi, S. (1999). Swelling–shrinkage properties and soil improvement of compacted expansive soil, Ning-Liang Highway, China. *Engineering Geology*, 53(3):351–358.

Dugdale, D. (1960). Yielding of steel sheets containing slits. *Journal of the Mechanics and Physics of Solids*, 8(2):100–104.

Easton, D. (2007). *The Rammed Earth House: Revised Edition*. Chelsea Green Publishing.

Festugato, L., Menger, E., Benezra, F., Kipper, E. A., and Consoli, N. C. (2017). Fibre-reinforced cemented soils compressive and tensile strength assessment as a function of filament length. *Geotextiles and Geomembranes*, 45(1):77–82.

Fisher, R. (1926). On the capillary forces in an ideal soil; correction of formulae given by W.B. Haines. *The Journal of Agricultural Science*, 16(3):492–505.

Galán Marín, C., Rivera Gómez, C., and Petric, J. (2010). Clay-based composite stabilized with natural polymer and fibre. *Construction and Building Materials*, 24(8):1462–1468.

Gelard, D., Fontaine, L., Maximilien, S., Olagnon, C., Laurent, J., Houben, H., and Van Damme, H. (2007). When physics revisit earth construction: Recent advances in the understanding of the cohesion mechanisms of earthen materials. In *Proceedings of the International Symposium on Earthen Structures.*, pages 294–302, Bangalore. Indian Institute of Science.

Gens, A. (2010). Soil–environment interactions in geotechnical engineering. *Géotechnique*, 60(1):3–74.

Gerard, P., Mahdad, M., McCormack, A., and François, B. (2015). A unified failure criterion for unstabilized rammed earth materials upon varying relative humidity conditions. *Construction and Building Materials*, 95:437–447.

Griffith, A. (1921). The phenomena of rupture and flow in solids. *Philosophical Transactions of the Royal Society of London. Series A, containing papers of a mathematical or physical character*, 221:163–198.

Grim, R. (1962). *Applied Clay Mineralogy*. McGraw-Hill Book Company, Inc.

Guinea, G., Planas, J., and Elices, M. (1992). Measurement of the fracture energy using three-point bend tests: Part 1–Influence of experimental procedures. *Materials and Structures*, 25(4):212–218.

Hall, M. (2007). Assessing the environmental performance of stabilised rammed earth walls using a climatic simulation chamber. *Building and Environment*, 42(1):139–145.

Hall, M. and Djerbib, Y. (2004a). Moisture ingress in rammed earth: Part 1 - The effect of soil particle-size distribution on the rate of capillary suction. *Construction and Building Materials*, 18(4):269–280.

Hall, M. and Djerbib, Y. (2004b). Rammed earth sample production: context, recommendations and consistency. *Construction and Building Materials*, 18(4):281–286.

Hall, M. and Djerbib, Y. (2006). Moisture ingress in rammed earth: Part 2 - The effect of soil particle-size distribution on the absorption of static pressure-driven water. *Construction and Building Materials*, 20(6):374–383.

Hall, M., Lindsay, R., and Krayenhoff, M., editors (2012). *Modern earth buildings - Materials, engineering, construction and applications*. Woodhead Publishing Limited.

Hall, M., Najim, K., and Keikhaei Dehdezi, P. (2012). Soil stabilisation and earth construction: materials, properties and techniques. In Hall, M., Lindsay, R., and Krayenhoff, M., editors, *Modern Earth Buildings: Materials, Engineering, Constructions and Applications*, chapter 9, pages 222–255. Woodhead Publishing Limited, Cambridge, UK.

Hallett, P. and Newson, T. (2005). Describing soil crack formation using elastic–plastic fracture mechanics. *European Journal of Soil Science*, 56(1):31–38.

Harris, C. (1975). *Dictionary of architecture and construction*. McGraw-Hill.

Head, K. (1982). *Manual of soil laboratory testing*, volume 2. Pentech Press Ltd, Plymouth, UK.

Heath, A. (2008). A strain-based non-linear elastic model for geomaterials. *W.S.E.A.S. Transactions on Applied and Theoretical Mechanics*, 3(6):197–206.

Heath, A., Lawrence, M., Walker, P., and Fourie, C. (2009). The compressive strength of modern earth masonry. In *11th International Conference on Non-conventional Materials and Technologies (NOCMAT 2009)*. University of Bath.

Heath, A., Pestana, J., Harvey, J., and Bejerano, M. (2004). Normalizing the behavior of unsaturated granular pavement materials. *Journal of Geotechnical and Geoenvironmental Engineering*, 130(9):896–904.

Hejazi, S., Sheikhzadeh, M., Abtahi, S., and Zadhoush, A. (2012). A simple review of soil reinforcement by using natural and synthetic fibers. *Construction and Building Materials*, 30:100–116.

Hela, R. and Orsáková, D. (2013). The mechanical activation of fly ash. *Procedia Engineering*, 65:87–93.

Hillerborg, A. (1985). The theoretical basis of a method to determine the fracture energy G_F of concrete. *Materials and Structures*, 18(4):291–296.

Hillerborg, A., Modéer, M., and Petersson, P. (1976). Analysis of crack formation and crack growth in concrete by means of fracture mechanics and finite elements. *Cement and Concrete Research*, 6(6):773–781.

Houben, H. and Guillaud, H. (1994). *Earth Construction: A Comprehensive Guide*. ITDG Publishing, Marseille.

Hughes, B. and Bahramian, B. (1965). Cube tests and the uniaxial compressive strength of concrete. *Magazine of Concrete Research*, 17(53):177–182.

Inglethorpe, S., Morgan, D., Highley, D., and Bloodworth, A. (1993). Industrial Minerals Laboratory Manual: Bentonite. Technical report, British Geological Survey.

Inglis, C. (1913). Stresses in a plate due to the presence of cracks and sharp corners. *Institution of Naval Architects*, 55:219–241.

Irwin, G. (1957). Analysis of stresses and strains near the end of a crack traversing a plate. *Journal of Applied Mechanics*, 24:361–364.

Irwin, G. (1960). Structural Mechanics. In *Proceedings of the First Symposium of Naval Structural Mechanics*, Oxford. Pergamon Press.

Jaquin, P. (2008). *Analysis of Historic Rammed Earth Construction*. PhD thesis, University of Durham, UK.

Jaquin, P. and Augarde, C. (2012). *Earth Building: History, science and conservation*. BRE Press, Bracknell, UK.

Jaquin, P., Augarde, C., Gallipoli, D., and Toll, D. (2009). The strength of unstabilised rammed earth materials. *Géotechnique*, 59(5):487–490.

Jaquin, P., Augarde, C., and Gerrard, C. (2008a). Chronological description of the spatial development of rammed earth techniques. *International Journal of Architectural Heritage*, 2(4):377–400.

Jaquin, P., Augarde, C., and Legrand, L. (2008b). Unsaturated characteristics of rammed earth. In Toll, D., Augarde, C., Gallipoli, D., and Wheeler, S., editors, *Unsaturated Soils, Advances in Geo-Engineering: Proceedings of the 1st European Conference (E-UNSAT 2008)*, pages 417–422, Durham, UK. CRC Press.

Jayasinghe, C. and Kamaladasa, N. (2007). Compressive strength characteristics of cement stabilized rammed earth walls. *Construction and Building Materials*, 21(11):1971–1976.

Jenq, Y. and Shah, S. (1985). Two parameter fracture model for concrete. *Journal of Engineering Mechanics*, 111:1227–1241.

Jones, M. (2015). Where does the water go in earthen construction materials? BEng Research Project.

Kariyawasam, K. and Jayasinghe, C. (2016). Cement stabilized rammed earth as a sustainable construction material. *Construction and Building Materials*, 105:519–527.

Kenai, S., Bahar, R., and Benazzoug, M. (2006). Experimental analysis of the effect of some compaction methods on mechanical properties and durability of cement stabilized soil. *Journal of Materials Science*, 41(21):6956–6964.

Krafft, J., Sullivan, A., and Boyle, R. (1961). Effect of dimensions on fast fracture instability of notched sheets. In *Proceedings of the Crack Propagation Symposium*, volume 1, pages 8–26.

Krahn, J. and Fredlund, D. (1972). On total, matric and osmotic suction. *The Emergence of Unsaturated Soil Mechanics*, 114:339–348.

Kumar, S. and Tabor, E. (2003). Strength characteristics of silty clay reinforced with randomly oriented nylon fibers. *Electronic Journal of Geotechnical Engineering*, 8.

Lees, G., Abdelkater, M., and Hamdani, S. (1982). Effect of the clay fraction on some mechanical properties of lime-soil mixtures. *The Highway Engineer*, 29(11):2–11.

Lenci, S., Clementi, F., and Sadowski, T. (2012). Experimental determination of the fracture properties of unfired dry earth. *Engineering Fracture Mechanics*, 87:62–72.

Lenci, S., Piattoni, Q., Clementi, F., and Sadowski, T. (2009). A mechanical characterization of unfired dry earth: ultimate strength, damage and fracture parameters. In *Proceedings of XIX Aimeta Conference*, pages 14–17.

Lilley, D. and Robinson, J. (1995). Ultimate strength of rammed earth walls with openings. *Proceedings of the ICE - Structures and Buildings*, 110:278–87.

Linsbauer, H. and Tschegg, E. (1986). Fracture energy determination of concrete with cube-shaped specimens. *Zement und Beton*, 31:38–40. (in german).

Lourenço, S., Gallipoli, D., Augarde, C., Toll, D., Fisher, P., and Congreve, A. (2012). Formation and evolution of water menisci in unsaturated granular media. *Géotechnique*, 62(3):193–199.

Lourenço, S., Gallipoli, D., Toll, D. G., and Evans, F. D. (2006). Development of a commercial tensiometer for triaxial testing of unsaturated soils. In *Unsaturated Soils 2006*, pages 1875–1886.

Lourenco, S., Toll, D., Augarde, C., Gallipoli, D., Congreve, A., Smart, T., and Evans, F. (2008). Observations of unsaturated soils by Environmental Scanning Electron Microscopy in dynamic mode. In Toll, D., Augarde, C., Gallipoli, D., and Wheeler, S., editors, *Unsaturated Soils: Advances in Geo-Engineering*, pages 145–150, London. Taylor & Francis Group.

Maccarini, M. (1993). A comparison of direct shear box tests with triaxial compression tests for a residual soil. *Geotechnical & Geological Engineering*, 11(2):69–80.

Maniatidis, V. and Walker, P. (2008). Structural capacity of rammed earth in compression. *Journal of Materials in Civil Engineering*, 20(3):230–238.

Maskell, D., Heath, A., and Walker, P. (2013). Laboratory scale testing of extruded earth masonry units. *Materials & Design*, 45:359–364.

Miraftab, M. and Lickfold, A. (2008). Utilization of carpet waste in reinforcement of substandard soils. *Journal of industrial textiles*, 38(2):167–174.

Mirzababaei, M., Miraftab, M., Mohamed, M., and McMahon, P. (2012). Unconfined compression strength of reinforced clays with carpet waste fibers. *Journal of Geotechnical and Geoenvironmental Engineering*, 139(3):483–493.

Nakamura, Y. and Matsukawa, S. (1971). On Wetting Behavior and Surface Structure of Wool Fibers. *Textile Research Journal*, 41(12):1001–1002.

Nowamooz, H. and Chazallon, C. (2011). Finite element modelling of a rammed earth wall. *Construction and Building Materials*, 25(4):2112–2121.

Parisi, F., Asprone, D., Fenu, L., and Prota, A. (2014). Experimental characterization of Italian adobe bricks reinforced with straw fibres. In *Proceedings of the 9th international masonry conference.*, Guimarães, Portugal.

Petersson, P. (1980). Fracture energy of concrete: Method of determination. *Cement and Concrete Research*, 10(1):79–89.

Piattoni, Q., Quagliarini, E., and Lenci, S. (2011). Experimental analysis and modelling of the mechanical behaviour of earthen bricks. *Construction and Building Materials*, 25(4):2067–2075.

Powrie, W. (2013). *Soil Mechanics: Concepts and Applications*. CRC Press, Boca Raton.

Quagliarini, E. and Lenci, S. (2010). The influence of natural stabilizers and natural fibres on the mechanical properties of ancient Roman adobe bricks. *Journal of Cultural Heritage*, 11(3):309–314.

Rampino, C., Mancuso, C., and Vinale, F. (2000). Experimental behaviour and modelling of an unsaturated compacted soil. *Canadian Geotechnical Journal*, 37(4):748–763.

Readle, D., Coghlan, S., Smith, J., Corbin, A., and Augarde, C. (2015). Fibre reinforcement in earthen construction materials (available ahead of print). In *Proceedings of the ICE - Construction Materials*.

Reis, J. M. L. d. (2009). Effect of textile waste on the mechanical properties of polymer concrete. *Materials Research*, 12(1):63–67.

Rice, J. (1967). A path independent integral and the approximate analysis of strain concentration by notches and cracks. *Journal of Applied Mechanics*, 35:379–386.

Rice, J. (1968). Mathematical analysis in the mechanics of fracture. *Fracture: An Advanced Treatise*, 2:191–311.

RILEM (1985). Determination of the Fracture Energy of Mortar and Concrete by Means of Three-Point Bend Tests on Notched Beames. Technical Report 106, RILEM.

Rossi, P., Brühwiler, E., Chhuy, S., Jenq, Y.-S., and Shah, S. (1991). *Fracture mechanics test methods for concrete*, chapter 2: Fracture properties of concrete as determined by means of wedge splitting tests and tapered double cantilever beam tests, pages 87–128. Taylor & Francis.

Sánchez, F., Martín-del Río, J., López, F., and Alés, V. (2012). Methodological proposal for rammed-earth wall characterization: Understanding of material in preliminary studies. In Milto, V. and Cristini, editors, *Rammed Earth Conservation*, London. Taylor & Francis Group.

Schroeder, H. (2011). Moisture transfer and change in strength during the construction of earthen buildings. *Informes de la Construcción*, 63(523):107–116.

Schroeder, H. (2012). Modern earth building codes, standards and normative development. In Hall, M., Lindsay, R., and Krayenhoff, M., editors, *Modern Earth Building: Materials, Engineering, Constructions and Applications*, chapter 4, pages 72–109. Woodhead Publishing Limited.

Serrano, S., Barreneche, C., Rincón, L., Boer, D., and Cabeza, L. (2012). Stabilized rammed earth incorporating PCM: Optimization and improvement of thermal properties and life cycle assessment. *Energy Procedia*, 30:461–470.

Sherwood, P. (1993). *Soil stabilization with cement and lime*. H.M.S.O.

Smith, J. (2015). *Examining Soil Based Construction Materials through X-Ray Computed Tomography*. PhD thesis, Durham University.

Smith, J. and Augarde, C. (2013). A new classification for soil mixtures with application to earthen construction. Technical report, Durham University.

Smith, J., Augarde, C., and Beckett, C. (2014). The use of XRCT to investigate highly unsaturated soil mixtures. In Khalili, N., Russell, A. R., and Khoshghalb, A., editors, *Unsaturated Soils: Research and Applications*, pages 719–725, London. CRC Press.

Taylor, P., Fuller, R., and Luther, M. (2012). Validated model and study of a rammed earth wall building. In *ANZSES 2004: Solar 2004: Life, the universe and renewables*. Australian and New Zealand Solar Energy Society.

Terzaghi, K. (1936). The shearing resistance of saturated soils and the angle between the planes of shear. In *Proceedings of the 1st International Conference on Soil Mechanics and Foundation Engineering*, volume 1, pages 54–56, Cambridge, MA. Harvard University Press.

Toll, D. (1999). A Data Acquisition and Control System for Geotechnical Testing. In Kumar, B. and Topping, B., editors, *Computing Developments in Civil and Structural Engineering*, pages 237–242, Edinburgh, UK. Civil-Comp Press.

Tripura, D. D. and Singh, K. D. (2015). Axial load-capacity of rectangular cement stabilized rammed earth column. *Engineering Structures*, 99:402–412.

Tuller, M., Or, D., and Dudley, L. M. (1999). Adsorption and capillary condensation in porous media: Liquid retention and interfacial configurations in angular pores. *Water Resources Research*, 35(7):1949–1964.

Turgut, P. and Yesilata, B. (2008). Physico-mechanical and thermal performances of newly developed rubber-added bricks. *Energy and Buildings*, 40(5):679–688.

Vanapalli, S., Fredlund, D., Pufahl, D., and Clifton, A. (1996). Model for the prediction of shear strength with respect to soil suction. *Canadian Geotechnical Journal*, 33(3):379–392.

Venkatarama Reddy, B., Suresh, V., and Nanjunda Rao, K. (2016). Characteristic compressive strength of cement-stabilized rammed earth. *Journal of Materials in Civil Engineering*, page 04016203.

Walker, P., Keable, R., Martin, J., and Maniatidis, V. (2005). *Rammed earth: design and construction guidelines*. BRE Bookshop, Watford, UK.

Wang, J.-J., Zhu, J.-G., Chiu, C., and Zhang, H. (2007). Experimental study on fracture toughness and tensile strength of a clay. *Engineering Geology*, 94(1):65–75.

Wang, Y., Zureick, A.-H., Cho, B.-S., and Scott, D. (1994). Properties of fibre reinforced concrete using recycled fibres from carpet industrial waste. *Journal of materials science*, 29(16):4191–4199.

Wei, X., Hattab, M., Bompard, P., and Fleureau, J.-M. (2016). Highlighting some mechanisms of crack formation and propagation in clays on drying path. *Géotechnique*, 66:287–300.

Wetzig, K. and Schulze, D., editors (1995). *In situ Scanning Electron Microscopy in Materials Research*. Akademie Verlag Germany.

Zheng, Z. and Feldman, D. (1995). Synthetic fibre-reinforced concrete. *Progress in Polymer Science*, 20(2):185–210.

Appendix A

Unconfined compressive strength test: experimental data

Sample ID	UCS (MPa)
U-W0C0-1	-
U-W0C0-2	0.39
U-W0C0-3	0.36
U-W0C0-4	0.51
U-W0C0-5	0.50
U-W0C0-6	0.50
U-W0C2-1	0.67
U-W0C2-2	0.90
U-W0C2-3	0.56
U-W0C2-4	1.17
U-W0C2-5	1.24
U-W0C2-6	1.23
U-W0C4-1	1.18
U-W0C4-2	1.25
U-W0C4-3	0.99
U-W0C4-4	1.77
U-W0C4-5	1.82
U-W0C4-6	1.84
U-W0C6-1	1.57
U-W0C6-2	1.94
U-W0C6-3	2.23
U-W0C6-4	1.35
U-W0C6-5	2.68
U-W0C6-6	2.63
U-W0C8-1	1.98
U-W0C8-2	2.04
U-W0C8-3	2.17
U-W0C8-4	2.84
U-W0C8-5	2.97
U-W0C8-6	3.03
U-W0C10-1	2.99
U-W0C10-2	2.60
U-W0C10-3	2.57
U-W0C10-4	4.48
U-W0C10-5	4.43
U-W0C10-6	4.38

Sample ID	UCS (MPa)
U-W2C0-1	0.88
U-W2C0-2	0.81
U-W2C0-3	0.90
U-W2C0-4	0.79
U-W2C0-5	0.89
U-W2C0-6	0.86
U-W2C2-1	1.88
U-W2C2-2	1.90
U-W2C2-3	1.97
U-W2C2-4	1.85
U-W2C2-5	1.88
U-W2C2-6	1.88
U-W2C4-1	2.66
U-W2C4-2	2.58
U-W2C4-3	2.88
U-W2C4-4	2.50
U-W2C4-5	2.74
U-W2C4-6	2.73
U-W2C6-1	2.95
U-W2C6-2	2.97
U-W2C6-3	3.17
U-W2C6-4	2.85
U-W2C6-5	2.59
U-W2C6-6	3.01
U-W2C8-1	3.46
U-W2C8-2	3.73
U-W2C8-3	3.54
U-W2C8-4	3.44
U-W2C8-5	3.58
U-W2C8-6	3.60
U-W2C10-1	4.55
U-W2C10-2	4.15
U-W2C10-3	4.26
U-W2C10-4	4.21
U-W2C10-5	4.09
U-W2C10-6	4.21

Sample ID	UCS (MPa)
U-W4C0-1	0.90
U-W4C0-2	1.02
U-W4C0-3	-
U-W4C0-4	0.89
U-W4C0-5	0.95
U-W4C0-6	0.94
U-W4C2-1	1.54
U-W4C2-2	1.73
U-W4C2-3	-
U-W4C2-4	1.62
U-W4C2-5	1.67
U-W4C2-6	1.85
U-W4C4-1	2.33
U-W4C4-2	2.18
U-W4C4-3	2.57
U-W4C4-4	2.47
U-W4C4-5	2.47
U-W4C4-6	2.43
U-W4C6-1	3.13
U-W4C6-2	3.38
U-W4C6-3	3.55
U-W4C6-4	3.10
U-W4C6-5	3.47
U-W4C6-6	3.82
U-W4C8-1	3.16
U-W4C8-2	3.14
U-W4C8-3	3.11
U-W4C8-4	3.12
U-W4C8-5	2.83
U-W4C8-6	3.27
U-W4C10-1	4.34
U-W4C10-2	4.28
U-W4C10-3	4.06
U-W4C10-4	4.37
U-W4C10-5	4.09
U-W4C10-6	4.63

Appendix B

Direct shear test: experimental data

Sample ID	Applied normal stress (kPa)	Maximum shear force (N)	Maximum shear stress (kPa)	Horizontal displacement at max. shear stress (mm)	Vertical displacement at max. shear stress (mm)
D-W0C0-1	35.77	461.62	128.23	2.09	0.25
D-W0C0-2	35.77	482.17	133.94	1.22	0.15
D-W0C0-3	35.77	519.22	144.23	1.48	1.19
D-W0C0-4	60.29	761.58	211.55	2.20	-0.12
D-W0C0-5	60.29	724.54	201.26	2.48	-0.28
D-W0C0-6	60.29	699.67	194.35	1.76	-0.14
D-W0C0-7	24.87	499.15	138.65	1.88	0.39
D-W0C0-8	24.87	395.27	109.80	2.29	0.53
D-W0C2-1	24.87	582.97	161.94	1.57	0.68
D-W0C2-2	24.87	324.85	-	-	-
D-W0C2-3	49.39	562.58	156.27	2.24	0.24
D-W0C2-4	49.39	691.50	192.08	2.03	0.25
D-W0C2-5	73.92	966.08	268.36	2.56	0.40
D-W0C2-6	24.87	789.84	219.40	2.52	0.35
D-W0C4-1	24.87	617.50	171.53	1.72	0.55
D-W0C4-2	49.39	670.75	186.32	1.92	0.71
D-W0C4-3	24.87	588.00	163.33	1.60	0.52
D-W0C4-4	49.39	733.29	203.69	2.37	0.15
D-W0C4-5	73.92	905.15	251.43	2.06	0.60
D-W0C4-6	73.92	762.90	211.92	2.39	0.00
D-W0C6-1	24.87	491.09	136.41	1.76	0.96
D-W0C6-2	24.87	440.28	122.30	2.13	1.18
D-W0C6-3	49.39	999.97	277.77	3.01	0.54
D-W0C6-4	49.39	1036.99	288.05	2.01	0.53
D-W0C6-5	73.92	1220.53	339.04	2.62	0.66
D-W0C6-6	73.92	1124.27	312.30	2.49	0.55
D-W0C8-1	24.87	745.44	207.07	2.46	1.22
D-W0C8-2	73.92	1186.94	329.71	2.33	0.06
D-W0C8-3	73.92	1057.39	293.72	2.73	0.00
D-W0C8-4	49.39	770.61	214.06	2.44	0.10
D-W0C8-5	49.39	929.03	258.06	2.08	0.20
D-W0C8-6	24.87	738.51	205.14	2.16	0.64

Sample ID	Applied normal stress (kPa)	Maximum shear force (N)	Maximum shear stress (kPa)	Horizontal displacement at max. shear stress (mm)	Vertical displacement at max. shear stress (mm)
D-W0C10-1	24.87	632.61	-	-	-
D-W0C10-2	24.87	548.80	152.44	1.55	0.49
D-W0C10-3	49.39	1015.79	282.16	2.02	0.15
D-W0C10-4	49.39	1194.97	331.94	2.20	0.15
D-W0C10-5	73.92	942.11	261.70	2.61	0.21
D-W0C10-6	73.92	873.74	242.71	2.03	0.15
D-W1C0-1	24.87	428.37	118.99	1.57	0.00
D-W1C0-2	24.87	382.91	106.36	2.02	0.12
D-W1C0-3	49.39	758.08	210.58	2.67	0.46
D-W1C0-4	49.39	468.94	130.26	1.80	0.21
D-W1C0-5	73.92	678.73	188.54	2.74	0.10
D-W1C0-6	73.92	529.28	147.02	3.00	0.19
D-W1C2-1	24.87	630.42	175.12	2.09	0.30
D-W1C2-2	24.87	500.66	139.07	1.60	0.07
D-W1C2-3	49.39	624.50	173.47	2.24	0.25
D-W1C2-4	49.39	556.54	154.59	1.92	0.00
D-W1C2-5	73.92	619.74	172.15	1.54	0.05
D-W1C2-6	73.92	813.33	225.93	2.48	0.09
D-W1C4-1	24.87	513.95	142.76	1.92	0.60
D-W1C4-2	24.87	777.30	215.92	3.14	0.45
D-W1C4-3	49.39	903.84	251.07	2.57	0.15
D-W1C4-4	49.39	846.18	-	-	-
D-W1C4-5	73.92	1333.83	370.51	2.76	0.27
D-W1C4-6	73.92	733.51	203.75	2.77	0.15
D-W1C6-1	24.87	518.35	143.99	2.04	0.31
D-W1C6-2	24.87	584.72	162.42	2.73	0.69
D-W1C6-3	49.39	736.98	204.72	2.62	0.61
D-W1C6-4	49.39	706.30	196.19	2.04	0.39
D-W1C6-5	73.92	883.87	245.52	3.03	0.89
D-W1C6-6	73.92	807.81	224.39	3.03	0.87
D-W1C8-1	24.87	446.88	124.13	2.23	0.60
D-W1C8-2	24.87	433.48	120.41	2.12	0.35
D-W1C8-3	49.39	626.28	173.97	2.28	-0.05
D-W1C8-4	49.39	587.61	163.23	3.15	0.51
D-W1C8-5	73.92	674.15	187.26	1.85	-0.06
D-W1C8-6	73.92	591.74	164.37	2.39	-0.05
D-W1C10-1	24.87	868.54	241.26	3.10	0.25
D-W1C10-2	-	-	-	-	-
D-W1C10-3	49.39	636.00	176.67	2.22	0.65
D-W1C10-4	49.39	683.11	189.75	2.00	0.52
D-W1C10-5	73.92	789.92	219.42	2.80	0.60
D-W1C10-6	73.92	1206.42	335.12	2.21	0.10
D-W2C0-1	24.87	450.89	-	-	-
D-W2C0-2	24.87	348.91	96.92	2.53	0.42
D-W2C0-3	49.39	428.11	-	-	-
D-W2C0-4	49.39	461.43	128.18	2.03	0.05
D-W2C0-5	73.92	462.77	128.55	3.48	-0.05
D-W2C0-6	73.92	317.31	88.14	2.94	0.00

Sample ID	Applied normal stress (kPa)	Maximum shear force (N)	Maximum shear stress (kPa)	Horizontal displacement at max. shear stress (mm)	Vertical displacement at max. shear stress (mm)
D-W2C2-1	24.87	412.36	114.54	2.54	0.34
D-W2C1-2	24.87	244.41	67.89	1.87	-0.05
D-W2C1-3	49.39	441.23	122.56	1.89	0.01
D-W2C1-4	49.39	377.07	104.74	2.91	0.13
D-W2C1-5	73.92	592.98	164.72	2.98	-0.32
D-W2C1-6	73.92	544.80	151.33	2.25	0.00
D-W2C4-1	24.87	330.14	91.71	2.46	0.27
D-W2C4-2	24.87	148.49	41.25	1.76	-0.12
D-W2C4-3	49.39	498.23	138.40	2.89	0.25
D-W2C4-4	49.39	444.04	123.34	1.74	0.15
D-W2C4-5	73.92	305.80	84.94	1.80	0.15
D-W2C4-6	73.92	771.35	214.26	2.51	0.59
D-W2C6-1	24.87	388.93	108.04	1.65	0.25
D-W2C6-2	24.87	304.20	84.50	2.66	1.40
D-W2C6-3	49.39	633.55	175.99	1.75	0.25
D-W2C6-4	-	-	-	-	-
D-W2C6-5	-	-	-	-	-
D-W2C6-6	73.92	711.18	197.55	1.88	0.34
D-W2C8-1	-	-	-	-	-
D-W2C8-2	24.87	351.54	97.65	1.57	0.42
D-W2C8-3	49.39	740.80	205.78	2.35	0.45
D-W2C8-4	49.39	478.74	132.98	2.21	0.29
D-W2C8-5	73.92	737.15	204.76	2.50	0.12
D-W2C8-6	73.92	519.65	144.35	3.02	0.22
D-W2C10-1	24.87	463.00	128.61	2.67	1.90
D-W2C10-2	24.87	122.28	33.97	4.47	0.50
D-W2C10-3	49.39	271.62	75.45	1.71	-0.05
D-W2C10-4	49.39	800.13	222.26	2.10	0.42
D-W2C10-5	73.92	611.42	169.84	1.49	0.00
D-W2C10-6	73.92	352.34	97.87	5.31	0.60
D-W3C0-1	24.87	284.62	79.06	2.85	0.15
D-W3C0-2	24.87	151.17	41.99	2.31	0.21
D-W3C0-3	49.39	188.96	52.49	2.35	0.00
D-W3C0-4	49.39	245.69	68.25	2.85	-0.15
D-W3C0-5	73.92	268.68	74.63	2.99	-0.15
D-W3C0-6	73.92	385.42	107.06	1.74	-0.09
D-W3C2-1	24.87	200.35	55.65	3.33	0.60
D-W3C2-2	-	-	-	-	-
D-W3C2-3	49.39	353.28	98.13	1.79	0.00
D-W3C2-4	49.39	243.20	67.56	1.45	-0.23
D-W3C2-5	73.92	533.67	148.24	3.02	0.30
D-W3C2-6	-	-	-	-	-
D-W3C4-1	24.87	160.31	44.53	2.56	0.15
D-W3C4-2	24.87	315.45	87.63	3.35	0.11
D-W3C4-3	49.39	206.25	57.29	1.51	0.00
D-W3C4-4	49.39	286.24	79.51	4.07	0.41
D-W3C4-5	73.92	465.04	129.18	2.99	0.13
D-W3C4-6	73.92	680.06	188.91	1.94	0.01

Sample ID	Applied normal stress (kPa)	Maximum shear force (N)	Maximum shear stress (kPa)	Horizontal displacement at max. shear stress (mm)	Vertical displacement at max. shear stress (mm)
D-W3C6-1	24.87	160.85	44.68	4.76	0.74
D-W3C6-2	-	-	-	-	-
D-W3C6-3	49.39	514.31	142.86	3.61	0.44
D-W3C6-4	49.39	511.49	142.08	2.68	0.01
D-W3C6-5	73.92	319.29	88.69	2.02	0.00
D-W3C6-6	73.92	357.93	99.43	3.09	0.06
D-W3C8-1	24.87	262.01	72.78	2.08	0.50
D-W3C8-2	24.87	276.76	76.88	3.63	0.71
D-W3C8-3	49.39	292.90	81.36	4.41	0.30
D-W3C8-4	49.39	321.67	89.35	2.59	0.10
D-W3C8-5	73.92	274.06	76.13	2.45	0.03
D-W3C8-6	73.92	307.64	85.46	2.28	0.00
D-W3C10-1	24.87	111.31	30.92	1.77	0.08
D-W3C10-2	24.87	55.88	15.52	2.43	0.00
D-W3C10-3	49.39	372.82	103.56	3.03	0.46
D-W3C10-4	49.39	241.43	67.06	8.07	0.64
D-W3C10-5	73.92	338.32	93.98	2.37	-0.02
D-W3C10-6	73.92	383.44	106.51	1.54	0.02
D-L1-1	24.87	254.15	70.60	1.78	-0.01
D-L1-2	24.87	309.13	85.87	1.80	0.10
D-L1-3	49.39	401.13	111.43	1.89	0.15
D-L1-4	49.39	354.21	98.39	3.22	0.05
D-L1-5	73.92	355.40	98.72	2.23	0.00
D-L1-6	73.92	381.27	105.91	1.79	0.00
D-L2-1	24.87	419.81	116.61	1.48	0.15
D-L2-2	24.87	342.93	95.26	1.72	0.70
D-L2-3	49.39	426.19	118.39	1.75	0.00
D-L2-4	49.39	557.54	154.87	1.60	0.05
D-L2-5	73.92	634.36	176.21	1.34	0.15
D-L2-6	73.92	664.65	184.63	1.62	0.05
D-L3-1	24.87	373.89	103.86	1.38	-0.02
D-L3-2	24.87	298.45	82.90	2.10	0.43
D-L3-3	49.39	593.41	164.84	2.00	0.04
D-L3-4	49.39	612.60	170.17	1.70	0.10
D-L3-5	73.92	551.77	153.27	2.42	0.16
D-L3-6	73.92	814.85	226.35	2.15	0.00
D-L4-1	24.87	370.60	102.94	1.90	0.61
D-L4-2	24.87	349.19	97.00	1.92	0.10
D-L4-3	49.39	457.27	127.02	2.63	0.00
D-L4-4	49.39	474.33	131.76	1.81	0.10
D-L4-5	73.92	582.09	161.69	2.06	0.00
D-L4-6	73.92	459.88	127.74	1.97	0.19

Table B.1: Direct shear test individual sample data

Appendix C

Direct shear test: c-ϕ determination plots)

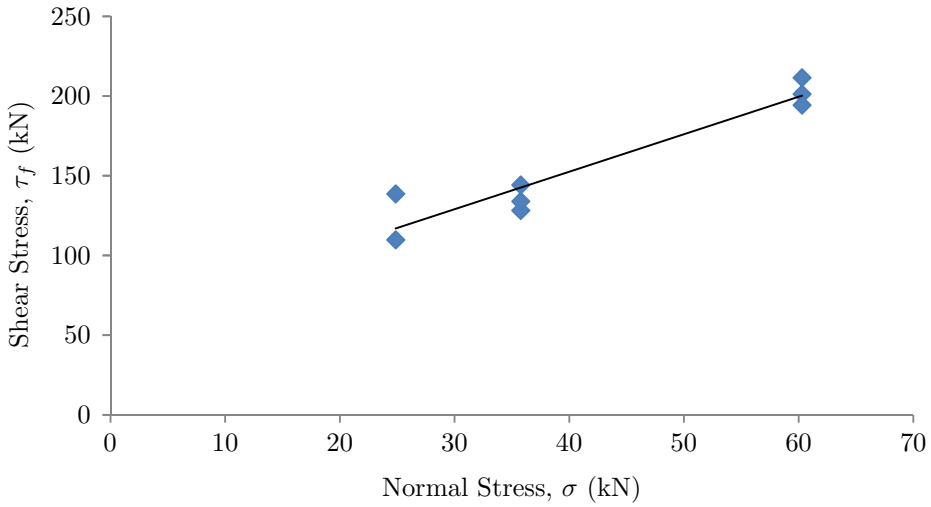

Figure C.1: Determination of c and ϕ for soil batch D-W0C0.

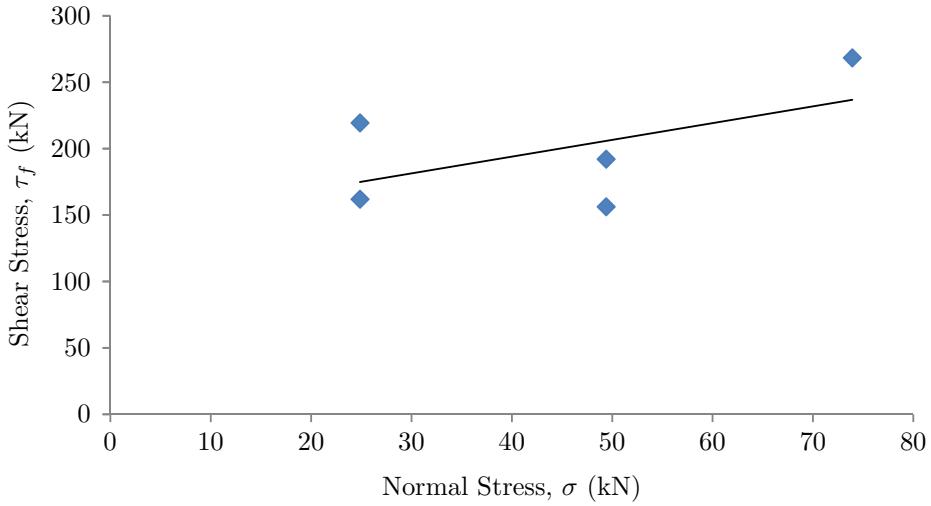

Figure C.2: Determination of c and ϕ for soil batch D-W0C2.

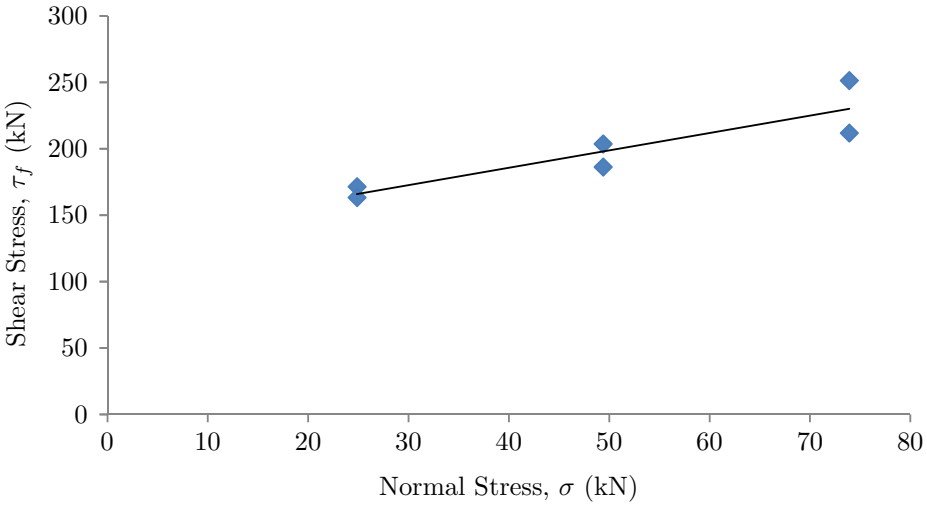

Figure C.3: Determination of c and ϕ for soil batch D-W0C4.

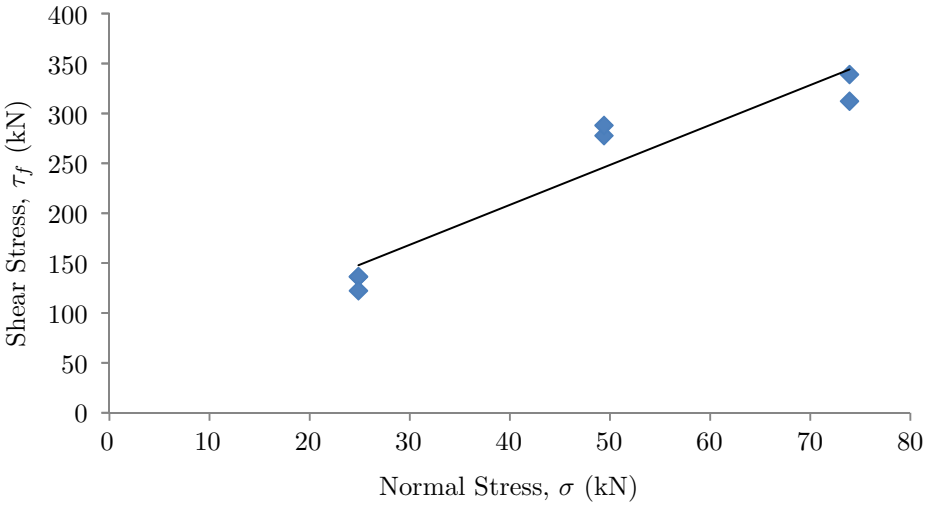

Figure C.4: Determination of c and ϕ for soil batch D-W0C6.

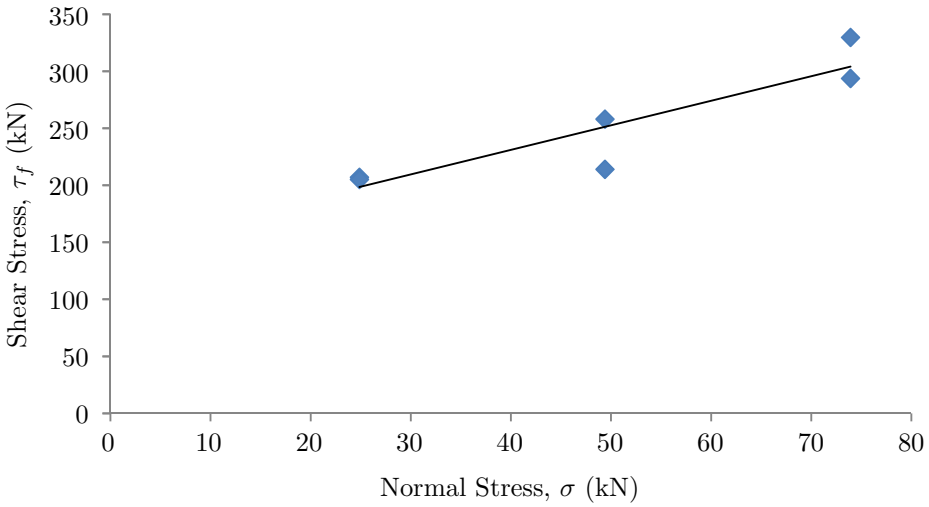

Figure C.5: Determination of c and ϕ for soil batch D-W0C8.

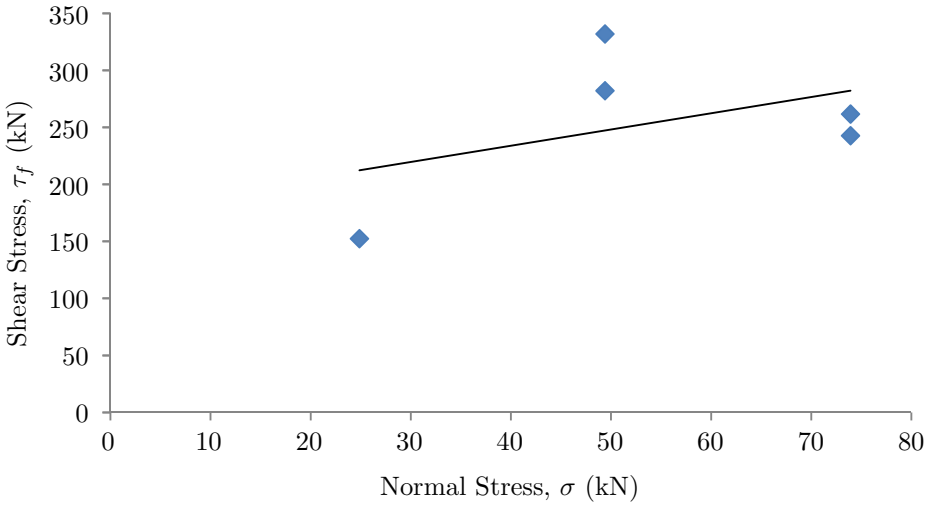

Figure C.6: Determination of c and ϕ for soil batch D-W0C10.

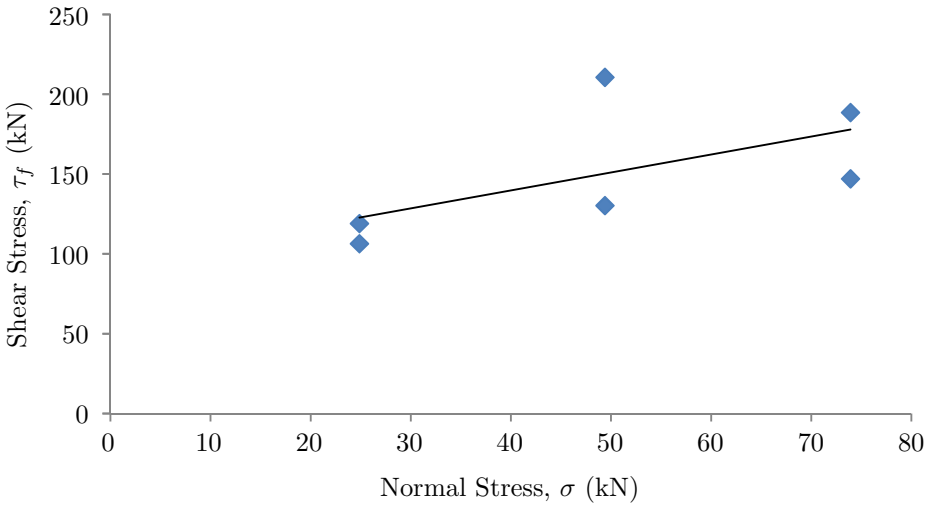

Figure C.7: Determination of c and ϕ for soil batch D-W1C0.

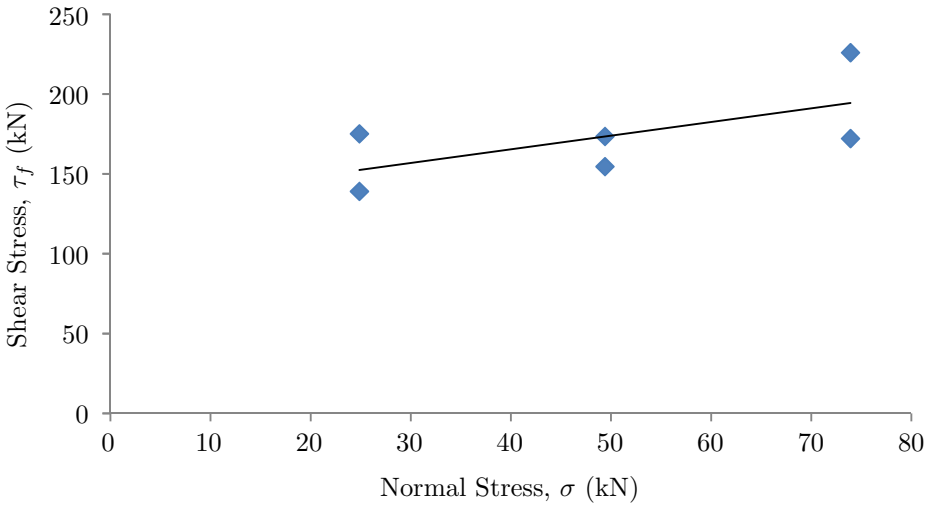

Figure C.8: Determination of c and ϕ for soil batch D-W1C2.

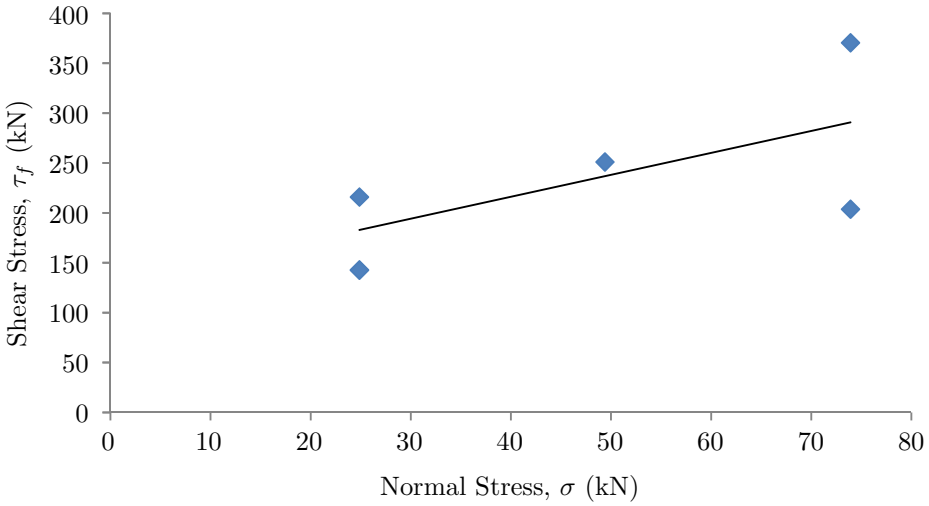

Figure C.9: Determination of c and ϕ for soil batch D-W1C4.

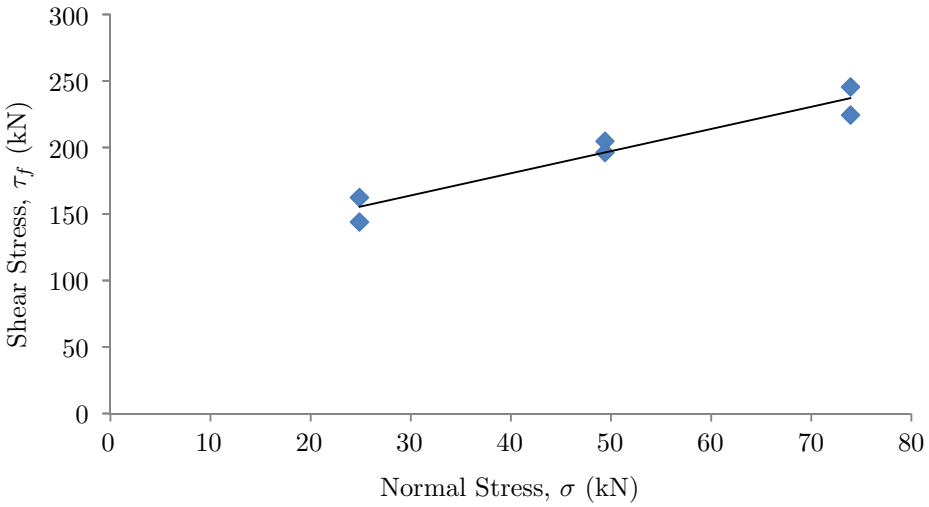

Figure C.10: Determination of c and ϕ for soil batch D-W1C6.

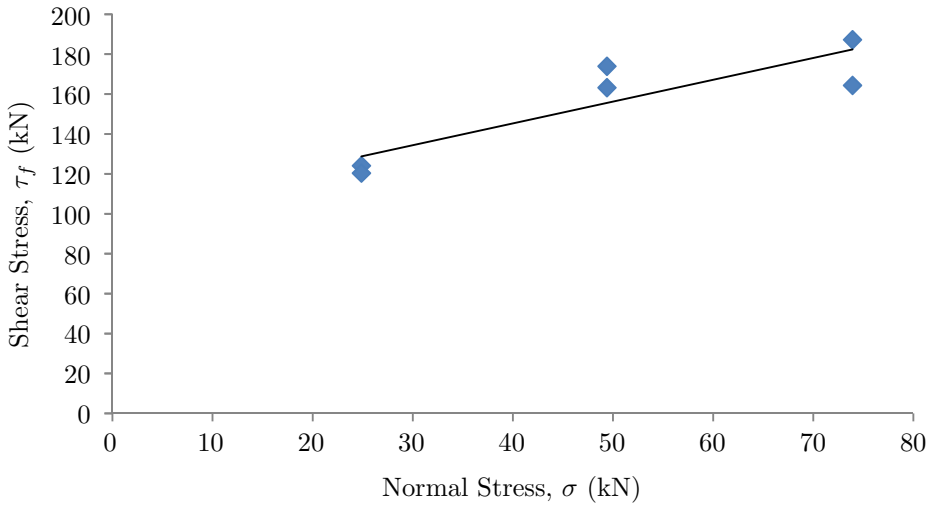

Figure C.11: Determination of c and ϕ for soil batch D-W1C8.

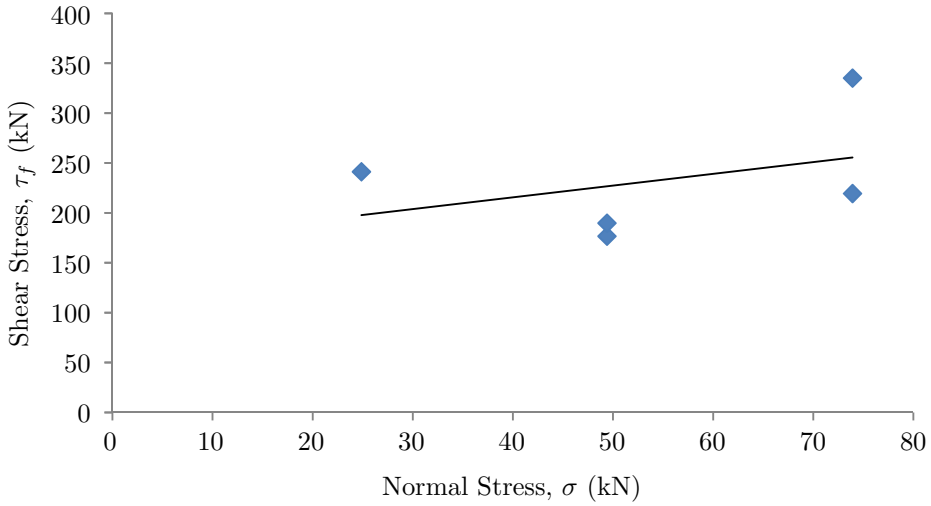

Figure C.12: Determination of c and ϕ for soil batch D-W1C10.

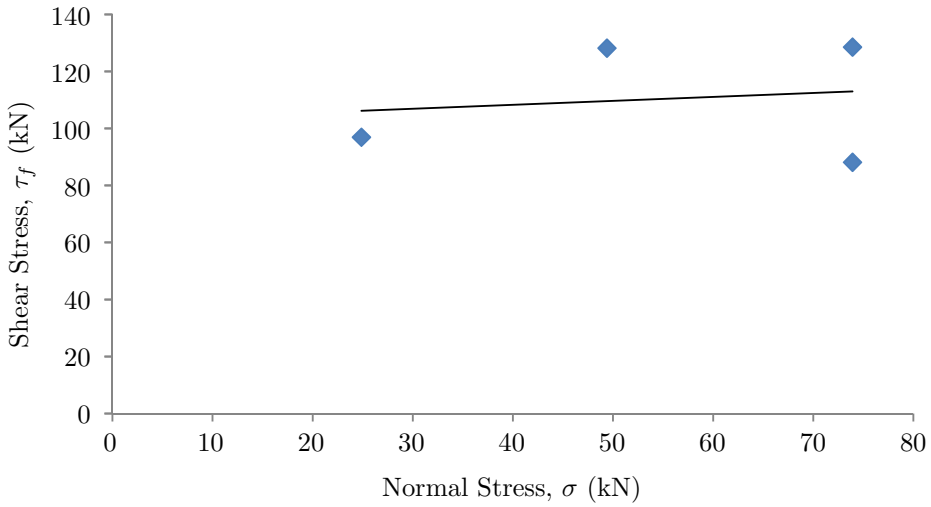

Figure C.13: Determination of c and ϕ for soil batch D-W2C0.

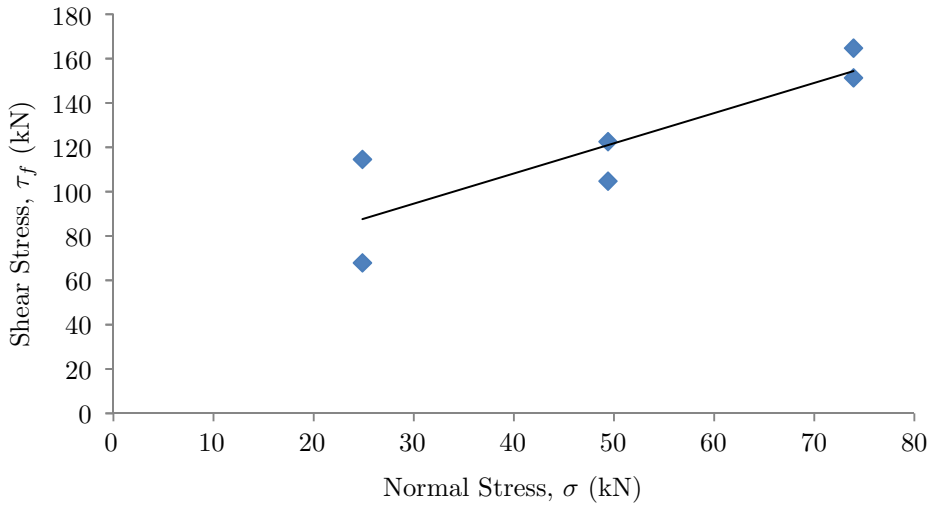

Figure C.14: Determination of c and ϕ for soil batch D-W2C2.

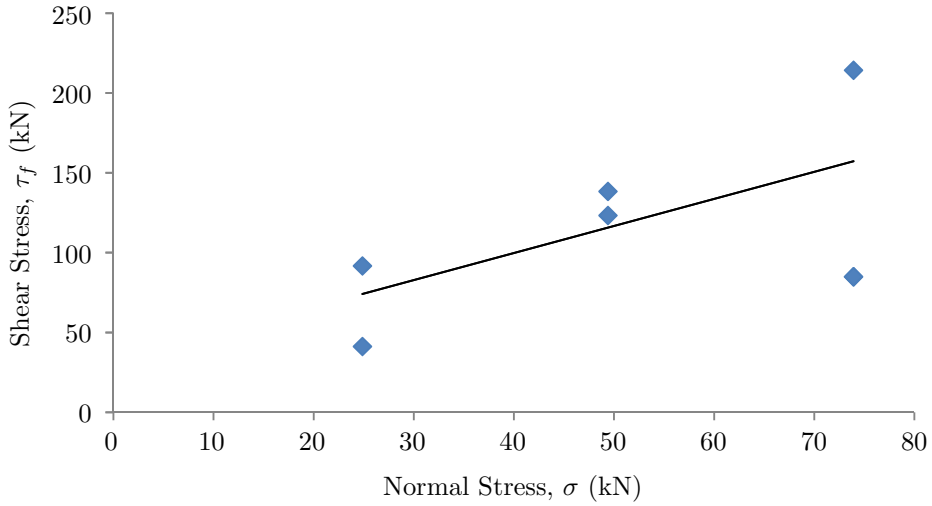

Figure C.15: Determination of c and ϕ for soil batch D-W2C4.

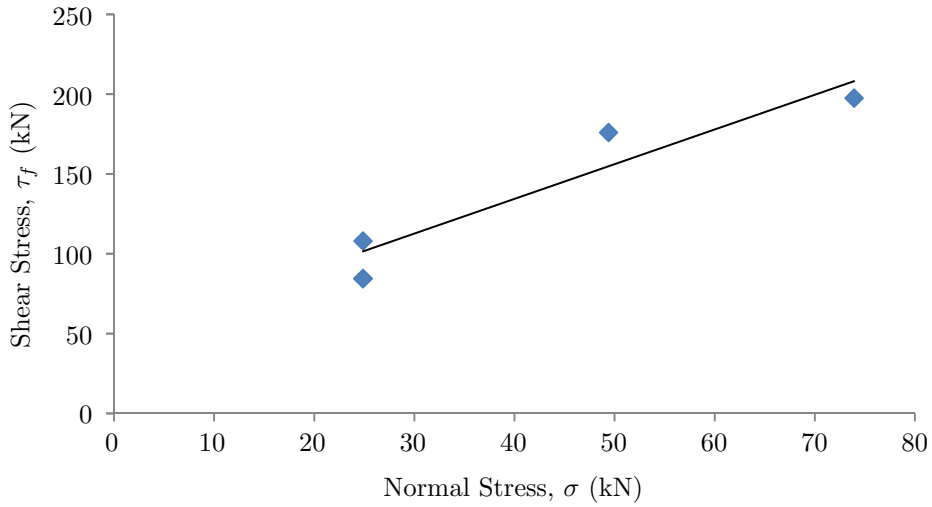

Figure C.16: Determination of c and ϕ for soil batch D-W2C6.

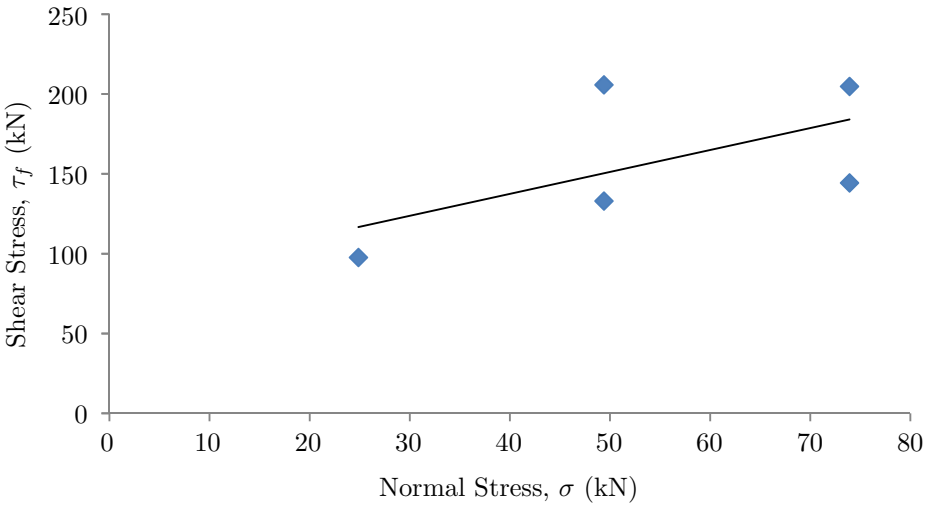

Figure C.17: Determination of c and ϕ for soil batch D-W2C8.

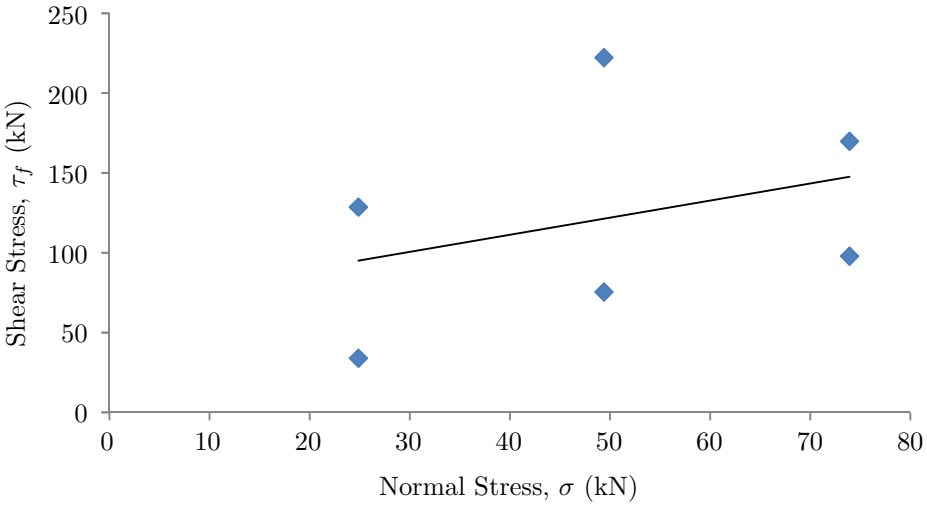

Figure C.18: Determination of c and ϕ for soil batch D-W2C10.

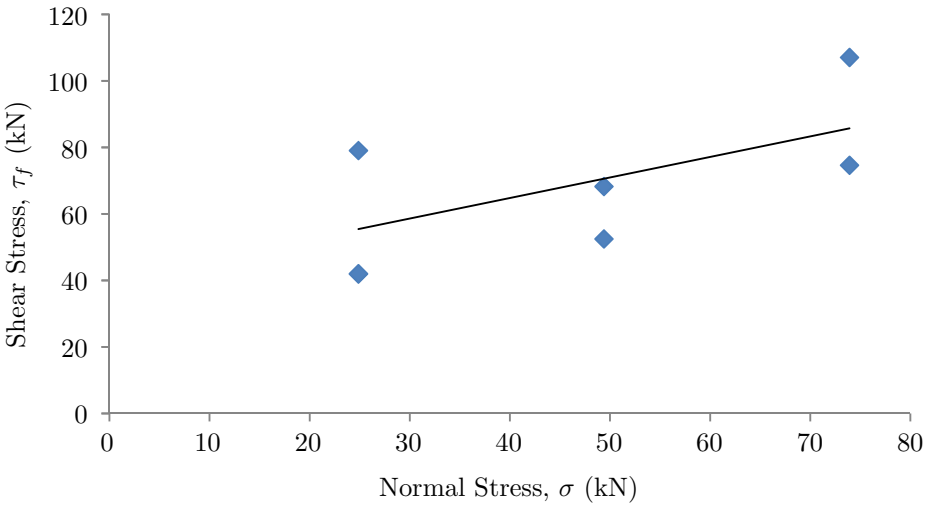

Figure C.19: Determination of c and ϕ for soil batch D-W3C0.

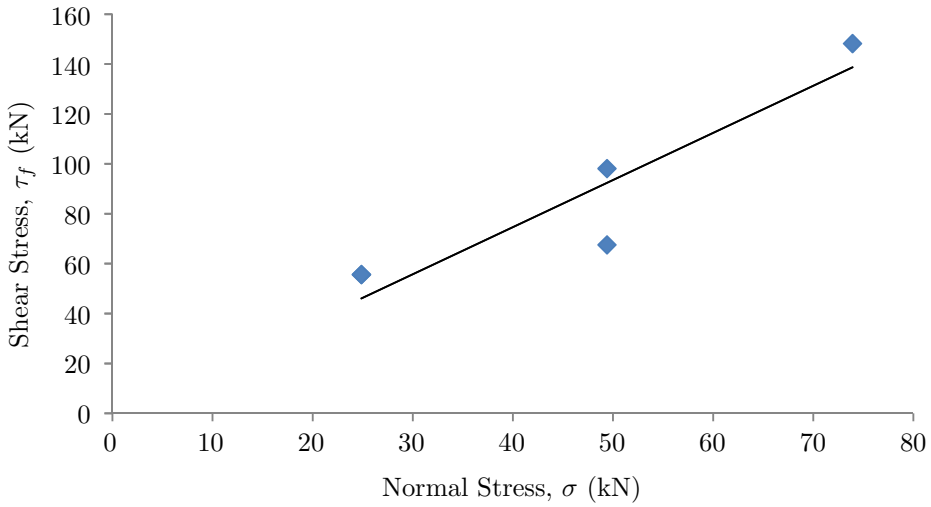

Figure C.20: Determination of c and ϕ for soil batch D-W3C2.

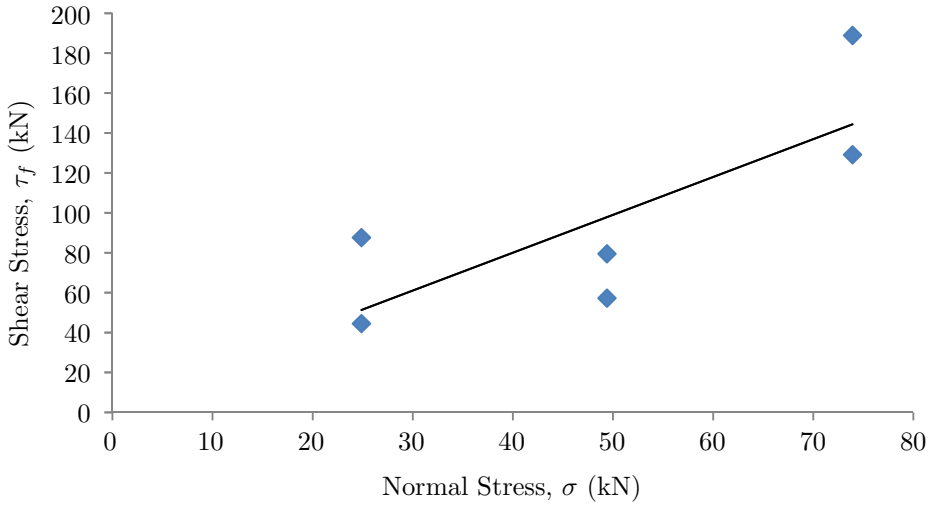

Figure C.21: Determination of c and ϕ for soil batch D-W3C4.

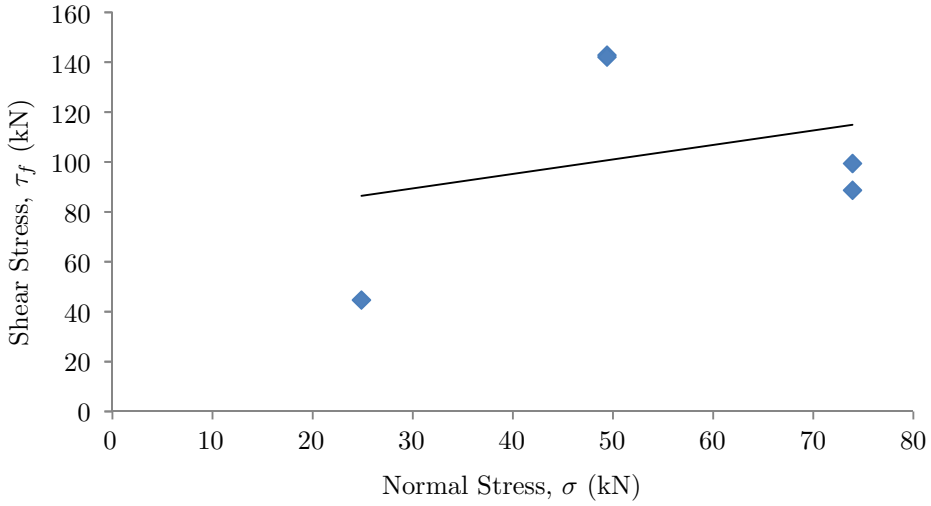

Figure C.22: Determination of c and ϕ for soil batch D-W3C6.

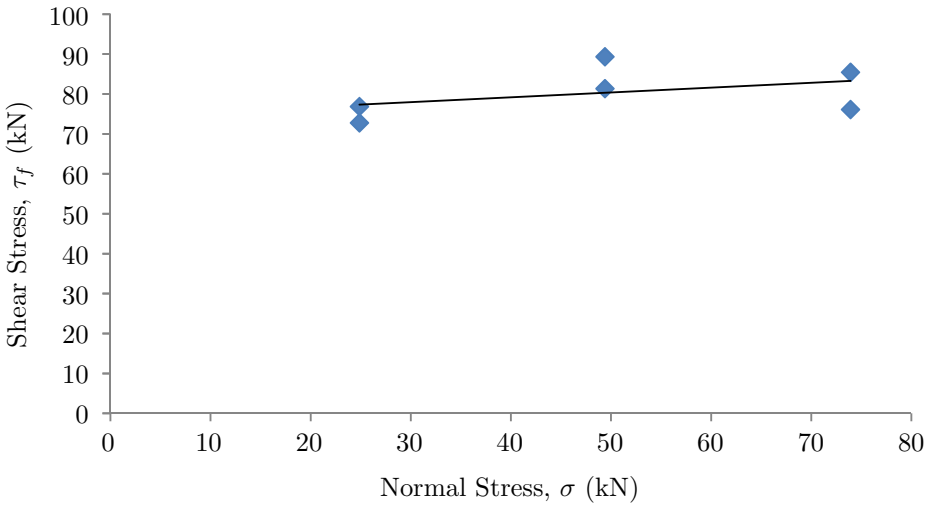

Figure C.23: Determination of c and ϕ for soil batch D-W3C8.

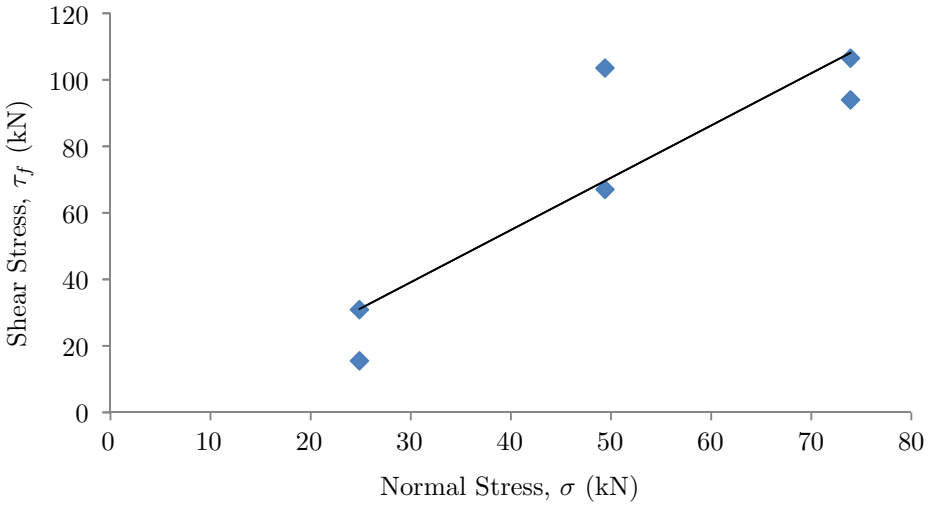

Figure C.24: Determination of c and ϕ for soil batch D-W3C10.

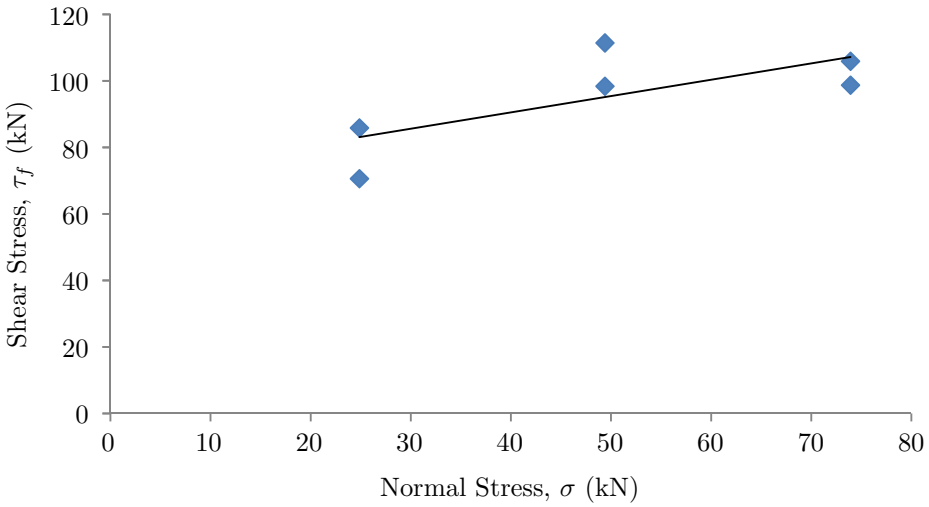

Figure C.25: Determination of c and ϕ for soil batch D-L1.

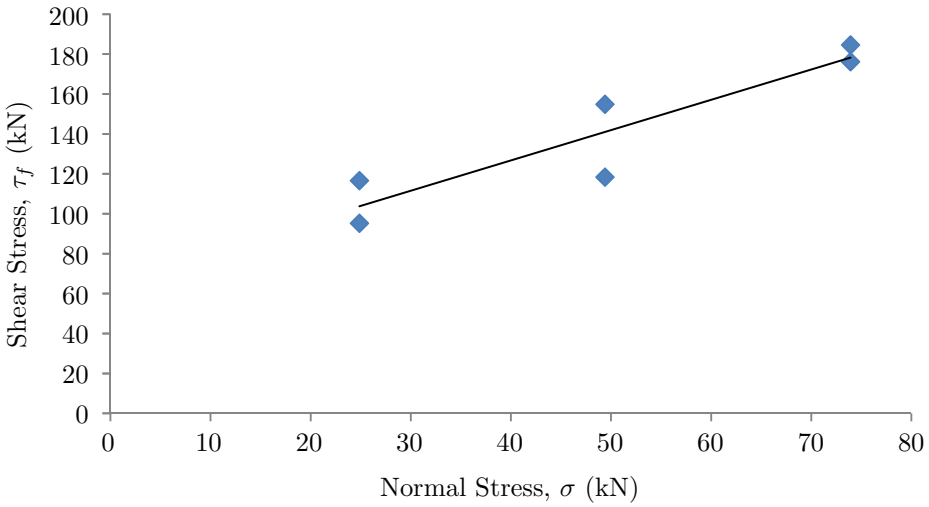

Figure C.26: Determination of c and ϕ for soil batch D-L2.

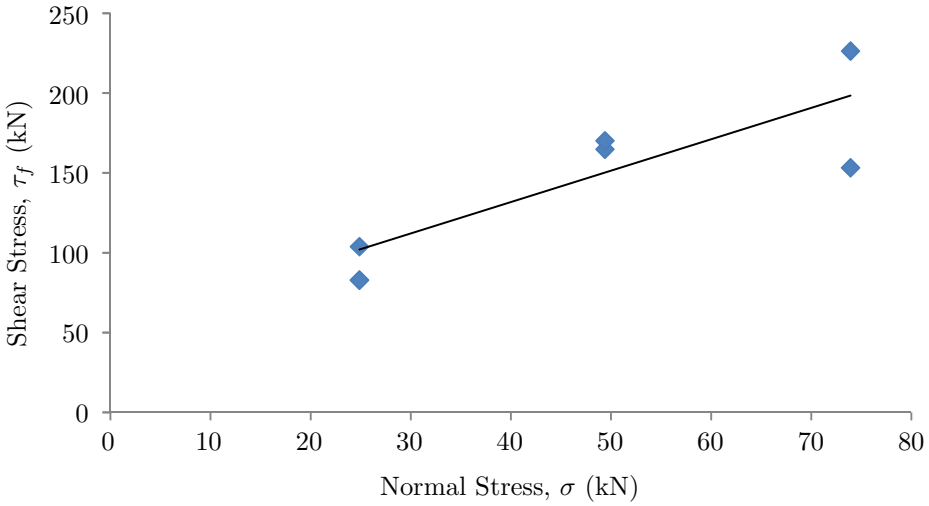

Figure C.27: Determination of c and ϕ for soil batch D-L3.

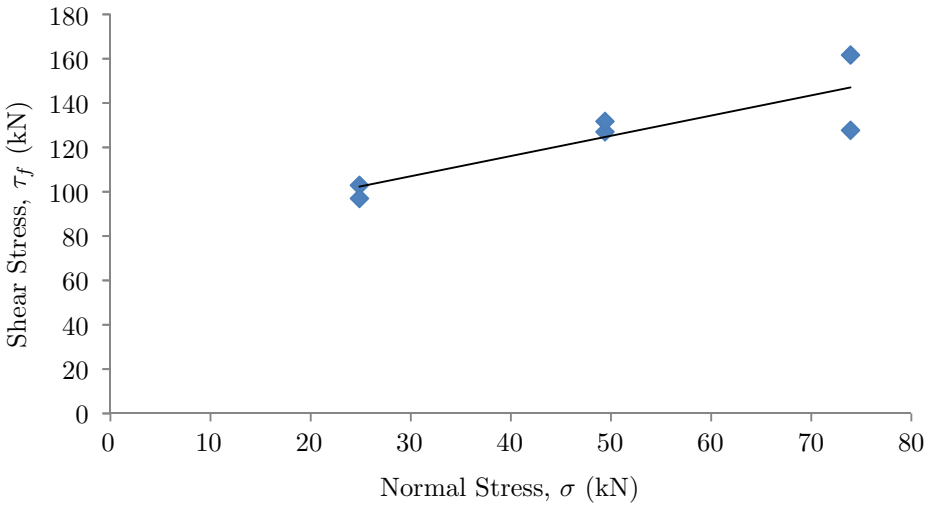

Figure C.28: Determination of c and ϕ for soil batch D-L4.